Université de Montréal

Characterization of microvascular stress and cell death responses triggered by renal ischemia-reperfusion injury and their roles in progressive fibrosis

par
Shanshan Lan

Programme de Sciences Biomédicales

Faculté de Médecine

Thèse présentée à la Faculté de Médecine
en vue de l'obtention du grade de Philosophiae Doctor (Ph.D)
en Sciences Biomédicales
option Générale

Décembre, 2020

Faculté des études supérieures et postdoctorales

Cette thèse intitulée

Characterization of microvascular stress and cell death responses triggered by renal ischemia-reperfusion injury and their roles in progressive fibrosis

Présentée par

Shanshan Lan

a été évaluée par un jury composé des personnes suivantes:

Emmanuelle Brochiero, Président-rapporteur

Marie-Josée Hébert, Directrice de recherche

Héloïse Cardinal, Co-directrice de recherche

Sylvain Meloche, Membre du jury

Tomoko Takano, Examinateur externe

Martin G. Sirois, Représentant du doyen

Résumé

L’insuffisance rénale aiguë (IRA) est une complication clinique associée à une mortalité significative. Parmi les diverses causes d'IRA, l'ischémie-reperfusion (IRI) est une étiologie importante, en particulier dans le contexte de la transplantation rénale.

Les types de mort cellulaire programmée (MCP) activées dans l'IRA induite par IRI ont été étudiées par des nombreux groupes. L’atteinte tubulaire épithéliale est classiquement considérée comme le principal contributeur à l'IRA.En effet, plusieurs morts programmées de cellules tubulaires ont été démontrées dans la littérature. Cependant, les lésions endothéliales microvasculaires rénales attirent davantage l'attention en tant qu'inducteurs cruciaux de dysfonctionnement microvasculaire et de fibrose rénale progressive. Ainsi, certaines équipes de recherche, dont la nôtre a rapporté le développement de l'apoptose endothéliale rénale en association avec l’IRI. Le but de mon travail était donc de caractériser les types de mort cellulaire microvasculaires secondaires à l’IRI et leur contribution à la dysfonction rénale.

Pour évaluer l'importance de l'apoptose dans l'IRA induite par IRI, nous avons utilisé un modèle murin d’IRI chez des souris caspase-3 knock-out (KO) et sauvages, avec clampage de l'artère rénale pendant 30 minutes (modèle IRA légère) ou 60 minutes (modèle IRA sévère). Dans le modèle IRA légère, notre résultat montre que la carence en caspase-3 empêche la mort apoptotique des cellules endothéliales dans toutes les phases de l'IRA, atténuant la raréfaction microvasculaire, le dépôt de collagène et la fibrose rénale. L’absence de caspase-3 favorise aussi le maintien d’une perméabilité endothéliale microvasculaire normale à long terme. Toutefois, l’invalidation de la caspase-3 aggrave la mort cellulaire tubulaire à court terme en favorisant la nécroptose, mais améliore l’homéostasie tubulaire à long terme grâce à la préservation des capillaires péritubulaires (PTCs) permettant un maintien de la perfusion tubulaire. En outre, le déficit en caspase-3 est également associé à un effet protecteur contre la raréfaction microvasculaire rénale, la fibrose rénale progressive, ainsi qu'une perméabilité endothéliale améliorée et une préservation de la fonction rénale dans le modèle d’IRA sévère.

En conclusion, nos résultats démontrent l'effet crucial de l’apoptose endothéliale microvasculaire en tant qu'inducteur de dysfonctionnement microvasculaire rénal, de raréfaction

microvasculaire et de fibrose rénale progressive dans la physiopathologie de l'IRA légère et sévère induite par l'IRI. Ils établissent aussi l'importance prédominante de l'atteinte microvasculaire plutôt que tubulaire épithéliale dans la prédiction de la perte de fonction rénale à long terme suite à une IRI.

Mots clés: Lésion rénale aiguë, lésion d'ischémie-reperfusion, apoptose, raréfaction microvasculaire, fibrose, perméabilité endothéliale, nécroptose.

Abstract

Acute kidney injury (AKI) is a crucial clinical event, with increasing incidence and mortality. Among various pathogenesis of AKI, ischemia-reperfusion injury (IRI) is an important etiology, especially in the renal post-transplant scenario.

The complex of programmed cell deaths (PCD) developed in IRI-induced AKI has been proven in a number of investigations. Renal tubular epithelial injury has been considered as the major contributor in AKI and multiple programmed tubular epithelial cell (TECs) deaths have been demonstrated in the literature. However, renal microvascular endothelial injury is attracting more attention as an important inducer of microvascular dysfunction and renal progressive fibrosis. Some investigators, including our team, have reported the development of renal endothelial apoptosis in the condition of ischemia.

Apoptosis, a commonly known programmed cell death, has been elucidated in both renal TECs and microvascular endothelial cells (ECs) post-IRI and the activation of caspase-3 functions as the key effector of caspase-dependent apoptosis. To verify the importance of apoptosis in IRI-induced AKI, we applied the *in vivo* murine renal IRI model in wild-type and caspase-3 KO mice, with clamping the renal artery for 30 minutes (mild AKI model) or 60 minutes (severe AKI model). In regard to the mild AKI model, our result demonstrates that caspase-3 deficiency prevents ECs apoptotic death in all phases of AKI, attenuating microvascular rarefaction, collagen deposition, and renal fibrosis, while maintaining physical endothelial permeability in the long-term. Meanwhile, caspase-3 deletion aggravates tubular injury in the short-term by promoting TECs necroptosis but ameliorates long-term tubular injury through preserved peritubular capillaries (PTCs) function. Furthermore, caspase-3 deficiency also demonstrated a protective effect against renal microvascular rarefaction, progressive renal fibrosis, as well as enhanced endothelial permeability in the severe AKI model.

Conclusively, our findings determine the crucial effect of microvascular endothelial apoptosis as an inducer of renal microvascular dysfunction, microvascular rarefaction, and progressive renal fibrosis in the pathophysiology of mild and severe AKI induced by IRI. Additionally, our results demonstrate the predominant importance of microvascular endothelial injury over tubular epithelial injury in predicting renal function loss at long-term post-IRI.

Keywords: Acute kidney injury, ischemia-reperfusion injury, apoptosis, microvascular rarefaction, fibrosis, endothelial permeability, necroptosis.

Table des matières

Liste des tableaux

Liste des figures

Liste des abréviations

ABMR	Antibody-Mediated Rejection
ADMA	Asymmetric Dimethylarginine
AKI	Acute Kidney Injury
AIF	Apoptosis Inducing Factor
Ang-2	Angiopoietin-2
Apaf-1	Apoptotic protease activating factor-1
Atgs	Autophagy related proteins
BAK	Homologue antagonist of Bcl-2
BAX	Bcl-2 associated X
BDD	Brain Death Donor
BH-3	Bcl-2 homology 3
bIRI	Bilateral IRI
BUN	Blood Urine Nitrogen
Caspase	Cysteine-aspartic-proteins
CKD	Chronic Kidney Disease
CKO	Conditional Knock-Out
CMJ	Cortico-Medullary Junction
Col IV	Collagen IV
CTGF	Connective Tissue Growth Factor
Cyp D	Cyclophilin D
DAMP	Damage-Associated Molecular Pattern
dATP	Deoxyadenosine triphosphate

DCD	Donation after Cardiac Circulatory Death
DCs	Dendritic Cells
DED	Death Effector Domain
Deptor	Dep-domain-containing mTOR interaction protein
DDL4	Delta-like Protein 4
DGF	Delayed Graft Function
DIC	Disseminated Intravascular Coagulation
DKD	Diabetic Kidney Disease
DN	Delayed Nephrectomy
DR	Death Receptor
ECM	Extracellular Matrix
ECs	Endothelial Cells
EGF	Epidermal Growth Factor
EM	Electron Microscopy
EMT	Epithelial-Mesenchymal Transition
EndoMT	Endothelial-Mesenchymal Transition
eNOS	Endothelial Nitric Oxide
EPCs	Endothelial Progenitor Cells
EPO	Erythropoietin
ER	Endoplasmic Reticulum
EVs	Extracellular Vesicles
ESRD	End-Stage Renal Disease
FADD	Fas-Associated Death Domain

Fas	Fatty acid synthase
FLIPs	FLICE-like Inhibitor Proteins
FoxO1	Forkhead Box O1
GFP	Green Fluorescent Protein
GFR	Glomerular Filtration Rate
GN	Glomerulonephritis
GPX4	Glutathione Peroxidase 4
HMGB1	High Mobility Group Box-1
HIF-1α	Hypoxia Inducible Factor-1α
HSC	Hematopoietic Stem Cells
HUVECs	Human Umbilical Vascular Endothelial Cells
ICAM-1	Intercellular Adhesion Molecule-1
IL	Interleukin
IR	Ischemia-Reperfusion
IRI	Ischemia-Reperfusion Injury
IS	Indoxyl Sulfate
KIM-1	Kiney Injury Molecule-1
KO	Knock-Out
LC3	Microtubule-associated protein 1A/1B light chain 3
LN	Lupus Nephritis
LPS	Lipopolysaccharide
MAPK	MAP kinase
MECA-32	Mouse Endothelial Cell Antigen-32

microCT	micro-Computed Tomography
MLKL	Mixed Linage Kinase Domain-Like Protein
MOMP	Mitochondrial Outer Membrane Permeability
MPT	Mitochondrial Permeability Transition
MPTP	MPT pore
mSIN1	Mamalian Stress-actived protein Kinase-Interaction Protein 1
mTOR	Mammalian Target of Rapamycin
mTORC	mTOR Complex
NADPH	Nicotinamide Adenine Dinucleotide Phosphate
NGAL	Neutrophil Gelatinase Associated Lipocaline
NLRs	NOD-like Receptors
NO	Nitric Oxide
NOS	Nitric Oxide Synthase
NPCD	Non-Programmed Cell Death
PAI-1	Plasminogen Activator Inhibitor-1
PAS	Phagophore Assembly Site
PBSCs	Peripheral Blood Stem Cells
PCD	Programmed Cell Death
PCs	p-Cresylsulfate
PDGF-A	Platelet Derived Growth Factor A
PI3K	Phsophoinositide 3-Kinase
PKB	Protein Kinase B
PS	Phosphatidylserine

PTCs	Peritubular Capillaries
PTCH1	Hedgehog Receptor Patched 1
PTECs	Proximal Tubular Epithelial Cells
Raptor	Regulatory-associated Protein of mTOR
RAS	Renin-Angiotensin System
Rictor	Rapamycin-insensitive companion of mTOR
RIPK1/3	Receptor-Interacting Protein Kinase 1/3
ROS	Reactive Oxygen Species
RRT	Renal Replacement Therapy
Scr	Serum creatinine
SDC-1	Syndecan-1
sFlt-1	Soluble fms-type Tyrosine Kinase-1
shRNA	Small hairpin RNA
siRNA	Small interfere RNA
SIRT1	Sirtuin 1
SLE	Systemic Lupus Erythematosus
SS	Serum Starvation
sTB	Soluble Thrombomodulin
tBid	Truncated Bid
TECs	Tubular Epithelial Cells
TGF-β	Transforming Growth Factor-β
TIMP-2	Tissue Iinhibitor of Metalloproteinases-2
TLRs	Toll Like Receptors

TNF-α	Tumor Necrosis Factor-α
TNFR	Tumor Necrosis Factor Receptor
tPA	Tissue Plasminogen Activator
TRADD	TNF Receptor Type-1-associated Death Domain Protein
uIRI	Unilateral IRI
ULK1/2	Unc-51-like Kinase
uPA	Urokinase Plasminogen Activator
uPAR	uPA Receptor
UTs	Uremic Toxins
UUO	Unilateral Ureteral Obstruction
VCAM-1	Vascular Cell Adhesion Protein 1
VEGF-A	Vascular Endothelial Growth Factor A
WPB	Weibel-Palade Body
WT	Wild-Type
α-SMA	Alpha-Smooth Muscle Actin

Remerciements

Après mes études doctorales de 6 ans, finalement j'arrive presque au terminus de cette période charnière. Je voudrais remercier beaucoup de personnes, qui m'ont donné grande aide et support. Je n'aurais jamais pu relever ce grand défi sans eux.

Quand je suis arrivée à Montréal en 2014, je ne savais pas que la langue utilisée au laboratoire était le français. En fait, je m'étais un peu perdue à ce moment-là. Donc, j'ai commencé à étudier le français à l'Université de Montréal. Tout le monde au laboratoire était un peu mon professeur en français; chacun m'a aidée à corriger mes expressions et ma grammaire. Même si ça me prenait beaucoup du temps à m'adapter à ce nouvel environnement, j'ai fini par m'y faire, et ce de mieux en mieux après toutes ces années.

D'abord, j'aimerais remercier ma directrice Dre. Marie-Josée Hébert, qui m'a donné l'opportunité d'étudier dans cet environnement de recherche idéal. De plus, je me considère chanceuse d'avoir obtenu l'approbation du laboratoire juste avant la date d'échéance de ma bourse. En tant que directrice, elle est intelligente, gentille, et toujours énergique. À chaque rencontre académique, elle soulève toujours des points intéressants en plus de m'inspirer de façon continue. Je suis impressionnée qu'elle m'encourage toujours, que le résultat soit positif ou négatif. Elle est toujours prête à m'aider et à m'offrir des suggestions, que ce soit sur mon travail, dans ma vie ou pour mon futur.

Après, je dois remercier Dre. Héloïse Cardinal, ma co-directrice de recherche, une femme si charmante. Plusieurs amis m'ont demandé qui est la femme élégante sur les portes de l'ascenseur au sous-sol. Elle est très gentille et m'a beaucoup appris sur la recherche clinique et les statistiques.

Ensuite, j'aimerai remercier toutes les personnes au labo, particulièrement Dre. Mélanie Dieudé. Elle est toujours là pour nous écouter et nous aider à résoudre nos problèmes, activement et patiemment.

Mentions spéciales aussi à Francis et Julie, pour les suggestions pour mon projet et pour la correction de mon article. À Annie et Stéphanie, merci beaucoup pour répondre patiemment à mes questions au laboratoire. Alexandre, merci beaucoup pour corriger mes devoirs de français

souvent (et aussi mes remerciements). Aussi à Hyunyun, bienvenue dans notre équipe et merci beaucoup pour tes petits cadeaux qui me font penser à la maison. En plus, un grand merci à Dr. Qi, un excellent microchirurgien et professeur. Il ne m'a pas seulement enseigné des techniques de chirurgies, mais aussi la méthode de résolution de problèmes.

Je remercie tous les membres de mon comité d'évaluation de pré-doctorat, Dre. Emmanuelle Brochiero, Dr. Alain Rivard et Dre. Véronique Moulin à l'Université Laval. Ils m'ont aidé à sortir de l'échec à ma première tentative pour assurer mon passage à ma deuxième évaluation. J'exprime ma gratitude à Dre. Natalie Patey, qui m'a guidée dans l'évaluation des pathologies rénales avec son expertise et sa patience.

Enfin, je voudrais remercier spécialement ma famille et mes amis. Merci à mon cher mari de comprendre et supporter tous les choix que j'ai fait, notamment ma décision d'étudier au Canada. Et merci beaucoup pour son amour constant. Merci à mes parents, malgré leur tempérament conservateur, qui ont tout de même respecté ma décision, même s'ils me manquent beaucoup, particulièrement pendant la période de pandémie. Je remercier également tous mes amis avec qui j'ai bien passé un temps agréable; c'est vous qui ne me faites pas sentir comme une étrangère ici.

J'arrive à la fin de mes études doctorales, mais ce sera aussi un début pour ma vie future. Cet épisode d'expériences m'a amené un grand défi, dont le plus grand acquis est de toujours essayer de trouver une façon de surmonter les difficultés. Je crois que je suis devenue une meilleure version de moi-même de jour en jour.

Introduction

Acute kidney injury (AKI) is a clinical event associated with high morbidity and mortality, and AKI can be triggered by various factors. Ischemia-reperfusion (IR) injury is one of the most common inducers of AKI. However, the lack of an effective clinical strategy makes AKI research an urgent need, to cover the clinical manifestations, pathophysiology, and potential therapeutic strategy.

AKI induced by IR is a major clinical challenge in kidney transplantation, and renal dysfunction post-ischemia-reperfusion injury (IRI) is highly associated with long-term renal damage progression and graft survival.

Pathophysiological changes of IRI-induced AKI display a series of complicated alternations. Manifestations in different clinical phases vary within different renal compartments, and various cell death pathways co-exist in the scenario of IRI. Furthermore, renal parenchymal cells can activate multiple cell response pathways according to their microenvironment, cell type, IR severity, and multiple influence factors. This study focuses on the mechanistic exploration of renal pathophysiology post-IRI in both mild and severe AKI forms, focusing predominantly on renal microvascular injury and renal fibrogenesis in the long-term. The perspective of this project is to explore potential renal endothelial injury biomarkers, which could contribute to predicting early-stage renal microvascular injury post-IRI.

1. Acute kidney injury (AKI) induced by ischemia-reperfusion (IR)

1.1 Renal anatomy and renal physiology

The kidney is a vital organ located in the retroperitoneal cavity. It is composed of nephrons, collecting tubes, and vasculature (Kaye and Goldberg 1982). On the cellular level, the kidney includes multiple types of cells performing a series of different physiological functions.

The nephron is the basic functional unit of the kidney. The number of nephrons ranges between 900,000 to 1 million in a healthy kidney, which could range from 20,000 to more than 2.5

million depending on individual status (Bertram, Douglas-Denton et al. 2011). One nephron is composed of one glomerulus and one tubule that receives its filtrate. The glomeruli are responsible for blood filtration, and blood passing through glomerular capillaries is filtered to form primitive urine. The latter then undergoes a series of modifications through secretion and reabsorption in the tubular system. The reabsorbed elements re-enter the circulation system through the peritubular capillaries (PTCs). Urine then enters the collecting duct system, where it continues to be concentrated (Cambar, Dorian et al. 1987, Jamison 1987).

The most important physiological renal functions are filtering and secreting metabolic waste products, mainly nitrogenous metabolites. Blood urea nitrogen and serum creatinine are the most commonly used biochemical markers of renal function evaluation (Basile, Anderson et al. 2012), with circulating levels rising as kidney function declines. In addition, the kidney has endocrine functions. The active form of vitamin D is produced in the proximal tubular epithelial cells (PTECs) by hydroxylation of its hepatic precursor, 25(OH) vitamin D3 to form 1.25(OH)D3. Therefore, the kidneys have an essential role in calcium-phosphate regulation, as 1.25(OH)D3 increases the digestive absorption of calcium and phosphate. As well as vitamin D, erythropoietin is also produced by renal cells in response to hypoxia and stimulates the production of red blood cells. Moreover, renin is secreted in the juxta-glomerular system in response to variations in blood volume, leading to the activation of the renin-angiotensin-aldosterone system, the main effects of which are vasoconstriction and water-sodium retention (Ionescu-Tirgoviste and Bodoia 1969, Erslev 1975, Pedersen, Ghazarian et al. 1976).

The primary renal compartments can be divided into the cortex and the medulla, from the outer layer to the inner layer. Each section, including the cortical section surrounding part of the medulla, is defined as a renal column. Renal tissue can be classified as renal tubular system and microvasculature according to cell type and function. The tubular system is responsible for reabsorption and secretion of urinary components, including the proximal tubule, Henle loop and distal convoluted tubule, which are mainly composed of epithelial cells. The proximal tubule mainly reabsorbs water, sodium, amino acid, and glucose, while the distal tubule adapts the composition of urine to the physiological state (Preuss 1993). The microvasculature is responsible for transporting blood and functions as a barrier between circulation and renal interstitial tissue. The renal vascular tree is composed of multiple types of endothelial cells

(ECs). Among these ECs, the endothelium in PTCs carries reabsorbed materials and participates in surrounding tubular epithelial function (Jourde-Chiche, Fakhouri et al. 2019).

1.2 Clinical features of AKI

AKI is a clinical event associated with an elevated burden of morbidity and mortality (Kanagasundaram 2015) for which there is currently no specific effective preventive or therapeutic strategy.

AKI is defined as a reduction in renal function, characterized by an increase in serum creatinine, an associated glomerular filtration rate (GFR) decline, and a decrease in urine output. In response to the need for standardization of definitions, various criteria have been developed for the diagnosis and severity assessment of AKI: the RIFLE, AKIN, and KDIGO criteria. The KDIGO criteria are the most recent and currently accepted criteria for AKI diagnosis (Rewa and Bagshaw 2014). Among these three definitions, the RIFLE classification was the earliest international criteria system for AKI, introduced in 2004. The AKIN category, which applied to pediatric AKI cases, was presented afterward. Later on, the KDIGO criteria became the most commonly used classification for pediatric cases and chronic kidney disease (CKD) progression (Roy and Devarajan 2019).

Stage	Serum Creatinine	Urine Output
1	1.5–1.9 times baseline	<0.5 mL/kg/h for 6–12 h
	OR	
	≥0.3 mg/dL increase	
2	2.0–2.9 times baseline	<0.5 mL/kg/h for ≥ 12 h
3	3.0 times baseline	<0.3 mL/kg/h for ≥ 24 h
	OR	OR
	Increase in serum creatinine to ≥4.0 mg/dL	Anuria for ≥ 12 h
	OR	
	Initiation of renal replacement therapy	
	OR	
	In patients <18 years. Decrease in eGFR to <35 mL/min/1.73 m^2	

Tableau I. KDIGO-2012 AKI classification and criteria (Acosta-Ochoa, Bustamante-Munguira et al. 2019).

The incidence of AKI has been continuously increasing in recent years. For instance, its incidence in admission patients went from 4.9% to 7.2% in the USA within the past 20 years (Nash, Hafeez et al. 2002). In a previous report, the incidence of AKI could reach 25% and was associated with a 28-90% rate of hospital mortality in the hospitalized population (Uchino, Bellomo et al. 2006). The rise of incidence may be due to an increase in risk factors, such as age, CKD development, existing chronic diseases such as diabetes, increased nephrotoxic medication, cardiac surgery, also increased clinical practice related to renal transplants. A USA report suggested that the incidence of dialysis-requiring AKI in hospitalized patients rose from 222 to 533 per million people from 2000 to 2009 (Hsu, McCulloch et al. 2013). These clinical cohort studies show an increase in renal replacement therapy (RRT) requirements, mainly for post-cardiac surgery and major vascular surgeries. The incidence of AKI in ICU was reported as 2/3 by Hoste's team (Hoste and Kellum 2006). Mortality among AKI patients in the ICU was higher than 50% in a multicentric study (Uchino, Kellum et al. 2005).

There are three major categories of AKI etiology: prerenal, renal, and postrenal.

A decrease in renal blood pressure produces prerenal AKI without renal parenchymal injury. The kidneys receive about 25% of the cardiac output. Hence, reductions in blood volume or pressure can cause a crucial impact on renal dysfunction (Rewa and Bagshaw 2014). AKI could be induced in the context of hypovolaemia/circulatory volume reduction, e.g., vomiting, burn injury, hemorrhage, or hypotension. Additionally, AKI can occur in normal circulatory volume, e.g., sepsis, cardiac failure. Prerenal AKI leads to the activation of compensatory mechanisms such as vasoconstrictive responses and the reabsorption of sodium/chloride ions inducing circulating volume conservation (Lameire, Van Biesen et al. 2005).

Renal AKI could be triggered by injuries directly targeting renal parenchyma. The most common etiologies in this category are IRI and nephrotoxic medications/substances. In pediatric cases, acute glomerulonephritis (GN), nephrotic syndrome, and sepsis are the most common AKI etiologies. Other rare etiologies have been reported, such as purpura, disseminated intravascular coagulation (DIC), systemic lupus erythematosus (SLE), or hemolytic uremic syndrome, which induce coagulation in the microvasculature (Cao, Yi et al. 2013).

Postrenal AKI is caused by any obstruction of urine outflow. Obstruction of the urinary tract is common in aged men with prostatic problems, kidney stones, and abdominal cancer patients (Bhandari, Johnston et al. 1995). Most postrenal causes can be amended by relieving the obstruction, depending on the original disease (Lameire, Van Biesen et al. 2005).

AKI is characterized by a sudden decrease in renal function, with nitrogen waste product accumulation. Symptoms include fatigue, nausea, vomiting, edema, impaired cognition, and reduced urine output. Electrolyte (e.g., hyperkalemia) and acid-base (acidosis) disorders often develop and represent criteria for RRT. Although this may be harder to appreciate from a clinical standpoint, AKI plays a vital role in inflammation regulation and the development of immunosuppression (Dirkes 2016).

Serum creatinine (Scr) and blood urea nitrogen (BUN) (Daniels and Bunchman) are recognized as the most commonly used biochemical markers for evaluating renal function in clinical settings. However, BUN can be influenced by nutritional status, medication utilization, muscle mass, age, and fluid volume, making it a sub-optimal biomarker of renal function. On the other hand, Scr does reflect renal function only if there is a greater than 50% decrease in GFR reduction (Benoit, Ciccia et al. 2020). Therefore, there is an impending need to explore novel sensitive biomarkers predicting early-stage renal dysfunction, even in mild renal damage. Most of the currently investigated biomarkers specifically detect tubular damage in AKI. However, candidate biomarkers predicting renal vascular injury and dysfunction should also be sought since vascular injury is associated with long-term renal impairment.

1.3 Treatment and prognosis

When AKI supervenes, symptomatic and supportive treatments, including RRT, are undertaken to restore renal function when possible. The prognosis is associated with the severity of the underlying conditions leading to AKI and the comorbidity burden (Waikar, Liu et al. 2008). The risk of developing CKD is higher in patients who have survived AKI than those in healthy controls (Ishani, Xue et al. 2009, Lo, Go et al. 2009). In the absence of adequate preventive measures and specific treatments, AKI's prognosis has improved little in recent decades. A better understanding of the pathophysiological mechanisms is necessary to improve clinical outcomes (Alge and Arthur 2015).

For AKI patients in ICU, even a slight elevation of Scr is highly associated with a risk of death. Besides the expected recognized clinical outcomes, AKI could also induce severe problems which extend beyond ICU stays, such as immune disorder, infection, and rapid CKD progression (Singbartl and Kellum 2012). Therefore, management of AKI patients in ICU is crucial for patient survival. As the most common detrimental etiologies of these patients are fluid volume reduction or hypoperfusion and acute tubular necrosis, intravascular fluid evaluation and urinary analysis are considered as a management guide. Fluid volume expansion, vasoconstrictors, diuretics, and renal replacement are also considered as the management strategies (Yunos, Kim et al. 2011, Joannidis, Druml et al. 2017, Mohsenin 2017).

2. Pathophysiology of IRI-induced AKI

Among various etiologies, one of the most common cause of AKI is IRI which can be prompted by various factors including: hypotension, surgeries involving clamping of the renal arteries or supra-renal aorta, vasoconstrictive medications, renal artery thrombosis/embolism, trauma, etc. A certain degree of renal IRI is always present in the context of kidney transplantation, as organ retrieval and storage are associated with a disruption in oxygen and nutrient delivery. In the setting of kidney transplantation, AKI manifests as delayed graft function (DGF), defined as a need for RRT in the first week post-transplant or a slower decline in serum creatinine post-transplant (Yarlagadda, Coca et al. 2009).

Due to the low oxygen supply and renal vascular architecture, the outer medulla is very sensitive to the decrease in oxygen supply associated with renal ischemia (Karlberg, Norlen et al. 1983). Reduction in nutrient and oxygen supply, in turn, damages the tubular epithelial compartment. Also, immune cells are activated and cytokines are released, which further attacks tubular cells. These responses trigger the interruption of glomerular filtration and tubular secretion, as tubular epithelial cells (TECs) are damaged and sloughed in the renal tubules. Meanwhile, tissue repair is activated in the kidney (Duann, Lianos et al. 2016). Mild AKI can recover without functional loss; however, long-term progressive renal damage can develop if repair capacity is insufficient (Weiss, Meersch et al. 2019).

Tissue homeostasis is essential to stabilize vital parameters and perform basic functions in the initiation phase of AKI. Ischemia and reactive oxygen species (ROS) released by reperfusion

lead to acute tissue insults. Following these insults, the body begins to restore a homeostatic state. This process starts with removing damaged cells through interactions between cell death and inflammation responses. More specifically, dying cells release signals that recruit immune cells and trigger pro-inflammatory and anti-inflammatory responses. The pro-inflammatory immune responses amplify tissue damage, creating a feedback loop that brings about the AKI maintenance phase, which can last several days to several months, even once the initial cause has disappeared (Bonventre 2007, Malek and Nematbakhsh 2015). Although the mechanisms and role of tissue insults for each compartment are discussed separately in the following chapters, it should be kept in mind that the pathophysiological process is composed of networked interactions between these compartments.

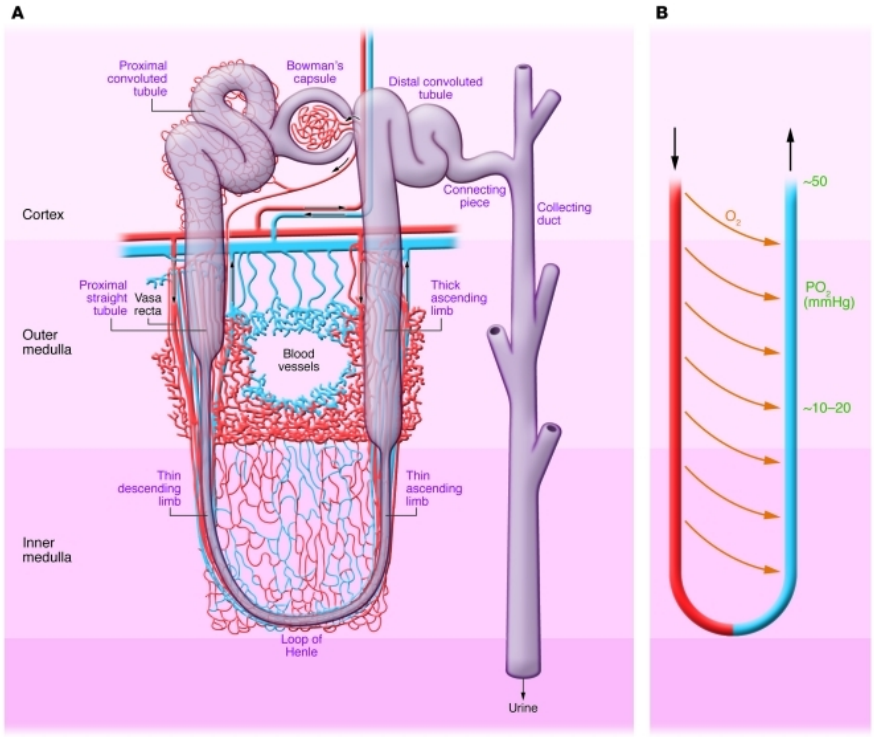

Figure 1. Corticomedullary oxygen gradient and medullary microvascular anatomy (Bonventre and Yang 2011).

2.1 Clinical phases

Clinically, AKI progression can be divided into four phases: initiation phase, extension phase, maintenance phase, and recovery phase (Basile, Anderson et al. 2012).

The initiation phase develops as a quick response to renal blood supply interruption, with rapid reduction in cytoplasmic ATP levels, leading to acute cellular injury. One of the critical targets in the initiation phase is TECs. The ischemic insult causes structural and functional changes in proximal TECs. Although the duration of ischemia is usually short, the dysfunction of TECs and microvascular endothelial cells (ECs) can vary according to the length and severity of ischemia. Both TECs and ECs keep on being injured even after reperfusion. Ischemia induces chemokine and cytokine up-regulation, initiating inflammation activation. Microvascular endothelium and smooth muscle cell damage in the initiation phase contribute to renal microvascular changes post-AKI (Matthys, Patton et al. 1983, Kwon, Phillips et al. 2002).

The extension phase is characterized by secondary hypoxia and the inflammation cascade. These alterations mainly occur at the renal cortico-medullary junction because of its sensitivity to ischemia. During this extension phase, renal microvascular endothelial injury plays a predominant role following the effect of ischemia on the tubular epithelial compartment, and inflammation (Kelly, Baird et al. 2001). After tubular epithelial cell damage, microvascular endothelial cell death, including programmed necrosis and apoptosis, are present at the cortico-medullary junction (CMJ). These are characterized as endothelial integrity disruption and endothelial permeability disorder, followed by microvascular collapse and microvascular rarefaction (Horbelt, Lee et al. 2007). Microvascular structures in the CMJ section are susceptible to ischemic stimuli due to a limited vascular network, which is then incapable of supplying vital oxygen and nutrients to the renal parenchymal tissue. As progressive cell damage at the CMJ is undergoing, a decline in GFR is further observed. In addition, the inflammatory cascade can be accelerated by the continuous release of cytokines and chemokines (Donnahoo, Meng et al. 1999). The inflammatory cascade activation is initiated 2 hours after ischemia and achieves a peak of immune cell infiltration approximately 24 hours later (Willinger, Schramek et al. 1992).

The maintenance phase is characterized by cellular recovery, including cell migration, proliferation, and repair by various cell types. The goal of the maintenance phase is to get back to the initial tubular integrity and function. GFR is usually stable at this point, while its decrease reflects the severity of the primary insult. Proximal tubular epithelial cells and distal convoluted tubular epithelial cells both contribute to tubular repair post-AKI. A fate-mapping tracing study demonstrated that resident TECs are the primary source of tubular repair (Humphreys, Valerius et al. 2008). No conclusive data showed that tubular progenitor cells located outside the nephron mediate epithelial repair; however, the possibility of resident tubular progenitor cell repair remains (Kumar 2018). Immune cells, such as macrophages and dendritic cells (DCs), also present a tissue repair effect beyond their pro-inflammatory role by promoting cytokines production such as IL-22 (Kulkarni, Hartter et al. 2014). In endothelial repair, PTCs connect the efferent arterioles of the cortex and the descending and ascending vasa recta of the CMJ. The endothelial repair post-AKI, including PTCs repair, is not well understood. Renal ECs display a limited regeneration capacity. However, angiogenesis is important for tissue function preservation and favors new capillary production and existing capillary intussusception after an ischemic attack (Tanaka and Nangaku 2013, Schellinger, Cordasic et al. 2017). Nevertheless, it is still unclear if PTCs are compromised in post-injury angiogenesis. Endothelial progenitor cells (EPCs) were shown to support endothelial repair by neovascularization and re-endothelization. Still, these processes have been demonstrated via a paracrine pathway but not by ECs differentiation per se (Hristov, Erl et al. 2003, Asahara and Kawamoto 2004). Myofibroblast differentiation in the renal interstitium is also involved in adaptive and maladaptive repair, contributing to chronic transition by accumulating fibrotic tissue. These alterations, including cell migration and proliferation, gradually lead to improvement in cellular and compartment functions (Basile, Anderson et al. 2012).

In the recovery phase, tubular epithelial cell differentiation, the reestablishment of cellular and tubular structure, and physiological function recover slowly (Nony and Schnellmann 2003). In the microvascular compartment, vascular cell repair is relatively limited, although response mechanisms can be activated (angiogenesis, myofibroblast differentiation, etc.). However, incomplete recovery can lead to chronic renal damage progression by activating profibrotic pathways such as transforming growth factor-β (TGF-β), connective tissue growth factor

(CTGF), Snail pathways, and collagen deposition implicated in AKI-CKD transition (Guzzi, Cirillo et al. 2019).

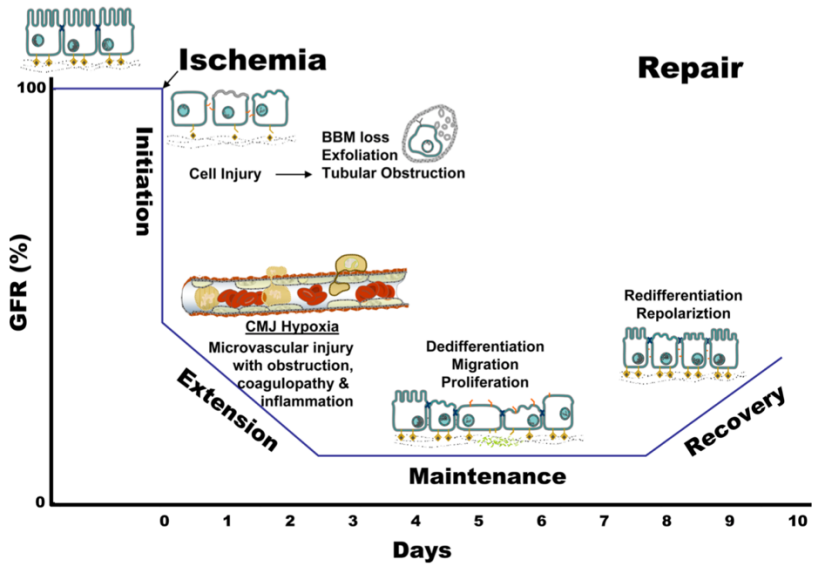

Figure 2. Pathophysiological phases of AKI (Basile, Anderson et al. 2012).

2.2 Cell death

Cell death can be classified into two broad, exclusive categories: non-programmed cell death (NPCD) and programmed cell death (PCD) (Galluzzi, Bravo-San Pedro et al. 2015). NPCD is triggered by severe stimuli, e.g., heat shock, exposure to cytotoxic agents, ischemia in multiple organs (stroke and myocardial infarction), etc. Although it plays an essential role in tissue damage, it is less interesting to investigate because it cannot be inhibited by pharmacological or genetic approaches (Galluzzi, Vitale et al. 2012). PCD is regulated and executed by the cell's molecular machinery. There are several modes of PCD, depending on the different molecular machinery involved. PCD includes apoptosis, necroptosis, pyroptosis, cornification, entosis, mitotic catastrophe, netose, and parthanatos (Linkermann, Chen et al. 2014, Conrad, Angeli et al. 2016).

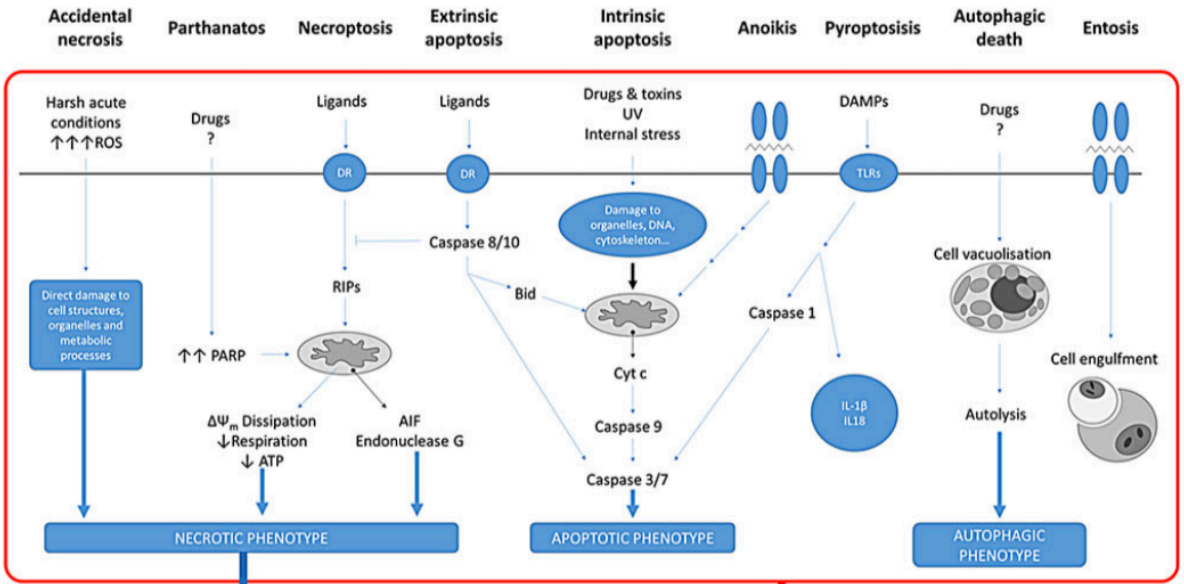

Figure 3. Schematic representation of the main signaling pathways of different cell death modes, and the pathophysiological mechanisms activated by cell death modes in acute kidney injury (Linkermann, Chen et al. 2014).

2.2.1 Apoptosis

Apoptosis (from the ancient Greek term "falling") is a process of programmed cell death that occurs in multicellular organisms (Kerr, Wyllie et al. 1972). Apoptotic morphological changes are characteristic, including budding of the cytoplasmic membrane, chromatin condensation, and DNA fragmentation. The molecular mechanisms of apoptosis are very complex and sophisticated.

2.2.1.1. Morphology of apoptosis

Apoptotic cells present a shrunken cytoskeleton, with laminin and actin cleavage. Cellular nuclear condensation, DNA fragmentation, and membrane blebbing can be found due to chromatin break. Apoptotic cells keep shrinking until they form a package for removal by macrophages, as these phagocytic cells participate in apoptotic cell cleaning (Hassan, Watari et al. 2014). Late stages of apoptosis also feature secretion of apoptotic bodies and smaller exosome-like particles (Dieude, Bell et al. 2015).

2.2.1.2. Markers of apoptosis

Apoptosis occurs in both physiological and pathophysiological circumstances. Markers and regulators of apoptosis are investigated in various scenarios.

Caspase family proteins, such as caspase-3, caspase-6, and caspase-7, are considered as the apoptotic key mediators and executors in multiple studies (Slee, Adrain et al. 2001, Homsi, Janino et al. 2006, Sirois, Raymond et al. 2011, Chen, Engle et al. 2015). Several caspase inhibitors, such as z-DEVD-fmk, Z-VAD-fmk, and their analogs are applied to probe apoptosis induction (Bullok, Maxwell et al. 2007). Besides the caspase family, other regulated proteins are also used for monitoring apoptosis development. Bcl-2 family is a crucial apoptotic regulated protein, which is also associated with the autophagy pathway. Detection of Bcl-2 expression was used to predict anti-tumor response in patients (Ozretic, Alvir et al. 2018). Bcl-2-associated X proteins (BAX)/Bcl-2 antagonist counterparts (BAK) function as pro-apoptosis proteins in mitochondria and are used to monitor the intrinsic apoptotic pathway (Jezek, Chang et al. 2019).

Anionic phospholipid phosphatidylserine (PS) is turned to the cellular surface following caspase-3 activation during apoptosis, an almost universal phenomenon. Annexin V is used as the most common imaging probe to detect exposed PS. However, limitations of using Annexin V as a biomarker of apoptosis also exist. For instance, difficulty in distinguishing necrosis and the imperfect pharmacokinetics of Annexin V protein are the two significant disadvantages (Niu and Chen 2010). PS is also exposed on the surface of the cell membrane in the development of necrosis secondary to apoptosis due to plasma membrane disruption, preventing Annexin V staining from distinguishing apoptosis and necrosis (Niu and Chen 2010). Another disadvantage of Annexin is the imperfect pharmacokinetics of radiolabelling, with a high background in the abdominal area. Also, the binding of Annexin V with PE is a $Ca2^{+}$-dependant mode. Therefore, some novel imaging markers begin to attract the interest of investigators. For example, positively charged bis (zin-dipicolulamine) (Zn-DPA) is a synthetic protein targeting PS, which is translocated to the outer membrane leaflet during apoptosis. Zn-PDA binds to exposed PS on the cell surfaces. This synthetic marker mimics the function of Annexin V, labeling apoptotic cells by binding PS in a murine model (Kwong, Hoang et al. 2014). The C2A domain of synaptotagmin I also binds to PS in a calcium-dependent way (Wang, Fang et al. 2008),

detecting PS on the cellular surface and detecting collapsed mitochondrial membrane potential. In addition, 18F-fluorobenzyl triphenylphosphonium, a PET agent, was reported as a novel marker of apoptosis. This new apoptotic marker was found to detect apoptosis by tracing mitochondrial membrane collapse in H345 cells (Madar, Ravert et al. 2007). Hence, a variety of novel biomarkers for apoptosis are currently being studied.

2.2.1.3 Molecular regulation

(1) Initiation of apoptosis

Many stimuli can trigger apoptosis. Two classical apoptosis pathways depend on the initiating signals: the extrinsic pathway and the intrinsic pathway (Gastman 2001).

In the intrinsic pathway, apoptosis is triggered by intracellular stress, for example, DNA damage, oxygenated free radicals, or cytosolic calcium overload. These signals lead to the permeabilization of the mitochondrial outer membrane (MOMP), which is crucial to the initiation of intrinsic pathway apoptosis. The MOMP is controlled by the Bcl-2 family, which comprises several proteins that share the domain of Bcl-2 homology. The Bcl-2 family can be divided into three subgroups: functionally and structurally distinct proteins composed only of BH-3 domains (BCL-2 homology 3), anti-apoptotic guard proteins, and pro-apoptotic effector proteins. Stimulated by intracellular stress, proteins composed only of BH-3 domains (e.g., PUMA, NOXA) are activated. This activation inhibits anti-apoptotic guardian proteins (Bcl-2), resulting in the oligomerization of BAX and BAK. The mitochondrial transmembrane potential is then deregulated, and mediators usually hidden in the mitochondria's intermembrane space are released in the cytosol (Hassan, Watari et al. 2014, Galluzzi, Bravo-San Pedro et al. 2015).

The released mediators are divided into two groups according to their effect on cysteine-aspartic-proteases (caspases) (MacPherson, Mills et al. 2019). The first group includes cytochrome c, Smac/DIABLO, and the serine protease HtrA2/Omi. They result in the activation of the caspase cascade for the execution of apoptosis. For example, the release of cytochrome c leads to the assembly of the apoptosome, which is composed of cytochrome c, apoptotic protease activating factor-1 (Apaf-1), and deoxyadenosine triphosphate (dATP), an activator complex for caspase-9. The activated caspase-9 will then direct the cell towards the execution of apoptosis by cleaving and activating effector caspases. The second group includes the apoptosis-

inducing factor (Annaldas, Saifi et al. 2019) and endonuclease G, which can move in the nucleus and cause DNA fragmentation in a caspase-independent way (Bonora, Wieckowski et al. 2015).

In the extrinsic pathway, apoptosis is initiated by the interaction between death receptors and their ligands. Different death receptors and ligands have been identified, including tumor necrosis factor-α (TNF-α)/TNF-Receptor 1, Fatty acid synthetase (Fas), Ligand/Fas-Receptor, Apo3L/death receptor (DR) 3, Apo2L/DR4, and Apo2L/DR5. To illustrate their roles, we will use the Fas signaling pathway example, which is one of the most understood. Following activation of Fas and FasL, the death domain associates with Fas-associated protein with death domain (FADD) and procaspase-8. The FLICE-like inhibitory protein (FLIPs) is an enzymatically inactive counterpart. Its presence in high titer can inhibit apoptosis. The formation of the above-mentioned complex leads to the auto-catalytic activation of procaspase-8, which blocks the inhibitory role of FLIPs, then activates effector caspases (Zhang, Hartig et al. 2005, Hassan, Watari et al. 2014).

There are "cross-talk" mechanisms between the extrinsic and intrinsic pathways of apoptosis. Bid is a member of the Bcl-2 family. After its cleavage by activated caspase-8, truncated Bid (tBid), Bid's C-terminal fragment, is released into the cytosol. The combination of tBid with the mitochondrial outer membrane facilitates the recruitment of BAX, which then activates apoptosis by the intrinsic route (Wang and Tjandra 2013).

(2) Execution of apoptosis

Caspases are a family of cysteine-aspartic proteases that play a crucial role in programmed cell death and inflammation. They are produced in the form of pro-caspases, which are inactive monomers. These monomers are composed of an N-terminal pro-domain, which contains an aspartate site for (auto) proteolysis, a small subunit, and a large subunit. The length of the N-terminal pro-domains varies depending on the function of the caspase. The effector caspases (caspase-3, -6, -7) have short pro-domains, while the inflammatory initiation (caspase-1, -4, -5) and initiating (caspase-8, -9, -10) caspases have long pro-domains, which contain a caspase recruitment domain (CARD) or an effector of death domain (Cavaille-Coll, Bala et al. 2013). Activation of caspases requires dimerization and often cleavage. Recruited by CARD or death

effector domain, different adapter proteins can facilitate the dimerization and activation of caspases (Gastman 2001, Slee, Adrain et al. 2001).

Caspase-3 is the most critical effector caspase. Activation of caspase-3 results in the cleavage of various substrates, including proteins linked to actin microfilaments, the caspase-activated DNase inhibitor (CADI), etc. Cleavage of these substrates ultimately results in budding of the cytoplasmic membrane, chromatin condensation, and DNA fragmentation in apoptotic cells (Slee, Adrain et al. 2001, Hassan, Watari et al. 2014).

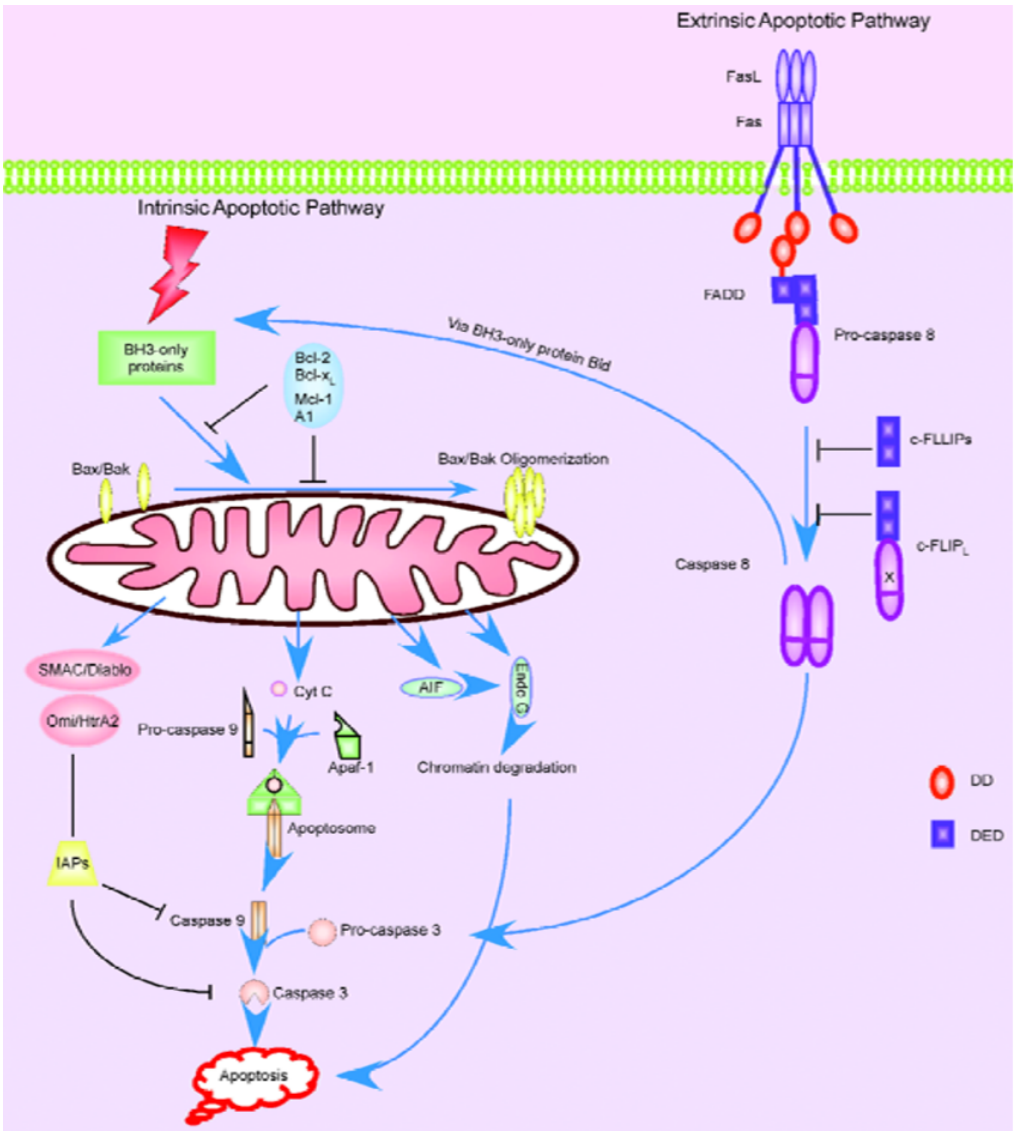

Figure 4. Apoptotic pathway (Zhang, Hartig et al. 2005).

2.2.1.4 Apoptosis in AKI

Although tubular necrosis has long been recognized as a classic pathophysiological finding in AKI, the extent of tubular cell necrosis observed on the kidney biopsy of patients with AKI is not associated with subsequent estimated glomerular filtration rate (Waikar and McMahon 2018). The degree of tubular necrosis demonstrates no significant association with long-term renal dysfunction. The poor correlation with renal function suggested alternative cell death possibilities, including apoptosis and autophagic cell death.

In the microenvironment of AKI induced by ischemia, hypovolemia, hypotension, and renal transplantation, apoptosis displays an important role. Both intrinsic and extrinsic pathways can be initiated, especially in the tubular epithelial compartment. Proximal tubular epithelial cells are sensitive to ischemic insult, undergoing multiple pathophysiological changes, involving cell detachment from the basement membrane, cell death, cell dysfunction, responding to the lack of blood supply, and reperfusion injury.

Many investigations proved that apoptosis contributes to ischemia-induced renal injury, with apoptosis detection by various approaches, including Hoechst staining, caspase-3 activity, apoptosis-inducing factor (Annaldas, Saifi et al.) or cytochrome C release, TUNEL, etc. (Bonegio and Lieberthal 2002, Saikumar and Venkatachalam 2003).

2.2.2 Necroptosis

Necrosis is a form of cell death by autolysis. Previously, it was considered an "accidental" and unscheduled cell death. The discovery of chemical inhibitors of necrosis and genetic evidence that the existence of programmed necrosis or necroptosis, has challenged this dogma (Conrad, Angeli et al. 2016).

2.2.2.1 Morphology of necroptosis

Necrosis is characterized by the breakdown of plasma membrane structure, accompanied by the release of intercellular components. Cellular immunogenic proteins and organelles can be released from the cytoplasm, such as interleukin-1 (IL-1), IL-33, high mobility group box-1(HMGB1), and RNA, initiating immune cascade (Linkermann, Hackl et al. 2013). Research work demonstrated that programmed necrosis also develops in AKI cases, which was previously

mistakenly recognized as non-programmed necrosis, partly attributed to similar morphological findings with non-programmed necrosis. Since programmed necrosis has been attracting the attention of investigators in recent years, more and more investigations focusing on it were reported in multiple scenarios. One of the most investigated types of programmed necrosis is necroptosis.

2.2.2.2. Markers of necroptosis

Necroptosis is programmed necrosis induced by the TNF family, mediated by RIKP family proteins. Receptor-interacting kinase 1 (RIPK1) is recruited in the cytoplasm and activated, it then binds to RIPK3 and phosphorylates it. Once activated, RIPK3 phosphorylates mixed lineage kinase domain-like protein (MLKL) to form a complex, triggering cells to undergo necroptosis (Zhao, Jitkaew et al. 2012). Therefore, RIPK3 and MLKL are largely used as markers of necroptosis.

2.2.2.3 Molecular regulation

Necroptosis is characterized by the activation of the **RIPK1-RIPK3-MLKL axis**. The RIPK1 pathway is the most elucidated, thanks to the availability of different inhibitors targeting these key molecules. Necrostatin-1, an allosteric inhibitor of RIPK1, was the first inhibitor of necroptosis to be discovered (Teng, Degterev et al. 2005, Linkermann, Hackl et al. 2013, Linkermann, Chen et al. 2014).

Most of the stimuli involved in initiating the RIPK1 pathway are not unique to necroptosis, as they can also cause activation of apoptosis. As mentioned above, **following TNF-receptor (TNFR) activation, the formation of complex II could direct the cell to apoptosis. In cases where caspase-8 is inhibited, or RIPK3 is overexpressed, the necrosome is formed by the aggregation of RIPK1 and RIPK3 and then activates the MLKL by phosphorylation, which directs the cell to necroptosis** (Galluzzi, Pietrocola et al. 2014, Linkermann, Chen et al. 2014, Vanden Berghe, Linkermann et al. 2014). Besides the RIPK1-RIPK3-MLKL pathway, the MPT pathway is recognized as another signal pathway of necroptosis. The MPT pathway shares the same initiation stages as intrinsic apoptosis. It is known that the mitochondrial permeability transition (MPT) pathway is regulated by cyclophilin D (CypD). Still, the

mechanism of regulation of CypD on MPT has not yet been well described (Galluzzi, Kepp et al. 2014).

2.2.3 Other forms of regulated cell deaths

Some other regulated cell death pathways have been reported, and some of those have also been observed in the context of AKI.

2.2.3.1 Pyroptosis

Pyroptosis is a pro-inflammatory PCD characterized by the activation of caspase-1. In response to stimuli, the NOD-like receptors (NLRs) or the cytosolic DNA sensor absent in melanoma 2 (AIM2) recruit the speck proteins associated with apoptosis containing a CARD, forming the inflammasome, which is a supramolecular complex. The inflammasome induces the activation of caspase-1 by dimerization and auto-proteolysis. Activated caspase-1 cleaves pro-IL-1β and pro-IL-18, resulting in the maturation and secretion of IL-1β and IL-18 (Tonnus and Linkermann 2019) (Aachoui, Sagulenko et al. 2013). It should be noted that activated caspase-1 can induce apoptosis by activating caspase-7 (Seo, Choi et al. 2019).

2.2.3.2 Ferroptosis

Another form of regulated necrosis, ferroptosis, was identified by Stockwell's team (Yagoda, von Rechenberg et al. 2007), induced by a compound (erastin) in RAS-transformed cancer cells.

Ferroptosis is a necrotic, iron-dependent pathway where glutathione metabolism is involved. A plasma membrane exchanger was found to fuel cells with cysteine, initiating glutathione synthesis for ROS clearing action by glutathione peroxidase 4(GPX4) (Yang, SriRamaratnam et al. 2014), which is an enzyme necessary for removing H_2O_2 to prevent lysosomal membrane permeabilization. In the condition of cellular stimuli, a decrease of GPX4 activity induces an increasing level of H_2O_2, further leading to lipid peroxidation following necrotic cell death.

The intervention of ferrostatin-1, a small molecule inhibiting ferroptosis, effectively prevents necrotic cell death in renal tubular cell lines treated by iron and hydroxyquinoline, the stabilizer of H_2O_2 (Skouta, Dixon et al. 2014).

2.2.3.3 Programmed necrosis regulated by MPT

The mitochondrion is a crucial cellular organelle for energy fueling and is also a research target for the cell death mechanism (Tait and Green 2010). Mitochondrial outer membrane MOMP is considered a critical point during apoptosis, and mitochondria can also trigger necrosis in the form of MPT (Kim, He et al. 2003). CypD, a matrix protein, mediates the opening of the MPT pore (MPTP). However, the mechanism of regulation of MPTP by CypD still needs to be described. P53 was reported to be involved in this process, but its precise role is still unclear (Karch and Molkentin 2012).

2.2.4 Autophagy

Autophagy was first discovered by De Duve in 1983 (de Duve 1983) and is generally considered a pro-survival response to stress, in both physiological and pathological conditions. In physiological conditions, autophagy activation was described in contexts of starvation, growth factor depletion, hypoxia, etc. In pathological cases, it is commonly recognized that autophagy activation is abnormal in aging, cancer, neurodegenerative diseases, liver disease, muscle disease, infection, and cardiovascular disorders (Levine and Kroemer 2008, Kroemer 2015, Klionsky, Abdelmohsen et al. 2016, Moulis and Vindis 2017, Kardideh, Samimi et al. 2019). It is characterized by a degradation process triggered by the deprivation of nutrients and growth factors. The process of autophagy includes initiation, elongation, and fusion with the lysosome.

There are at least three forms of autophagy: microautophagy, chaperone-mediated autophagy, and macroautophagy. Most studies focus on macroautophagy, which is characterized by the transport of cytoplasmic material in double-membrane vesicles (autophagosomes), which associate with lysosomes for the degradation and recycling of their content. There are three critical enzymes in the initiation of macroautophagy: phosphoinositide 3-kinase (PI3KC1), protein kinase B (PKB), and the target of rapamycin in mammals (mTOR). Also, autophagy-related proteins (Atgs) are the leading players in the execution of autophagy. In the physiological context, growth factors transmit proliferation signals through their membrane receptors, which will activate the PI3KC1-PKB-mTOR chain. Once mTOR is activated, it inhibits Unc-51-like kinases (ULK1/2) by phosphorylation. In the context of growth factor deprivation, inactivation of mTOR results in the release of ULK1/2, leading to the formation of phagophores by activating

Beclin1 and PI3KC3. The Atg12-Atg5-Atg16 complex is recruited for phagophore elongation. The light chain 3 of protein Ia/Ib is associated with microtubules-associated protein 1A/1B light chain 3 (LC3), which is lipidized on the autophagosome membrane, converting to LC3-II. This lipidation form of LC3 (LC3-II) contributes to the autophagosome's closure, and the augmented portion of LC3II indicates dynamic autophagosomal formation and enhanced autophagic flux. The Atg7/8 are required for the recruitment of Atg5 and LC3. The last step of autophagy is the fusion of the autophagosome with the lysosome, leading to the degradation of its internal content by lysosomal enzymes. mTORs could also be directly inactivated by the lack of nutrients, triggering the downstream process (Kroemer 2015, Klionsky, Abdelmohsen et al. 2016).

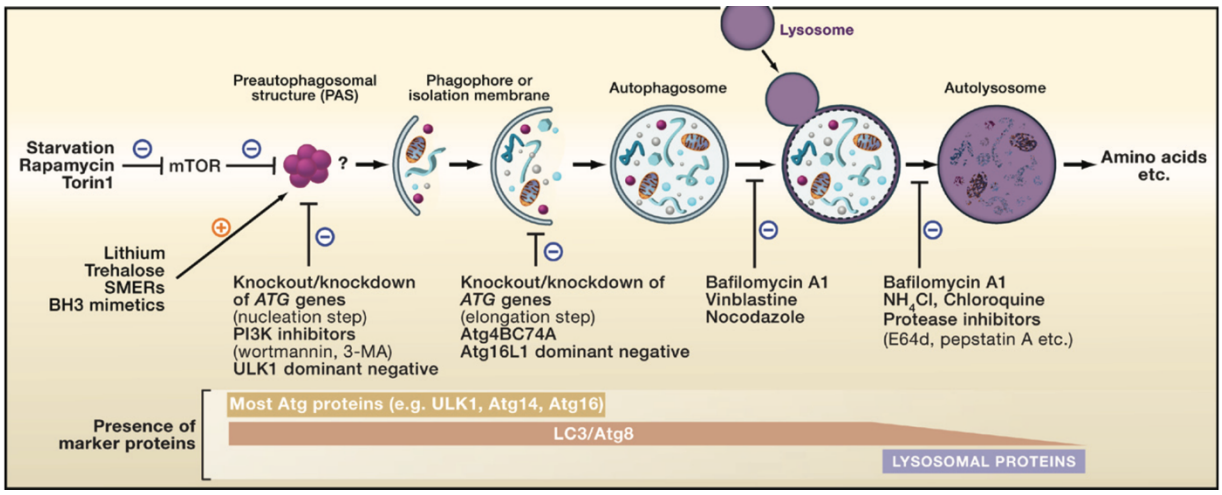

Figure 5. Process of macroautophagy (Mizushima, Yoshimori et al. 2010)

2.2.4.1 Morphology of autophagy

Due to the complexity of detecting the autophagy flux, the traditional electron microscopy method is still the gold standard for visualizing autophagy. Mammalian autophagy was first reported in the 1950s. As characterized by its ultrastructural morphology, the autophagosome is described as a double-membrane structure containing cytoplasmic material such as mitochondrial and endoplasmic reticulum (ER) fragments (van der Vaart, Mari et al. 2008). The autophagosome is usually an easily identified specific structure of autophagy. Another unique characteristic is the formation of autophagolysosome by fusing autophagosome and lysosome.

Autophagolysosome's size differs due to the amount of internal undigested cytoplasmic contents (Mizushima, Yoshimori et al. 2010).

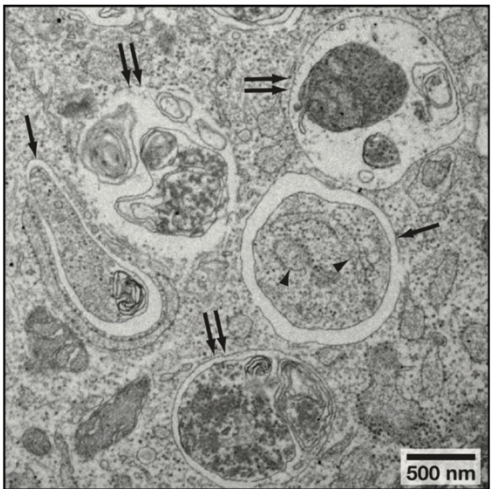

Figure 6. Autophagosome and Autolysosome Morphology (Mizushima, Yoshimori et al. 2010).

2.2.4.2 Markers in autophagic flux monitoring

Various autophagy-related molecules and proteins have been proposed as monitoring markers. Autophagy includes multiple steps and is a dynamic process with autophagosome formation and autophagolysosome degradation peaking at different time points. For setting up an optimal monitoring procedure, both dynamic changes of autophagosome and autophagolysosome should be considered. No marker is sufficient to monitor autophagic flux because of the complicated involvement of a series of regulators. However, here are a few candidates that have recently been studied.

Atg8/LC3: In recent investigations, Atg8/LC3 is the most used autophagy detecting marker since it is essential for autophagosome formation. However, another LC3 isoform, mammalian Atg-8 like protein (GABARAPs), should be considered as well. Because monitoring the full dynamic range of autophagy is complex, multiple markers should be used to monitor different phases of autophagy (Klionsky, Abdelmohsen et al. 2016).

Atg 9: Atg family proteins are closely associated with eukaryote autophagy flux, but only Atg9 is the integral membrane protein involved in autophagosome formation. Atg9 could be partially visualized by colocalizing with green fluorescence protein (GFP) because it binds with LC3 puncta (Young, Chan et al. 2006). Atg9 in yeast can move between the phagophore assembly site (PAS) and cytoplasm, functioning as the precursor of the phagophore (Mari, Griffith et al. 2010).

Atg5: Atg5/Atg12/Atg16 complex is an indispensable contributor to phagophore elongation during the autophagic flux, and can also be applied as a marker for visualizing autophagy. These three Atg proteins can be observed by fluorescence technique in the cytoplasm. (Mizushima, Kuma et al. 2003). In physiological conditions, Atg5, Atg12, and Atg16 are diffusely located in the cytoplasm, but in stress-induced autophagy, such as starvation or ischemia, apparently an increased number of cells with a punctate form of Atg5, Atg12, Atg16 can be observed. Additionally, upstream blocking of autophagosome forming leads to this Atg puncta decrease, while downstream inhibition of autophagosome elongation results in Atg 5, Atg 12, Atg 16 puncta accumulation due to insufficient use (Atala 2012).

BECN1: BECN1 and PIL3C3/VSP34 are essential participants in autophagy activation and initiation. Multiple researchers have used them to observe the autophagic flux (Cao and Klionsky 2007, Yang and Klionsky 2010). BECN1 can be downregulated by anti-apoptosis-associated protein BCL2 binding. In this case, autophagy is activated by BECN1, which is cleaved from BCL2, through phosphorylating BECN1 by BH3 protein (a pro-apoptosis protein). The association between BECN1 and BCL2 is complicated. BECN1-independent pathways trigger some types of cellular autophagy, but BECN1 cleaved by the caspase family could not induce autophagy in some cell types (Kang, Zeh et al. 2011), indicating the complexity of apoptosis and autophagy switch.

2.2.4.3 Autophagy-regulating molecules

Autophagy is a complicated process that multiple molecules can regulate. Two categories of molecules can target autophagy: autophagic inhibitors and autophagic inducers. Pharmacological blocking agents inhibit autophagic flux by targeting different steps.

(1) Autophagy inhibitors

Bafilomycin A1, chloroquine, and ammonium chloride inhibit the fusion of the autophagosome with lysosomes by increasing intracellular pH (Klionsky, Elazar et al. 2008). Bafilomycin A1 is an inhibitor of Na^+/H^+-ATPase, interrupting the proton gradient (Yoshimori, Yamamoto et al. 1991). Bafilomycin A1 is a useful tool for *in vitro* research but rarely applied in *in vivo* experiments because of the high cost and inadequacy of long-term study (Iwai-Kanai, Yuan et al. 2008).

Chloroquine is the commonly used medication in animal models for blocking autophagic flux. Chloroquine is an anti-inflammatory medication used in the treatment of malaria and inflammatory diseases for decades. It is widely accepted as a potential intervention in the autophagy process because of its low price and biological safety *in vivo* (Gurney, Huang et al. 2015).

Colchicine and vinblastine also inhibit the autophagosome-lysosome fusion step by depolymerizing microtubules. Leupeptin, E64d, and pepstatin A are blockers that inhibit lysosome hydrolases and proteases (Klionsky, Abdelmohsen et al. 2016).

However, these drugs mentioned above are not specific for regulating autophagy flux. Most of them have multiple effects on cells, such as inflammatory regulation and cell proliferation. This limitation makes the understanding of autophagy in certain conditions complicated. Theoretically, combined with the transgenic method when possible is a better option for autophagy research. Autophagy (Atg) protein depletion functions as a more specific tool for autophagy regulation, but Atg proteins also present different autophagy-independent impacts, e.g., endocytosis, cell death mediation, immunity (Kroemer and Levine 2008). Therefore, targeting multiple Atg genes working at different phases of autophagy is recommended, which truly represents the case of autophagy inhibition (Iwai-Kanai, Yuan et al. 2008, Mizushima, Yoshimori et al. 2010, Moulis and Vindis 2017).

Drugs	Comments	Administration	Doses	Limitations/ Advantages
Leupeptin	Cystein, serine, threonine proteases inhibitor	Intraperitoneally	9–40 mg/kg	Most commonly used in vivo
E64d	Cystein proteases inhibitor	Orally (food)		Preferentially used in vitro
Pepstatin A	Aspartyl proteases inhibitor	Intraperitoneally	20 mg/kg	
	Lysosomal protein degradation blockage			Should or can be used in combination
Bafilomycin A1	Na+/H+-ATPase inhibitor	Intraperitoneally	0.1–1mg/kg	Costly and unsuitable in vivo
Chloroquine	Lysosomotropic compounds	Intraperitoneally	10–100 mg/kg	Quite inexpensive and suitable in vivo, most commonly used
Ammonium chloride (NH4Cl)		Orally (drinking water)		Less frequent
	Autophagosome-lysosome fusion blockage			
Colchicine	Microtubules depolymerizing agents	Intraperitoneally	0.4–2 mg/kg	Lack of specificity, clastogenic effects
Vinblastine				
	Autophagosome-lysosome fusion blockage			

Tableau II. Pharmacological inhibitors of autophagy (Moulis and Vindis 2017).

(2) Autophagy inducers

Several current approaches to induce autophagy such as caloric restriction and exercise can improve health, and some nutrient factors like caffeine and vitamin D can also induce autophagy. Some agents and medications presenting an induction of autophagy have been considered as a clinical strategy for treatment of cancers, neurodegenerative disorders, diabetic nephropathy, etc. (Sarkar 2013, Lonskaya, Hebron et al. 2014).

One of the most common approaches to autophagy induction is activating nutrient signaling pathways. The common downstream target is the mechanistic target of Rapamycin (mTOR), which is suppressive of autophagy in physiological conditions. In environmental stress, mTOR could be inhibited by activating its inhibitors, such as Rapamycin, then initiating autophagy pathway. However, Rapamycin has various functions, including immunosuppression, inhibiting cellular proliferation, activating autophagy (Li, Kim et al. 2014). Rapamycin down-regulates cell proliferation by inhibiting the mTOR signal. As Rapamycin possesses multiple action

mechanisms, it is not a perfect autophagic inducer as it is not explicitly directed at autophagy and can affect various responses and cellular metabolism.

In addition, resveratrol and spermidine are also being used as autophagy inducers *in vivo*. Resveratrol has been demonstrated to regulate cardioprotection associated with wine intake and functions as an autophagy inducer. Its role as an autophagy inducer is controlled by an NAD^+-dependent deacetylase sirtuin1 (SIRT1) activation (Morselli, Maiuri et al. 2010). Also, resveratrol has been observed as having an anti-cancer effect in various *in vitro* models by inhibiting mTOR 1 complex activity (Tian, Song et al. 2019). However, the mechanism by which resveratrol induces autophagy is not yet completely understood in certain cancer scenarios, which still needs further illustration in the future.

Spermidine could reduce aged oxidative injury by autophagy activation. Recent data show that spermidine is associated with cardioprotection in old mice by upregulating autophagy and mitophagy in cardiocytes (Eisenberg, Abdellatif et al. 2016).

The lack of specific autophagy inducers makes the evaluation of autophagy intervention challenging. Potential pharmaceutical autophagy inducers present multiple functions beyond autophagic induction. Specific strategies cover tissue-specific gene therapy or drug-like peptides. For gene therapy, Atg7 or beclin1 displayed a protective effect in neurodegenerative disorders, diabetes, and cystic fibrosis (Levine, Packer et al. 2015). Another possible option is to increase autophagy substrate and upregulate lysosome activity (Randow and Youle 2014). Still, a novel approach is needed to verify compound which better clear autophagy substrates.

2.2.4.4 Autophagy in AKI

AKI involves various insults, such as ischemia and nutrient and oxygen deprivation, triggering autophagy activation. Generally, autophagy functions as a protective cell survival pathway by degrading damaged organelles and cytoplasmic constituents (Mizushima and Komatsu 2011). Therefore, enhancement of autophagy has been proposed as a potential therapeutic strategy for rescuing AKI.

Autophagy has been demonstrated *in vivo* and *in vitro* in IRI models (Chien, Shyue et al. 2007, Liu, Feng et al. 2012). Multiple investigations have reported on the effect of autophagy post-IRI. The protective effect of autophagy post-IRI was found in conditional renal proximal tubular

Atg5 or Atg7 knock-out (KO) mice (Jiang, Liu et al. 2010, Kimura, Takabatake et al. 2011). Mice deficient in Atg5 in proximal and distal tubules exposed to IRI displayed greater tubular injury and renal failure compared to WT animals. In comparison, the absence of Atg5 in distal tubules was not associated with greater AKI severity after IRI (Chien, Shyue et al. 2007, Liu, Feng et al. 2012).

Compared with the large body of literature on autophagy in renal tubular epithelial cells (Tian, Wang et al. 2020) (Kaushal and Shah 2016), autophagy research on the endothelial compartment is scarce. The contribution of endothelial autophagy in AKI is poorly understood, and the impact of endothelial autophagy on microvascular dysfunction is unknown. Several reports recently demonstrated that induction of autophagy in endothelial cells in the context of AKI might regulate renal fibrosis post-IRI (Patschan, Schwarze et al. 2016). Nevertheless, the importance of endothelial autophagy on molecular mechanisms of AKI and on AKI to CKD transition has not been clarified. Also, current methods of activating autophagy by pharmacological inducers have multiple limitations, as these inducers could also impact some cellular biological metabolism. Therefore, the potential beneficial effects of inducing endothelial autophagy in AKI need to be studied in greater detail.

2.2.5 Cell death pathways of importance in the present project

Based on the above-mentioned cell death pathways discovered in AKI, we could conclude that cell death crosstalk post-AKI is a complex process, depending on injury severity, cell type, regulation of specific mediators, and molecular switch among different cell response pathways. However, tubular epithelial apoptosis and programmed necrosis have been highlighted in both patient samples and animal models (Havasi and Borkan 2011). Therefore, my project aims to observe these two programmed cell death pathways within the tubular epithelial and endothelial microvascular compartments.

Although TECs injury was regarded as an essential feature of AKI in the past, renal microvascular injury is attracting more attention due to the link with long-term renal dysfunction. The molecular pathways mediating injury to microvascular ECs during AKI progression remains unclear. Reports from several teams described the upregulation of caspase-3, a key mediator of caspase-dependent apoptosis, in renal TECs and ECs in the short-term of AKI

induced by IRI. Caspase-3 silencing by small interfering RNAs (siRNA) was shown in both attenuation and aggravation of renal dysfunction (Yang, Hosgood et al. 2011, Yang, Zhao et al. 2014, Nydam, Plenter et al. 2018). Investigation of the endothelial cell response is another focus in our study.

2.3 Tubular injury

IRI-induced AKI is a complex pathophysiological process, with injuries affecting multiple renal compartments 1) tubular injury, 2) microvascular injury, 3) glomerular injury, 4) interstitial inflammation. We will describe tissue injury beginning with tubular injury.

2.3.1 Pathophysiological manifestations of tubular injury

The two main functions of the renal tubules are absorption and secretion. In AKI induced by IRI, the most vulnerable cells are the epithelial cells of the proximal tubules and the ascending branches of Henle's loop (Sharfuddin and Molitoris 2011, Zuk and Bonventre 2016) due to the high metabolic rate for performing active transport, and also due to a limited capacity for anaerobic metabolism. Therefore, the alteration of these tubules is considered a critical pathological characteristic (Bohle, Grund et al. 1977). The pathological manifestations vary according to the severity and evolution of AKI, including loss of brush border, tubular dilation, the formation of cylinders, tubular necrosis, and denudation of the basement membrane (Huen, Huynh et al. 2015).

Programmed cell death pathways have been shown to play an essential role in tubular damage. Several apoptotic and necroptotic regulators are overexpressed in the context of AKI, including p53, caspase-3, and RIPK3 (Bonegio and Lieberthal 2002, Linkermann, Hackl et al. 2013, Pavlosky, Lau et al. 2014, Chen, Fang et al. 2018). Multiple examples showed that inhibition of PCD (apoptosis and necroptosis) could reduce the severity of AKI in the context of IRI. For instance, the genetic deletion of TNF-α or TNFR2, which are involved in the induction of apoptosis and necroptosis, reduced AKI severity induced by cisplatin (Ramesh and Reeves 2004). Conditional suppression of BAX in PTECs, an essential regulator in the intrinsic apoptosis pathway and the MPT-mediated necroptosis pathway, improved renal dysfunction caused by IRI (Wei, Dong et al. 2013). There is growing evidence suggesting a predominant

role of necroptosis in tubular damage. Inhibition of the RIPK1-RIPK3 pathway, either by using necrostatin, an inhibitor of RIPK1 or in mice genetically deficient of RIPK3, reduced renal tubular lesions and early renal dysfunction in AKI models (Linkermann, Hackl et al. 2013, Chen, Fang et al. 2018). In a murine IRI model followed by kidney transplantation, RIPK3 KO kidney allografts showed improved renal function and prolonged survival after transplantation. In contrast, genetic inhibition of caspase-8 by small hairpin RNA (shRNA) showed worsening of necroptosis and renal dysfunction (Lau, Wang et al. 2013).

Autophagy also plays a vital role in tubular damage induced by IRI; Atg 5-deficient mice demonstrate an increase in apoptosis in tubular cells and aggravated renal dysfunction, indicating a protective effect of autophagy in tubular injury caused by IRI (Kimura, Takabatake et al. 2011, Liu, Feng et al. 2012, Yoshii, Kuma et al. 2017).

Besides autophagy inhibitors, the impact of other pharmacological agents targeting PCD was reported in animal AKI models. Pan-caspase inhibitor Z-VAD-fmk was used in cold conservation in a murine renal transplant model. It decreased serum creatinine levels and reduced tubular apoptosis (Nydam, Plenter et al. 2018). In a porcine kidney transplant model, caspase-3 siRNA attenuated IR-induced renal damage and apoptosis (Yang, Hosgood et al. 2011). Intravenous administration of I5NP, a selectively trophic synthetic p53 siRNA selectively trophic in the tubular compartment, was proven to prevent serum creatinine elevation of IRI in a rat model (Powell, Tsapepas et al. 2013).

2.3.2 Biomarkers of tubular injury

Injured PTECs release various molecules into the tubular lumen. Multiple biomarkers of tubular injury have been reported, including lipocalin associated with neutrophils and gelatinase (NGAL), kidney injury molecule-1 (KIM-1), tissue inhibitor of metalloproteinases-2 (TIMP-2), insulin-like growth factor-binding protein 7(IGFBP7), Cystatin C, IL-18, high mobility group box 1(HMGB1) (Waikar, Liu et al. 2008, Rabadi, Ghaly et al. 2012, Meersch, Schmidt et al. 2014, Obermuller, Geiger et al. 2014, Tian, Zhang et al. 2015, Schaub and Parikh 2016, Guan, Chen et al. 2017, Luthra and Tyagi 2019, Zhang, Dong et al. 2019).

The NGAL protein belongs to the lipocalin family and is primarily expressed in tubular epithelial cells. Investigations have reported that NGAL is secreted after renal ischemic insult

or nephrotoxin. At the earliest, serum NGAL can be measured two hours after injury and it reaches a peak at around six hours, and this peak is maintained for several days and then gradually decreases. The promising predictive effect of NGAL in AKI and CKD, as well as in other clinical cases, makes it a potential biomarker of detecting renal tubular injury in early stages. Moreover, some clinical trials of NGAL have already started.

KIM-1 is a type I transmembrane glycoprotein that is undetectable in normal kidneys. Following renal insults, it is rapidly overexpressed at the apical membrane of the PTECs in animals and humans (Bonventre, Vaidya et al. 2010, Alge and Arthur 2015, Dong, Zhang et al. 2019). The soluble form of human KIM-1 is detectable in the urine of patients with acute tubular necrosis and can be used as a biomarker for tubular damage (Han, Bailly et al. 2002).

IL-18 is a pro-inflammatory cytokine of the IL-1 family of cytokines and is synthesized as an inactive 23 kDa precursor by several cell types, including monocytes, macrophages, and PTECs. It is transformed into its active form by caspase-1 and increased in the case of tubular inflammation (Dinarello 1999), and IL-18 is overexpressed in AKI caused by IRI. In humans, the urinary level of IL-18 increases 24 to 48 hours before the elevation of serum creatinine, and its concentration correlates with the severity of AKI (Obermuller, Geiger et al. 2014, Alge and Arthur 2015).

Cystatin C is a small molecular protein produced continuously by all nucleated cells. The level of urinary cystatin C is increased in AKI models, including the injection of gentamicin or cisplatin and IRI (Ferrannini, Vischini et al. 2008, Krawczeski, Vandevoorde et al. 2010, Ma, Li et al. 2010, Wan, Wang et al. 2013, Pirgakis, Makris et al. 2014, Lagos-Arevalo, Palijan et al. 2015, Saydam, Turkmen et al. 2018, Benoit, Ciccia et al. 2020). In humans, urinary and plasmatic cystatin C levels are associated with a tubular injury prior to serum creatinine increase in AKI, both in pediatric and adult patients (Koyner, Bennett et al. 2008, Togashi, Sakaguchi et al. 2012, Park, Choi et al. 2013, Wan, Wang et al. 2013, Lagos-Arevalo, Palijan et al. 2015, Benoit, Ciccia et al. 2020). These reports provide evidence that cystatin C could be considered a potential biomarker for AKI. However, serum cystatin C was reported to poorly predict AKI in critically ill children (Hamed, El-Sherbini et al. 2013). Therefore, further observation of cystatin C in various clinical conditions is still in need.

HMGB1 behaves as damage-associated molecular pattern (DAMP) and pro-inflammatory factor. It is widely expressed in almost all types of mammalian cells, which can be translocated from the nucleus to the cytoplasm, then released to the extracellular matrix. HMGB1 binds to immune cells receptors to promote the release of inflammatory factors, such as IL-6, tumor necrosis factor alpha (TNF)-α. The inflammatory factors in turn further increase the extracellular release of HGMB1, forming a circle of inflammation amplification (Rieckmann, Tuscano et al. 1997). Studies focusing on the HGMB1 pathway in hypoxia models have also been published, including the renal IRI model (Rabadi, Ghaly et al. 2012, Tian, Zhang et al. 2015, Zhang, Dong et al. 2019). There is evidence that HMGB1 is translocated and upregulated after hypoxia treatment in a rat model (Zhang, Dong et al. 2019). Another report in a mice IRI model demonstrated that HMGB1 is released from TECs and ECs of PTC 1-hour post-ischemia, and the release of HMGB1 correlates with the duration of ischemia. Also, intraperitoneal administration of a HMGB1 neutralizing antibody prevented HGMB1 release from ECs, displaying ameliorated short-term and long-term renal function (Rabadi, Ghaly et al. 2012).

In summary, the tubular epithelial compartment is attacked by IR from the earliest stage. Ischemic injury dysregulates absorption and secretion following TECs damage. Two major programmed cell death pathways s in TECs, apoptosis and necroptosis are contributing to tubular injury. Based on the specific absorption functions of different tubular segments, certain proteins expressed within TECs are regarded as tubular injury markers, such as KIM-1, NGAL, Cystatin-C, etc.

2.4 Microvascular injury

2.4.1 Microvascular anatomy

The renal microvasculature has a unique structure and is comprised of glomerular capillaries and PTCs. The vasculature branches from the renal arteries into a series of large arteries, supplying arteriolar blood to the superficial cortex via the interlobular arteries, and ends in a network of afferent arterioles and glomerular capillaries. PTCs can have two origins, the interlobular arteries and the afferent glomerular arterioles. **Since 90% of blood flow is directed to the superficial cortical area, there is a decreasing oxygenation gradient from the cortical**

region to the medullary zone. Due to these anatomical features, the CMJ is a more vulnerable section in IRI (Zimmerhackl, Robertson et al. 1985, Sampaio and Aragao 1990).

In the context of IRI-induced AKI, renal microvascular damage usually has few remarkable pathological features beyond microvascular congestion in CMJ, **which is recognized by the aggregation of erythrocytes, also referred to as rouleaux formation**. Although damage to tubular epithelial cells has been recognized for decades as playing a pivotal role in AKI, there is a growing body of research that has shown that renal microvascular damage is a significant factor in renal dysfunction (Basile, Donohoe et al. 2001, Basile 2004, Basile 2007, Sharfuddin and Molitoris 2011).

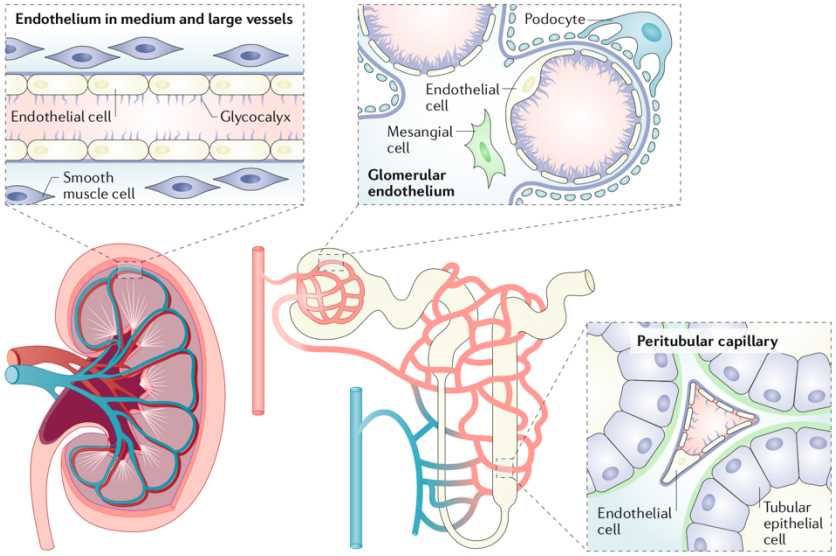

Figure 7. Different microvascular endothelial cells in the kidney (Jourde-Chiche, Fakhouri et al. 2019).

2.4.2 Mechanism of microvascular injury

In a physiological context, ECs essentially form a continuous barrier across all the vessels of organs. An intact endothelium is required for normal vascular tone regulation, platelet activity, adhesion to leukocytes, and angiogenesis. In AKI cases caused by IRI, hypoxia and oxidative stress cause changes in the glycocalyx, which leads to activation of ECs. The new markers expressed on the surface of these activated ECs promote the recruitment and adhesion of leukocytes and platelets, which leads to the deterioration of microcirculation and endothelial

dysfunction, such as soluble thrombomodulin (sTB), VCAM-1, ICAM-1, E-selectin, Syndecan-1, etc (Katayama, Nunomiya et al. 2017, Inkinen, Pettila et al. 2019, Ohnishi, Yasudo et al. 2019, Yu, McNeil et al. 2019, Zhang, Li et al. 2019).

The types of cell death involved in microvascular damage are unclear. A study has shown that in an animal model of renal IRI, caspase-3 is activated in ECs, suggesting that apoptosis plays a role in the death of ECs in this context (Horbelt, Lee et al. 2007). Our team has also described a protective role for caspase-3 deficiency in microvascular injury post-IRI (Yang, Lan et al. 2018).

2.4.3 Impact of microvascular injury

In pathophysiological settings, including AKI, a series of microvascular endothelial injuries can be triggered. Endothelial dysfunction is defined by decreased synthesis; the release of nitric oxide (NO) derived from the endothelium. It can influence vasoconstriction, endothelial permeability, coagulation, and inflammatory responses (Brodsky, Yamamoto et al. 2002, Yamamoto, Tada et al. 2002).

Vasoconstriction is the crucial feature of endothelial dysfunction in AKI. Several studies have shown an essential role in reducing renal blood flow in AKI, and certain inhibitors that target these pathways improve AKI (Basile and Yoder 2014). Nitric oxide synthases (NOS) are a family of oxidoreductases responsible for producing NO, which is a potent vasodilator in mammals (Weiner, Knowles et al. 1994)). eNOS is a type of NOS produced by ECs. The absence of eNOS exacerbates renal dysfunction in an animal model of endotoxin-induced AKI (Wang, Mitra et al. 2004). Administration of NO or its precursor (L-arginine) improves renal function in animal models of IRI-induced AKI (Popolo, Adesso et al. 2014). The mechanisms involved in altered eNOS activity are still unclear, probably associated with endothelial damage or free radical activity. The administration of an agent increasing free radicals resulted in decreased renal blood flow (Harris, Ju et al. 2001).

An intact endothelium is essential for maintaining normal microvascular permeability. Another crucial functional change in endothelial dysfunction is the increase of microvascular endothelial permeability or microvascular leakage. The mechanisms involved in increased permeability have not been fully elucidated; most mechanistic studies are based on *in vitro* systems which

have shown that increased permeability is induced by the alteration of the cytoskeleton, dissociation of cell-endothelial junctions, and increased endothelium-leukocyte interactions (Kwon, Phillips et al. 2002, Sutton, Mang et al. 2003, Verma and Molitoris 2015).

Activation of coagulation is a crucial step for microcirculatory dysfunction. Under physiological conditions, ECs inhibit coagulation by regulating a series of cytokines, including protein C, thrombomodulin, specific proteoglycans, and the tissue plasminogen activator (tPA). Thrombomodulin is a thrombin co-factor that reduces blood clotting by converting thrombin to an anticoagulant enzyme. Endothelial insults induce a decrease of thrombin-thrombomodulin complex and reduce the level of activated protein C, leading to the local generation of thrombin. It is this loop that causes a pro-coagulant response (Sadler 1997).

In summary, in the context of IRI-induced AKI, microvascular damage causes endothelial dysfunction, which contributes to renal dysfunction in several ways: 1. increased vasoconstriction, which can affect post-IRI perfusion; 2. increased permeability and coagulation, which can also alter the post-IRI perfusion by exacerbating the aggregation of erythrocytes in the microcirculation; 3. the increase in permeability and adhesion molecules which worsens inflammatory response (Kinsey, Li et al. 2008, Meng 2019).

2.5 Inflammation

Inflammation is a complex response to an apparent detrimental pathogen that contributes to tissue injury and promotes tissue repair. Excessive inflammation can trigger an autoimmune response, tissue fibrogenesis, and long-term damage. Cytokines released locally and recruitment of leukocytes *in situ* are characteristic of early inflammation occurring in the initiation phase of AKI (Rabb, Griffin et al. 2016).

Inflammation in various cell types (epithelial cells, ECs, inflammatory cells) can be elicited through the innate and adaptive immune systems (Kurts, Panzer et al. 2013). The innate immune system defends the body against pathogens as an early phenomenon, performed by several families of membrane or cytoplasm receptors sensitive to pathogen-released signals. Blocking innate immune system receptors, such as TLR2, can prevent AKI progression in animal models. Clinical studies using TLR2 blocking agents have also been launched in humans in the USA

and Europe, intending to prevent reperfusion injury post renal transplant and other clinical conditions (Shigeoka, Holscher et al. 2007, Reilly, Miller et al. 2013). In this phase I clinical study, OPN-305 (a humanized IgG4 monoclonal TLR2 antibody) and placebo were administrated randomly to healthy males. TLR2 blocking on monocytes was found from 14 days to later than 90 days post TLR2 stimulation, accompanied by inhibition of interleukin-6 production.

Various immune cells are involved in AKI and some of them are harmful, including neutrophils, monocytes/macrophages, dendritic cells (DCs), NKT cells, NK cells, and B cells. Other immune cells seem to play a protective role, such as Tregs. Macrophages play entirely different roles according to cell subtypes. M1 macrophages exert a pro-inflammatory role, contributing to tissue damage in the early stage. M2 macrophages function as anti-inflammatory players post-ischemic AKI and improve renal tissue regeneration in the recovery phase (Jang and Rabb 2015).

An increase in the number of neutrophils in the kidney has been observed in early-stage animal models of IRI (Bonventre 2007). Two important causes of this accumulation of leukocytes are the obstruction of the renal microcirculation and participation of adhesion molecules, including the selectin molecules and the intercellular adhesion molecule-1 (ICAM-1). Ischemic insults have been shown to increase the expression of P-selection and E-selectin on the surface of ECs. Also, inhibition of E-selectin and ICAM-1 by different experimental approaches in animal models of IRI-induced AKI reduced leukocyte infiltration and attenuated renal dysfunction (Cotran and Mayadas-Norton 1998, Okugawa, Miki et al. 2010, Barber, Grigg et al. 2018, Hu, Liu et al. 2018, Parodis, Gokaraju et al. 2020). In the late phase of AKI, macrophages and T lymphocytes are the predominant immune cells, while neutrophils are less common.

2.6 Repair and regeneration post-IRI

2.6.1 Tubular epithelial cell repair and regeneration

Following cell death of TECs and immune responses secondary to IRI, damaged tubules begin to regenerate. New cells migrate, proliferate, and differentiate in the damaged regions by

reconstituting a functional tubular epithelium. Studies have identified three possible sources for these cells:

2.6.1.1 Dedifferentiation of damaged TECs

Although an essential role for stem cells from bone marrow was put forward some years ago, several studies have demonstrated the predominant role of epithelial cells in repopulating tubules (Ferenbach and Bonventre 2015). This contribution of epithelial cells in tubular repair in the context of renal IRI is confirmed by genetic fate-mapping techniques, which demonstrate that the majority of regenerated TECs originate from resident tubules (Humphreys 2018). Using genetic line analysis, another study confirmed the dedifferentiation of TECs and their role in post-IRI tubular regeneration (Polichnowski, Griffin et al. 2020).

2.6.1.2 Stem cells from the bone marrow

The first evidence comes from a clinical study that examined male transplant patients who received kidneys from female donors. In those who recovered from acute tubular necrosis, TECs that had Y chromosomes were found (Jiang, Jahagirdar et al. 2002). This finding was then confirmed in an IRI animal model, where female mice transplanted with hematopoietic stem cells from male mice had TECs derived from males post-IRI (Lin, Cordes et al. 2003).

However, several published articles (Duffield, Park et al. 2005, Lin, Moran et al. 2005, Togel, Hu et al. 2005) have concluded that the source of repaired tubular cells was primarily from the endogenous renal population, not from bone marrow, which suggested renal tubular regeneration did not benefit from the proliferation of bone marrow-derived cells. Therefore, the contribution of bone marrow stem cells in tubular repair is still a controversial subject.

2.6.1.3 Renal or progenitor stem cells

Numerous studies have demonstrated the existence of renal progenitor cells, but their role in IRI is still debated (Becherucci, Mazzinghi et al. 2009, Kitamura, Nakano et al. 2018).

Failure of tubular regeneration leads to tubular atrophy, which is one of the key pathological features of CKD. There is growing evidence suggesting that hypoxia caused by microvascular

depletion is the driving force for impaired tubular regeneration and post-IRI fibrosis (Tanaka, Tanaka et al. 2014, Venkatachalam, Weinberg et al. 2015).

2.6.2 Endothelial repair and regeneration

2.6.2.1 Limited endothelial repair

In contrast to tubular epithelial cells, the repair and regeneration capacity of endothelial cells are limited. In the context of renal damage, ECs detach into the circulation, but the proliferation and migration of resident and neighboring endothelial cells are not sufficient to restore the microvascular endothelium. Therefore, endothelial progenitor cells (EPCs) are an essential cell source for the repair process. One study proved that the EPC level in the serum is associated with vascular dysfunction (Bakogiannis, Tousoulis et al. 2012). EPCs enhanced by erythropoietin (Finn, Fernandezrepollet et al.) prior to and during ischemia displayed a protective role on renal function in an animal model of renal IRI, with less of an increase in serum creatinine and a reduction in tubular necrosis. However, in this study, the direct impact of EPCs on the vascular compartment was not reported (Cakiroglu, Enders-Comberg et al. 2016) (Li, Black et al. 2012).

2.6.2.2 Angiogenesis

Angiogenesis is another repair pathway contributing to restoring the integrity of the microvascular endothelium. Angiogenesis is mainly regulated by vascular endothelial growth factor A (VEGF-A). VEGF is primarily distributed in podocytes and thick ascending limbs, also in proximal and distal tubular epithelial cells (Tanaka, Tanaka et al. 2015). VEGF expression was decreased in a model of obstructive nephropathy (Burt, Forbes et al. 2007). The VEGF pathway is also altered in ischemic injury, and VEGF administration results in preserving the microvasculature. It is commonly recognized that VEGF receptors (VEGFR) located on ECs can be classified as VEGFR1, which has an anti-angiogenic role, and VEGFR2, which has a pro-angiogenic role. The relative importance of these two types of VEGFR determines the angiogenic fate of ECs (Mayer 2011). In a rat renal IRI model, VEGF mRNA and protein expression were down-regulated post bilateral 45-minute ischemia (Basile, Fredrich et al. 2008). These results demonstrated the association between the VEGF pathway and renal

revascularization post-IRI. The VEGF transcription and expression level down-regulation suggest a pro-angiogenic role of the microvasculature. VEGF is crucial to preserve microvasculature. However, overexpression of VEGF displays a detrimental effect in a murine transgenic model; increased VEGF level suggests renal fibrotic progression (Hakroush, Moeller et al. 2009).

Besides the VEGF pathway, hypoxia-inducible factor (Molnar, Kumpers et al.) is another regulator in the condition of hypoxia. This transcriptional factor consists of two subunits, HIF-α and HIF-β. HIF-α expression is highly associated with oxygen pressure and has two active forms, HIF-1α and HIF-2α, functioning as an adaptor of hypoxia. HIF-1α is mainly expressed in TECs while HIF-2α in ECs and fibroblasts. In hypoxia conditions, initiating angiogenesis by HIF activation is a promising strategy; HIF accumulation was shown to form new vasculature in an animal study (Leite de Oliveira, Deschoemaeker et al. 2012).

2.6.3 Microvascular rarefaction

The renal microvasculature is composed of the glomerular capillaries and PTCs. The progression of AKI to CKD is associated with a progressive loss of PTCs, and PTC damage also influences the long-term post-IRI outcome (Basile, Donohoe et al. 2001, Basile, Fredrich et al. 2004). Clinical and animal studies demonstrate that in other kidney diseases, including glomerulonephritis and obstructive nephropathy, there is also an inverse correlation between microvascular density and the severity of fibrosis (Ohashi, Kitamura et al. 2000, Ohashi, Shimizu et al. 2002). Together, these results strongly suggest that the depletion of PTCs plays a central role in fibrotic progression and renal dysfunction.

In addition to cell death of ECs, loss of pericytes and altered angiogenesis also contribute to microvascular rarefaction. Pericytes are located on the abluminal side of PTCs. After ischemia, pericytes detach from the endothelium and facilitate renal fibrogenesis. The loss of endothelium-pericytes intense contact contributes to endothelial instability, which further induces haemorrhage, permeability augmentation, or microvascular rarefaction (Kida and Duffield 2011).

Microvascular rarefaction, especially PTC rarefaction, can occur subsequent to IR-induced AKI. In pathophysiological conditions, including IRI, aging, angiotensin-II infusion,

glomerulonephritis, etc., PTC rarefaction is presented as an irreversible renal capillary loss observed in the renal biopsies. In humans, PTCs are injured, and their density is decreased in association with renal interstitial fibrosis (Choi, Chakraborty et al. 2000). **PTC rarefaction and renal endothelial dysfunction result in chronic renal interstitial hypoxia, which leads to hypertrophied remaining nephrons. These atrophic renal areas further exacerbate the hypoxic insult. Chronic hypoxia partly induced by PTC rarefaction is recognized as a pivotal contributor to renal fibrogenesi**s (Basile 2004).

After pericyte detachment from capillaries, pericytes are activated and contribute to fibrosis by dedifferentiating into myofibroblasts. However, the injured endothelium is now devoid of close contact with pericytes, and the crosstalk between endothelial cells and pericytes vital for vessel stability is lost. In other organs, the endothelium lacking pericytes is unstable, prone to aneurysm, hemorrhage, or drop-out (rarefaction). In recent studies, Lin's team has shown that blockade of VEGFR 2 on ECs following renal injury abrogated pericyte detachment, attenuating both PTCs loss and fibrosis during progressive renal injury induced by unilateral ureteral obstruction (UUO) or IRI, suggesting a crosstalk between pericyte damage and capillary loss, as well as fibrosis (Lin, Chang et al. 2011).

The association between loss of PTCs and renal fibrosis post-IRI has been reported in numerous studies (Basile 2004, Basile 2007, Horbelt, Lee et al. 2007, Polichnowski 2018, Basile 2019, Menshikh, Scarfe et al. 2019). In this context, three possible significant mechanisms of PTC rarefaction are prone to induce renal fibrosis: secondary hypoxia following PTCs loss triggers fibrogenesis; pathophysiological changes in the renal medulla exacerbate sodium ion-sensitive hypertension; differentiation of myofibroblasts further accentuates interstitial fibrosis (Basile and Yoder 2014).

Microvascular rarefaction post-IRI was considered a permanent loss due to the limited capacity of proliferation and regeneration (Basile, Friedrich et al. 2011). However, recent investigations of the delayed contralateral nephrectomy (DN) IRI model demonstrated a recovery of capillary density in the long-term by presenting CD31 positive vessels in murine renal tissue (Menshikh, Scarfe et al. 2019). This DN-IRI model is not commonly used as an experimental model due to its repeated invasive operations, making it cost and resources consuming. However, its advantage is to increase the animal survival rate due to the compensated function of the delayed

removed kidney. The DN-IRI model has been performed both in mice and rat models (Finn 1980) and was shown to facilitate renal function and renal tissue repair post-IRI. Reports have demonstrated that nephrectomy contributes to functional nephrons recruitment, which would have become atrophic (Finn, Fernandezrepollet et al. 1984, Fu, Tang et al. 2018, Wei, Wang et al. 2019). The protective role of the DN-IRI model is probably mediated by an increase in GFR and functional nephrons. Nevertheless, it is still not clear whether PTC rarefaction works as the cause or the result.

2.6.4 Renal fibrosis post-AKI

Fibrosis is defined by the aberrant and excessive deposition of extracellular matrix proteins (ECM), which leads to changes in tissue architecture and function loss in fibrotic regions. Regardless of the etiology, renal fibrosis is a common pathological CKD feature (Babickova, Klinkhammer et al. 2017). It is associated with end-stage renal failure, and effective preventive strategies for fibrosis are crucial to prevent irreversible loss of renal function (Leung, Tonelli et al. 2013, Prakoura, Hadchouel et al. 2019). As mentioned above, tissue insults induce an inflammatory response, which causes an increase in both pro-inflammatory cytokines and profibrotic cytokines. The latter inevitably leads to activation of cells producing ECM, which is undoubtedly a significant renal fibrogenesis event (Strutz and Muller 2006). Fibrosis is a series of complicated processes, some critical procedures and signal pathways involved in fibrosis are described in the following pages.

2.6.4.1 Myofibroblast differentiation

It is generally accepted that myofibroblasts are the primary cell type responsible for synthesizing and accumulating extracellular matrix leading to renal fibrosis. Several different sources, with other mechanisms, have been proposed as contributors to the myofibroblast pool during the renal fibrosis process (Strutz and Zeisberg 2006).

(1) Origins of myofibroblasts

Resident fibroblasts: Fibroblasts are spindle-shaped mesenchymal cells that play a crucial role in the homeostasis of the ECM. They are the first identified source and are still considered the most important source of myofibroblasts (Meng 2019, Yuan, Tan et al. 2019). Interstitial

fibroblasts are characterized by the production of fibronectin. When activated by profibrotic stimuli, fibroblasts differentiate into proto-myofibroblasts by expressing fibronectin containing an additional domain A (ED-A fibronectin), filamentous actin, and focal adhesions. This transition is reversible. **Proto-myofibroblasts can then differentiate into myofibroblasts, characterized by the expression of smooth muscle actin α (α-SMA). α-SMA is a reliable marker for differentiation into myofibroblasts** (Li, Yu et al. 2019, Wang, Li et al. 2019, Yuan, Tan et al. 2019).

Pericytes: Pericytes are cells that surround and stabilize ECs within capillaries. Following tissue insults, pericytes detach from the endothelium, undergo migration and proliferation, and differentiate into myofibroblasts. By using genetic mapping techniques in a mouse model of IRI-induced renal fibrosis, pericytes/perivascular fibroblasts have been identified as the dominant source of myofibroblasts (Humphreys, Lin et al. 2010, Kida and Duffield 2011, Piera-Velazquez, Li et al. 2011, Chang, Chou et al. 2012).

Circulating fibrocytes: Circulating fibrocytes are a subpopulation of monocytes derived from the bone marrow; they express the hematopoietic cell marker CD45 and have specific fibroblast characteristics, e.g., the spindle shape, the production capacity of type I collagen. An animal model of renal fibrosis induced by IRI where rats were transplanted with marked bone marrow cells demonstrated that bone marrow cells contribute to 30% of the myofibroblast population, indicating an essential role in fibrocytes (Broekema, Harmsen et al. 2007).

(2) Mechanisms implicated in myofibroblast differentiation

TGF-β/CTGF axis: TGF-β is one of the primary mediators in inducing myofibroblast differentiation. During stimulation with TGF-β, fibroblasts are activated and undergo a phenotypic transition to a myofibroblast phenotype. Several pathways are involved in this differentiation induced by TGF-β, in particular the Smad3, FAK, JNK, TAK, and PI3-kinase/Akt pathways (Xu, Lamouille et al. 2009, Dobaczewski, Bujak et al. 2010).

CTGF is another potent inducer of differentiation into myofibroblasts. CTGF expression is activated downstream of the TGF-β signaling pathway, amplifying the TGF-β pathway by positive feedback (Cheng, Thuillier et al. 2006, Wang, Chen et al. 2019, Yin and Liu 2019). Our team demonstrated that CTGF could induce differentiation into myofibroblasts in a TGF-β

independent way (Laplante, Sirois et al. 2010, Bernard, Dieude et al. 2014). In a clinical study and an animal model of allogenic renal transplantation, the presence of high levels of urinary CTGF correlated with the development of interstitial fibrosis (Yue, Xia et al. 2010, Kuypers, Metalidis et al. 2012).

ROS: Reactive oxygen species (ROS) are oxygenated chemical species such as oxygen anions, free radicals, and H_2O_2. There are two primary sources of ROS production in cells: mitochondria (which generate ROS as a by-product of respiration) and nicotinamide adenine dinucleotide phosphate (NADPH) oxidase (Scherz-Shouval and Elazar 2011, Rahal, Kumar et al. 2014). NADPH oxidases are the primary source of ROS, which promotes fibrotic processes. The signaling pathways involved in ROS-induced differentiation into myofibroblasts are not yet fully understood. NOX enzymes in the NADPH family have been suggested to induce differentiation into myofibroblasts via the MEK-ERK1/2 pathway (Barnes and Gorin 2011).

Autophagy-mTORC2: The autophagy pathway is a pro-survival stress response. Studies have shown that autophagy plays an important role in the fibrotic process by using multiple experimental approaches. Induction of autophagy has been shown to promote the survival of synovial fibroblasts (Shin, Han et al. 2010). In a clinical study, autophagy was associated with the differentiation into myofibroblasts in the oral mucosa (Vescarelli, Pilloni et al. 2017). In liver fibrosis models, a decrease in autophagy has been shown to reduce the differentiation of liver stellate cells into myofibroblasts, leading to a reduction in fibrosis (Hernandez-Gea, Ghiassi-Nejad et al. 2012). However, it is interesting to note that it has also been reported that the inhibition of autophagy accentuates fibrosis instead of reducing fibrosis in specific experimental approaches; for example, autophagy deficiency increased cardiac interstitial fibrosis in a study using a murine model of cardiomyopathy (Tannous, Zhu et al. 2008); and another publication demonstrated the inhibition of autophagy promoted myofibroblast differentiation in an *in vitro* COPD model (Fujita, Araya et al. 2015). It has been proposed that autophagy in different cell types could have different impacts on the fibrotic process. Based on these studies, autophagy is suggested vital to myofibroblasts differentiation in various cell types.

mTOR is a serine/threonine kinase that controls many cellular processes. Two kinds of mTOR complex are structurally and functionally distinct: mTOR complex 1 (mTORC1) and mTOR complex 2 (mTORC2). mTORC1 is composed of the protein associated with the regulation of

mTOR, Raptor (protein associated with regulation of mTOR), the mammalian lethal with Sec 13 protein 8/G-protein β-protein subunit-like (mLST8/GβL), the substrate 40 kDa of Akt/PKB (PRAS40), and the DEP-domain-containing mTOR interacting (Deptor) protein. MTORC2 is composed of the rapamycin-insensitive companion of mTOR (Rictor), mammalian stress-activated protein kinase-interacting protein 1 (mSIN1), the protein observed with Rictor1/2 (Protor1/2), mLST8/GβL, and Deptor (Huang and Fingar 2014). The specific ablation of Rictor in fibroblasts leads to a decrease in fibrosis and the level of α-SMA in a mouse model of unilateral ureteral obstruction, suggesting an essential role of mTORC2 in the differentiation into myofibroblasts (Li, Tan et al. 2015). Using an *in vitro* fibroblast system, our team also demonstrated that autophagy could activate differentiation of fibroblasts into myofibroblasts in a mTORC2-dependent manner (Bernard, Dieude et al. 2014).

Senescence: Cellular senescence or biological aging is the deterioration of cellular function, involving an increased death rate or damaged function of proliferation and differentiation, including remodeling of chromatin, autophagy activation, and proinflammatory protein secretion (Waters, Blokland et al. 2018). The link between cell senescence and differentiation into myofibroblasts has been found in specific contexts. It has been demonstrated in a murine model of skin wound closure that senescent fibroblasts appear early in the wound. Senescent fibroblasts accelerate the closing by inducing differentiation into myofibroblasts via the secretion of platelet-derived growth factor AA (PDGF-AA) (Demaria, Ohtani et al. 2014). Our team also reported autophagy activation by inhibiting mTOR2 fueled senescence and myofibroblast differentiation in vitro human fibroblasts (Bernard, Yang et al. 2020).

2.6.4.2 Other cellular pathways contributing to fibrosis

(1) Epithelial-mesenchymal transition (EMT)

EMT is a cellular process characterized by the loss of cell polarity and the change in cell form from cuboid to fibroblastoid, by under-regulation of epithelial markers and over-regulation of mesenchymal markers (Luo, Cai et al. 2019, Hu, Zhang et al. 2020). The function of EMT in kidney fibrosis is still in debate. Multiple investigations reporting mesenchymal markers after tubular epithelial cells are damaged or exposed to cytokine *in vitro*, but *in vivo* studies suggest the presence of EMT in the kidney fibrotic process is limited (Iwano, Plieth et al. 2002). One

study using Cre/Lox technique for genetic labeling did not find evidence for the migration of epithelial cells outside of the tubular basement membrane into the interstitial space in a murine Unilateral Ureteral Obstruction (UUO) model, which did not support EMT as contributing to fibrosis (Humphreys, Lin et al. 2010).

When fluorescence labeling and genetic crossing were used to trace the origin of myofibroblasts, no evidence of epithelial cell origin was found. Moreover, pericytes work as precursors of myofibroblasts (Humphreys, Lin et al. 2010).

(2) Endothelial-mesenchymal transition (EndoMT)

EndoMT is considered a unique form of EMT where ECs are induced to switch to a mesenchymal cell phenotype. EndoMT has been observed in renal dysfunction caused by multiple etiologies, including IRI, UUO, and streptozotocin-induced diabetic kidney disease (DKD) (Li, Qu et al. 2009). One study investigated EndoMT in three different murine renal fibrosis models, UUO, streptozotocin induction, and Alport renal disease. This study showed that up to 50% of fibroblasts had the endothelial marker CD31 and the myofibroblast marker α-SMA. Cell tracing observations on Tie-2/Cre mice also suggested an endothelial source of myofibroblasts (Zeisberg, Potenta et al. 2008).

In the context of IRI-induced AKI, using genetic mapping techniques, a study showed that a population of myofibroblasts is of endothelial origin (Basile, Friedrich et al. 2011). EndoMT contributes to renal dysfunction in patients post sepsis-induced AKI (Stasi, Intini et al. 2017), and could be induced by renal IRI and antibody-mediated rejection (ABMR) in the transplant setting (Xu-Dubois, Peltier et al. 2016). Although EndoMT has been shown to be involved in animal organ fibrosis progression, the extensive contribution of EndoMT has not yet been thoroughly investigated and remains a controversial topic. One study labeled fibroblast using a murine collagen-GFP fused model, but most fibroblasts originated from resident fibroblast cells, not from ECs or epithelial cells (Moore-Morris, Guimaraes-Camboa et al. 2014).

EndoMT is regulated by TGF-β, AKT, and mTOR pathways, causing the loss of ECs markers and the acquisition of myofibroblast features, such as α-SMA N-cadherin (Dejana, Hirschi et al. 2017). TGF-β receptor endothelial conditional knock-out heterozygous mice show increased angiogenic capacity after UUO (Xavier, Vasko et al. 2015).

Pericytes:

In a fate-tracing study of myofibroblasts post-UUO and IRI, no evidence of tubular epithelial origin was found. Still, α-SMA positive myofibroblasts with pericyte markers PDGF receptor β (PDGFRβ) and CD73 were documented (Humphreys, Lin et al. 2010). Other investigators reported that a population of PDGFRβ positive cells were characterized as mesenchymal-like cells and contributed to renal fibrogenesis. Simultaneously, a deficiency in zinc-finger transcription factor GL11+ on pericytes attenuated renal fibrosis induced by UUO (Kramann, Schneider et al. 2015). Although pericyte to mesenchymal transition is documented in kidney disease, pericytes are not considered significant renal fibrosis drivers because only a small amount of myofibroblasts originate from NG2 positive pericytes (LeBleu, Taduri et al. 2013).

While EMT does not seem to play a significant role in renal fibrosis, tubular epithelial cells could upregulate profibrotic factors, which can, in turn, affect pericytes. Hedgehog signal is regulated by tubular epithelial cells, while Hedgehog receptor patched 1 (PTCH1) and effector GLI1 and GLI2 are expressed on pericytes (Fabian, Penchev et al. 2012). Also, tubular epithelial cells express Wnt signal factor Wnt1, promoting pericyte to mesenchymal transition by mediating the Wnt–βcatenin signal (Xiao, Zhou et al. 2016).

In addition to transitioning to myofibroblasts, pericytes can detach from endothelial cells in AKI, disrupting the microvascular structure and facilitating capillary loss and secondary tubular hypoxia, which in turn promote fibrosis (Schrimpf, Teebken et al. 2014).

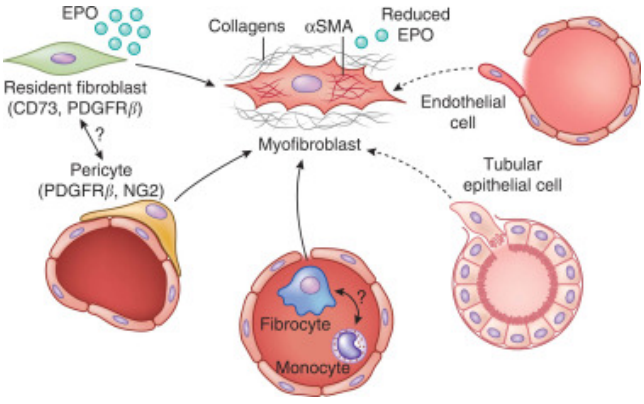

Figure 8. Sources of renal myofibroblasts (Mack and Yanagita 2015).

In summary, tubular epithelial cells present an adequate capacity for regeneration and repair, while repair and regenerative capacities in the microvascular endothelial compartment are much more limited. Therefore, microvascular rarefaction is a crucial characteristic of microvascular loss, and some other mechanisms beyond tissue repair are involved in renal microvascular preservation or revascularization, such as angiogenesis. Renal fibrosis develops as an irreversible form of tissue scar formation secondary to incomplete renal tissue repair, with the feature of myofibroblasts dedifferentiation and renal structural disorder. Some other signals also contribute to renal fibrosis progression, e.g., EndMT, EndoMT, and pericyte-myofibroblast differentiation.

2.7 Chronic kidney disease (CKD) and AKI-CKD transition

2.7.1 Definition of CKD

CKD is now recognized as a severe clinical event. CKD incidence among patients over 65 years old is around 10% in the USA. This population of patients has excessively high morbidity, mortality, and a strong tendency for end-stage renal disease (ESRD) progression. Therefore, the management of CKD is critical due to the severe clinical outcome and economic burden of ESRD (Kalamas and Niemann 2013).

CKD is defined according to the level of renal dysfunction, usually diagnosed by the 2002 National Kidney Foundation Kidney Disease Outcomes Quality Initiative guidelines (NKF KDOQI). This criterion includes five stages classified according to the glomerular filtration rate (GFR) and related symptoms, such as proteinuria, and abnormal renal biopsy.

National Kidney Foundation K/DOQI: stages of chronic kidney disease (CKD)

Stage of CKD	Description	GFR (mL/min/1.73 m^2)
I	Kidney damage with normal or increased GFR (eg, early diabetic nephropathy)	≥90 mL/min
II	Kidney damage with mildly reduced GFR	60–89
III	Moderately reduced GFR	30–59
IV	Severely reduced GFR	15–29
V	End-stage renal disease	<15 or need for dialysis

Tableau III. Definition and classification of CKD (Kalamas and Niemann 2013).

2.7.2 AKI to CKD transition

AKI and CKD were considered two independent clinical events, attributed to the concept that the kidney has enough repair capacity for full functional recovery. However, renal recovery post AKI has now been recognized as more insufficient than assumed. A transition from AKI to CKD develops in many cases of AKI (Maekawa and Inagi 2019). The precise mechanism of AKI-CKD transition is still not well understood, however, multiple alterations were involved in the progression to CDK, e.g., chronic hypoxia leading to further tubulointerstitial fibrosis, microvascular loss, microvascular dysfunction. In regard to molecular and cellular alteration, ER stress and tubular phenotype changes (tubular cell senescence) and tubular inflammation were also observed by different investigations (Ferenbach and Bonventre 2015, Sturmlechner, Durik et al. 2017).

Effective prevention of AKI-CKD transition is crucial for maintaining renal function. Observation targeting ER stress and mitochondrial stress demonstrated that these stresses promoted CKD transition through activation of tubular cell senescence and initiation of inflammation (Zhang, Sha et al. 2018). Another study focusing on cGAS-STING and SASP pathways displayed a potential contribution to AKI-CKD transition of tubular senescence and inflammation. However, investigating the molecular mechanism of CKD transition still needs to be further explored (Maekawa and Inagi 2019).

In brief, mounting evidence suggests insufficient renal functional recovery post-AKI explaining to some degree the trend toward AKI-CKD transition and the importance of preventing CKD development.

3. Characteristics of multiple rodent AKI-CKD models

IRI induced by renal artery clamping is the most commonly used and best characterized AKI experimental animal model. It was developed in a number of species, including murine and porcine models (Yang, Hosgood et al. 2011, de Braganca, Volpini et al. 2016, Perry, Huang et al. 2016, Black, Lever et al. 2018, Kitamura, Nakano et al. 2018, Dong, Zhang et al. 2019). The IRI model is relevant to clinical situations such as vascular occlusion, hypotension, dehydration, and, most importantly, renal transplantation. The renal ischemic insult contains an ischemic phase and a reperfusion phase, initiating a cluster of cell responses that induce tubular epithelial

damage, inflammation, and microvascular dysfunction. Renal dysfunction continues to develop several weeks to months after IRI in rodent models, enabling possible research strategies focused on the characterization of AKI-CKD transition. Generally, animal IRI models of AKI-CKD transition include bilateral IRI, unilateral IRI, unilateral IRI plus nephrectomy, and multiple IRI.

3.1 bilateral IRI (bIRI)

bIRI is performed by clamping the renal artery of both kidneys. Basile's team used bIRI rat model for 60 minutes to investigate long-term damage post-AKI. It was found that abnormal tubular morphology was present at four weeks post-operation. However, interstitial fibrosis developed at 40 weeks involving TGF-1 up-regulation and capillary loss in the outer medulla (Basile, Donohoe et al. 2001). This study demonstrated that severe IRI could induce long-term fibrosis with loss of peritubular capillaries. Other bIRI models with different clamping times were also performed.

In addition to clamping time, the ischemic temperature is another important factor regulating the severity of ischemic damage. Based on the literature and our preliminary work, homeothermic monitoring and rectal probing during manipulation are required (Wei and Dong 2012, Marschner, Schafer et al. 2016). Different IRI severity can be induced by modifying temperatures and ischemia times, providing various damage scenarios for generating moderate AKI or severe AKI followed by progressive CKD transition.

bIRI is a model of hemodynamics similar to patient, however, there are also apparent disadvantages. The optimal surgery condition should be tested; if the injury is too severe, the animal cannot survive in the long-term; if too mild, renal dysfunction recovers to normal quickly, which stops CKD development.

3.2 unilateral IRI (uIRI)

uIRI is performed by clamping only one renal artery while the contralateral kidney is kept intact. Some studies induced uIRI by clamping the renal artery for 30 minutes at 37°C (Skrypnyk, Harris et al. 2013, Ehling, Babickova et al. 2016, Chen, Fang et al. 2018, Yang, Lan et al. 2018, Dong, Zhang et al. 2019, Menshikh, Scarfe et al. 2019). One study observed epigenetic

alternations of several genes post IR and lipopolysaccharide (LPS) insults. As a result, TNF and NGAL were transcriptionally upregulated in both models, and KIM-1 was overexpressed in the IRI model (Zager, Johnson et al. 2011). Another investigation performing clamping for 45 minutes also found abnormalities of tubular epithelial morphology, inflammation, and renal fibrosis at ten weeks post-ischemia (Lech, Grobmayr et al. 2014). These investigations confirmed that uIRI is a useful model to study chronic renal damage due to the high survival rate. However, this is also a disadvantage since the intact contralateral kidney's compensation role makes it challenging to monitor renal dysfunction at different stages, which implies that this model is a good choice to study long-term histological findings post-IRI but not to assess its renal functional consequences (decreased estimated GFR).

3.3 unilateral IRI plus nephrectomy (uIRIx)

The uIRIx model is similar to that of the uIRI but involves contralateral nephrectomy, therefore avoiding the compensatory role of the contralateral kidney. One research work inducing IRI in rats by 60-minute unilateral renal artery occlusion plus nephrectomy found that renal function was better preserved if the contralateral kidney was excised before ischemia (Finn, Fernandezrepollet et al. 1984), but this study doesnot apply to the AKI-CKD transition. Another study using delayed nephrectomy demonstrated that the nephrectomy group displayed reduced fibrosis in the long term (Yang, Besschetnova et al. 2010). Also, an observation comparing moderate and severe uIRIx models, by simultaneously performing nephrectomy simultaneously in a moderate model for 26 minutes of ischemia in a moderate model and eight days delayed nephrectomy for 30 minutes in a severe model, respectively (Skrypnyk, Harris et al. 2013). **These works suggested that the uIRIx model could induce chronic kidney damage with a stable survival rate and ameliorate progressive renal injury**. However, delayed nephrectomy is beneficial for animal survival, especially in severe models, which does not perfectly mimic real-life situations in the clinic.

3.4 multiple IRI

Multiple IRI is usually used to induce renal fibrosis. Firstly, Zager and his colleagues demonstrated that repeated bIRI in a rat model did not result in a more significant loss of GFR

and had a protective role in renal function, with no further elevation of serum creatinine and BUN after 6 days (Zager, Baltes et al. 1984). Similar clinical research is called "preconditioning intervention," which has suggested better preservation of renal function through preconditioning treatment (Yeh, Hsu et al. 2010, Ferreyra, Vargas et al. 2013, Zhou, Liu et al. 2020). Further investigations are required to understand this multiple IRI model better. The influence of ischemic times, the interval time of subsequent ischemic injury, and other factors require in-depth study.

In short, all these models present development of CKD transition post-AKI to some degree, demonstrated by the serum and urine parameters test conforming with the definition of AKI. At the same time, renal progressive damage and fibrosis could be found in the long term attributed to incomplete repair. Among these IRI murine models, uIRIx was chosen for the animal model in our study due to its similar scenario with the clinical renal replacement procedures. In addition, as it differs from uIRI, uIRIx can avoid contralateral renal function compensation after nephrectomy.

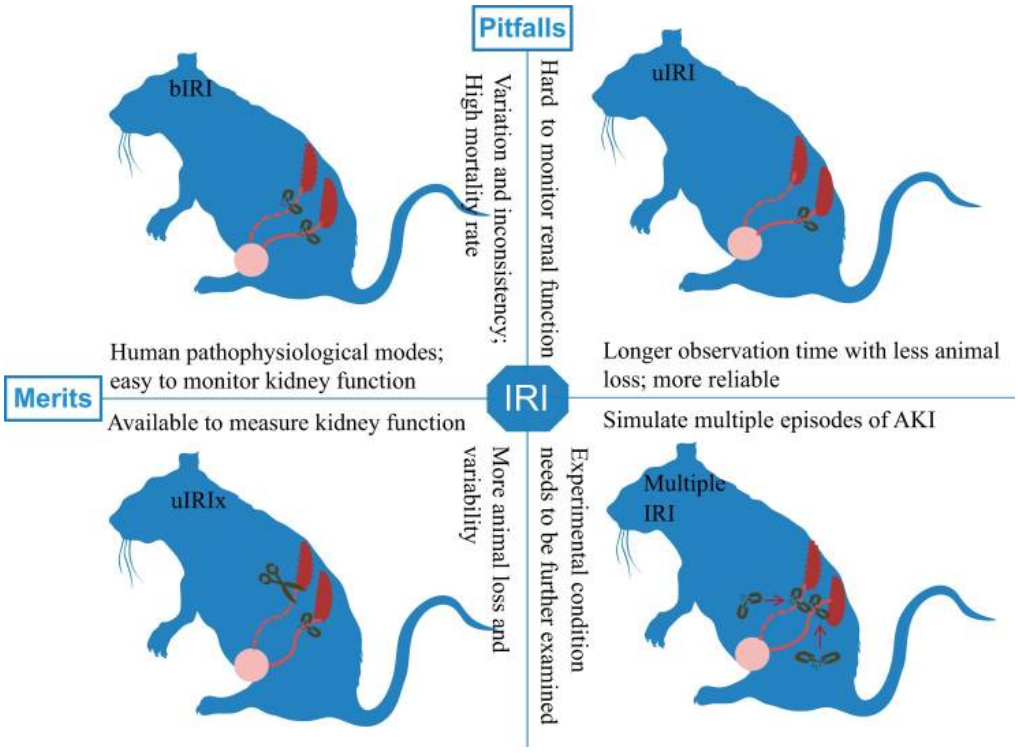

Figure 9. Comparison of multiple animal IRI models (Fu, Tang et al. 2018).

Rationale and hypothesis

Rationale

IRI is one of the most common causes of AKI and a significant risk factor for CKD. Renal transplant is inevitably associated with IRI, which can lead to AKI in the immediate post-transplant period resulting in delayed graft function (DGF). In turn, DGF is highly associated with poor kidney graft function and survival. It is now generally accepted that tubular and microvascular insults are two critically important features of IRI-induced AKI. Programmed cell death plays a predominant role in tubular epithelial cell damage and endothelial damage. Tubular epithelial injury was considered the primary cellular target in the past, however, mounting evidence has identified microvascular injury as a pivotal contributor to progressive renal damage and renal fibrosis. Therefore, this study focuses more on endothelial dysfunction in IRI cases. In our previous work and reports from other teams, apoptosis was found as an essential endothelial cell death pathway in the scenario of serum starvation *in vitro* and clinical kidney transplant (Cailhier, Laplante et al. 2006, Laplante, Sirois et al. 2010, Yang, Hosgood et al. 2011, Yang, Zhao et al. 2014, Dieude, Bell et al. 2015, Cardinal, Dieude et al. 2018). Activation of caspase-3, a crucial mediator in apoptosis, has been reported in tubular epithelial cells and ECs in the context of AKI. The relative importance of caspase-3 activation in tubular and microvascular insults induced by IRI and the functional effects of the damage to these compartments remain unclear.

Microvascular endothelial injury releases a series of signals that trigger microvascular permeability disorders and subsequent microvascular rarefaction, which further induces long-term renal dysfunction and interstitial fibrosis. Whether caspase-3 contributes to microvascular dysfunction and microvascular rarefaction post-IRI remains uncertain at present.

Hypothesis

1. Apoptosis is the predominant mode of endothelial cell death in the context of AKI induced by IRI. Caspase-3 deficiency has a protective effect against microvascular dysfunction post mild and severe IRI.

2. Caspase-3 deficiency prevents renal microvascular rarefaction, renal fibrogenesis, and long-term renal dysfunction post-IRI.

Objectives

1. To define the effect of caspase-3 in renal microvascular dysfunction after mild and severe renal IRI.
2. To define the molecular mechanism of microvascular endothelial protection associated with caspase-3 inhibition.
3. To investigate the interplay between endothelial cell death and microvascular rarefaction, and also renal fibrosis in the long term.

Methods

1. In vitro experiments: human tubular epithelial cells (K2 cells) and human umbilical vascular cells (HUVECs) were exposed to mild hypoxia-reoxygenation (mimicking mild AKI in vivo).
2. In vivo experiments: unilateral renal artery clamping plus contralateral nephrectomy (30 minutes and 60 minutes) were performed in wild-type mice (C57BL/6) and caspase-3 KO mice. Mice were sacrificed at 1, 2, 3, 7, and 21 days post-IRI. BUN and serum creatinine were tested to monitor renal function, histological evaluation was performed to evaluate tubular and endothelial dysfunction, and microvascular rarefaction and fibrosis in the long term. Micro-Computed Tomography (microCT) and intra-vital imaging were used for assessing renal microvascular permeability and renal microvascular density.

Results

Manuscript 1: Caspase-3 is a pivotal regulator of microvascular rarefaction and renal fibrosis after ischemia-reperfusion injury

Bing Yang, [1,2,3] ***Shanshan Lan***, [1,2,3] Mélanie Dieudé, [1,2,3] Jean-Paul Sabo-Vatasescu,[1] Annie Karakeussian-Rimbaud, [1,2] Julie Turgeon, [1,2] Shijie Qi, [1,2] Lakshman Gunaratnam,[2,4] Natalie Patey,[1,2,3,5]and Marie-Josée Hébert[1,2,3]

1 Research Centre, Centre hospitalier de l'Université de Montréal, Montreal, Quebec, Canada; 2 Canadian National Transplant Research Program, Edmonton, Alberta, Canada; 3 Université de Montréal, Montreal, Quebec, Canada; 4 London Health Sciences Centre, Schulich School of Medicine and Dentistry, The University of Western Ontario, London, Ontario, Canada; and5 Department of Pathology, Centre hospitalier universitaire Sainte-Justine, Université de Montréal, Montreal, Quebec, Canada. B.Y. and S.L. are co-first authors.

Author order: Co-first author

Contribution: S.L., B.Y., and M.-J.H. designed experiments. S.L., B.Y., M.-J.H., and N.P. analyzed the data, and wrote the manuscript. B.Y., S.L., A.K.-R., J.-P.S.-V., J.T., and S.Q. performed experiments. M.D. participated in analyzing the data and the preparation of the manuscript. L.G. performed the KIM-1 immunohistochemical staining.

As a co-first author, Shanshan Lan participated in experiments design and murine microsurgery troubleshooting and standardization. In the part of in vivo experiments, Shanshan was responsible for setting up the animal IRI model, collecting biological samples pre-op and at different time points post-op, animal sacrifice, necropsy, samples collection, and preservation. Shanshan Lan also completed BUN test, immunohistochemistry staining with Dr. Bing Yang, and pathological evaluation with Dr. Bing Yang and Dr. Natalie Patey. In the part of in vitro experiments, Shanshan finished one replicate of HUVECs and K2 cell culture, protein exaction and western blot manipulation, and semi-quantification analysis. In writing, Shanshan made part of the figures and finished figure modification according to the revision comments.

This manuscript was published in the Journal of American Society of Nephrology (JASN) in 2018.

Caspase-3 is a pivotal regulator of microvascular rarefaction and renal fibrosis after ischemia-reperfusion injury

Bing Yang [1,3,4#], Shanshan Lan [1,3,4#], Mélanie Dieudé [1,3,4], Jean-Paul Sabo-Vatasescu[1], Annie Karakeussian-Rimbaud[1,3,4], Julie Turgeon [1,3,4], Shijie Qi [1,3], Lakshman Gunaratnam [3,5], Natalie Patey [1,2,3,4*]and Marie-Josée Hébert[1,3,4*]

[1]Research centre, Centre hospitalier de l'Université de Montréal (CRCHUM), Montreal, QC, Canada

[2]Department of pathology, CHU Ste-Justine, Université de Montréal, Montreal, QC, Canada.

[3]Canadian National Transplant Research Program

[4]Université de Montréal, Montréal, QC, Canada

[5]London Health Sciences Centre, Schulich School of Medicine and Dentistry, The University of Western Ontario, London, ON, Canada

co-first authors.

[*]**Corresponding authors, both authors contributed equally:**

Marie-Josée Hébert MD, marie-josee.hebert.chum@ssss.gouv.qc.ca

Natalie Patey MD, natalie.patey.hsj@ssss.gouv.qc.ca

Research Centre, Centre hospitalier de l'Université de Montréal (CRCHUM)

900 rue St-Denis, Tour Viger, Montréal, QC, H2X 0X9

Tel: 514-890-8000 ext. 25017, Fax: 514-412-7624

Running title: Importance of caspase-3 in ischemia-reperfusion injury

Word count: abstract 234; text 3214.

Abstract

Ischemia-reperfusion injury (IRI) is a major risk factor of chronic renal failure. Here, we characterize the different modes of programmed cell death in the tubular and microvascular compartments during the various stages of IRI-induced acute kidney injury (AKI) and their relative importance on renal fibrogenesis. Unilateral renal artery clamping for 30 minutes with contralateral nephrectomy was performed in wild-type mice (C57BL/6) or caspase-$3^{-/-}$ mice. In the early stage of AKI, caspase-$3^{-/-}$ mice showed aggravated tubular epithelial cell (TEC) injury with higher urine cystatin C levels, tubular injury scores, and serum creatinine levels compared with the wild type. Electron microscopy, Receptor-interacting serine/threonine-protein kinase 3(RIPK3) immunohistochemistry and phosphorylated RIPK3 levels demonstrated enhanced TEC necroptosis in caspase-$3^{-/-}$ mice. In contrast, microvascular congestion and activation were reduced in the early and extension phases of AKI in caspase-$3^{-/-}$ mice. In the long term, microvascular rarefaction was reduced in caspase-$3^{-/-}$ mice. This was associated with reduced renal fibrosis, decreased expression of α-smooth muscle actin and reduced collagen deposition within peritubular capillaries. Preservation of the peritubular microvasculature in caspase-$3^{-/-}$ mice led to reduced tubular ischemia, with lower hypoxia-inducible factor 1 α (HIF1α) expression and ameliorated tubular injury scores 3 weeks after IRI.

Collectively, these results establish the pivotal importance of caspase-3 in regulating microvascular apoptosis and fibrosis after IRI. These findings also demonstrate the predominant role of microvascular over tubular injury as driver of progressive renal damage and fibrosis after IRI.

Introduction

Acute kidney injury (AKI) is a major risk factor of progressive renal insufficiency. More than 20% of hospitalized adults worldwide experience some level of AKI[1-3] prompted most commonly by ischemia-reperfusion injury (IRI) and sepsis.[4] The severity and number of AKI episodes in various patient cohorts predict progressive long-term renal dysfunction.[3, 5] This association holds true whether or not patients presented renal conditions prior to AKI.[6] Also, in renal transplant patients, AKI at the time of transplantation portends reduced renal allograft survival, independently from the risk of rejection.[7]

Programmed death of tubular epithelial cells is a classical hallmark of AKI.[4] Apoptotic renal tubular cells, as assessed either through TUNEL staining, immunohistochemistry for the effector caspase-3, or electron microscopy, have been highlighted in animal models of AKI and human renal biopsy samples.[8-12] The presence of renal tubular cells with a morphology suggestive of necrosis is also a classical finding in AKI.[13, 14] Although both apoptotic and necrotic tubular epithelial cells are present in the acute phase of AKI, mounting evidence suggests a predominant role for regulated necrosis, or necroptosis, in acute renal dysfunction. Receptor-interacting serine/threonine-protein kinases 1 and 3 (RIPK1 and RIPK3) and mixed lineage kinase domain–like protein (MLKL) regulate necroptosis in various cell types, including renal tubular cells.[15] Inhibition of RIPK3 activation, either through the use of the RIPK1 inhibitor necrostatin or in mice genetically deficient for RIPK3, reduces early renal tubular injury and renal dysfunction in models of IRI or cisplatin-induced AKI.[16, 17] In murine models of IRI followed by renal transplantation, RIPK3$^{-/-}$ kidney allografts showed improved renal function and longer survival post transplantation.[18]

Although tubular epithelial cell injury has been recognized for decades as an important characteristic of AKI, renal microvascular injury is now appreciated as an important contributor to renal dysfunction.[4, 19-21] In the early phase of AKI, endothelial activation, dysfunction, and apoptosis promote inflammatory leukocyte trafficking, complement activation, and thrombosis. The reduced blood flow and vascular congestion that ensue contribute to the extension phase of AKI, producing further epithelial injury. In the long term, loss of peritubular capillaries (PTC) lead to chronic hypoxia, which translates into increased expression of hypoxia inducible factor 1 α (HIF-1α) within tubular epithelial cells, renal fibrosis, and progressive loss of renal function.[4, 22-24] In transplanted kidneys, the magnitude of microvascular involution during the first 3 months following transplantation is a major predictor of long-term renal allograft function.[7]

The molecular pathways and programs that control renal microvascular cell death and involution during the various stages of AKI remain debated. Upregulation of caspase-3, the main effector of apoptosis, has been described in both renal tubular and microvascular endothelial cells in the early stages of IRI-induced AKI.[22, 25] Caspase-3 inactivation with siRNAs prior to IRI yielded contradictory results in different animal models, with both cases of ameliorated and deteriorated renal dysfunction observed following IRI.[25-27] In addition, the relative importance of caspase-3 in the regulation of different modes of cell death within renal tubular and microvascular compartments throughout the early, extension, and pro-fibrotic phases of AKI remains to be characterized.

Here, we used caspase-$3^{-/-}$ mice to delineate the mechanisms of tubular and microvascular damage throughout the various phases of IRI-induced AKI. We report that early tubular injury and renal dysfunction are increased in caspase-$3^{-/-}$ mice, whereas microvascular integrity is

ameliorated throughout the various phases. In the long term, caspase-$3^{-/-}$ mice show reduced microvascular drop-out, decreased tubular ischemia, and reduced interstitial fibrosis, establishing a major role for caspase-3 activation in microvascular rarefaction and renal fibrosis.

Results

Caspase-3 deficiency aggravates early tubular epithelial injury following ischemia-reperfusion

Renal artery clamping for 30 minutes followed by contralateral nephrectomy is a classical model of IRI. Unexpectedly, caspase-$3^{-/-}$ mice showed accentuated renal dysfunction following renal artery clamping (Figure 1). Serum creatinine levels were significantly higher in caspase-$3^{-/-}$mice at day 1 post IRI, and rapidly returned to levels comparable to wild-type mice thereafter (Figure 1A). Renal tubular injury scores were significantly higher at 1 and 2 days post IRI in caspase-$3^{-/-}$ mice (Figure 1B, 1C), suggesting accentuation of tubular injury. Urinary cystatin C was also increased in caspase-$3^{-/-}$ mice at day 1 post-IRI (Figure 1C and Supplementary Figure 1). Immunostaining for KIM-1 also showed significantly increased levels at day 1 post—IRI (Figure 1 D) providing further evidence of enhanced epithelial injury in the absence of caspase-3. Immunostaining for activated caspase-3 was unsurprisingly present in wild-type mice after IRI but not in caspase-3 deficient mice (Supplementary Figure 2). In wild-type mice, the increase in the number of caspase-3 positive cells was not statistically significant when compared to baseline in the first week after IRI (Supplementary Figure 2). Furthermore, influx of CD45+ leukocytes was also higher in caspase-$3^{-/-}$ mice at 1 day post IRI, demonstrating enhanced inflammation in association with increased tubular injury (Supplementary Figure 1b).

Interestingly, influx of CD45+ leukocytes at 2, 3 and 7 days post-IRI were not different between caspase-$3^{-/-}$ mice and wild-type controls.

We then investigated the morphological characteristics of tubular cell death at day 1 post IRI. Light microscopy revealed severe features of acute tubular necrosis in caspase-$3^{-/-}$ mice, particularly renal tubule denudation, tubular dilation caused by tubular cell flattening, and extensive cast formation (Figure 1B). Renal tubular epithelial cell swelling and sloughing were common, suggesting extensive necrotic cell death, whereas nuclear condensation typical of apoptosis was typically absent in caspase-$3^{-/-}$ mice (Figure 1B).

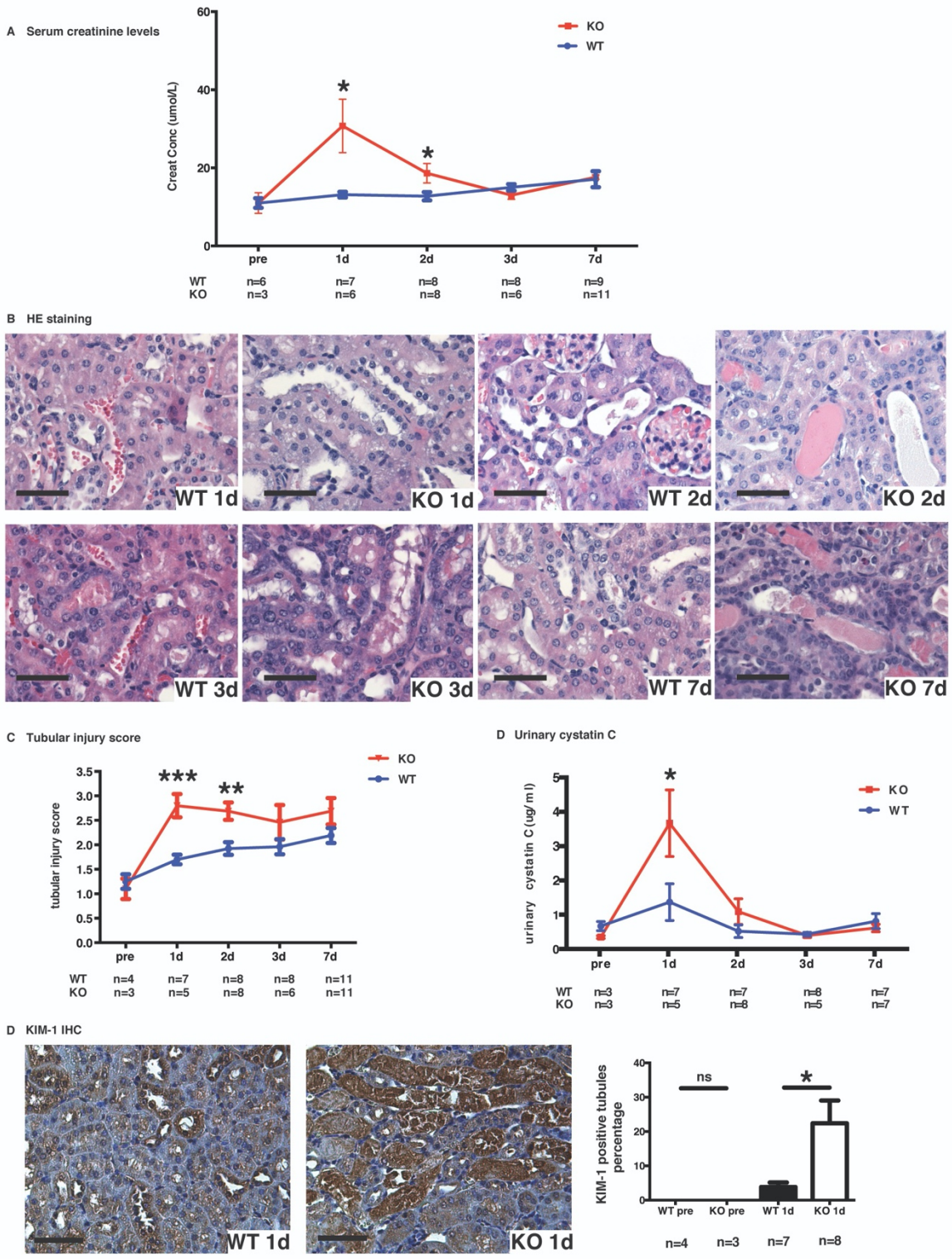

Figure 1: Caspase-3 deficiency aggravates IRI-induced tubular injury.

Electron microscopy confirmed these findings and highlighted the presence of severely damaged tubules containing remnants of tubular epithelial cells detached from the basement membrane in caspase-$3^{-/-}$ mice at 1 day post IRI. Tubular epithelial cells were swollen with degenerative damages in mitochondria, showing intense vacuolization and membrane rupture that are both consistent with necrosis (Figure 2A). In caspase-$3^{-/-}$ mice, there were few, if any, tubular epithelial cells showing ultrastructural features of apoptotic cell death, such as chromatin condensation and fragmentation. In wild-type mice, tubular epithelial cell injury was less prominent and characterized mainly by loss of brush borders and microvilli and basolateral infoldings in the proximal tubules (Figure 2A). These findings suggested enhanced necrosis in tubular epithelial cells of caspase-$3^{-/-}$ mice. To evaluate whether markers of necroptosis, a genetically regulated form of necrosis, were enhanced in caspase-$3^{-/-}$ mice, we performed RIPK3 immunostaining in kidney sections at 1 day post IRI. Indeed, RIPK3 immunostaining was found to be enhanced in damaged tubules, consistent with accentuation of tubular necroptosis in caspase-$3^{-/-}$ mice following IRI (Figure 2B). We also assessed levels of phosphorylated RIPK3 in whole kidney extracts and found significantly increased pRIPK3 levels in caspase-$3^{-/-}$ mice. We also evaluated whether injection of the pan-caspase inhibitor ZVAD-FMK would accentuate AKI in wild-type and caspase-$3^{-/-}$ mice. ZVAD-FMK significantly increased serum creatinine levels at day 1 post-IRI in caspase-$3^{-/-}$ mice but not in wild-type controls (Supplementary Figure 3), suggesting that caspases other than caspase-3 may contribute to the response to IRI in caspase-3 deficient animals. Collectively, these results demonstrate that caspase-3 deficiency increases the propensity to tubular injury in the early stage of IRI-induced AKI by enhancing the activation of the necroptotic response.

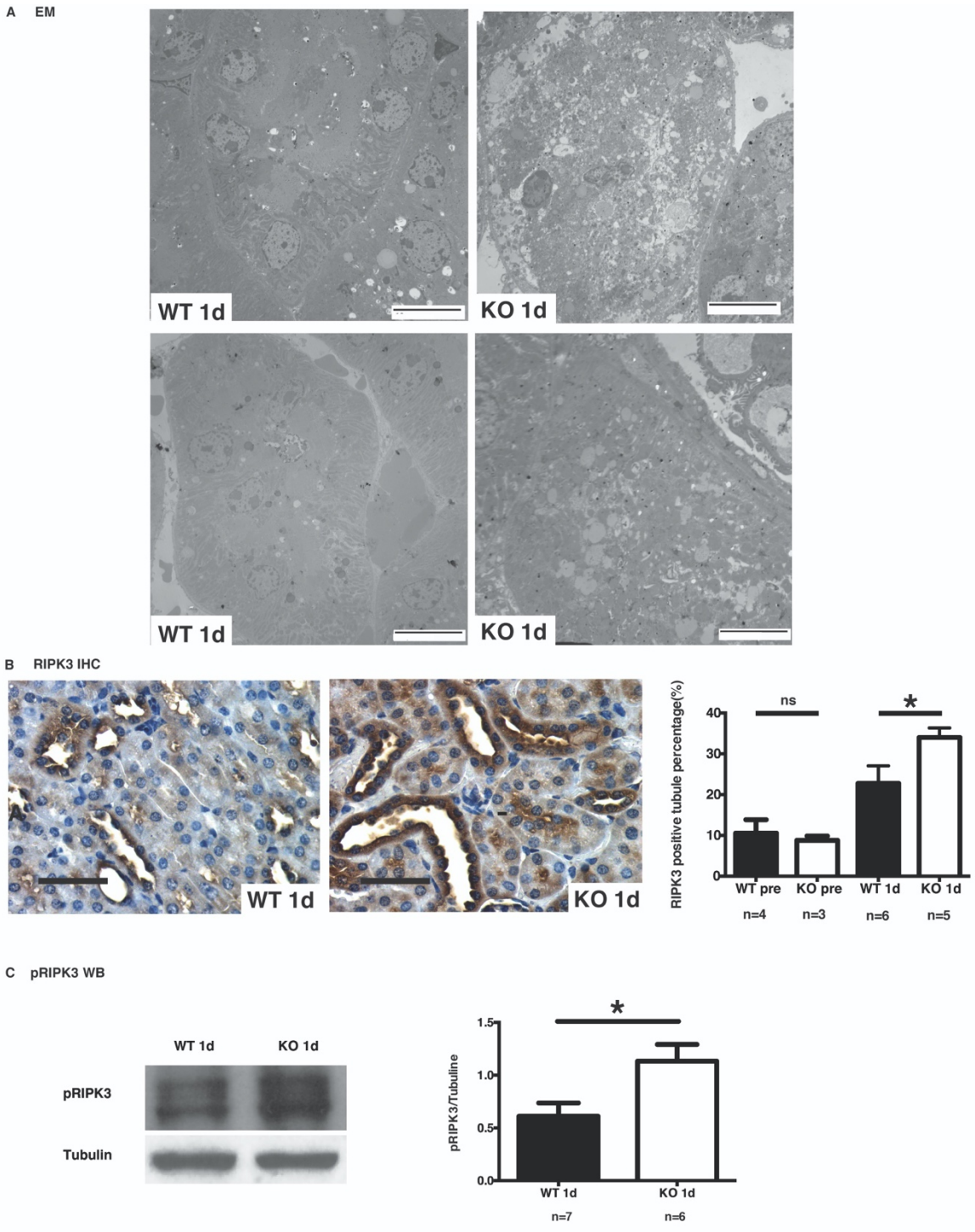

Figure 2: Caspase-3 deficiency increases IRI-induced necroptosis in tubular cells.

Caspase-3 deficiency attenuates microvascular injury and preserves microvascular integrity

We then evaluated whether microvascular endothelial cells were similarly affected by caspase-3 deficiency. Intriguingly, rouleaux formation, a read-out of microvascular congestion, tended to be attenuated in caspase-$3^{-/-}$ mice at days 1 and 2, but was significantly reduced at day 3 (Figure 3A). CD34, a marker of endothelial progenitor cells,[28] was significantly higher 1 day post IRI (Supplementary Figure 4A). There was no difference at baseline in the number of bone marrow CD34+/CD45+ bone marrow cells in caspase-$3^{-/-}$ and wild-type mice (Supplementary Figure 4B). As evidence of better preservation of microvascular integrity in caspase-$3^{-/-}$ mice during the extension phase of AKI, staining of mouse endothelial cell antigen (MECA-32), a marker of microvascular endothelial cells,[29] was found to be significantly increased within peritubular capillaries in caspase-$3^{-/-}$ mice compared to wild-type mice at day 3 post IRI (Figure 3B). Electron microscopy results were also consistent with this observation. Wild-type mice showed widespread signs of peritubular microvascular damage with reduced endothelial fenestration, and irregularities in the endothelium and basement membrane at day 3 post IRI (Figure 3C). In contrast, these changes were uncommon in caspase-$3^{-/-}$ mice, where fenestration of peritubular endothelial cells was preserved (Figure 3C). Collectively, these results suggest that caspase-3 deficiency aggravates tubular injury while concomitantly preserving the integrity of the microvasculature.

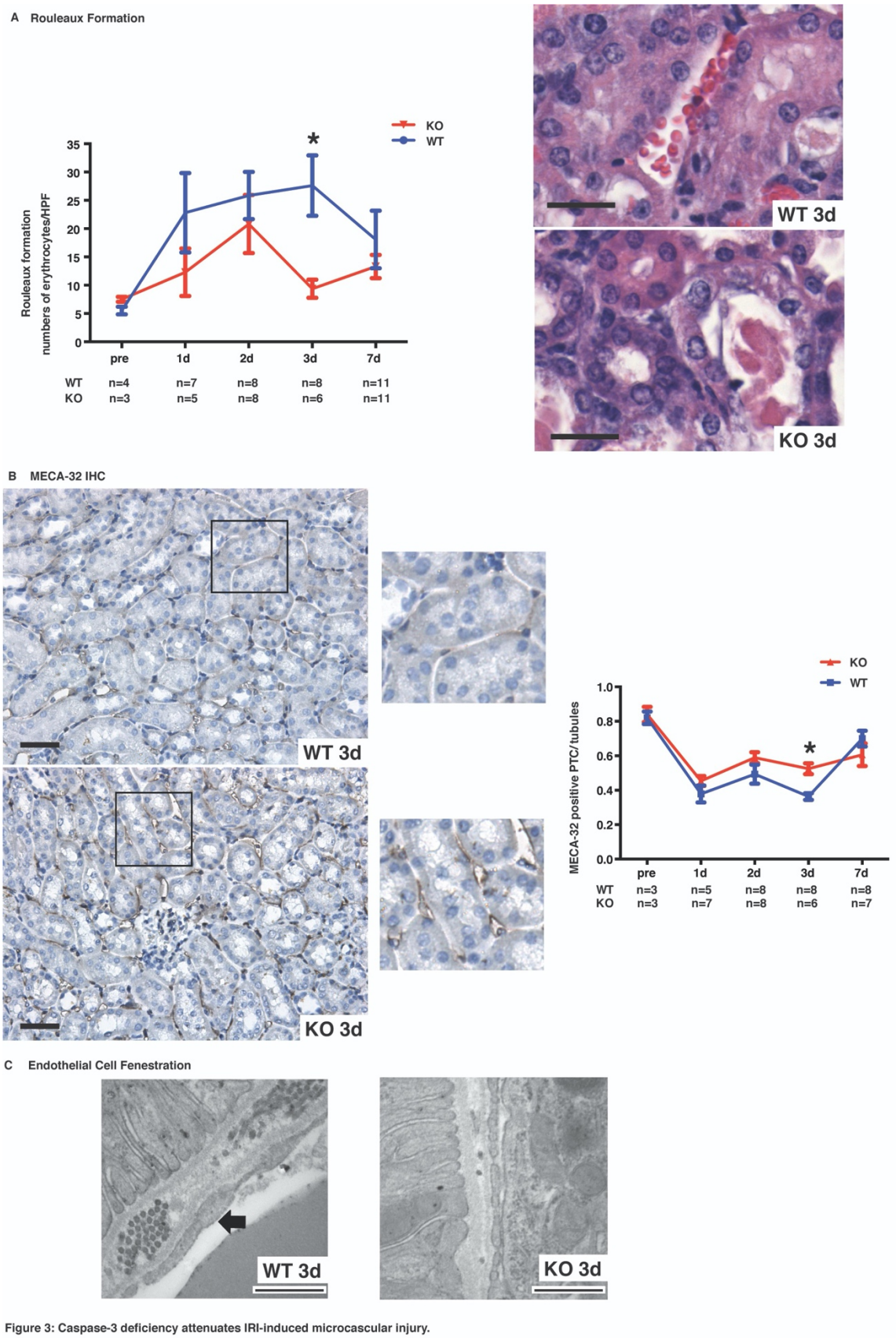

Figure 3: Caspase-3 deficiency attenuates IRI-induced microcascular injury.

To further assess this finding, we evaluated kinetics and modes of cell death in human endothelial and renal tubular epithelial cells exposed to oxygen and nutrient deprivation *in vitro*. Exposure to hypoxia and serum deprivation for 4 hours followed by reoxygenation led to a significant increase in apoptosis in endothelial cells but not in epithelial cells (Figure 8). Only after 24 hours of hypoxia and serum starvation did we find a similar level of apoptosis in renal epithelial cells. However, this was associated with a concomitant and significant increase in the number of necrotic cells (Figure 8C). Silencing caspase-3 in endothelial cells significantly reduced the number of apoptotic cells without increasing necrosis. In epithelial cells however, caspase-3 silencing did not impact levels of apoptosis but significantly increased the number of necrotic cells. Collectively, these results confirm that different types of death programs and different kinetics of cell death are activated in endothelial and renal tubular epithelial cells upon oxygen and serum deprivation.

Caspase-3 deficiency attenuates activation of fibrogenic pathways post IRI

Previously, we showed that caspase-3 activation within apoptotic endothelial cells leads to the release of the fibrogenic mediator connective tissue growth factor (CTGF).[30] Higher circulating levels of CTGF predict renal fibrosis and reduced renal allograft function in renal transplant patients.[31, 32] Consistent with reduced vascular cell damage in caspase-$3^{-/-}$ mice, we found a surge in circulating CTGF levels at day 2 post-IRI whereas CTGF remained stable in caspase-$3^{-/-}$ mice (Figure 4A). Microvascular injury and dysfunction is known to lead to increased α-smooth muscle actin (α-SMA) expression.[33] α-SMA upregulation increased steadily in the first week post-IRI in wild-type mice whereas caspase-$3^{-/-}$ mice showed a slower increase with significantly less peritubular α-SMA staining at day 3 post-IRI (Figure 4B). Collectively, these

results confirm better preservation of microvascular integrity in the early and extension stages of AKI in caspase-$3^{-/-}$ mice.

During the extension and repair phases of AKI, microvascular rarefaction plays a key role in renal fibrogenesis, at least in part through induction of renal tubular ischemia associated with HIF-1α overexpression and activation of downstream fibrogenic pathways.[4, 34, 35] The molecular mechanisms controlling microvascular rarefaction remain ill-defined. We therefore evaluated the impact of caspase-3 invalidation on microvascular rarefaction and fibrogenesis. Collagen deposition, as evaluated with Sirius Red staining, was significantly lower in caspase-$3^{-/-}$ mice at day 7 post IRI compared with wild-type mice. In the latter, intense Sirius Red staining was present within peritubular spaces, whereas glomerular and macrovascular compartments were largely negative (Figure 4C).

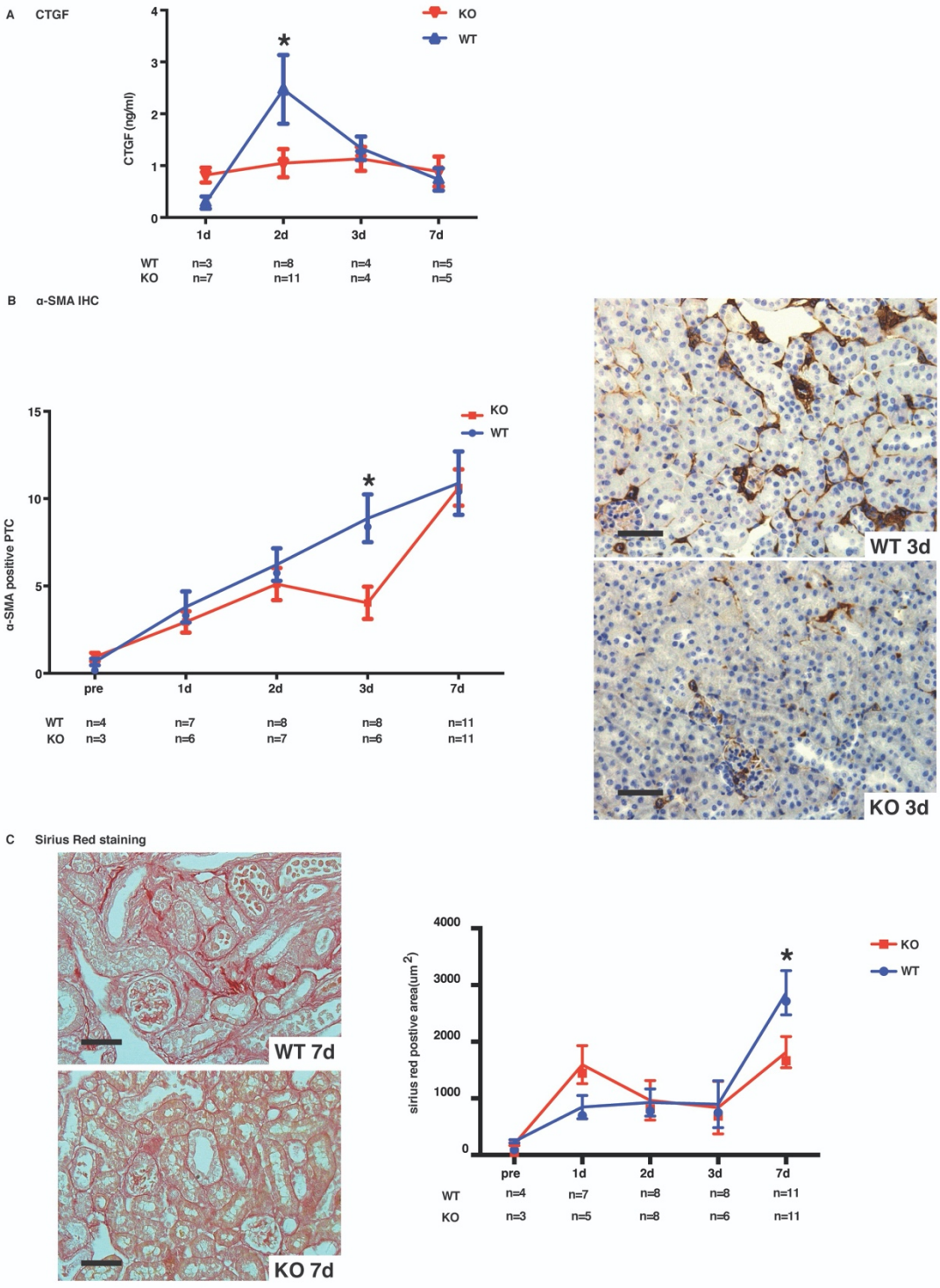

Figure 4: Caspase-3 deficiency attenuates IRI-induced upregulation of pro-fibrotic markers.

Electron microscopy also highlighted preservation of microvascular integrity in caspase-3$^{-/-}$ mice (Figure 6). In wild-type mice, peritubular capillaries showed characteristic apoptotic ultrastructural changes within peritubular capillaries, such as chromatin condensation and formation of apoptotic bodies (Figure 6). These changes were absent in caspase-3$^{-/-}$ mice. In addition, αSMA staining within peritubular capillaries was significantly reduced in caspase-3$^{-/-}$ mice, consistent with better microvascular homeostasis and reduced fibrogenesis (Figure 5B). α-SMA levels in whole kidney extracts were also evaluated by western blotting and confirmed reduced α-SMA levels in caspase-3$^{-/-}$ mice (Figure 5C and Supplementary Figure 5B). We also evaluated whether increased α-SMA staining was present specifically in peritubular capillaries or whether other components of the vascular compartment, such as glomeruli, were affected. Peritubular α-SMA staining increased over time in wild-type mice whereas caspase-3$^{-/-}$ mice showed a slower increase in α-SMA levels with significantly lower levels at day 21 post-IRI compared to wild-type mice. The kinetics of glomerular α-SMA staining were however similar at all time points in caspase-3$^{-/-}$ mice and wild-type controls. This suggested a major role for caspase-3 within peritubular capillaries but not in glomeruli. In support of this conclusion, Sirius Red staining was also significantly reduced within peritubular capillaries in caspase-3$^{-/-}$ mice, indicating reduced collagen deposition (Figure 5D). Collectively, these results demonstrate a sustained advantage for caspase-3$^{-/-}$ mice in preserving the integrity of the peritubular capillary network and reducing fibrosis after IRI, and highlight a novel role for caspase-3 in the regulation of microvascular rarefaction.

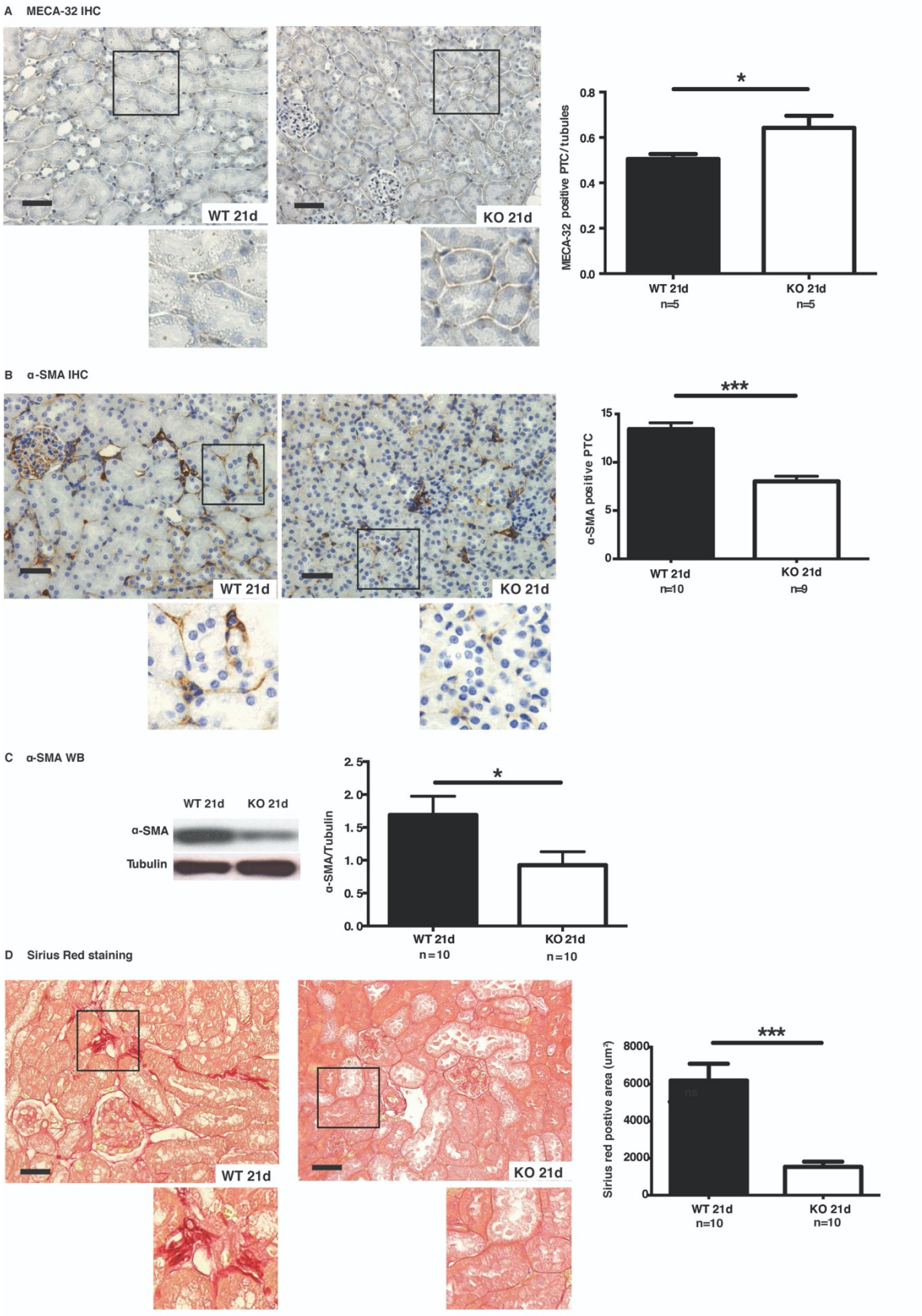

Figure 5: Caspase-3 deficiency attenuates IRI-induced microvascular rarefaction and fibrosis.

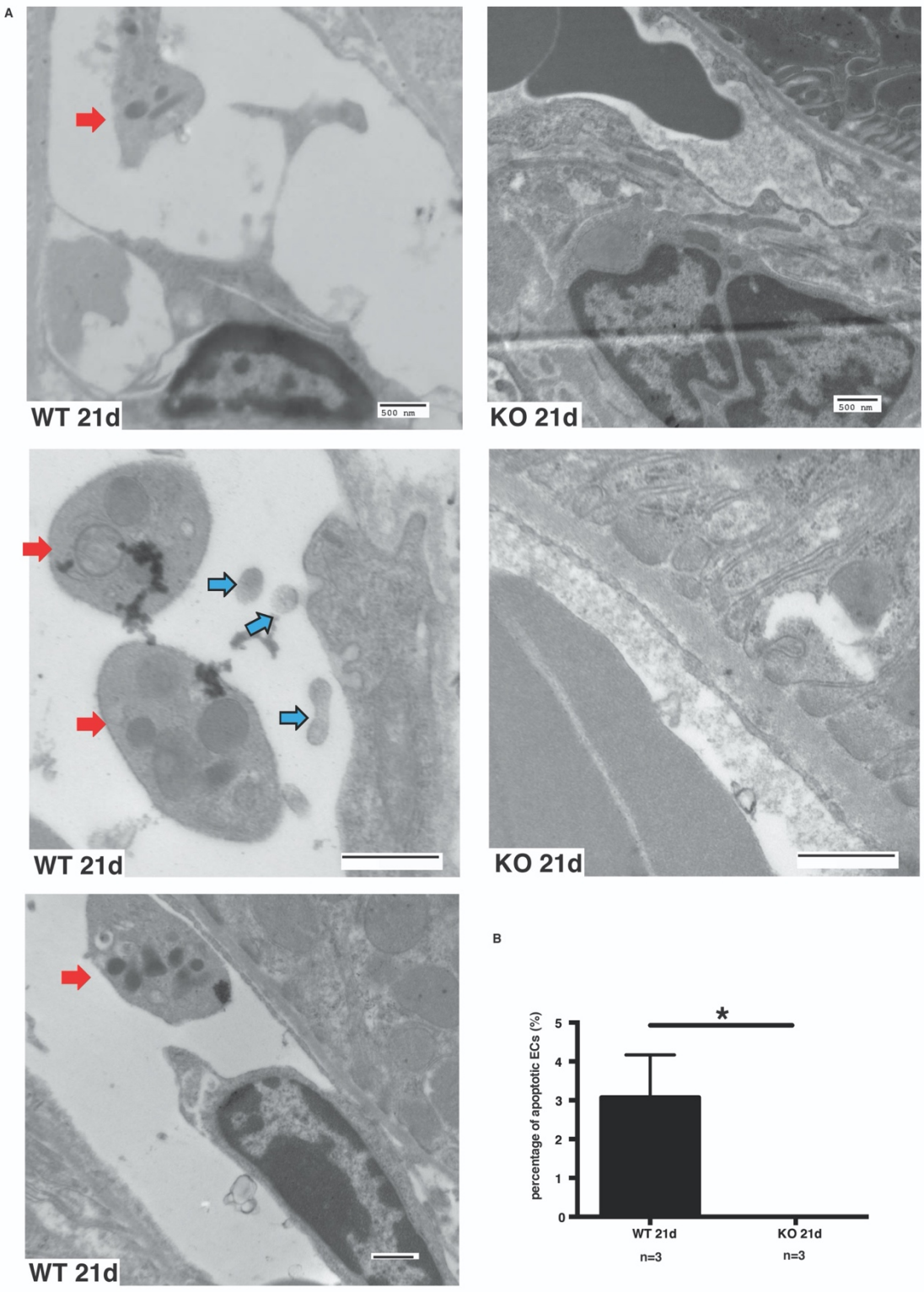

Figure 6: Caspase-3 deficiency prevents IRI-induced long-term renal endothelial cell death.

Microvascular drop-out can lead to a state of tubular ischemia characterized by HIF-1α overexpression, which in turn favors tubular atrophy and renal dysfunction.[34] We found that expression of tubular HIF-1α was significantly reduced in caspase-$3^{-/-}$ mice at 21 days post IRI (Figure 7A,B and Supplementary Figure 6A). Western blots for HIF-1α in whole kidney extracts confirmed significantly reduced HIF-1α levels in caspase-$3^{-/-}$ mice at day 21 post-IRI (Figure 7B). Immunostaining for activated caspase-3 showed that the number of caspase-3 positive cells was maximal at day 21 post-IRI in wild-type mice, suggesting persistent cell death over time (Supplementary Figure 2). Tubular injury scores rose steadily after IRI in wild-mice whereas caspase-$3^{-/-}$ mice showed a sharper decline after the initial surge with significantly lower levels at day post-IRI compared to wild-type mice (Supplementary Figure 6B). Serum creatinine levels were not different in wild-type and caspase-$3^{-/-}$ mice at day 21 post-IRI highlighting the known lack of sensitivity of creatinine as a biomarker of renal fibrosis.[14] Collectively, these results suggest that preservation of microvascular integrity in caspase-3–deficient mice with lower levels of tubular ischemia in the long term benefits tubular homeostasis and prevents peritubular fibrosis (Figure 9).

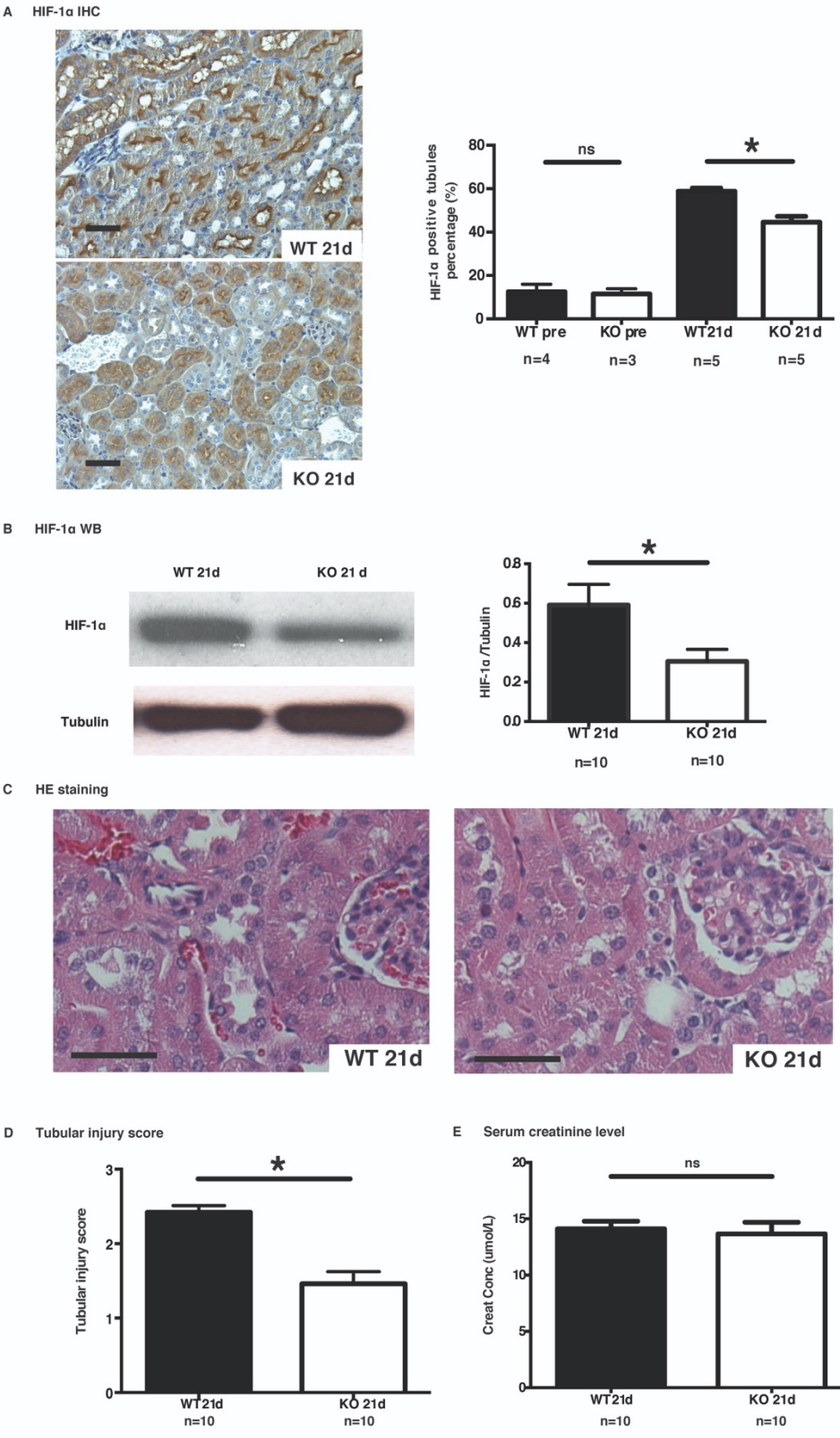

Figure 7: Caspase-3 deficiency prevents IRI-induced long-term tubular injury.

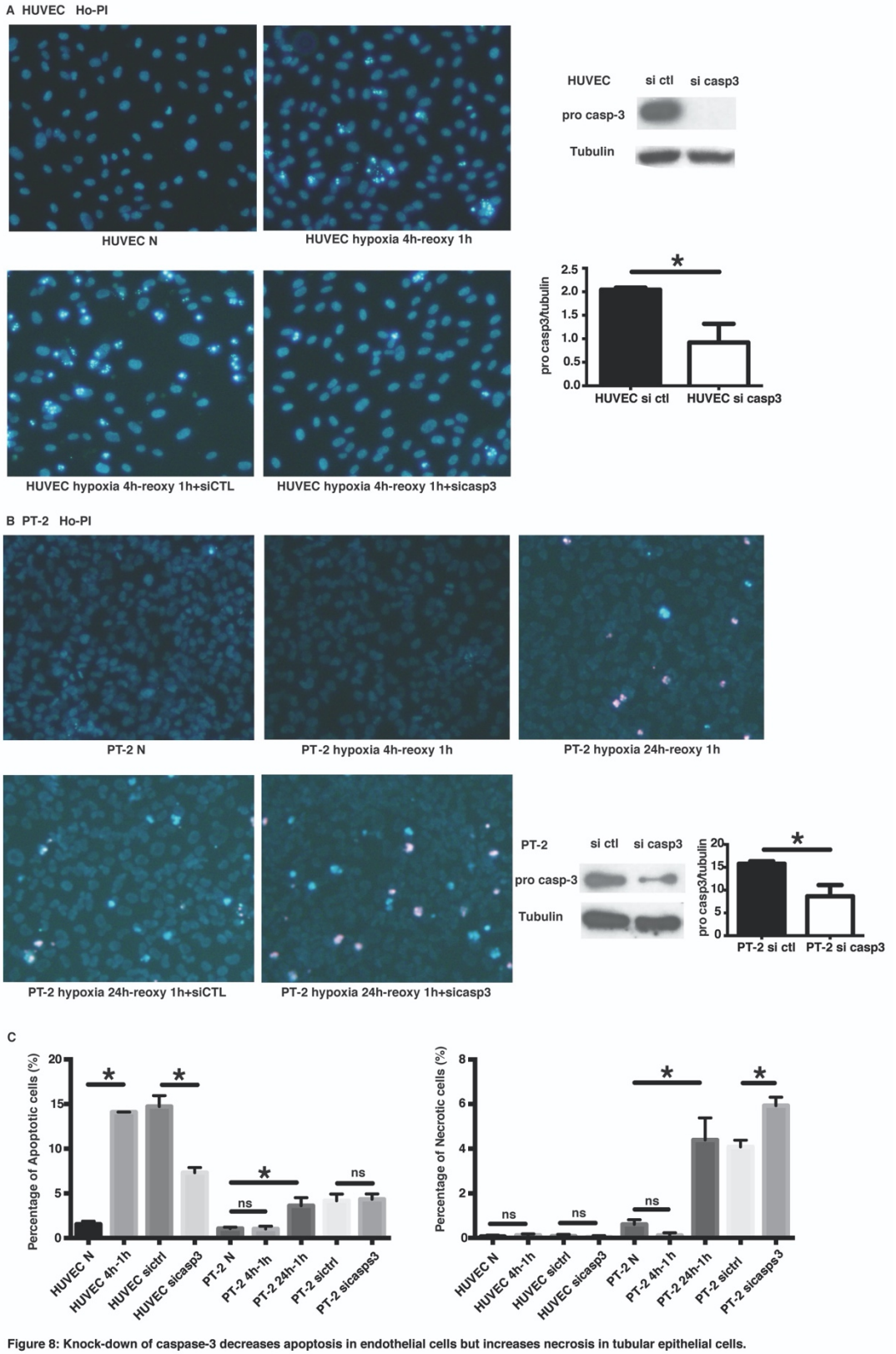

Figure 8: Knock-down of caspase-3 decreases apoptosis in endothelial cells but increases necrosis in tubular epithelial cells.

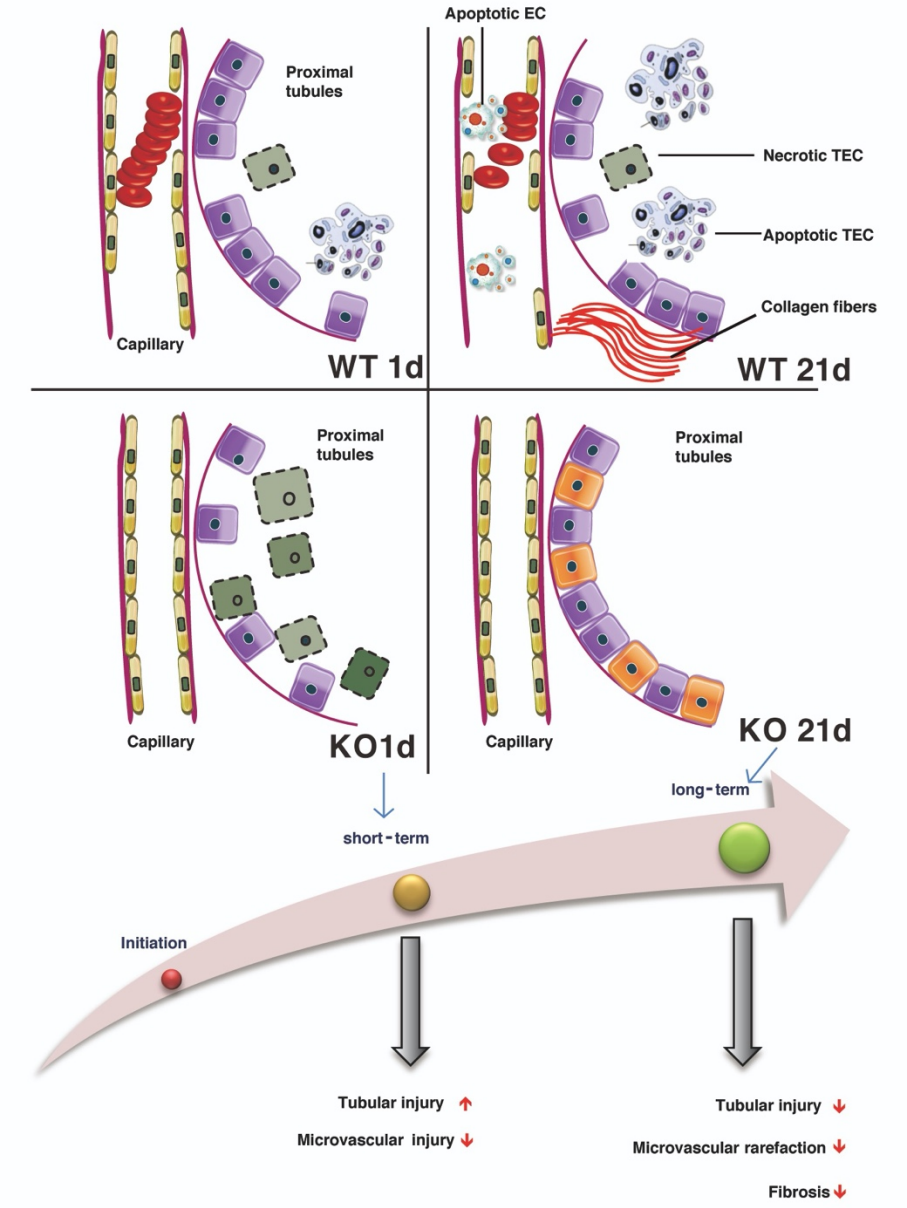

Figure 9: Caspase-3 is a pivotal regulator of peritubular capillary rarefaction and renal dysfunction.

Discussion

IRI is one of the most common causes of AKI and a major risk factor for chronic renal failure. In this study, we identified caspase-3 as a central regulator of peritubular capillary injury and microvascular rarefaction and fibrosis post IRI.

Intriguingly, our results showed a deleterious impact of caspase-3 invalidation on renal function and tubular epithelial cell injury in the early stage of AKI. Caspase-$3^{-/-}$ mice displayed enhanced tubular injury scores, increased urinary cystatin C, increased KIM-1 levels, and deteriorated serum creatinine at 1 day post IRI. We demonstrated that, by electron microscopy RIPK3 staining and evaluation of phosphorylated RIPK3 levels, that absence of caspase-3 redirects tubular cell death towards necroptosis. These results are consistent with mounting evidence highlighting a major role for necroptosis as the predominant type of renal tubular demise in the early stage of AKI.[13, 15, 36, 37] Our results also highlight that failure to activate tubular apoptosis upon IRI favors RIPK3 activation and leads to accentuated renal dysfunction in the early stage of AKI.

However, the present results are in stark contrast with a previous report by Zhang et al describing a protective role for small interfering RNA (siRNA) targeting caspase-3 when infused intravenously prior to renal IRI.[25] One major difference between the two studies is the method of caspase-3 invalidation. It is possible that intravenous infusion of caspase-3 siRNA prior to IRI in the study by Zhang could have led to preferential caspase-3 silencing within the vasculature. The relative levels of caspase-3 silencing in renal tubules compared with the microvasculature were not addressed in the study by Zhang. Nonetheless, this prompted us to evaluate the relative contributions of caspase-3 in both cellular compartments in our system.

In the early stage of AKI, caspase-3$^{-/-}$ mice showed enhanced tubular injury, yet reduced microvascular damage as demonstrated by rouleaux formation, staining for CD34, and MECA-32 and electron microscopy. Collectively, our results highlight different modes of regulated cell death in renal tubules compared with peritubular capillaries after IRI. Whereas necroptotic pathways have been shown to play a predominant role in regulated epithelial cell death post IRI,[16, 36] our results show that microvascular endothelial cell injury occurs through apoptosis and is under the control of caspase-3. Necroptosis does not represent a major default death pathway for vascular cells, since the absence of caspase-3 does not enhance mode of cell death within the vascular compartment after IRI and does not favor the development of necrotic cell death upon exposure to oxygen and serum deprivation *in vitro*. This highlights the complexity and potential cross-talk between various modes of cell death. For example, caspase-3 is a classic effector of apoptosis but in certain condition can also trigger necrosis by cleaving the gasdermin GSDME.[38] Also, caspases are increasingly appreciated as regulators of multiple functions in addition to cell death, such as cellular remodeling, stem cell fate determination, spermatogenesis, and erythroid differentiation.[39] In the present study, we demonstrated reduced endothelial peritubular cell death in caspase-3 deficient mice. However, this does not exclude the potential contribution of other caspase-3 dependent pathways in the preservation of peritubular capillary density. Whether absence of caspase-3 could favor progenitor cell trafficking and microvascular repair is a possibility that will be addressed in future studies.

Another important finding that stems from this study is the different impact of tubular versus endothelial cell death on progressive renal dysfunction. Progression from AKI to chronic kidney disease (CKD) is a common clinical event. Large cohort studies have highlighted the robust predictive impact of AKI on risk of chronic renal failure.[6] Although the precise cellular

mechanisms explaining the major role of AKI in progressive renal failure are still debated, most clinical studies have identified diabetes, hypertension, severity of AKI, and preexisting CKD as predictors of CKD. Notably, these predictors are all major cardiovascular risk factors, suggesting a relationship between vascular vulnerability and progressive renal dysfunction post IRI. The present results now provide molecular and cellular insights into the pathways controlling microvascular injury and the major role of caspase-3 dependent microvascular injury in long-term renal dysfunction after IRI. The presence of increased tubular damage concomitant with microvascular protection early after IRI in caspase-$3^{-/-}$ mice allowed us to discriminate the relative importance of both cell compartments in progressive renal dysfunction. Early accentuation of renal tubular injury did not portend negative long-term renal outcomes in caspase-$3^{-/-}$ mice. Preservation of microvascular integrity was present both in the early and late phases of AKI in caspase-$3^{-/-}$ mice. This translated into reduced levels of fibrogenic markers, such as circulating CTGF levels, renal α-SMA expression, and collagen deposition. In late stages, better preservation of microvascular integrity protected tubules from ischemia, with reduced HIF-1α expression, reduced apoptosis and tubular injury scores. These results are in keeping with recent elegant studies demonstrating a pivotal role for peritubular capillary damage in progressive renal fibrosis and dysfunction.[29, 40] In various experimental models, including IRI, progressive renal disease was associated with the development abnormal ultrastructural findings in peritubular capillaries such as widening of the subendothelial space, reduced numbers of fenestration and increased thickness of the basement membrane. Increased microvascular permeability was also described. These results and the present work suggest that upon renal injury the peritubular microvasculature undergoes significant ultrastructural and functional changes of importance in the development of fibrosis. [29, 40]

Collectively, our results provide novel insights into the molecular mechanisms controlling microvascular drop-out, and identify caspase-3 as a novel and pivotal upstream regulator of microvascular rarefaction and renal fibrogenesis after IRI. They also demonstrate a predominant role for microvascular versus epithelial injury in regulating the development of fibrosis following renal IRI.

Concise methods

Animals and Surgical Procedures:

6-to-8-week–old female C57BL/6 mice were purchased from Charles River Laboratories (Wilmington, MA, USA). CASP3-deficient mice on C57BL/6 congenic background, aged 6 to 8 weeks, were derived from breeding pairs of heterozygous CASP3-deficient (B6.129S1-C3t^{m1Flv}/J) mice obtained from Jackson Laboratory (JAX stock #006233, Bar Harbor, Me). Generation of these mice was previously described[41]. These homozygotes mice are viable, reach adulthood, and show a variety of hyperplasias and disorganized cell deployment in the brain [42]. They are also congenitally deaf [43] and have cataracts at the anterior lens pole [44]. All mice were kept in 12-hour light/dark cycles, with normal food provided ad libitum. All mice were kept in 12-hour light/dark cycles, with normal food provided ad libitum. IRI was performed as described previously.[45] Briefly, 2% isoflurane inhalation was used as anesthesia, and mice were then fixed on a heating blanket (37 ℃). After opening the abdominal cavity via midline incision, a micro-aneurysm clip was placed on the left renal pedicle. Complete ischemia was indicated by color change of the kidney from red to dark purple. After 30 minutes, the micro-aneurysm clip was released, and the right kidney was removed. Mice were sacrificed at day 1, 2, 3, 7, or 21 post surgery; the left kidneys, sera, and urine were collected. All the animal experimental

protocols were reviewed and approved by the Centre hospitalier de l'Université de Montréal (CRCHUM) Comité Institutionnel de Protection des Animaux (CIPA).

Flow cytometry

Mouse bone marrow was collected on WT(C57BL/6) and Caspase $3^{-/-}$ mice as described. Single-cells suspensions were then immediately stained for flow cytometry[46]. All of the experiments were performed on BD LSRII flow cytometer (Becton Dickinson, San Jose, CA, USA). Viable cells were gated using Live/dead Fixable aqua dead cell stain kit (Aquavid) (Molecular probes, Eugene, OR, USA), CD34+ CD45+ progenitor cells were determined by using anti-mouse CD34-BV421 (BD Bioscience, San Jose, CA, USA) and anti-mouse CD45-APC (BD Bioscience, San Jose, CA, USA). All data were analyzed with FlowJo software 10.0 (Ashland, OR, USA). Results were expressed as the percentage of CD34+CD45+ cells among viable bone marrow cells.

Biochemical Evaluation of Renal Function

Serum Creatinine:

Serum creatinine levels were determined using Vitro CREA Slides and Vitro Chemistry Products (Vitro 250/350 Chemistry System; Ortho Clinical Diagnostics; Raritan, NJ, USA).

Histopathological Examination

Tubular Injury Score:

Tubular injury score was estimated in hematoxylin and eosin (H&E)–stained renal tissue, as described previously.[47] Renal tubular damage was graded on six levels based on the loss of brush

border, tubular dilation, cast formation, tubular necrosis, and neutrophil infiltration. Ten high-power fields (200X) were chosen randomly, five of them were taken in the renal cortex and five at the cortico-medullary junction, and each field was scored from 0 to 5 (0: normal; 1: mild injury, involvement of 0%-10%; 2: moderate injury, involvement of 11%-25%; 3: severe injury, involvement of 26%-49%; 4: high severe injury, involvement of 50%-75%; 5: extensive injury, involvement of >75%). All assessments were done by two investigators blinded to experimental conditions.

Peritubular Capillary Vascular Congestion:

On H&E-stained sections, numbers of aggregated erythrocytes inside peritubular capillaries were counted in ten randomly chosen high-power fields by two investigators blinded to experimental conditions.

Immunohistochemistry

Ischemic kidneys were retrieved without perfusion pre-surgery or at days 1, 2, 3, 7, and 21 post-surgery, fixed in 10% formalin, embedded in paraffin, and subsequently cut into 4-µm slices. Immunohistochemistry staining was performed on paraffin-embedded slices as described previously.(40) The antibodies used in this study were KIM-1 (1/8; R&D systems; Minneapolis, USA), RIPK3 (1/500; Abcam; Toronto, Canada), MECA-32 (1/20; Biolegend; San Diego, USA), HIF-1α (1/500; Abcam; Toronto, Canada), α-SMA (1/500; clone 1A4; Dako), CD45 (1/60,BD Bioscience, San Jose, CA, USA), CD34 (pre-diluated, Dako QBend10 IR632) VCAM-1 (1/200; Abcam; Toronto, Canada) and caspase-3 (1/50; Biocare Medical; Pacheco, USA). For all immunohistochemistry stainings, 5 randomly chosen high power fields (magnification 200X) were captured using the Leica DM4000B microscope (Leica

Microsystems; Germany) per mice. Quantifications were done by two investigators blinded to experimental conditions.

Sirius Red Staining:

Sirius Red staining was carried out using the Picro Sirius Red Stain Kit (Abcam; Toronto, Canada) according to the manufacturer ‘s instructions.

5 randomly chosen high power fields (magnification 200X) were captured using the Leica DM4000B microscope (Leica Microsystems; Germany) per mice. Quantification was performed with ImageJ (NIH; USA) by two investigators blinded to experimental conditions.

Electron Microscopy Examination

Renal tissue was cut into small pieces that were fixed with 3% glutaraldehyde, post-fixed with 1% osmium tetroxide, and incubated consecutively in an ascending acetone series (50%, 70%, and 90%), with a final incubation in 100% ethanol for hydration. After incubation in acetone, the tissue was embedded in Epon. 1-nm sections were cut and stained using uranyl acetate and lead citrate. Electron microscopy images were taken with the Phillips EM208 electron microscope.

Enzyme-Linked Immunosorbent Assay

Serum levels of connective tissue growth factor (CTGF) and urinary levels of cystatin C were determined using the following commercial enzyme-linked immunosorbent assay (ELISA) kits according to the manufacturer’s instructions: mouse CTGF (Elabscience; E-EL-M0340; Bethesda, USA), and mouse Cystatin C (Abcam; ab201280; Toronto, Canada).

Cell culture and small interfering RNAs

Human umbilical vascular endothelial cells (HUVEC, cat# 200p-05n) were purchased from Cell application Inc (San Diego, US) and then were grown in endothelial cell basal medium (Lonza, CC-3121, Basel, Switzerland) and used at passages three through four. PT-2 tubular epithelial cells (TECs) (kind gift of A Jevnikar) is a human renal tubular cell line isolated and cloned from centrifuged urine, which was obtained from a transplant recipient undergoing acute rejection .[48] Morphologically, PT-2 cells have a typical proximal tubular cell-like shape. They are γ GTP+, cytokeratin+ vimentin+ with high alkaline phosphatase activity, which are characteristic of epithelialcells. However, the expression of E-cadherin and aminopeptidase N (CD13) in PT-2 cells are low.[48]

PT-2 cells were cultured in a medium that is constituted with following products [Dulbecco's modified Eagle's medium (DMEM): Hams F12] (50:50) (Invitrogen-Gibco, Carlsbad, CA, USA), 5% fetal bovine serum (Invitrogen, Waltham, USA), hormone mix [5 μg/mL insulin, 1.25 ng/mL prostaglandin E1, 34 pg/mL triiodothyronine, 5 μg/mL transferrin, 1.73 ng/mL sodium selenite and 18 ng/mL of hydrocortisone] and 25 ng/mL epidermal growth factor.

For hypoxia-reoxygenation treatment, HUVECs and PT-2 cells were grown in normal medium till 90% confluence, then exposed to serum-free (SS) medium (RPMI, Gibco, Carlsbad, CA, USA) in a hypoxia incubator (5% O_2, 5% CO_2, 90% N_2), for 4 hours or 24 hours, respectively. The cells were then changed with normal medium and incubate in normal oxygen incubator (21% O2, 5% CO2, 74% N2) for one hour.

For Caspase-3 silencing, HUVECs and PT-2 cells grown in normal conditions were transfected with siCaspase-3 (Dharmacon, L-004307-00-0005), or siControl (Dharmacon, D-001810-03). We used the MATra si Reagent (iba Solutions for Life Sciences, Goettingen, Germany)

according to the manufacturer's guidelines. The final concentrations of siRNAs were 12nM for HUVECs and 18nM for PT-2 cells.

Fluorescence microscopy to quantify the cells with chromatin condensation and cell membrane permeabilization

Epifluorescence microscopy was performed using unfixed/unpermeabilized adherent cells. Cells were stained with Hoechst 33342 (2′-(4-ethoxyphenyl)-5-(4-methyl-1-piperazinyl)-2.5′-bi-1H-benzimidazole) (Ho, Sigma Aldrich,ON,CA) and propidium iodide (PI, Invitrogen, Waltham, USA), as has been previously described.[49]

Immunoblotting

Homogenized renal tissue and cell lysate were separated onto 12 or 15% SDS-PAGE gels, transferred onto nitrocellulose or polyvinylidene difluoride (for pro-caspase-3 detection) membranes then probed by the following antibodies: Anti-RIP3 (phospho S227) (Abcam; Toronto, Canada), HIF-1α (Abcam; Toronto, Canada), α-SMA (clone 1A4; Dako), pro-Caspase 3 (Invitrogen, Waltham, USA).

Statistics

All data were expressed as means ± standard error of the mean (SEM). Comparisons between groups were conducted with the unpaired Student's *t*-test using Prism 5 (GraphPad Software Inc.), where $P < 0.05$ was considered significant for all tests.

Acknowledgments

This work was supported by research grants from the Canadian Institutes of Health Research (CIHR) (MOP-123436 and PJT-148884), B.Y. is a recipient of a research fellowship from the University of Montreal Nephrology Research Consortium and a CNTRP student. SL is a recipient of Merit scholarship for foreign students from Fonds de recherche du Québec – Nature et technologies (FRQNT) and CNTRP student. M.J.H. is the holder of the Shire Chair in Nephrology, Transplantation and Renal Regeneration of l'Université de Montréal. We thank the J.-L. Levesque Foundation for renewed support. The authors would like to thank Antony M. Jevnikar from the Lawson Health Research Institute (Western University, London, Ontario) who kindled provided PT-2 cells. We thank the CHUM Research Centre's cytometry, cell imaging and molecular pathology core facility for their technical help, and Ms. Josée-Marie Dubé for helping taking electron microscopy photos.

Disclosures

none.

References

1. Susantitaphong, P, Cruz, DN, Cerda, J, Abulfaraj, M, Alqahtani, F, Koulouridis, I, Jaber, BL: World incidence of AKI: a meta-analysis. *Clin J Am Soc Nephrol,* 8**:** 1482-1493. doi: 1410.2215/CJN.00710113. Epub 00712013 Jun 00710116., 2013.

2. Bedford, M, Farmer, C, Levin, A, Ali, T, Stevens, P: Acute kidney injury and CKD: chicken or egg? *Am J Kidney Dis,* 59**:** 485-491. doi: 410.1053/j.ajkd.2011.1009.1010., 2012.

3. Ishani, A, Xue, JL, Himmelfarb, J, Eggers, PW, Kimmel, PL, Molitoris, BA, Collins, AJ: Acute kidney injury increases risk of ESRD among elderly. *J Am Soc Nephrol,* 20**:** 223-228. doi: 210.1681/ASN.2007080837. Epub 2007082008 Nov 2007080819., 2009.

4. Molitoris, BA: Therapeutic translation in acute kidney injury: the epithelial/endothelial axis. *J Clin Invest,* 124**:** 2355-2363. doi: 2310.1172/JCI72269. Epub 72014 Jun 72262., 2014.

5. Amdur, RL, Chawla, LS, Amodeo, S, Kimmel, PL, Palant, CE: Outcomes following diagnosis of acute renal failure in U.S. veterans: focus on acute tubular necrosis. *Kidney Int,* 76**:** 1089-1097. doi: 1010.1038/ki.2009.1332. Epub 2009 Sep 1089., 2009.

6. Lo, LJ, Go, AS, Chertow, GM, McCulloch, CE, Fan, D, Ordonez, JD, Hsu, CY: Dialysis-requiring acute renal failure increases the risk of progressive chronic kidney disease. *Kidney Int,* 76**:** 893-899. doi: 810.1038/ki.2009.1289. Epub 2009 Jul 1029., 2009.

7. Steegh, FM, Gelens, MA, Nieman, FH, van Hooff, JP, Cleutjens, JP, van Suylen, RJ, Daemen, MJ, van Heurn, EL, Christiaans, MH, Peutz-Kootstra, CJ: Early loss of peritubular capillaries after kidney transplantation. *J Am Soc Nephrol,* 22**:** 1024-1029. doi: 1010.1681/ASN.2010050531. Epub 2010052011 May 2010050512., 2011.

8. Nogae, S, Miyazaki, M, Kobayashi, N, Saito, T, Abe, K, Saito, H, Nakane, PK, Nakanishi, Y, Koji, T: Induction of apoptosis in ischemia-reperfusion model of mouse kidney: possible involvement of Fas. *J Am Soc Nephrol,* 9**:** 620-631., 1998.

9. Toronyi, E, Lord, R, Bowen, ID, Perner, F, Szende, B: Renal tubular cell necrosis and apoptosis in transplanted kidneys. *Cell Biol Int,* 25**:** 267-270., 2001.

10. Jaffe, R, Ariel, I, Beeri, R, Paltiel, O, Hiss, Y, Rosen, S, Brezis, M: Frequent apoptosis in human kidneys after acute renal hypoperfusion. *Exp Nephrol,* 5**:** 399-403., 1997.

11. Havasi, A, Borkan, SC: Apoptosis and acute kidney injury. *Kidney Int,* 80**:** 29-40. doi: 10.1038/ki.2011.1120. Epub 2011 May 1011., 2011.

12. Kishino, M, Yukawa, K, Hoshino, K, Kimura, A, Shirasawa, N, Otani, H, Tanaka, T, Owada-Makabe, K, Tsubota, Y, Maeda, M, Ichinose, M, Takeda, K, Akira, S, Mune, M: Deletion of the kinase domain in death-associated protein kinase attenuates tubular cell apoptosis in renal ischemia-reperfusion injury. *J Am Soc Nephrol,* 15**:** 1826-1834., 2004.

13. Kers, J, Leemans, JC, Linkermann, A: An Overview of Pathways of Regulated Necrosis in Acute Kidney Injury. *Semin Nephrol,* 36**:** 139-152. doi: 110.1016/j.semnephrol.2016.1003.1002., 2016.

14. Moledina, DG, Parikh, CR: Phenotyping of Acute Kidney Injury: Beyond Serum Creatinine. *Seminars in Nephrology,* 38**:** 3-11.

15. Linkermann, A, Chen, G, Dong, G, Kunzendorf, U, Krautwald, S, Dong, Z: Regulated cell death in AKI. *J Am Soc Nephrol,* 25**:** 2689-2701, 2014.

16. Linkermann, A, Brasen, JH, Himmerkus, N, Liu, S, Huber, TB, Kunzendorf, U, Krautwald, S: Rip1 (receptor-interacting protein kinase 1) mediates necroptosis and contributes to renal ischemia/reperfusion injury. *Kidney Int,* 81**:** 751-761. doi: 710.1038/ki.2011.1450. Epub 2012 Jan 1011., 2012.

17. Xu, Y, Ma, H, Shao, J, Wu, J, Zhou, L, Zhang, Z, Wang, Y, Huang, Z, Ren, J, Liu, S, Chen, X, Han, J: A Role for Tubular Necroptosis in Cisplatin-Induced AKI. *J Am Soc Nephrol,* 26**:** 2647-2658. doi: 2610.1681/ASN.2014080741. Epub 2014082015 Mar 2014080718., 2015.

18. Lau, A, Wang, S, Jiang, J, Haig, A, Pavlosky, A, Linkermann, A, Zhang, ZX, Jevnikar, AM: RIPK3-mediated necroptosis promotes donor kidney inflammatory injury and reduces allograft survival. *Am J Transplant,* 13**:** 2805-2818. doi: 2810.1111/ajt.12447. Epub 12013 Sep 12418., 2013.

19. Sharfuddin, AA, Molitoris, BA: Pathophysiology of ischemic acute kidney injury. *Nat Rev Nephrol,* 7**:** 189-200. doi: 110.1038/nrneph.2011.1016. Epub 2011 Mar 1031., 2011.

20. Basile, DP: The endothelial cell in ischemic acute kidney injury: implications for acute and chronic function. *Kidney Int,* 72**:** 151-156. Epub 2007 May 2002., 2007.

21. Basile, DP, Friedrich, JL, Spahic, J, Knipe, N, Mang, H, Leonard, EC, Changizi-Ashtiyani, S, Bacallao, RL, Molitoris, BA, Sutton, TA: Impaired endothelial proliferation and mesenchymal transition contribute to vascular rarefaction following acute kidney injury. *Am J Physiol Renal Physiol,* 300**:** F721-733. doi: 710.1152/ajprenal.00546.02010. Epub 02010 Dec 00541., 2011.

22. Horbelt, M, Lee, SY, Mang, HE, Knipe, NL, Sado, Y, Kribben, A, Sutton, TA: Acute and chronic microvascular alterations in a mouse model of ischemic acute kidney injury. *Am J Physiol Renal Physiol,* 293**:** F688-695. Epub 2007 Jul 2011., 2007.

23. Basile, DP, Donohoe, DL, Roethe, K, Mattson, DL: Chronic renal hypoxia after acute ischemic injury: effects of L-arginine on hypoxia and secondary damage. *Am J Physiol Renal Physiol,* 284**:** F338-348. Epub 2002 Oct 2001., 2003.

24. Basile, DP, Donohoe, D, Roethe, K, Osborn, JL: Renal ischemic injury results in permanent damage to peritubular capillaries and influences long-term function. *Am J Physiol Renal Physiol,* 281**:** F887-899., 2001.

25. Zhang, X, Zheng, X, Sun, H, Feng, B, Chen, G, Vladau, C, Li, M, Chen, D, Suzuki, M, Min, L, Liu, W, Garcia, B, Zhong, R, Min, WP: Prevention of renal ischemic injury by silencing the expression of renal caspase 3 and caspase 8. *Transplantation,* 82**:** 1728-1732., 2006.

26. Yang, C, Jia, Y, Zhao, T, Xue, Y, Zhao, Z, Zhang, J, Wang, J, Wang, X, Qiu, Y, Lin, M, Zhu, D, Qi, G, Qiu, Y, Tang, Q, Rong, R, Xu, M, Ni, S, Lai, B, Nicholson, ML, Zhu, T, Yang, B: Naked caspase 3 small interfering RNA is effective in cold preservation but not in autotransplantation of porcine kidneys. *J Surg Res,* 181**:** 342-354. doi: 310.1016/j.jss.2012.1007.1015. Epub 2012 Jul 1026., 2013.

27. Yang, C, Zhao, T, Zhao, Z, Jia, Y, Li, L, Zhang, Y, Song, M, Rong, R, Xu, M, Nicholson, ML, Zhu, T, Yang, B: Serum-stabilized naked caspase-3 siRNA protects autotransplant kidneys in a porcine model. *Mol Ther,* 22**:** 1817-1828. doi: 1810.1038/mt.2014.1111. Epub 2014 Jun 1816., 2014.

28. Fina, L, Molgaard, HV, Robertson, D, Bradley, NJ, Monaghan, P, Delia, D, Sutherland, DR, Baker, MA, Greaves, MF: Expression of the CD34 gene in vascular endothelial cells. *Blood,* 75**:** 2417-2426., 1990.

29. Babickova, J, Klinkhammer, BM, Buhl, EM, Djudjaj, S, Hoss, M, Heymann, F, Tacke, F, Floege, J, Becker, JU, Boor, P: Regardless of etiology, progressive renal disease causes ultrastructural and functional alterations of peritubular capillaries. *Kidney Int,* 91**:** 70-85. doi: 10.1016/j.kint.2016.1007.1038. Epub 2016 Sep 1024., 2017.

30. Laplante, P, Sirois, I, Raymond, MA, Kokta, V, Beliveau, A, Prat, A, Pshezhetsky, AV, Hebert, MJ: Caspase-3-mediated secretion of connective tissue growth factor by apoptotic

endothelial cells promotes fibrosis. *Cell Death Differ,* 17**:** 291-303. doi: 210.1038/cdd.2009.1124. Epub 2009 Sep 1034., 2010.

31. Cheng, O, Thuillier, R, Sampson, E, Schultz, G, Ruiz, P, Zhang, X, Yuen, PS, Mannon, RB: Connective tissue growth factor is a biomarker and mediator of kidney allograft fibrosis. *Am J Transplant,* 6**:** 2292-2306. Epub 2006 Aug 2294., 2006.

32. Mannon, RB, Fairchild, R: Allograft fibrosis--unmasking the players at the dance. *Am J Transplant,* 10**:** 201-202., 2010.

33. Humphreys, BD, Lin, SL, Kobayashi, A, Hudson, TE, Nowlin, BT, Bonventre, JV, Valerius, MT, McMahon, AP, Duffield, JS: Fate tracing reveals the pericyte and not epithelial origin of myofibroblasts in kidney fibrosis. *Am J Pathol,* 176**:** 85-97. doi: 10.2353/ajpath.2010.090517. Epub 092009 Dec 090511., 2010.

34. Kapitsinou, PP, Sano, H, Michael, M, Kobayashi, H, Davidoff, O, Bian, A, Yao, B, Zhang, MZ, Harris, RC, Duffy, KJ, Erickson-Miller, CL, Sutton, TA, Haase, VH: Endothelial HIF-2 mediates protection and recovery from ischemic kidney injury. *J Clin Invest,* 124**:** 2396-2409. doi: 2310.1172/JCI69073. Epub 62014 May 69071., 2014.

35. Dagher, PC, Hato, T, Mang, HE, Plotkin, Z, Richardson, QV, Massad, M, Mai, E, Kuehl, SE, Graham, P, Kumar, R, Sutton, TA: Inhibition of Toll-Like Receptor 4 Signaling Mitigates Microvascular Loss but Not Fibrosis in a Model of Ischemic Acute Kidney Injury. *Int J Mol Sci,* 17(5). E647. doi: 610.3390/ijms17050647., 2016.

36. Linkermann, A, Brasen, JH, Darding, M, Jin, MK, Sanz, AB, Heller, JO, De Zen, F, Weinlich, R, Ortiz, A, Walczak, H, Weinberg, JM, Green, DR, Kunzendorf, U, Krautwald, S: Two independent pathways of regulated necrosis mediate ischemia-reperfusion injury. *Proc Natl Acad Sci U S A,* 110**:** 12024-12029. doi: 12010.11073/pnas.1305538110. Epub 1305532013 Jul 1305538111., 2013.

37. Linkermann, A: Nonapoptotic cell death in acute kidney injury and transplantation. *Kidney Int,* 89**:** 46-57. doi: 10.1016/j.kint.2015.1010.1008., 2016.

38. Wang, Y, Gao, W, Shi, X, Ding, J, Liu, W, He, H, Wang, K, Shao, F: Chemotherapy drugs induce pyroptosis through caspase-3 cleavage of a gasdermin.

39. Julien, O, Wells, JA: Caspases and their substrates. *Cell Death And Differentiation,* 24**:** 1380, 2017.

40. Ehling, J, Babickova, J, Gremse, F, Klinkhammer, BM, Baetke, S, Knuechel, R, Kiessling, F, Floege, J, Lammers, T, Boor, P: Quantitative Micro-Computed Tomography Imaging of Vascular Dysfunction in Progressive Kidney Diseases. *J Am Soc Nephrol,* 27**:** 520-532. doi: 510.1681/ASN.2015020204. Epub 2015022015 Jul 2015020220., 2016.

41. Kuida, K, Zheng, TS, Na, S, Kuan, C, Yang, D, Karasuyama, H, Rakic, P, Flavell, RA: Decreased apoptosis in the brain and premature lethality in CPP32-deficient mice. *Nature,* 384**:** 368-372, 1996.

42. Leonard, JR, Klocke, BJ, D'Sa, C, Flavell, RA, Roth, KA: Strain-dependent neurodevelopmental abnormalities in caspase-3-deficient mice. *Journal of neuropathology and experimental neurology,* 61**:** 673-677, 2002.

43. Takahashi, K, Kamiya, K, Urase, K, Suga, M, Takizawa, T, Mori, H, Yoshikawa, Y, Ichimura, K, Kuida, K, Momoi, T: Caspase-3-deficiency induces hyperplasia of supporting cells and degeneration of sensory cells resulting in the hearing loss. *Brain research,* 894**:** 359-367, 2001.

44. Zeiss, CJ, Neal, J, Johnson, EA: Caspase-3 in postnatal retinal development and degeneration. *Investigative ophthalmology & visual science,* 45**:** 964-970, 2004.

45. Wei, Q, Dong, Z: Mouse model of ischemic acute kidney injury: technical notes and tricks. *Am J Physiol Renal Physiol,* 303**:** F1487-1494. doi: 1410.1152/ajprenal.00352.02012. Epub 02012 Sep 00319., 2012.

46. Madaan, A, Verma, R, Singh, AT, Jain, SK, Jaggi, M: A stepwise procedure for isolation of murine bone marrow and generation of dendritic cells. *2014*, 2014.

47. Leemans, JC, Stokman, G, Claessen, N, Rouschop, KM, Teske, GJ, Kirschning, CJ, Akira, S, van der Poll, T, Weening, JJ, Florquin, S: Renal-associated TLR2 mediates ischemia/reperfusion injury in the kidney. *J Clin Invest,* 115**:** 2894-2903., 2005.

48. Wang, S, Zhang, ZX, Yin, Z, Liu, W, Garcia, B, Huang, X, Acott, P, Jevnikar, AM: Anti-IL-2 receptor antibody decreases cytokine-induced apoptosis of human renal tubular epithelial cells (TEC). *Nephrology, dialysis, transplantation : official publication of the European Dialysis and Transplant Association - European Renal Association,* 26**:** 2144-2153, 2011.

49. Pallet, N, Sirois, I, Bell, C, Hanafi, LA, Hamelin, K, Dieude, M, Rondeau, C, Thibault, P, Desjardins, M, Hebert, MJ: A comprehensive characterization of membrane vesicles released by autophagic human endothelial cells. *Proteomics,* 13**:** 1108-1120, 2013.

Figure legends

Figure 1: Caspase-3 deficiency aggravates IRI-induced tubular injury. A) Serum creatinine levels in wild-type (WT) and caspase-3-/- (KO) mice at baseline (pre op), and 1, 2, 3, and 7 days post IRI. B) Representative hematoxylin and eosin (H&E)–stained renal sections from WT and KO mice at 1, 2, 3 and 7 days post IRI (magnification 200X). C) Left panel: Mean tubular injury scores of ten randomly chosen high-power fields (magnification 200X) in mice kidney sections post IRI. Right Panel: Urinary levels of cystatin C in WT and KO mice at baseline (pre op) and 1, 2, 3 or 7 days post-IRI. D) Left panels: representative Kidney Injury Molecule 1(KIM-1) immunohistochemistry in renal cortical sections from WT and KO at day 1 post-IRI (magnification 200X). Right panel: quantification of KIM-1 immunohistochemistry–stained murine renal cortical sections at baseline (pre op) and 1 day post IRI. All bar scales =50μm. Values are mean ± SEM.*$P < 0.05$, compared between WT and KO at the same time-point.

Figure 2: Caspase-3 deficiency increases IRI-induced necroptosis in tubular cells. A) Representative electron microscopy showing renal tubules from wild-type (left) and caspase-3-/- (right) mice that underwent IRI and were sacrificed 1 day post IRI (magnification 1000X). Bar scales =10μm. Tubules from KO mice show severe necrotic changes with loss or tubular cell membrane integrity and widespread accumulation of cellular debris within tubules. B) Left panels: representative RIPK3 immunohistochemistry in renal cortical sections from wild-type (WT) and caspase-3-/- (KO) mice that underwent IRI and were sacrificed 1 day post IRI (magnification 200X). Right panel: quantification of RIPK3 immunohistochemistry–stained murine renal cortical sections at baseline (pre-op) and 1 day post IRI, bar scales =50μm. C) Left panels: representative western blot (WB) of phosphorylated RIPK3(pRIPK3) in renal tissue from WT and KO mice that underwent IRI and were sacrificed 1 day post IRI Right panel:

quantification of pRIPK3 WB at day 1 post IRI. Values are mean ± SEM.*P < 0.05, compared between WT and KO at the same time point.

Figure 3: Caspase-3 deficiency attenuates IRI-induced microvascular injury. A) Left panel: quantification of rouleaux formation in H&E-stained kidney sections at baseline (pre-op) and from mice that underwent IRI and were sacrificed at 1, 2, 3, or 7 days post IRI. Right panel: representative H&E-stained murine renal cortical sections at 3 days post IRI (magnification 400X), bar scale=20μm. B): Left panel: representative images of MECA-32 immunohistochemistry in renal cortical sections from wild-type and caspase-3-/- mice that underwent IRI and were sacrificed 3 days post IRI (magnification 200X). Right panel: quantification of MECA-32 in murine renal cortical medullary junction sections at baseline (pre-op)and 1, 2, 3, or 7 days post IRI, bar scale=50μm. C) Representative electron microscopy images of renal endothelial cells in wild-type (left panel) and caspase-3-/- (right panel) mice that underwent IRI and were sacrificed 3 days post IRI. Loss of endothelial fenestration is found in WT mice (arrow) whereas KO show preserved fenestrae (magnification 10000X), bar scales =500nm. Values are mean ± SEM.*P < 0.05, compared between WT and KO at the same time point.

Figure 4: Caspase-3 deficiency attenuates IRI-induced upregulation of pro-fibrotic markers. A) Serum levels of CTGF in wild-type (WT) and caspase-3-/- (KO) mice that underwent IRI and were sacrificed at 1,2,3 or 7 days post IRI. B) Left panel: quantification of α-SMA immunohistochemistry in renal cortical sections from wild-type and caspase-3-/- mice at baseline (pre) or at 1, 2, 3, or 7 days post IRI (magnification 200X). Right panel: representative α-SMA staining in murine renal cortical sections at day 3 after surgery. bar scale=50μm. C) Left panels: representative images of Sirius Red staining in renal cortical

medullary junction sections from wild-type (upper panel) and caspase-3-/- (lower panel) mice that underwent IRI and were sacrificed 7 days post IRI (magnification 200X). Right panel: quantification of Sirius Red staining in murine renal cortical medullary junction sections at baseline and 1, 2, 3, or 7 days post IRI. Bar scale =50μm. Values are mean ± SEM.*P < 0.05, compared between WT and KO at the same time point.

Figure 5: Caspase-3 deficiency attenuates IRI-induced microvascular rarefaction and fibrosis. A) Left panels: representative images of MECA-32 immunohistochemistry in cortical medullary junction sections from wild-type and caspase-3-/- mice that underwent IRI and were sacrificed 21 days post IRI (magnification 200X). Right panel: quantification of MECA-32 staining in murine renal cortical sections at 21 days post IRI. Bar scale= 50μm. B) Left panels: representative image of α-SMA immunohistochemistry of renal cortical sections from wild-type and caspase-3-/- mice that underwent IRI and were sacrificed 21 days post IRI (N = 10 per group; magnification 200X and 400X). Right panels: quantification of α-SMA staining in PTC in murine renal cortical sections at 21 days post IRI. Bar scale =50μm. C) Left panels: representative western blot of α-SMA from wild-type and caspase-3-/- mice that underwent IRI and were sacrificed 21 day post IRI. Right panel: quantification of α-SMA WB at 21 day post IRI. D) Left panels: representative image of Sirius Red staining of renal cortical medullary junction sections from wild-type and caspase-3-/- mice that underwent IRI and were sacrificed 21 days post IRI (magnification 200X). Right panels: quantification of Sirius Red staining of murine renal cortical medullary junction sections at 21 days post IRI. Bar scale =50μm. Values are mean ± SEM.*P < 0.05, ***p<0.001, compared between WT and KO at the same time point.

Figure 6: Caspase-3 deficiency prevents IRI-induced long term endothelial cell death. A) representative electronic microscopic images of endothelial cell apoptotic death from wild-type

and caspase-3-/- mice that underwent IRI and were sacrificed 21 days post IRI. Bar scale=500nm. Red arrows indicate apoptotic bodies and blue arrows indicate exosome-like membrane vesicles, (magnification 10000X). B) quantification of apoptotic cells in wild-type and caspase-3-/- mice that underwent IRI and were sacrificed 21 days post IRI. Values are mean ± SEM.*P < 0.05, compared between WT and KO at the same time point.

Figure 7: Caspase-3 deficiency prevents IRI-induced long-term tubular injury. A) Left panel: representative images of HIF-1α staining in murine renal cortical sections 21 days after surgery. Right panel: quantification of HIF-1α immunohistochemistry in renal cortical sections from wild-type and caspase-3-/- mice at baseline and 21 days post IRI; magnification 200X). B) Left panels: representative WB images of HIF-1α in renal tissue 21 days post IRI. Right panel: quantification of HIF-1α WB detection at 21 day post IRI. C) Representative H&E-stained murine renal cortical sections 21d post IRI (magnification 200X). D) Mean tubular injury scores of ten randomly chosen high-power fields in wild-type and caspase-3-/- mice that underwent IRI and were sacrificed at 21d post IRI. E) Serum creatinine levels in wild-type and caspase-3-/- mice that underwent IRI and were sacrificed at 21 days post IRI. All bar scales =50μm. Values are mean ± SEM.*P < 0.05, compared between WT and KO at the same time point.

Figure 8: Knock-down of caspase-3 decreases apoptosis in endothelial cells but increases necrosis in tubular epithelial cells. A) Left panel: representative images of Ho-PI staining in Human Umbilical Vein Endothelial Cells (HUVECs) exposed to hypoxia (5% O_2) for 4 hours followed by reoxygenation for 1 hour in serum free medium. Right panels: representative images of western blot (upper panel) and quantification (lower panel) for pro-caspase-3 in HUVECs transfected with siRNA ctrl or caspase-3 (N=3 independent experiments). B) Left panel: representative images of HO-PI staining of Human Renal Proximal Tubular Epithelial

Cells (PT-2) exposed to hypoxia (5% O_2) for 4 or 24 hours followed by reoxygenation for 1 hour in serum free medium. Right panels: representative images of western blot (upper panel) and quantification (lower panel) for pro-caspase-3 in PT-2 cells transfected with siRNA ctrl or caspase-3 (N=3 independent experiments). C) Left panel: quantification of apoptotic death in HUVEC and PT-2 cells exposed to hypoxia-reoxygenation in serum free medium. Right panel: quantification of necrotic death in HUVEC and PT-2 cells exposed to hypoxia-reoxygenation in serum free medium. Values are mean ± SEM.*$P < 0.05$.

Figure 9: Schematic representation of the impact of caspase-3 deficiency on microvascular rarefaction and renal dysfunction post IRI. Caspase-3 is a pivotal regulator of peritubular capillary rarefaction and renal dysfunction. Early tubular injury and renal dysfunction are increased in caspase-3-/- mice, whereas microvascular integrity is ameliorated throughout the various phases. In the long term, caspase-3-/- mice show reduced microvascular drop-out, decreased tubular injury, and reduced interstitial fibrosis.

Supplementary figure legends

Supplementary Figure 1a: Caspase-3 deficiency aggravates IRI-induced tubular injury. A) Representative H&E–stained murine renal cortical sections at baseline (N ≥ 3 per group; magnification 200X). Bar scale =50μm. B) Urinary levels of cystatin C in wild-type and caspase-3-/- mice at baseline and at days 1,2,3,7 or 21 post IRI. C) Representative KIM-1 immunohistochemistry in renal cortical sections from wild-type and caspase-3-/- mice at baseline (N ≥ 3 per group; magnification 200X). Bar scale=50μm Values are mean ± SEM.*$P < 0.05$ compared between WT and KO at the same time point.

Supplementary Figure 1b: D) Left panels: representative images of CD45 immunohistochemistry in renal cortical sections from wild-type and caspase-3-/- days 1 and 7 post IRI Bar scale=50μm (magnification 200X). Right panels: quantification of CD45 in murine renal cortical sections at baseline and 1, 2, 3, 7 or 21 days post IRI. E) Left panel: representative images of vascular cell adhesion molecule-1 (VCAM-1) immunohistochemistry in renal cortical sections from wild-type and caspase-3-/- mice at baseline and 3 or 21 days post IRI. Bar scale=50μm (magnification 200X). Right panels: quantification of VCAM-1 immunohistochemistry Values are mean ± SEM.*P < 0.05, compared between WT and KO at the same time point.

Supplementary Figure 2: Caspase-3 activation post IRI. Upper panels: representative images of activated caspase-3 immunohistochemistry in renal cortical sections from wild-type and caspase-3-/- mice at baseline and 1,2,3,7 or 21 days after IRI (magnification 200X). Bar scale=50μm. Lower panel: quantification of activated caspase-3 staining in murine renal cortical sections from wild-type and caspase-3-/- mice at baseline and 1,2,3,7 or 21 days post IRI. Values are mean ± SEM. ***p<0.001, compared between baseline (pre) and other time points.

Supplementary Figure 3: **Pan-caspase inhibition further aggravates IRI-induced renal dysfunction.** Serum creatinine levels in wild-type and caspase-3-/- mice treated with the pan-caspase inhibitor Z-VAD-FMK or vehicle (DMSO) and sacrificed 1 day post IRI or sham treatment. Values are mean ± SEM.*P < 0.05.

Supplementary Figure 4: A) Left panel: representative images of CD34 immunohistochemistry in renal cortical sections from wild-type and caspase-3-/- mice at day 1 post IRI (magnification 200X). Right panels: quantification of CD34 in murine renal cortical sections at 1, 2, 3 or 7 days post IRI. Bar scale=50μm B) Left panel: quantification of

CD34+/CD45+ bone marrow derived cells in wild-type and caspase-3-/- mice at baseline. Right panels: representative FACs scatter plots for CD34+/CD45+ bone marrow derived cells. C) Representative image of MECA-32 immunohistochemistry in renal cortical sections from wild-type and caspase-3-/- mice at baseline (magnification 200X). Values are mean ± SEM.*P < 0.05, compared between WT and KO at the same time point.

Supplementary Figure 5: Caspase-3 deficiency attenuates IRI-induced microvascular rarefaction. A) Quantification of MECA-32 staining in murine renal cortical sections from wild-type and caspase-3-/- mice at baseline and 1,2,3,7 or 21 days post IRI. B) Quantification of α-SMA staining in PTC in murine renal cortical sections from wild-type and caspase-3-/- mice at baseline and at 1,2,3,7 or 21 days post IRI . C) Upper panel: representative images of glomerular α-SMA staining in wild-type and caspase-3-/- at baseline and 1,2,3,7 or 21 days after IRI (magnification 200X). Bar scale=50μm. Lower panel: Quantification of glomerular α-SMA staining in murine renal cortical sections from wild-type and caspase-3-/- mice at baseline and 1,2,3,7 or 21 days post IRI. Values are mean ± SEM.*P < 0.05, compared between WT and KO at the same time point.

Supplementary Figure 6: A) Representative image of HIF-1α staining in murine renal cortical sections from wild-type and caspase-3-/- mice that were sacrificed pre-operation (N ≥ 3 per group; magnification 200X). Bar scale=50μm B) Serum creatinine levels in wild-type and caspase-3-/- mice at baseline or at 1,2,3,7 or 21 days post IRI or sham treatment. C) Mean tubular injury scores of ten randomly chosen high-power fields in H&E-stained renal cortical sections from wild-type and caspase-3-/- mice at baseline and at 1,2,3,7 or 21 days post IRI. D) Quantification of rouleaux formation in H&E-stained renal cortical sections from wild-type and

caspase-3-/- mice at baseline and at 1,2,3,7 or 21 days post IRI. Values are mean ± SEM.*P < 0.05, compared between WT and KO at the same time point.

Supplementary Figure 7: Caspase-3 deficiency increases IRI-induced necroptosis in tubular cells. A) Representative H&E-stained murine renal cortical sections 1 day post IRI in wild-type and caspase-3-/- mice (magnification 400X). Bar scale =50μm B) Representative RIPK3 immunohistochemistry in renal cortical sections from wild-type and caspase-3-/- mice at baseline (magnification 200X).

Supplementary Figure 8: A) Representative α-SMA immunohistochemistry in murine renal cortical sections at baseline (N ≥ 3 per group). Bar scale=50μm B) Left panel: representative western blot images of α-SMA 3 days post IRI (N ≥ 6 per group). Right panel: quantification α-SMA western blot 3 days post IRI. C) Representative images of Sirius Red staining at renal cortical medullary junction sections from wild-type and caspase-3-/- mice at baseline (N ≥ 3 per group; magnification 200X). Bar scale=50μm Values are mean ± SEM.*P < 0.05, compared between WT and KO at the same time point.

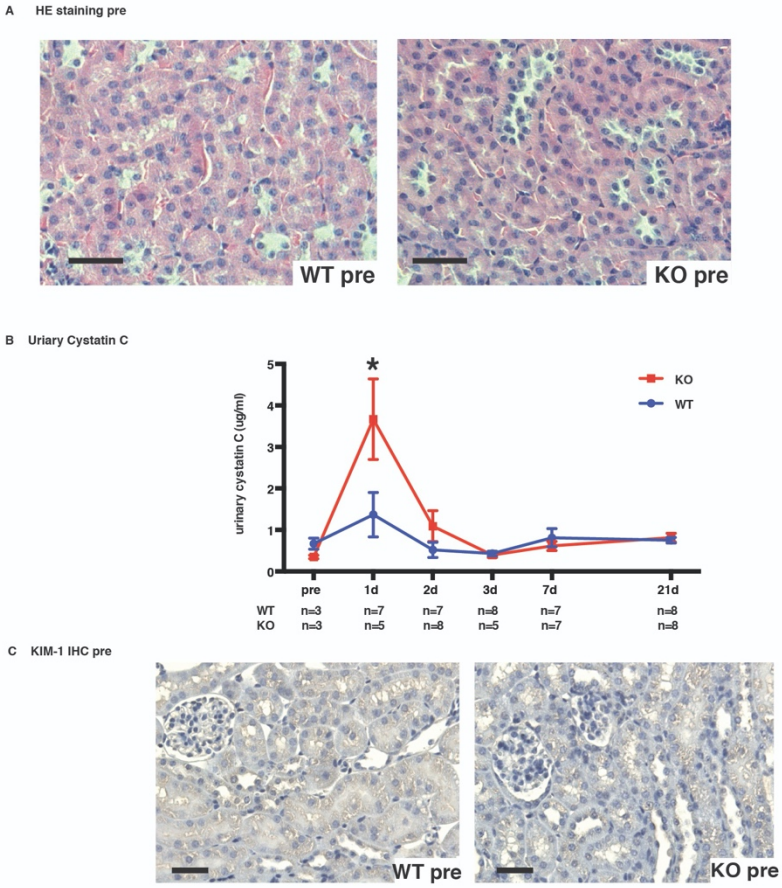

Figure S1a: Caspase-3 deficiency aggravates IRI-induced tubular injury.

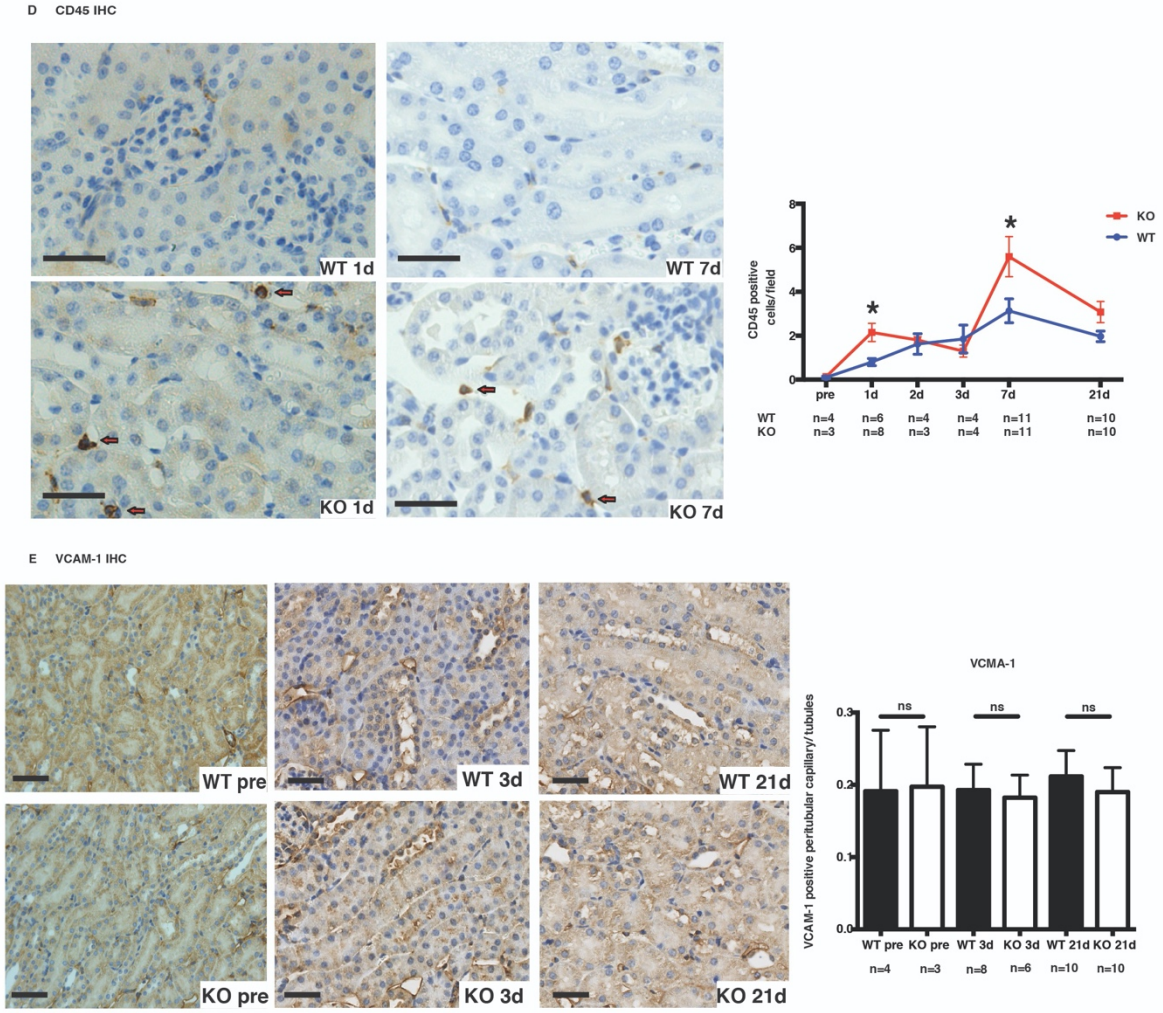

Figure S1b: Caspase-3 deficiency aggravates IRI-induced tubular injury.

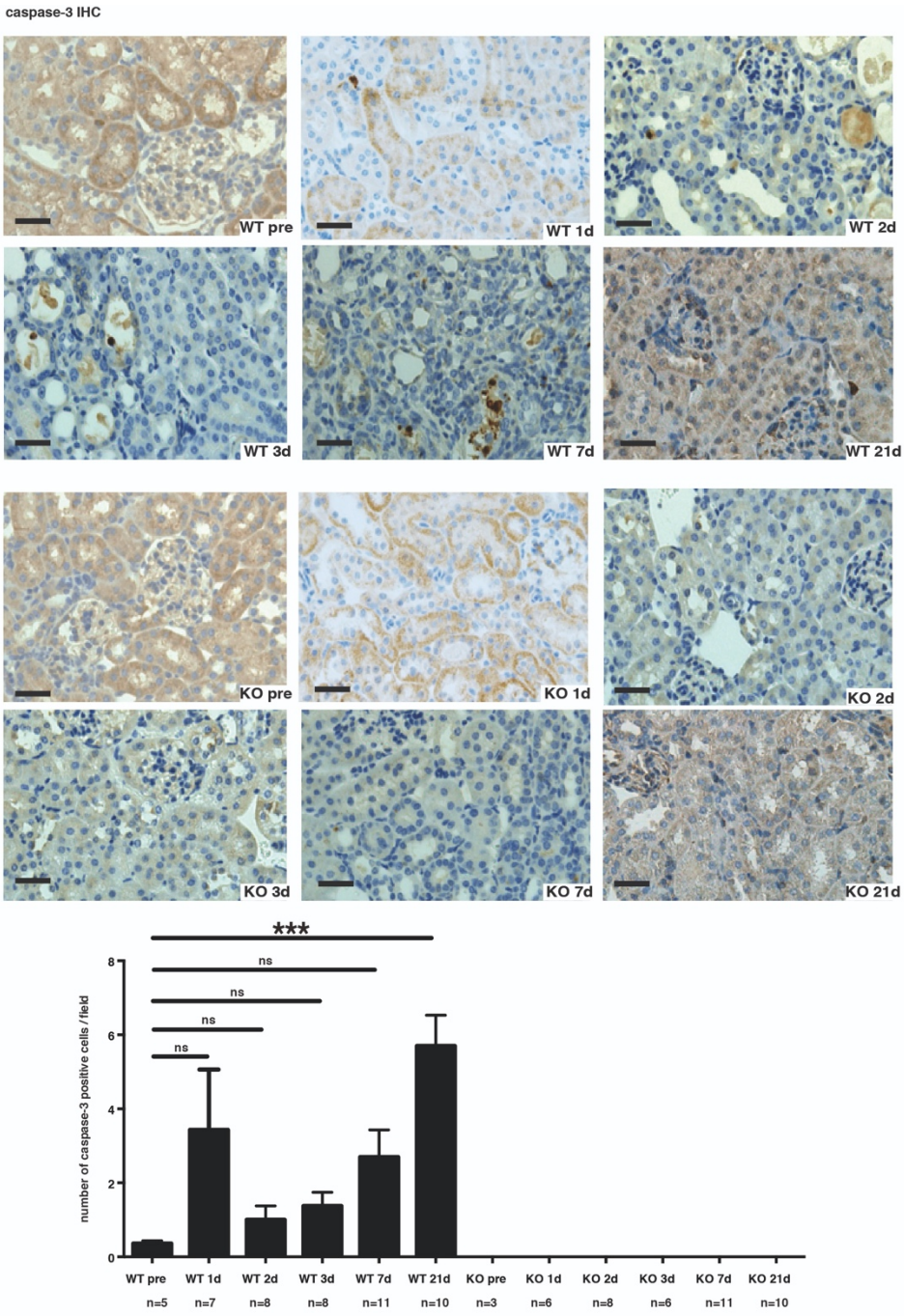

Figure S2: Caspase-3 activation post ischemia-reperfusion Injury.

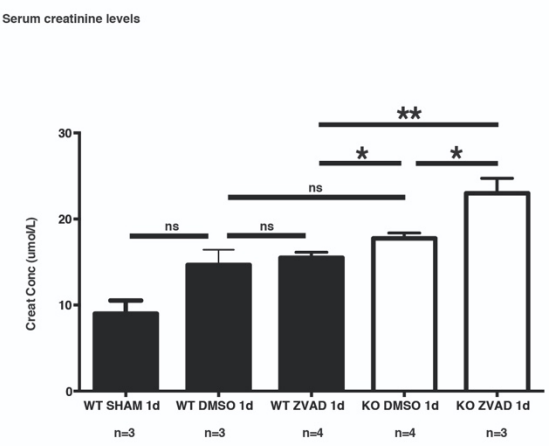

Figure S3: Pan-caspase inhibition further aggravates IRI induced renal dysfunction.

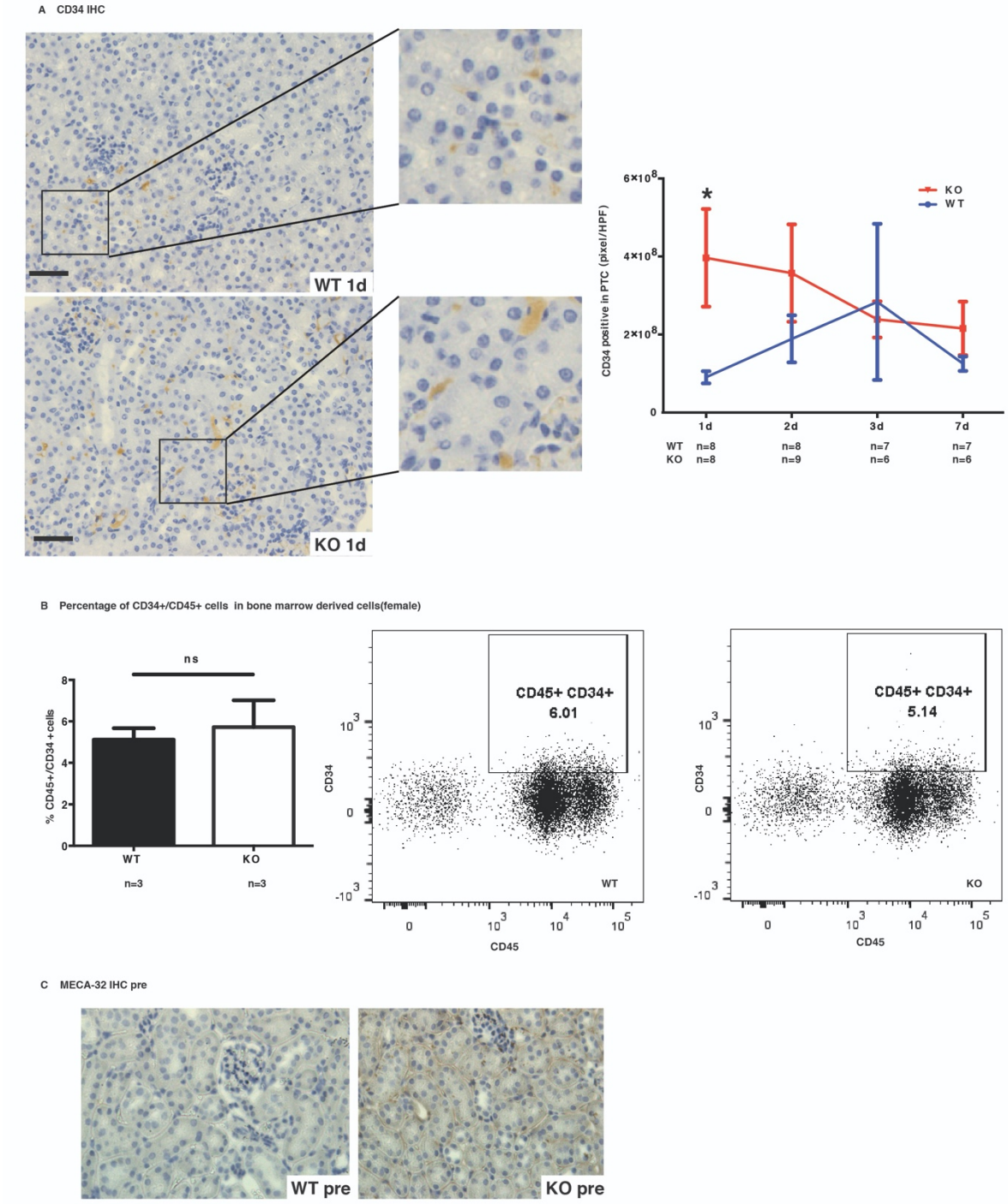

Figure S4: Caspase-3 deficiency benefits endothelial cells preservation after IRI.

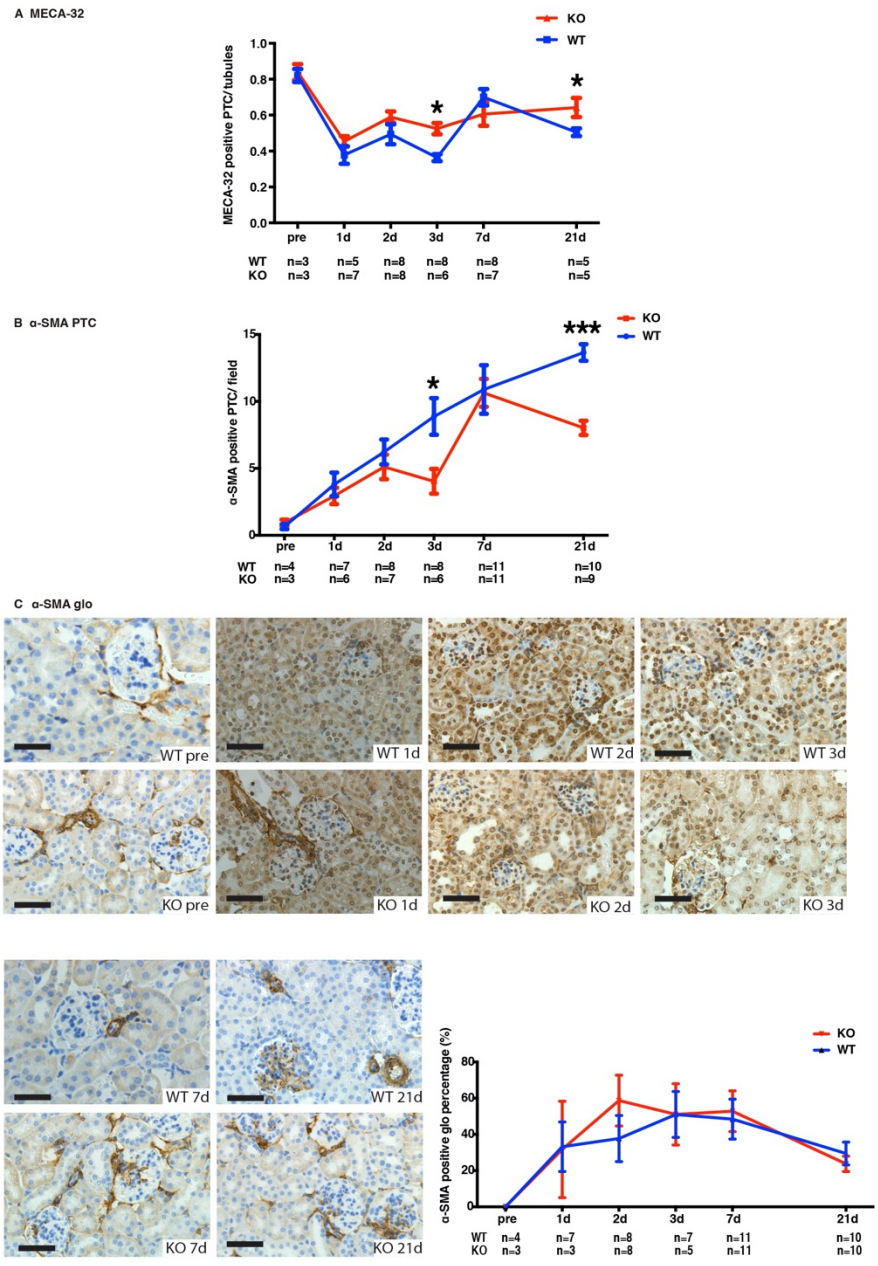

Figure S5: Caspase-3 deficiency attenuates IRI-induced microvascular rarefaction.

A HIF-1α IHC pre

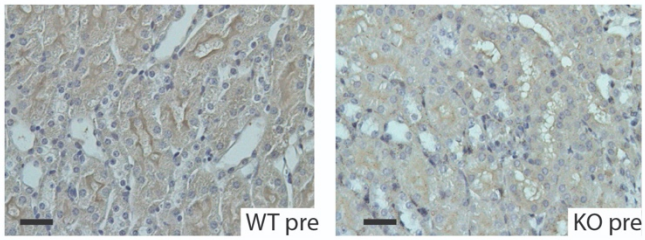

B Serum creatinine level

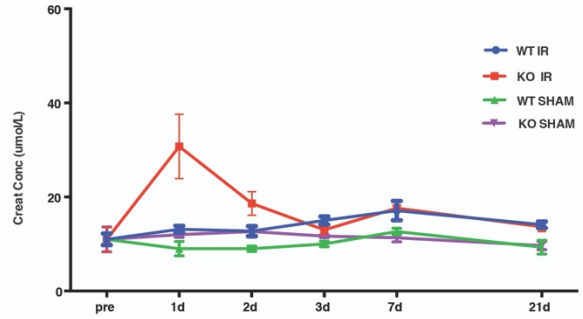

WT IR	n=6	n=7	n=8	n=8	n=9	n=10
KO IR	n=3	n=6	n=8	n=6	n=11	n=9
WT SHAM	n=3	n=3	n=3	n=3	n=3	n=3
KO SHAM	n=3	n=3	n=3	n=3	n=3	n=3

C Tubular injury score

D Rouleaux Formation

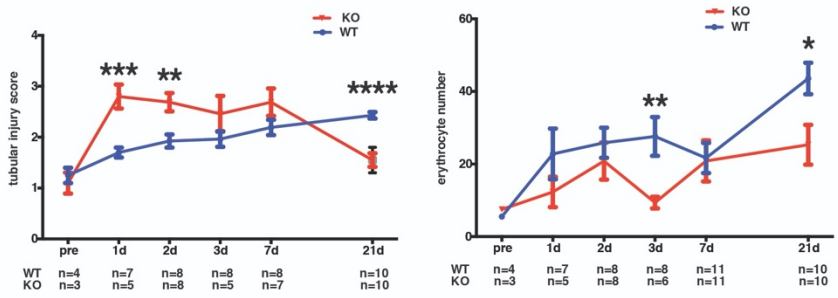

WT	n=4	n=7	n=8	n=8	n=8	n=10
KO	n=3	n=5	n=8	n=5	n=7	n=10

WT	n=4	n=7	n=8	n=8	n=11	n=10
KO	n=3	n=5	n=8	n=6	n=11	n=10

Figure S6: Caspase-3 deficiency prevents IRI-induced long-term renal dysfunction.

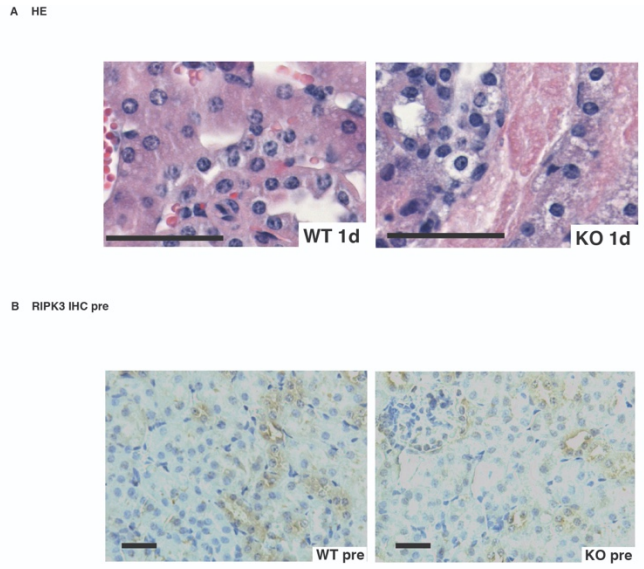

Figure S7: Caspase-3 deficiency increases IRI-induced necroptosis in tubular cells.

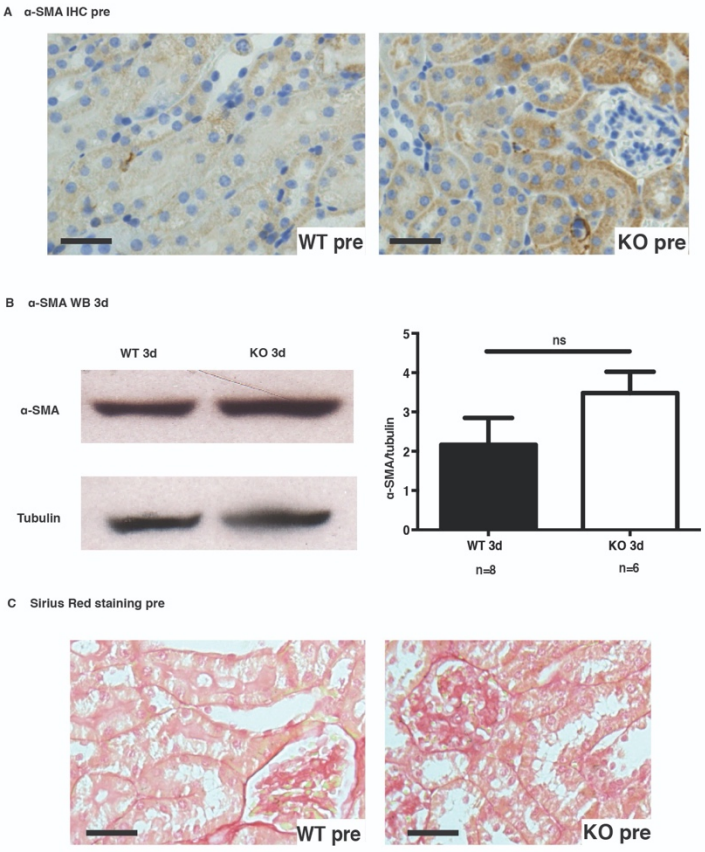

Figure S8: Caspase-3 deficiency attenuates IRI-induced upregulation of pro-fibrotic markers.

Manuscript 2: Caspase-3 dependent peritubular capillary dysfunction is pivotal for transition from acute to chronic kidney disease after acute ischemia-reperfusion injury

Shanshan Lan[1,2,3], Bing Yang[1,2,3], Francis Migneault[1,2], Julie Turgeon[1,2], Maude Bourgault[1], Mélanie Dieudé[1,2,3], Heloïse Cardinal[1,2,3], Michael. J. Hickey[5], Natacha Patey[1,3,4], Marie-Josée Hébert[1,2,3]

1. Research Centre, Centre hospitalier de l'Université de Montréal, Montreal, Quebec, Canada; 2. Canadian Donation Transplant Research Program, Edmonton, Alberta, Canada; 3, Université de Montréal, Montreal, Quebec, Canada; 4. Department of Pathology, Centre hospitalier universitaire Sainte-Justine, Université de Montréal, Montreal, Quebec, Canada; 5. Centre for Inflammatory Diseases, Monash University Department of Medicine, Monash Medical Centre, Clayton, Australia.

Author order: First author

Contribution: S.L. and M-J.H. designed and developed the research strategy. S.L. and B.Y. performed experiments. S.L., B.Y., M.J.H., M-J.H., and N.P. analyzed the slides, images and videos. S.L., B.Y., F.M., J.T., M.B., M.D. analyzed data. S.L., B.Y., F.M., J.T., M.D., M.J.H., H.C., and M-J.H. interpreted the results. S.L. and F.M. prepared the figures. S.L., F.M., and M.J.H. drafted the manuscript. S.L., F.M., H.C., and M.J.H. edited and revised the manuscript. S.L., B.Y., F.M., J.T., M.B., M.D., M.J.H., H.C., N.P., and M-J.H. approved the final version of the manuscript.

As the first author, Shanshan Lan participated in experiments design with Dr. Bing Yang and Dr. Marie-Josée Hébert. In the experimental section, Shanshan standardized the model of severe murine IRI and was also responsible for animal serum collection, animal sacrifice, necropsy, samples collection, and preservation. Then Shanshan Lan performed the BUN test, immunohistochemistry staining, and histochemistry staining on renal tissue slice. She also contributed to all pathological evaluation. In renal microvasculature imaging analysis, Shanshan Lan performed renal blood vessel perfusion, microCT scan, 3D image construction, and software analysis. In addition, Shanshan Lan performed murine jugular vein catheter installation and dye injection in the process of intra-vital imaging, with the coordination of the cellular

imaging platform of CRCHUM. Shanshan Lan wrote the manuscript and made the figures and videos as the first version before submission. In the step of revision, Shanshan modified the text, made new supplementary figures and videos accordingly.

This manuscript was accepted by the American Journal of Physiology-Renal Physiology in July 2021.

Caspase-3 dependent peritubular capillary dysfunction is pivotal for transition from acute to chronic kidney disease after acute ischemia-reperfusion injury

Shanshan Lan1,2,3, Bing Yang 1,2,3, Francis Migneault 1,2 Julie Turgeon 1,2, Maude Bourgault 1, Mélanie Dieudé 1,2,3, Héloïse Cardinal 1,2,3, Michael. J. Hickey 5, Natacha Patey 1,3,4, Marie-Josée Hébert* 1,2,3

1. Research Centre, Centre hospitalier de l'Université de Montréal, Montreal, Quebec, Canada;
2. Canadian Donation Transplant Research Program, Edmonton, Alberta, Canada;
3. Université de Montréal, Montreal, Quebec, Canada;
4. Department of Pathology, Centre hospitalier universitaire Sainte-Justine, Université de Montréal, Montreal, Quebec, Canada;
5. Centre for Inflammatory Diseases, Monash University Department of Medicine, Monash Medical Centre, Clayton, Victoria 3168, Australia.

Running Head: Central role of PTCs in AKI to CKD transition

Corresponding author:
Dr. Marie-Josée Hébert
CRCHUM, Faculty of Medicine, Université de Montréal,
900, rue Saint-Denis, Montreal, Quebec, Canada, H2X 0A9
Phone: +1- 514 890-8000, poste 25017
Fax : +1- 514 412-7624
Email: marie-josee.hebert@umontreal.ca

Abstract

Ischemia-reperfusion injury (IRI) is a major risk factor for chronic renal failure. Caspase-3, an effector responsible for apoptosis execution, is activated within peritubular capillary (PTC) in the early stage of IRI-induced acute kidney injury (AKI). Recently, we showed that caspase-3-dependent microvascular rarefaction plays a key role in fibrosis development after mild renal IRI. Here, we further characterize the role of caspase-3 in microvascular dysfunction and progressive renal failure in both mild and severe AKI, by performing unilateral renal artery clamping for 30/60 minutes with contralateral nephrectomy in wild-type (C57BL/6) or caspase-3-/- mice. In both forms of AKI, caspase-3-/- mice showed better long-term outcomes in spite of worse initial tubular injury. After 3 weeks, they showed reduced PTC injury, decreased PTC collagen deposition and α-SMA expression, and lower tubular injury scores when compared to wild-type animals. Caspase-3-/- mice with severe IRI also showed better preservation of long-term renal function. Intra-vital imaging and micro-computed tomography (microCT) revealed preserved PTC permeability and better terminal capillary density in caspase-3-/- mice. Collectively, these results demonstrate the pivotal importance of caspase-3 in regulating long-term renal function after IRI and establish the predominant role of PTC dysfunction as a major contributor to progressive renal dysfunction.

Introduction

Acute kidney injury (AKI) is one of the most powerful predictors of progressive renal failure in both native and transplanted kidneys (1). More than 20% of hospitalized adults worldwide experience some level of AKI (2-4) prompted most commonly by ischemia-reperfusion injury (IRI) and sepsis (5). IRI is an integral component of kidney transplantation and AKI occurs in 20%-50% of transplantations from deceased donors in the immediate postoperative period (6-8). The severity and number of AKI episodes in various patient cohorts predicts progressive long-term renal dysfunction and risk of end-stage renal failure (4, 9-12),. Long referred to as acute tubular necrosis, AKI is classically considered a disease of tubular epithelial cells. Increased cell death of tubular epithelial cells, in the form of apoptosis and necroptosis, is indeed an important characteristic of AKI and tends to occur predominantly at the cortico-medullary

junction where blood and oxygen supply is limited (13). However, microvascular injury has emerged in the past decade as a major and previously underappreciated factor regulating progressive renal dysfunction after AKI (5, 14-16). Loss of peritubular capillaries (PTC) favors chronic hypoxia leading to overexpression of hypoxia-inducible factor-1 α (HIF-1α) and fibrogenic factors which in turn favor myofibroblast differentiation and fibrosis (5, 15, 17-20). In transplanted kidneys, the magnitude of microvascular involution during the first 3 months following transplantation is a major negative predictor of long-term renal allograft function (21). Studies using in vivo imaging and electron microscopy demonstrated a tight correlation between PTC dysfunction/rarefaction and renal fibrosis in murine models of AKI and in human kidney biopsy samples (22-24).

Caspase-3 is an effector caspase responsible for the induction of apoptosis. Caspase-3 activation is present within PTC in the early stage of IRI-induced AKI (17, 25). Our group recently showed that caspase-3 dependent microvascular involution plays a predominant role in regulating the transition from AKI to fibrosis after mild renal IRI (26). Upon renal artery clamping, caspase-3-/- mice show early increases in tubular epithelial cell injury translating into more severe early renal dysfunction than wild-type controls. Incapacity to mount an apoptotic response in caspase-3 deficient mice redirects tubular epithelial cell death towards necroptosis, a more severe and inflammatory type of cell death. Yet, in spite of increased early tubular cell death and acute renal dysfunction, PTC are largely protected from IRI-induced cell death. Inhibition of PTC apoptosis does not fuel other forms of regulated cell death but rather prevents microvascular rarefaction and long-term renal fibrosis. There is no impact of caspase-3 deficiency on long-term renal function. These results confirm a predominant role for microvascular injury over early epithelial injury as a driver of renal fibrosis after IRI.

Renal fibrosis is classically considered a surrogate marker of progressive renal failure. Yet, recent data suggest that progressive renal dysfunction after AKI is not always correlated with renal fibrosis (24). Having identified a predominant role for caspase-3-dependent microvascular injury in renal fibrogenesis after mild IRI, we now aim at evaluating the impact of caspase-3 on microvascular function and integrity, fibrogenesis and renal function after severe IRI. In the present study, we compare early and late microvascular and tubular abnormalities in caspase-3 deficient mice exposed to mild and severe forms of IRI. Our goal is to assess whether caspase-

3 deficiency preserves microvascular integrity and function even in severe forms of AKI or rather increases PTC injury, as was the case for renal epithelial cells in mild forms of AKI.

Materiel and Methods

Animal and Surgical Procedures

We used 6-8 weeks old female C57BL/6 mice from Charles River Laboratories (Wilmington, MA,USA). CASP3-deficient (caspase-3-/-) mice on a C57BL/6 congenic background, aged 6–8 weeks, were derived from breeding pairs of heterozygous CASP3-deficient (B6.129S1-C3tm1Flv/J) mice obtained from Jackson Laboratory (stock #006233; Bar Harbor, ME). The generation of these mice was previously described (26). These homozygote mice were viable, reached adulthood, and showed a variety of hyperplasias and disorganized cell deployment in the brain. All mice were kept in 12-hour light/dark cycles, with normal food provided ad libitum. IRI by unilateral renal artery clamping plus contralateral nephrectomy was performed as described previously (26). Detailed surgical procedures can be found in Supplemental Material. Animals were divided into mild AKI (IR30m) and severe AKI (IR60m) and were sub-grouped into pre-operation, SHAM, 1 day, 2 days, 7 days, and 21 days post-operation groups. A maximum of 10 mice per sub-group were used. The number of mice per experiment is described in figure legends. Carprofen was injected subcutaneously daily until day 3 post-op. Mice with significant body weight loss were also injected with 0.5 mL saline + 0.3 mL 2,5% dextrose. Mice were euthanized by neck dislocation, after performing cardiac puncture under 2% isoflurane inhalation at baseline or on days 1, 2, 7, or 21 post-surgery and the left kidney, serum, and urine were collected.

Renal Function Biochemical Evaluation

Serum creatinine levels were determined using Vitro CREA slides and Vitro chemistry products (Vitro 250/350 Chemistry System; Ortho Clinical Diagnostics, Raritan, NJ), as described in our previous work (26, 27).

Renal Histopathological Examination

Tubular Injury Score

Tubular injury score was evaluated in murine renal tissue stained with haematoxylin and eosin (HE), as described previously (26). Ten high-power magnification fields (200X) were randomly chosen; five from the renal cortex and five from the cortico-medullary junction. Based on the percentage of affected tubules, the tubular injury score was classified as 0-5 (0: normal; 1: mild injury, involvement of 0%–10%; 2: moderate injury, involvement of 11%–25%; 3: severe injury, involvement of 26%–49%; 4: high severe injury, involvement of 50%–75%; 5: extensive injury, involvement of 75%). The criteria for tubular injury involved: brush border loss, tubular dilation, cast formation, tubular necrosis, as well as neutrophil infiltration. All assessments were done by two investigators blinded to experimental conditions (28).

Peritubular Capillary Vascular Congestion

Rouleaux formation, a read-out of peritubular capillary microvascular congestion, was estimated by counting accumulated erythrocytes inside peritubular capillaries (PTC) on HE-stained slides. Ten randomly chosen high magnification fields were counted per mouse by two investigators blinded to experimental conditions.

Immunohistochemistry

Mice were sacrificed at different time points (baseline, days 1, 2, 7 and 21). Kidneys were collected and fixed in 10% formalin, embedded in paraffin, and subsequently cut into 4-µm slices. Immunohistochemistry staining was performed on paraffin-embedded tissue as described previously (26). The antibodies used in this study were mouse endothelial cell antigen (MECA-32; 1:20; 120501; Biolegend, San Diego, CA, USA), HIF-1α (1:200; ab2185; Abcam, Cambridge, MA, USA), α-smooth muscle actin (α-SMA; 1:200, clone 1A4; Dako, Santa Clara, CA,USA). Stained slides were scanned (original magnification 200X) using an Olympus VS110 slide scanner and randomly chosen fields were evaluated. Quantification of MECA-32 staining in PTC were assessed by evaluating the ratio of positive PTC/ tubule number in five high-power magnification fields (200X) in cortical-medullary junction, and MECA-32 in glomeruli was quantified by accounting positive glomerulus in cortex in five high-power magnification fields (100X). Quantification of α-SMA staining in PTC were assessed by accounting positive PTC in ten high-power magnification fields (200X); α-SMA staining in glomeruli was performed in five high-power magnification fields (100X). All assessments were done by two independent

investigators blinded to experimental conditions. α-SMA staining in renal macrovessels was assessed using Visiomorph TM VIS Histoinformatics Software (Olympus) in the whole kidney.

Sirius Red Staining

Sirius Red staining was performed using Picro-Sirius Red Staining Kit (ab150681, Abcam, Cambridge, MA, USA) according to the manufacturer's instructions. All slides were scanned using an Olympus VS110 slide scanner microscope. Five randomly chosen high-power fields at the cortical-medullary junction (magnification 200X) were taken. Sirius red positive area within PTC and glomeruli were evaluated with ImageJ (National Institutes of Health) by two independent investigators blinded to experimental conditions.

Silver staining

Silver staining was done according to Jones' Methenamine Silver Stain (JMS) - Staining protocol (29). Stained slides were scanned using an Olympus VS110 slide scanner microscope. Five randomly chosen high-power fields in the renal cortical section (magnification 200X) were taken, and glomerulosclerosis scores were evaluated by two independent investigators blinded to experimental conditions. Based on involved glomerular percentage, glomerulosclerosis score was classified as 0-3 (0: no glomerulopathy-double contours affecting <10% peripheral capillary loop in the most severe attacked glomerulus. 1: double contours affecting up to 25% peripheral capillary loop in most affected non-sclerotic glomeruli. 2: double contours affecting up to 50% peripheral capillary loop in most affected non-sclerotic glomeruli. 3: double contours affecting >50% peripheral capillary loop in most affected non-sclerotic glomeruli) (30).

Electron Microscopy

Fresh murine renal tissue was fixed with 3% glutaraldehyde, post-fixed with 1% osmium tetroxide and embedded in Epon according to routine techniques. Ultrathin renal slices were obtained using an ultra-microtome (Leica Biosystems RM2245, Buffalo Grove, IL, USA) and mounted on naked nickel grids. Slices were stained with aqueous uranyl acetate and lead citrate as previously reported (31). Examination was performed using a Zeiss Axio Imager.A1 transmission electron microscope and electron micrographs were captured using a AxioCam, Zeiss digital camera. Images of renal peritubular capillaries were taken randomly in the cortex and cortico-medullary junction by two blinded investigators.

Ex-vivo renal microvasculacular microCT imaging

5 mL silicone rubber radiopaque contrast agent Microfil (Flow Tech Inc. Carver, MA, USA) was pump-perfused (0.5ml/min, catheter length: 12cm) via a left ventricle 23G catheter to allow 3D visualization of the renal microvasculature. The kidney was collected following polymerization for 4-6 hours at 4 °C and fixed in 1.5 mL tube for subsequent scan procedure (32, 33).

Ex-vivo micro-Computed Tomography (microCT) manipulation was performed using a high-resolution SkyScan 1176 scanner (SkyScan, Kontich, Belgium). The fixed kidney was positioned and scanned 360° around the vertical axis with a rotating speed of 0.3°, at a resolution of 9 um. Vascular volume was assessed following volume rendering and 3D reconstruction analysis (22). Terminal capillaries were counted using Imaris 9.2 software (Oxford Instruments plc).

Evans Blue ex-vivo extravasation test

Evans Blue (E2129, Sigma Aldrich, Burlington, MA, USA) (5mg/kg) was dissolved in D-PBS 1X (1 g/L glucose, 36 mg/L sodium pyruvate with calcium and magnesium) and injected intravenously via the tail vein. After 30 min of circulation, mice were perfused with 20 mL of 0,9% NaCl via the left ventricle to remove all the blood in the circulation. The ischemic kidney was collected, dried, weighed, and put in 100% formamide (4ml/g) at 56°C for 24h. Extracted Evans Blue was measured by spectrophotometry at 620 nm and expressed as mg/g bodyweight (34, 35).

Intra-vital mice kidney imaging

Intra-vital images were acquired using an Olympus FV1000 upright microscope (Olympus, Japan). At 21 days post-ischemia-reperfusion, mice were anesthetized with 2% isoflurane and 1% oxygen over all the surgery procedure and imaging session. Then mice were placed on a 37°C heated carpet with the right jugular vein catheterized for the administration of reagents. The kidney was exposed by dorsal incision and positioned on a special stage (36). After preparation procedure, mice were maintained under a 32°C environment and were monitored using Mouse Ox apparatus (Flow Tech Inc). All images were acquired using a XLUM Plan FL N 20x/1.00 Water objective. Ultrasound gel was used to establish the immersion between the

objective and the coverslip (#1.5, 0.17 mm) as it has the same refractive index as water. 2000 kDa Alexa Fluor 488nm conjugated dextran (FD 2000S, Sigma Aldrich, Burlington, MA, USA) (0.25 mg/kg) and Evans Blue (1 mg/kg) were injected via a jugular catheter. Live imaging was taken at pre-injection and 15 minutes post-injection. For excitation, 405 nm, 488 nm and 635 nm lasers were used for autofluorescence (AF), Dextran 488 and Evans Blue, respectively. For detection, photomultiplier tubes (PMT) detectors were set as follow: a first SDM490 was positioned in front of the first PMT associated with a BA 430-470 for AF detection; then a SDM560 was positioned in front of the second PMT associated with a BA 505-605 for Dextran 488 detection; and finally, a BA 655-755 filter was positioned in front of the third detector for Evans Blue detection. All channels were acquired simultaneously. Images were acquired in a 640x640 pixel format at zoom 3 (pixel resolution of 331nm) at 4 µs/pixel speed at different time points after Evans Blue injection: prior to injection, 30 sec, 3 min, 5 min, 10 min and15 min post-injection. For live videos, the frame interval between each image was 2.4 seconds. During live acquisition, the sample was scanned in x and y at zoom 1X until a region of interest was observed during or after Evans Blue injection. The zoom was then adapted to Zoom 3X to focus on this specific region of the kidney. For some interesting time-points/localizations, z-stack were acquired as followed: Zoom 3X, step size 2 µm, Z volume between 22 µm up to 44 µm depth. Images were acquired using the Olympus Fluoview software (v4.2.3.6, Olympus, Japan). Final images are 12 bits. Image analysis was performed using FIJI software (NIH, open source).

Quantification of microvascular permeability was assessed by measuring the number of Evans Blue leaking points per field. Capillary perfusion was evaluated by quantification of perfused versus non-perfused capillaries in each field. A capillary branch was defined as one segment between two nearby endpoints. Perfused capillaries with circulation were defined as yellow/green fluorescence in the lumen, and visible red blood cell circulation; non-perfused capillaries were defined as red fluorescence in the lumen (34). Perfused capillaries without circulation were defined as yellow/green fluorescence in the lumen but without cellular circulation.

Statistics

All data were expressed as means ± SEM. Biological and histological data were compared using unpaired *t*-test. Statistical analyses were performed using Prism 8 (Prism-GraphPad software, Inc). P values of 0.05 or less were considered significant.

Study approval

All animal experimental protocols (document number for animal use approval: 4I14057MJHs and IP18047MJHs) were reviewed and approved by the Centre hospitalier de l'Université de Montréal - Comité Institutionnel de Protection des Animaux.

Results

Caspase-3 deficiency preserves long-term renal function after severe AKI.

We showed previously that caspase-3 deficiency prevents microvascular rarefaction and long-term renal fibrosis after mild renal IRI despite early accentuation of tubular injury (26). We now compare the impact of caspase-3 deficiency in severe vs mild forms of IRI-induced AKI. Severe AKI was induced by clamping the renal artery for 60 minutes and mild AKI with renal artery clamping for 30 minutes. Both interventions were followed by contralateral nephrectomy. Serum creatinine levels were significantly higher in severe AKI compared to mild AKI, both in wild-type and caspase-3-/- mice at all time points (Fig. 1A). In caspase-3-/- mice, creatinine levels were significantly higher at day 1 and 2 post-IRI in mild AKI compared with wild-type controls (Fig. 1B). In the severe AKI groups, there was no difference in serum creatinine levels between caspase-3-/- mice and wild-type controls during the first-week post-IRI. At day 21 post-IRI, serum creatinine failed to go back to baseline in both wild-type and caspase-3-/- mice with severe AKI (Fig. 1A). Serum creatinine levels were statistically lower in caspase-3-/- mice with severe AKI compared with wild-type controls with severe AKI but there was no significant difference in mild AKI. Caspase-3-/- mice showed higher tubular injury scores than wild-type controls in both mild and severe AKI at day 1 post-IRI. These results are in line with our previous findings showing redirection towards tubular necroptosis in caspase-3-/- mice in the early phase of AKI (26). On day 21 post-IRI, tubular injury scores were significantly better in caspase3-/- mice compared to wild-type controls in both severe and mild AKI (Fig. 1B). Collectively, these results demonstrate that the severity of IRI predicts long-term renal

dysfunction while early tubular injury does not predict long-term tubular integrity and level of renal dysfunction (Fig. 1B, Fig. S1A).

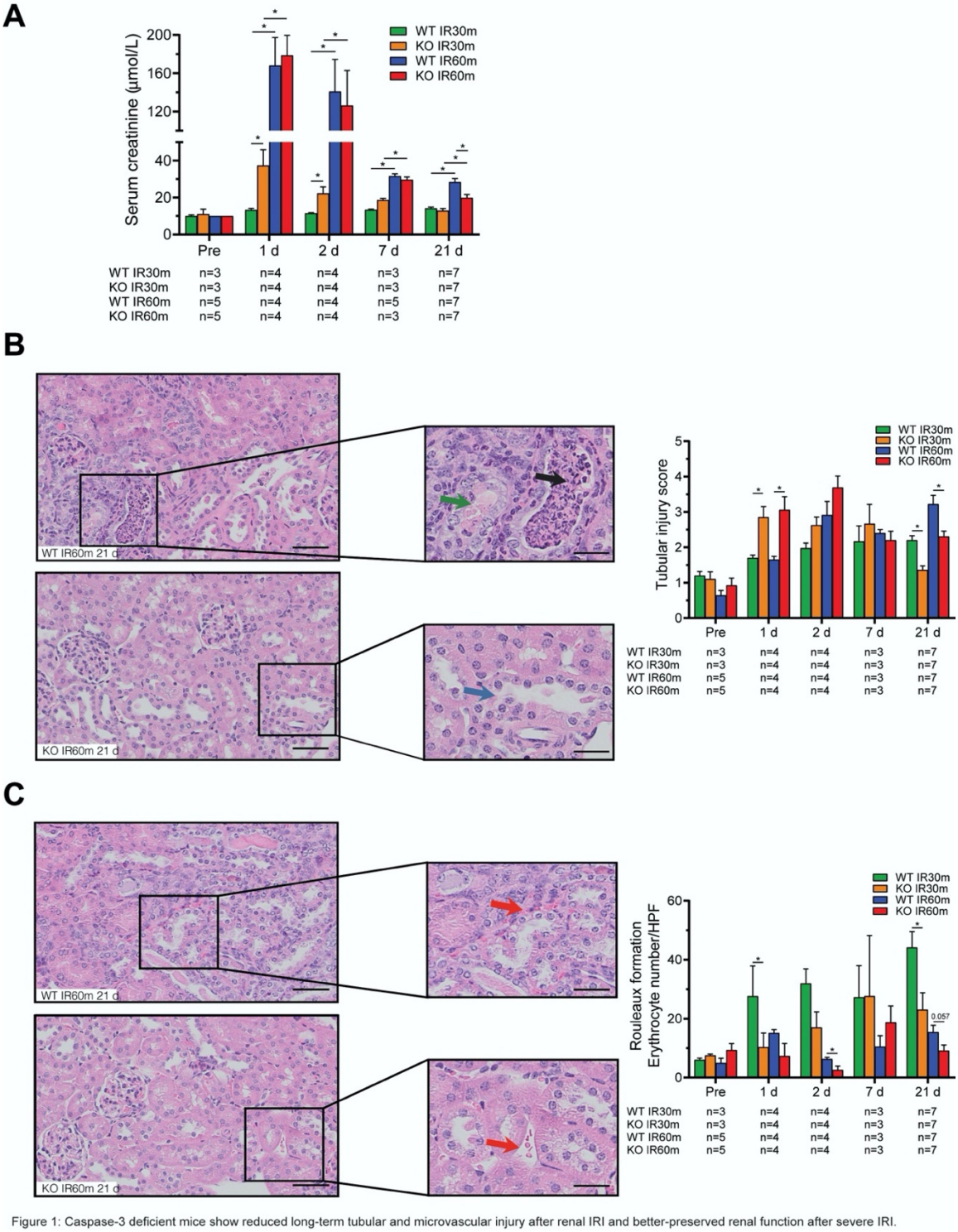

Figure 1: Caspase-3 deficient mice show reduced long-term tubular and microvascular injury after renal IRI and better-preserved renal function after severe IRI.

Caspase-3 deficiency improves long-term renal microvascular integrity and rarefaction after mild and severe forms of IRI-induced AKI.

Microvascular rarefaction is increasingly recognized as an important determinant of progressive renal failure after AKI (24, 37, 38). Therefore, we turned to evaluating the impact of caspase-3 on microvascular integrity in mild and severe forms of AKI (37). Rouleaux formation, a read-out of microvascular congestion, increased in the early phase of AKI in wild-type mice submitted to 30 min of artery clamping and increased further on the long term, suggesting sustained and progressive abnormalities in microvascular circulation (Fig. 1C). Caspase-$3^{-/-}$ mice showed significantly lower rouleaux levels both in the early (day 1) and chronic (day 21) phases of mild AKI (Fig. 1C, Fig. S1B). Intriguingly, severe AKI was associated with lower levels of rouleaux formation in wild-type and caspase-$3^{-/-}$ mice compared to mild AKI. Rouleaux formation at day 21 was significantly lower in caspase-$3^{-/-}$ mice with severe AKI compared with wild-type mice. These results suggest better preservation of microvascular circulation in caspase-$3^{-/-}$ mice, both in mild and severe forms of AKI. The lower levels of rouleaux formation with severe AKI were surprising and raised the possibility of enhanced microvascular rarefaction with severe AKI, preventing microvascular circulation and hence rouleaux formation. To test this possibility, we used immunostaining of murine endothelial cell antigen-32 (MECA-32), a marker of microvascular endothelial cells (34). On day 21 post-IRI, MECA-32 staining in cortico-medullary PTC was significantly reduced in wild-type mice exposed to mild AKI compared to sham-treated animals. MECA-32 was further reduced in wild-type mice exposed to severe AKI compared to sham. In both forms of AKI, caspase-$3^{-/-}$ mice showed significantly higher PTC MECA-32 staining than wild-type counterparts. (Fig. 2A, Fig. S2).

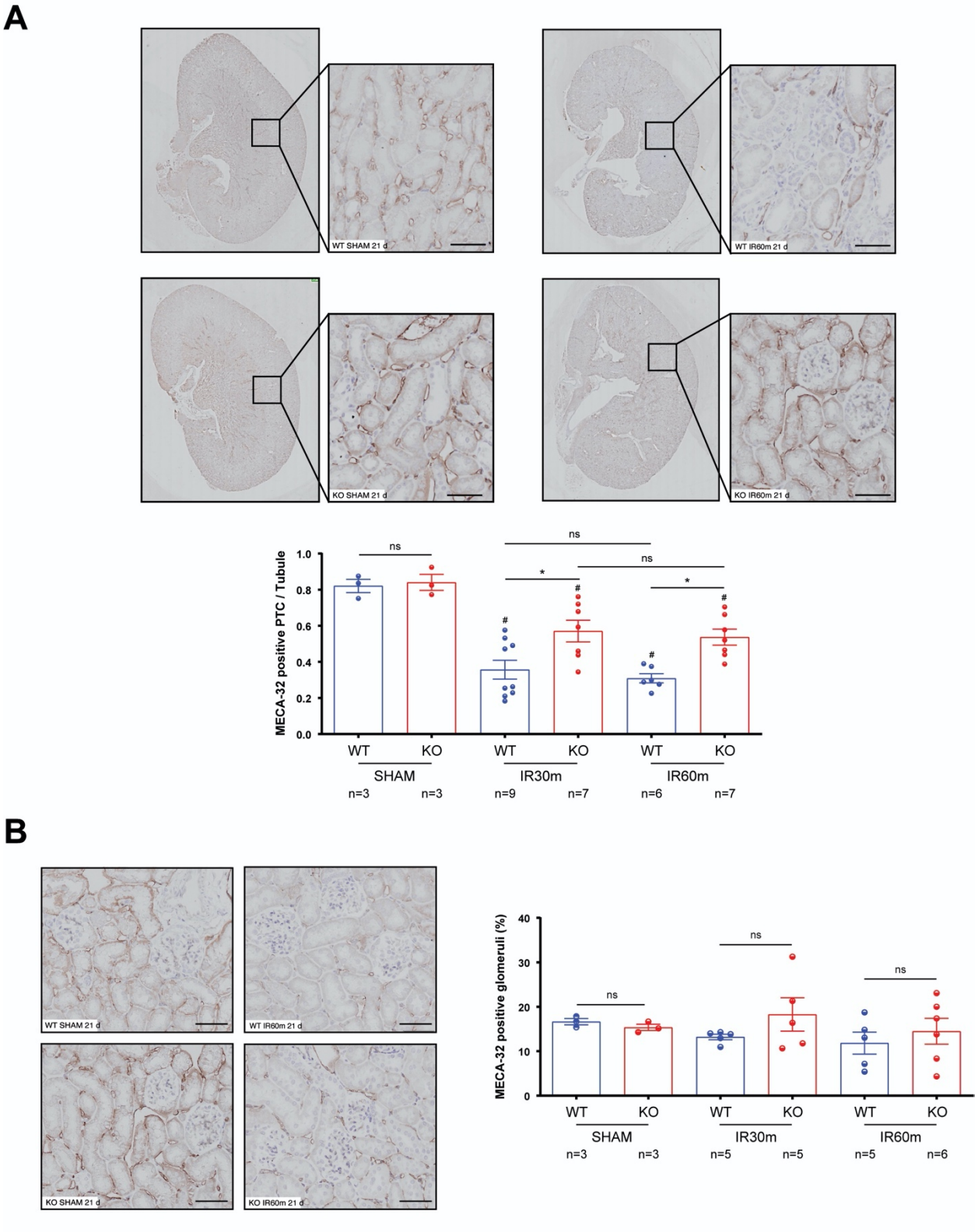

Figure 2: Caspase-3 deficiency preserves the integrity of peritubular capillaries post-IRI.

Electron microscopy also revealed the preservation of microvascular integrity in caspase-3$^{-/-}$ mice. Features of endothelial apoptosis, such as nuclear condensation, apoptotic bodies, apoptotic exosome-like vesicles, were found within PTC in wild-type but not in the caspase-3$^{-/-}$ mice (Fig. 3A-F). Rouleaux formation was also observed in PTC of wild-type mice, consistent with results on HE-stained tissue (Fig.1C). Wild-type mice also showed reduced endothelial fenestration and basement membrane irregularities at 21 d post-IRI (Fig. 3A-C). These features were limited in caspase-3$^{-/-}$ mice, where microvascular integrity was better preserved. (Fig. 3D-F). Caspase-3 immunohistochemistry staining revealed the presence of several positive endothelial-like cells within PTC in wild-type mice at 21 days post severe IRI (Fig. S3) unlike caspase-3$^{-/-}$ mice. Collectively, these results showed enhanced microvascular rarefaction with more severe forms of AKI and better PTC preservation in caspase-3 deficient mice. We also evaluated whether microvascular compartments other than PTC show differences in MECA-32 staining post-AKI. Glomerular MECA-32 staining was not modulated by AKI in wild-type or caspase-3$^{-/-}$ mice (Fig. 2B). In line with this result, glomerulosclerosis was not modulated post-AKI (Fig. S4). To further confirm these results, we assessed microvascular rarefaction with contrast-enhanced microCT. Total blood vessel volume decreased at day 21 post-IRI in mild and severe AKI when compared to baseline. There was however no significant difference between wild-type and caspase-3$^{-/-}$ mice (Fig. 4). However, significant differences were noted when considering terminal capillary volume. In wild-type mice, the number of terminal capillaries was lower than baseline in mild AKI and there was a further significant reduction in severe AKI. Caspase-3$^{-/-}$ mice showed significantly higher terminal capillary numbers than wild-type counterparts after mild and severe AKI (Fig. 4C). Collectively, these results demonstrate the importance of caspase-3 in controlling microvascular rarefaction in both mild and severe forms of AKI.

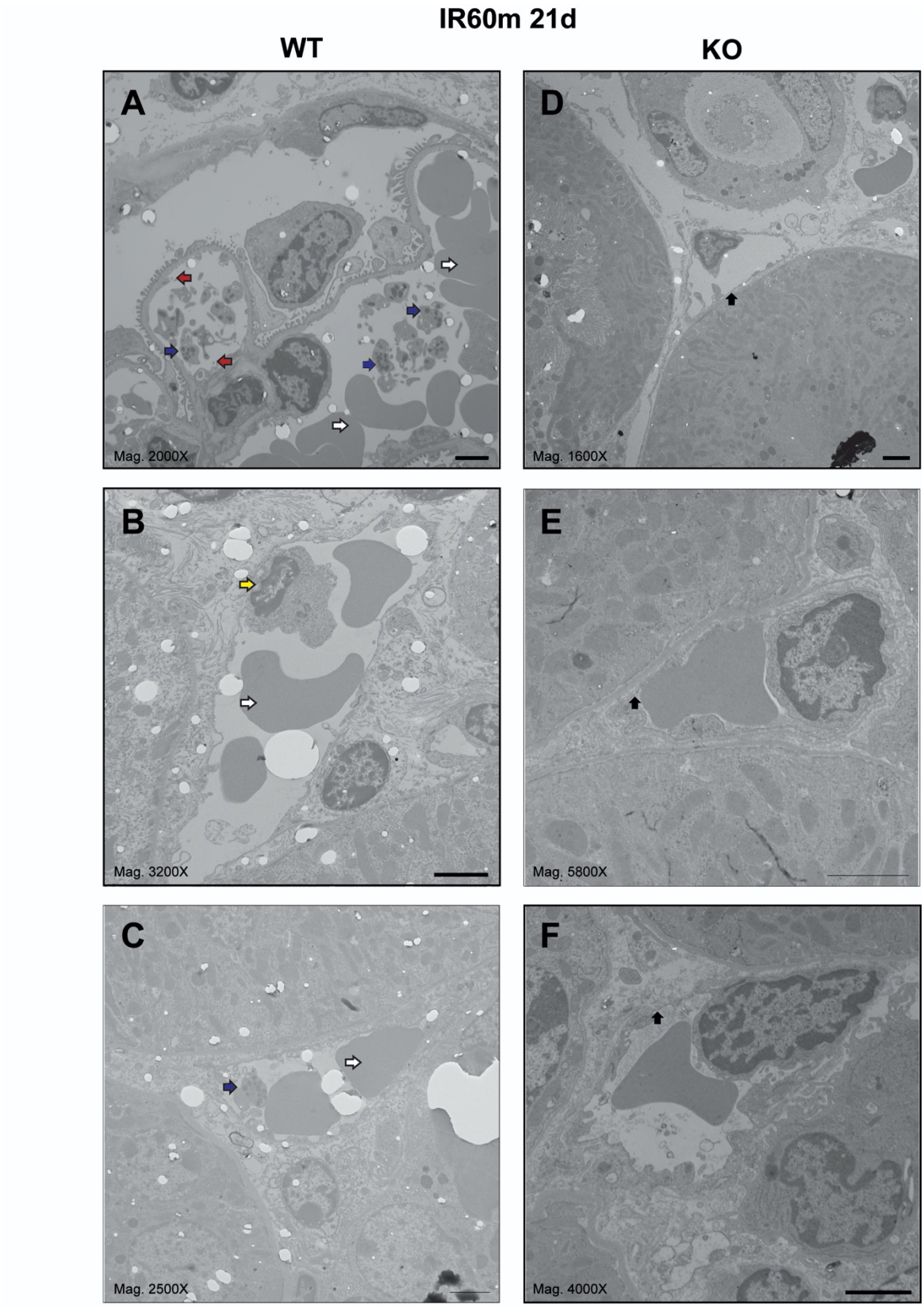

Figure 3: Caspase-3 deficiency prevents endothelial apoptosis post severe IRI.

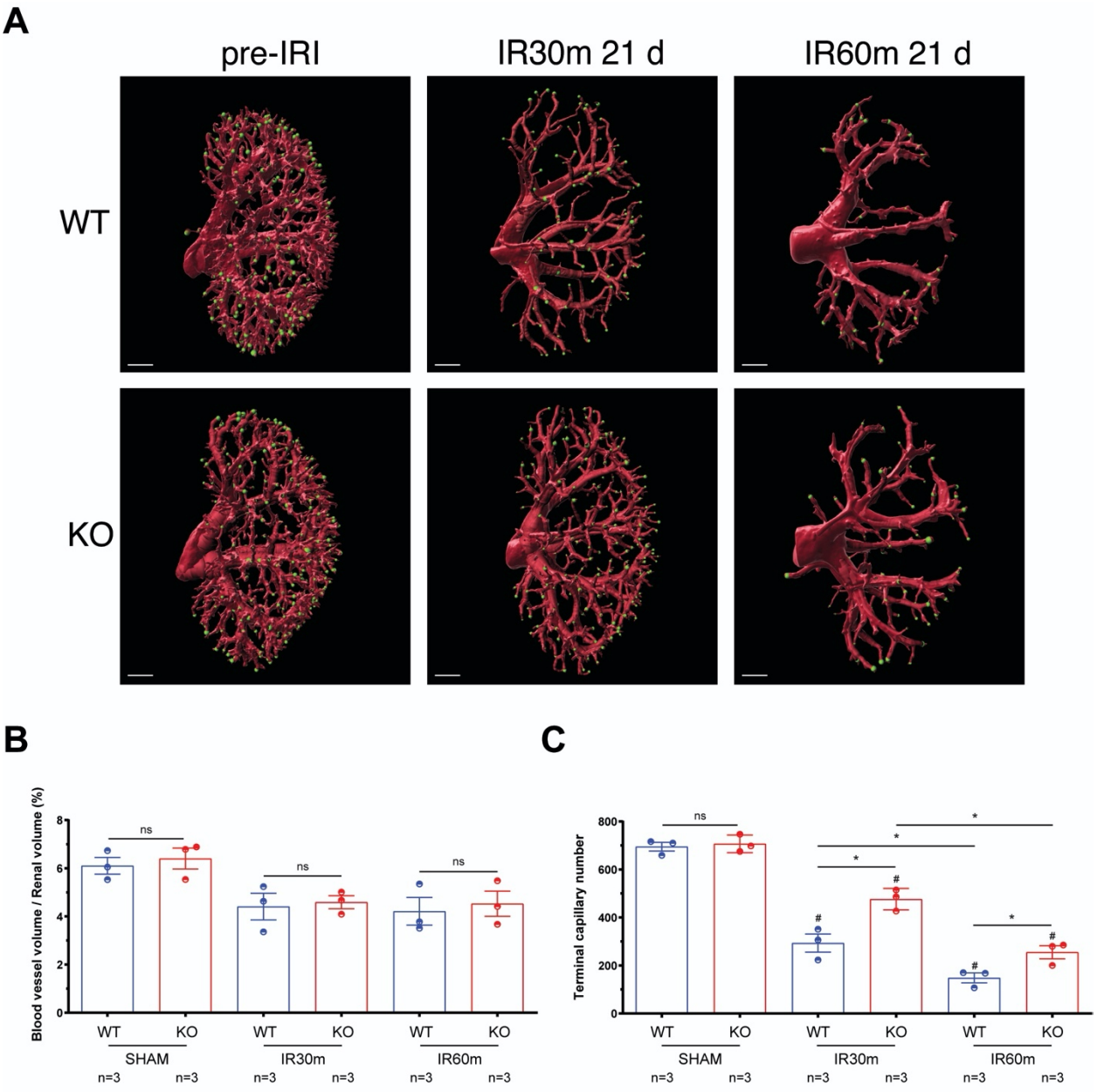

Figure 4: Caspase-3 deficiency prevents microvascular rarefaction of terminal capillary in mild and severe forms of IRI.

Caspase-3 deficiency prevents endothelial permeability disorder after mild and severe AKI.

Abnormal microvascular permeability is another feature of AKI to CKD transition and is thought to contribute to the development of a hypoxic microenvironment that fuels fibrogenesis, tubular injury and renal failure (37). We evaluated endothelial permeability post-IRI with intra-vital imaging using intra-vital confocal microscopy. Mice were injected with fluorescein isothiocyanate–labeled high molecular weight (2000 kDa) dextran to delineate the vasculature and with red fluorescent Evans Blue to detect extravasation. At day 21 post-IRI, wild-type mice with mild AKI showed abnormal PTC permeability with significantly increased global kidney Evans Blue extravasation compared with sham-treated mice (Fig. 5D). Caspase-$3^{-/-}$ mice with mild AKI showed reduced Evans Blue extravasation when compared to wild-type controls. There was however no difference between wild-type and Caspase-$3^{-/-}$ mice with severe AKI. We went on to characterize microscopic differences. Wild-type mice exposed to mild AKI showed areas of extravasation, the number of which was further enhanced in wild-type mice exposed to severe AKI. These extravasation areas were characterized by the presence of extravascular Evans Blue but not 2000 kDa dextran. We observed the appearance of Evans Blue within the peritubular or tubular lumen shortly after I.V. administration suggesting respectively PTC and glomerular membrane dysfunction after IRI (video 5-8). In both mild and severe AKI, caspase-$3^{-/-}$ mice showed significantly reduced length of non-perfused PTC when compared to wild-type mice (Fig. 5A, B, Video 1, 2, Fig. S5). The ratio of perfused capillaries decreased in wild-type mice exposed to mild AKI when compared to baseline and the decrease was further enhanced in wild-type mice exposed to severe AKI (Fig. 5C). Caspase-$3^{-/-}$ kidneys showed a higher number of perfused capillaries in mild and severe AKI as compared to wild-type kidneys (Fig. 5C, Video 3, Video 4, Fig. S6, Video 9). Prevention of PTC rarefaction leading to preservation of tubule perfusion was also reflected by lower expression of tubular HIF-1a in caspase-$3^{-/-}$ mice at 21 days post-IRI both in the cortex and cortico-medullary junction (Fig. S7). Collectively, these results demonstrate that AKI of increasing severity leads to enhanced permeability disturbances and that caspase-3 controls microvascular integrity and permeability after mild and severe AKI.

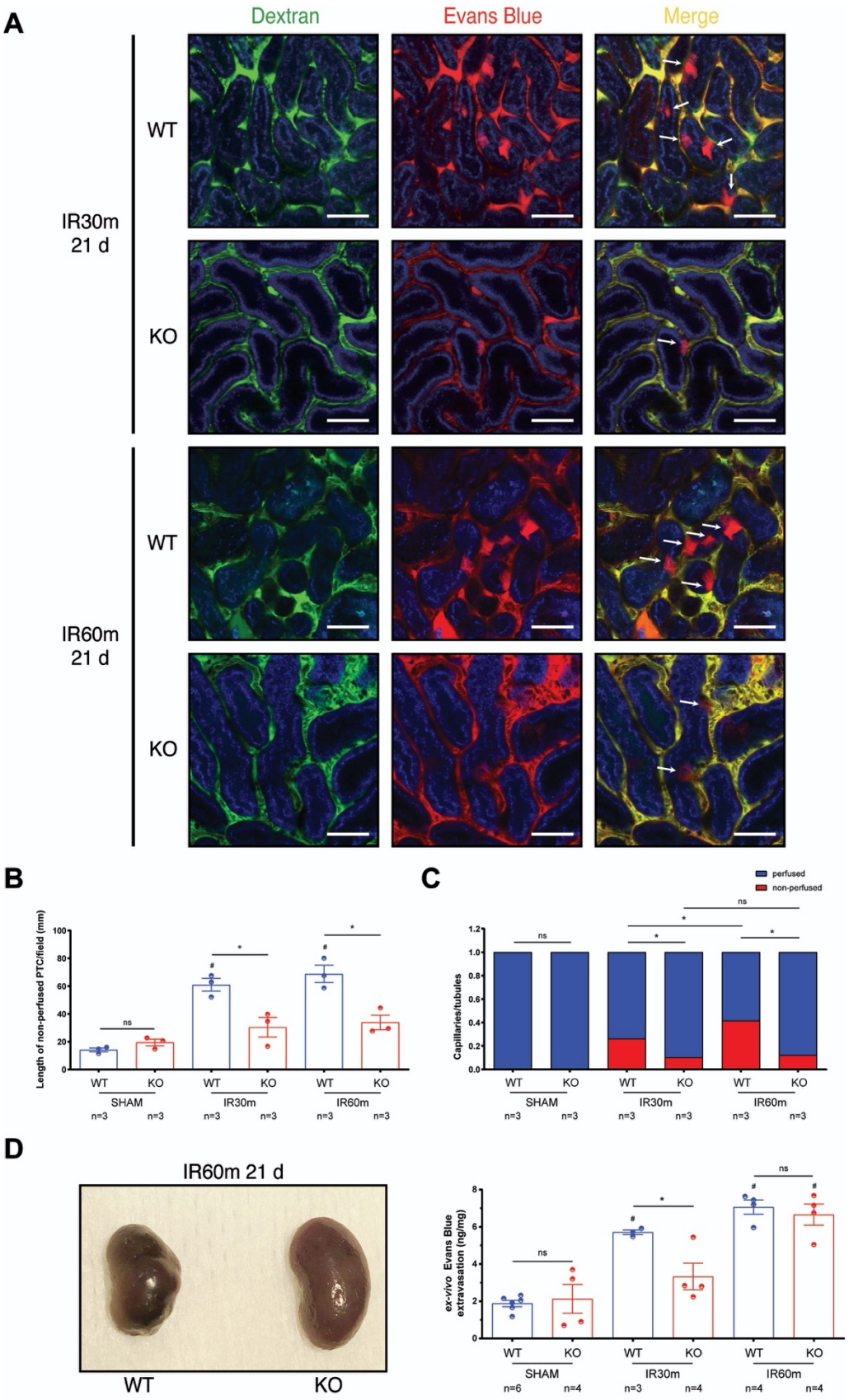

Figure 5: Caspase-3 deficient mice show reduced long-term endothelial permeability disturbances after mild and severe IRI.

Caspase-3 deficiency prevents renal fibrogenesis after AKI.

Progressive renal failure is classically accompanied by fibrosis characterized by increased collagen deposition and interstitial myofibroblast differentiation. Renal microvascular disturbances are frequently associated with renal fibrogenesis although recent data suggest that this association may not always hold true (24). Staining with Sirius red, a marker of collagen I and III, revealed a significant increase in peritubular collagen deposition at day 21 post-IRI in wild-type mice exposed to mild and severe AKI. Caspase-3 deficient mice showed reduced collagen deposition as compared with wild-type controls in both mild and severe forms of AKI (Fig. 6A). Increased collagen deposition with AKI was not present in all microvascular compartments as Sirius red staining in glomeruli was not modulated by AKI in wild-type or caspase-$3^{-/-}$ mice at day 21 post-IRI (Fig. 6B). Electron microscopy confirmed the accumulation of collagen within the peritubular basement membrane in wild-type mice (Fig. 6C). Myofibroblast differentiation, as evaluated with alpha-smooth muscle actin (α-SMA) staining, was assessed in PTC and glomeruli. On day 21 post-IRI, wild-type mice showed increased peritubular α-SMA staining in both forms of AKI. In both mild and severe forms of AKI, caspase-$3^{-/-}$ mice demonstrated less myofibroblast differentiation within renal PTC (Fig. 7A, B). However, there was no difference in α-SMA staining within glomeruli or macrovessels between wild-type or caspase-3 deficient mice (Fig. 7C, D). Collectively, these results highlight the association between PTC abnormalities and fibrogenesis and confirm the protective role of caspase-3 deficiency in preventing peritubular fibrosis.

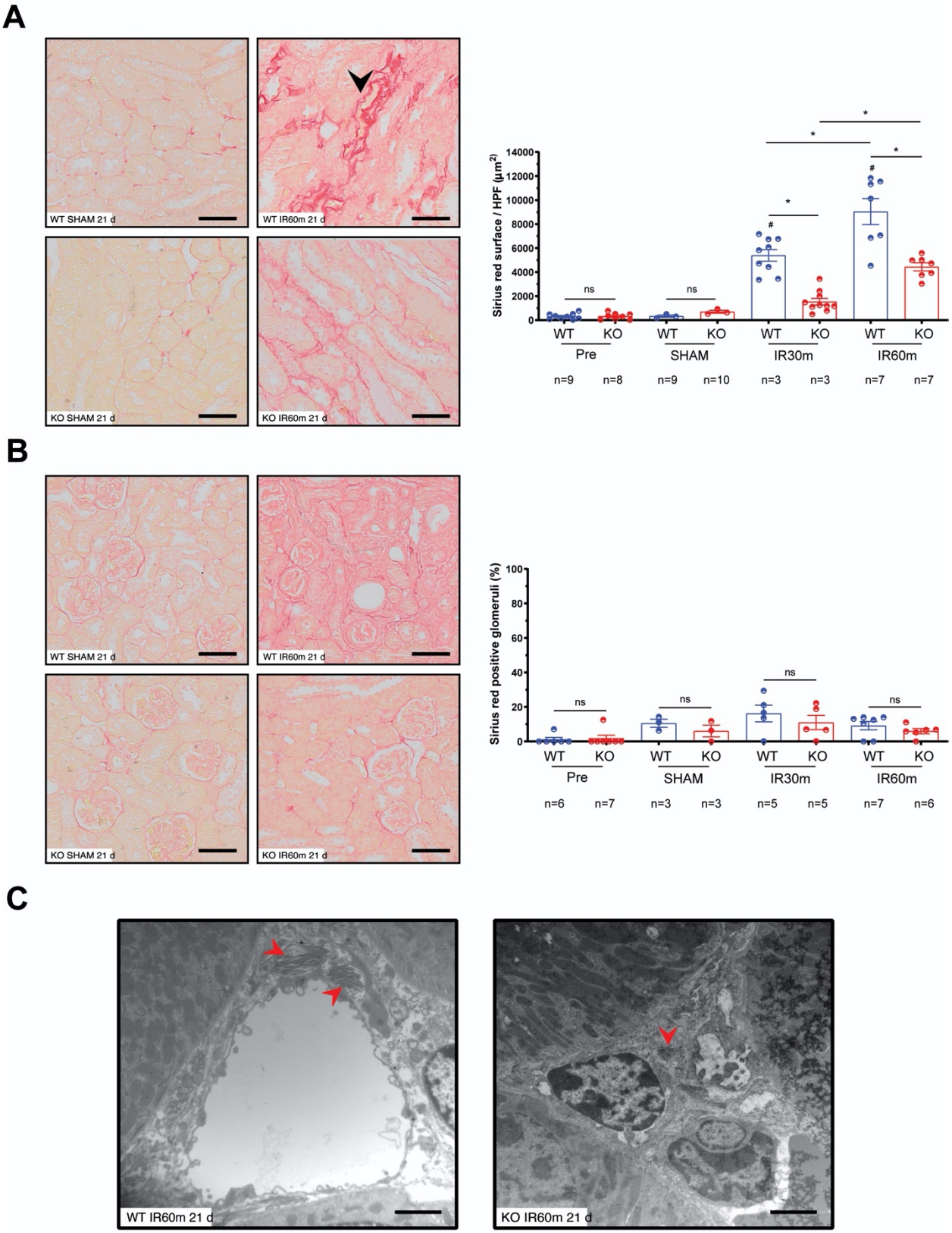

Figure 6: Caspase-3 deficiency attenuates long-term collagen deposition in peritubular capillary after mild and severe IRI.

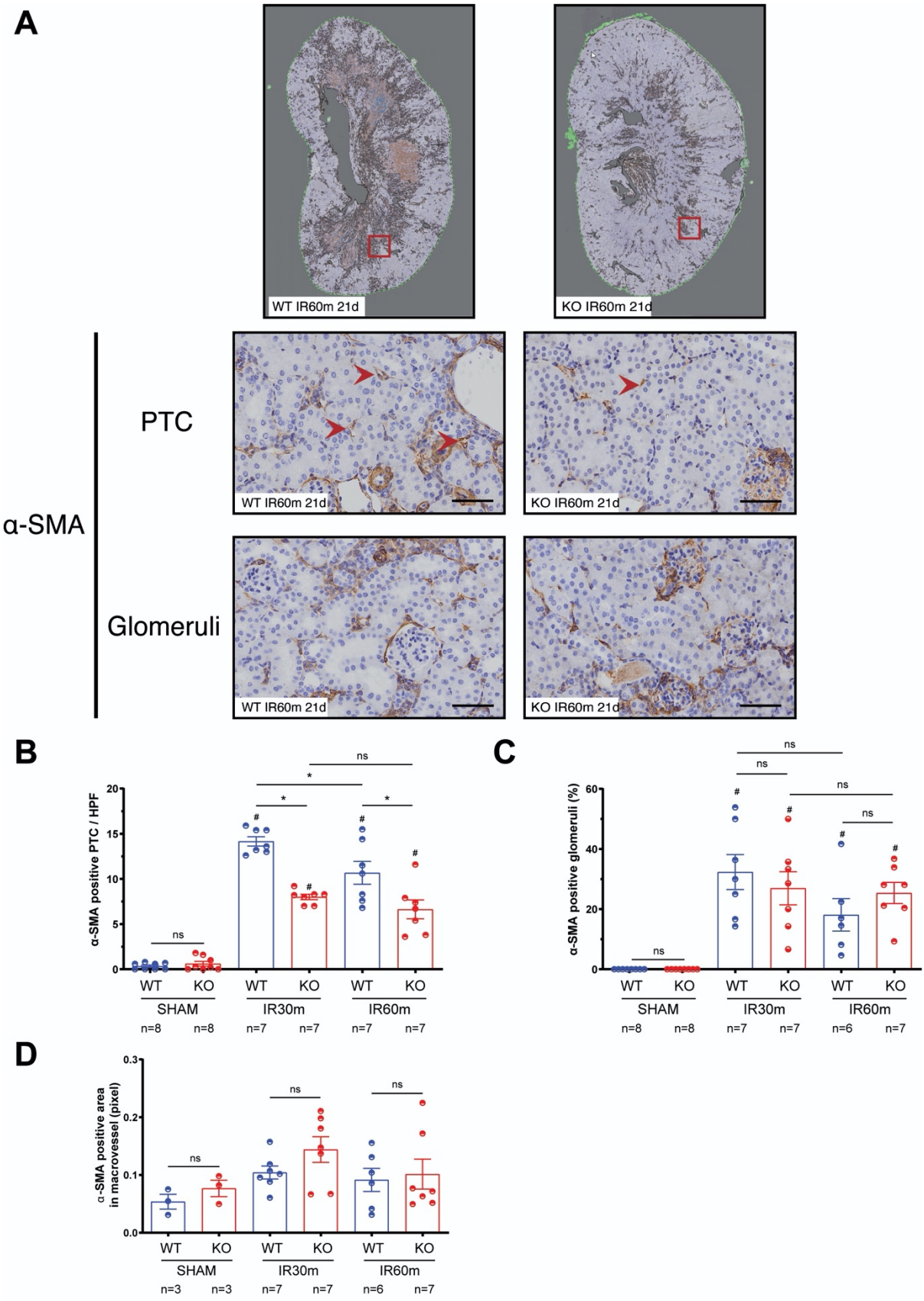

Figure 7: Caspase-3 deficient mice show reduced long-term renal fibrosis after mild and severe IRI.

Discussion

Microvascular rarefaction is increasingly appreciated as an important predictor of AKI to CKD transition following ischemia-reperfusion injury. Here we show that caspase-3 is a pivotal regulator of peritubular microvascular integrity and long-term dysfunction after IRI. The severity of acute IRI correlates in the long term with the severity of microvascular rarefaction, fibrosis, and loss of renal function. Severe AKI also leads to greater long-term perturbation of renal microvascular permeability (Fig. 8). We identify caspase-3 as a pivotal factor controlling microvascular homeostasis and renal function post-IRI. These results extend our previous observations pointing to an important role for caspase-3 in the regulation of microvascular rarefaction following mild IRI. In this study, we show that in mild and severe forms of AKI, caspase-3 control not only the number of surviving peritubular capillaries but also impacts their permeability and overall tubule-interstitial oxygenation. The beneficial impact of caspase-3 deficiency on long-term renal outcomes is present despite the early deterioration of epithelial injury, both in mild and severe forms of AKI, confirming the predominant role of microvascular injury over early epithelial damage in regulating AKI to CKD transition.

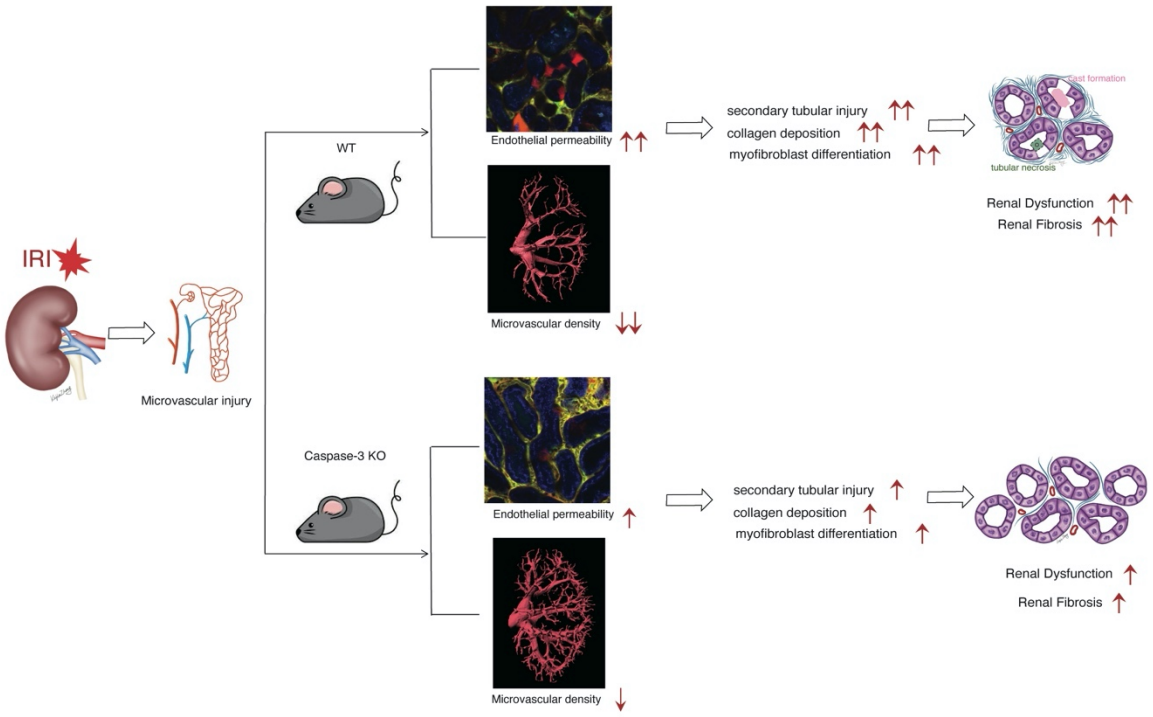

Figure 8: Impact of caspase-3 on microvascular endothelial injury and renal fibrosis and dysfunction post IRI.

A number of different murine IRI models (39-42) are available to investigate the pathophysiology of AKI-to-CKD transition. However, severe forms of AKI are less commonly investigated given the difficulty of ensuring animal survival in the long term (43, 44). Head-to-head comparisons of microvascular abnormalities after mild and severe IRI are therefore still lacking. Yet severe AKI is an important cause of progressive renal dysfunction in patients (45) and efforts are needed to better understand the mechanisms contributing to progressive renal failure in this context. In this study, we used unilateral renal artery clamping for 30 and 60 minutes along with contralateral nephrectomy, as means of comparing mild and severe forms of IRI on AKI-to-CKD transition. As expected, severe AKI led to higher serum creatinine levels at all time points when compared to mild AKI. Intriguingly, indices of microvascular congestion 2 days and 3 weeks after IRI were significantly less important in severe AKI compared to mild AKI. This finding led us to consider the possibility that severe IRI aggravates microvascular drop-out. In that case, congestion indices would be reduced not because of better microvascular integrity but rather by the disappearance of the microvascular network. Our results largely support this assumption. Immunohistochemistry for MECA-32, electron microscopy and *in vivo* imaging with 3D integral renal vasculature visualization confirmed enhanced and accelerated microvascular rarefaction with increased severity of IRI. Caspase-3 deficiency led to better preservation of the renal peritubular microvasculature both in mild and severe forms of AKI. 3D reconstructed kidney from microCT imaging showed enhanced reduction of terminal capillary volume with increasing severity of IRI and preservation of capillary volume in caspase-3 deficient animals. Microvascular analysis along with endothelial staining confirmed PTC rarefaction but showed no difference in glomerular histology in both forms of AKI. These findings are in line with observations showing little ultrastructural alterations of glomerular endothelial membranes following renal ischemia-reperfusion injury (46, 47).

Our results also point to caspase-3 as a pivotal regulator of PTC injury and dysfunction. IRI triggers breaks of intercellular adhesions leading to increased PTC permeability exemplified by leakiness of the contrast agent (48). Enhanced permeability likely represents a compensation mechanism aimed at preserving tissue perfusion after ischemia. However, in the long-term, leakiness leads to interstitial edema, capillary compression, and further perturbations in perfusion and oxygenation (49). Using intra-vital kidney imaging, we found abnormal PTC

leakiness with mild IRI and further enhanced permeability abnormalities with severe IRI. Enhanced capillary rarefaction with severe IRI was associated with more severe permeability disturbances and higher tubular expression of HIF-1α. Conversely, caspase-3 deficiency protected against permeability disturbances and microvascular drop-out and was associated with lower HIF-1α tubular levels. These results are in line with previous findings suggesting a major role for microvascular injury in fueling tubular ischemia that can, in turn, contribute to CKD transition (50). Microvascular permeability disturbances similar to the ones we described after severe IRI injury have been reported in association with a number of animal models of renal dysfunction such as ureteral obstruction and Col4a3-deficient mice, and in patient biopsy samples with progressive renal failure due to glomerulonephritis and interstitial nephritis (34). These similarities raise the possibility that microvascular rarefaction and permeability disturbances represent a common pathway of transition toward progressive loss of renal function, irrespective of the initial cause of renal dysfunction.

Renal fibrosis is a classical hallmark of progressive renal failure. The present work highlights a close association between the severity of microvascular disturbances, level of peritubular fibrosis, and loss of renal function. There was however no correlation between indices of early tubular injury and long-term renal fibrosis or renal function. In caspase-3 deficient mice, early renal dysfunction and tubular injury scores were worse than wild-type controls in both forms of IRI. Yet caspase-3 deficient mice showed lower renal fibrosis and reduced dysfunction in the long term. Collectively, our results point to the importance of turning our attention to markers of microvascular injury as potential predictors of AKI to CKD transition. Currently, AKI severity is evaluated with clinical criteria, such as an increase in serum creatinine, decreased urine output, and the need for renal replacement therapy. Most biomarkers of AKI, such as cystatin C, kidney-injury-molecule-1 (KIM-1), and neutrophil gelatinase-associated lipocalin (NGAL) monitor levels of tubular injury (51, 52). However, the present results and an increasing body of literature suggest that early tubular injury is unlikely to predict transition to CKD if not associated with concomitant microvascular injury and PTC drop-out (53, 54). There is an urgent need for biomarkers that could allow a reliable and non-invasive assessment of the degree of PTC damage following IRI. Several new candidates are emerging and should be the scope of future studies. Our group showed that endothelial cells release apoptotic exosome-like

membrane vesicles which can be tracked in circulation following ischemia-reperfusion episodes, including renal IRI (55). Several endothelial associated proteins and molecules have been considered as potential biomarker candidates at an early stage, such as E-selectin, P-selectin, vascular endothelial growth factor (VEGF), glycocalyx, endothelin-1, angiopoietins, intercellular adhesion molecule (ICAM), vascular cell adhesion molecule (VCAM) (56-62). It will be crucial to assess the capacity of these biomarkers and others to predict AKI to CKD transition and long-term renal outcomes after IRI. As acute microvascular dysfunction following IRI has been documented in lungs, liver and intestine (63-66), better means of assessing microvascular damage could prove useful in delineating the relationship between microvascular drop-out and fibrosis in a number of conditions.

Our results also point to caspase-3 as a potential target of intervention for the prevention of CKD transition following AKI. Caspase-3 inhibitors and siRNA have been tested on early renal outcomes in a number of IRI animal models with somewhat conflicting results (67-70). Caspase-3 siRNA intervention also displayed a protective role on renal function in a porcine kidney autotransplant model (70). Although caspase inhibition has yet to be tested in human renal IRI, a pan-caspase inhibitor has been evaluated in clinical trials in the context of liver transplantation (NCT00080236), IDNN-6556 (pan-caspase inhibitor) administration in cold perfusate protected liver damage against IRI initiated apoptosis (71). But, to our knowledge, only early time points were assessed. Further clinical studies addressing the use of caspase inhibition in the prevention of progressive renal dysfunction after IRI are still lacking. Our current results point to the need to address this question in future clinical studies that will look into acute and long-term consequences of renal IRI in patients.

In conclusion, the severity of PTC disturbances after IRI is a major predictor of AKI to CKD transition. Caspase-3 is an important mediator in AKI, due to its crucial regulatory effect on apoptosis and its downstream consequence on microvascular function and rarefaction, fibrogenesis, and renal function post-IRI. These results open new directions for defining predictors of AKI to CKD transition and identify caspase-3 as a novel target of intervention for preserving long-term renal function.

Author contributions

S.L. and M.J.H. conceived and designed the research strategy. S.L. and B.Y. performed experiments. S.L., B.Y., M.H., M.J.H., and N.P. analyzed the slides, images and videos. S.L., B.Y., F.M., J.T., M.B., M.D. analyzed data. S.L., B.Y., F.M., J.T., M.D., M.H., H.C., and M.J.H. interpreted the results. S.L. and F.M. prepared figures. S.L., F.M., and M.J.H. drafted the manuscript. S.L., F.M., H.C., and M.J.H. edited and revised the manuscript. S.L., B.Y., F.M., J.T., M.B., M.D., M.H., H.C., N.P., and M.J.H. approved the final version of the manuscript.

Acknowledgment

The authors acknowledge support from the Canadian Institutes of Health Research (MOP-123436 and PJT-148884) and the Canadian Donation Transplantation Research Program (CDTRP). Marie-Josée Hébert holds the Shire Chair in Nephrology, Transplantation and Renal Regeneration of Université de Montréal. We also thank the J.-L. Lévesque Foundation for renewed support. Shanshan Lan was supported by the Canadian Society of Transplantation (CST) Research Training Award and is a CDTRP trainee. We thank Dr. Junzheng Peng of the Cardiovascular phenotype core facility of the Centre Hospitalier de l'Université de Montréal Research Centre (CRCHUM) for assisting in microCT imaging and Dr. Aurélie Cleret-Buhot of the Cell Imaging core facility of the CRCHUM for performing the confocal microscopy acquisitions. We thank the CRCHUM molecular pathology platform and animal facility for their service. Many thanks to Dr. Shijie Qi for thoughtful advice and to Hyunyun Kim for his assistance with murine renal pathology evaluation. Also great thanks to Dr. Kejia Zhang for his drawing contribution in Figure 8 and graphic abstract.

The authors have no conflict of interest to declare.

References

1. Chawla LS, Eggers PW, Star RA, and Kimmel PL. Acute kidney injury and chronic kidney disease as interconnected syndromes. N Engl J Med. 2014;371(1):58-66.

2. Susantitaphong P, Cruz DN, Cerda J, Abulfaraj M, Alqahtani F, Koulouridis I, et al. World incidence of AKI: a meta-analysis. Clin J Am Soc Nephrol. 2013;8(9):1482-93. doi: 10.2215/CJN.00710113. Epub 2013 Jun 6.

3. Bedford M, Farmer C, Levin A, Ali T, and Stevens P. Acute kidney injury and CKD: chicken or egg? *Am J Kidney Dis.* 2012;59(4):485-91. doi: 10.1053/j.ajkd.2011.09.010.

4. Ishani A, Xue JL, Himmelfarb J, Eggers PW, Kimmel PL, Molitoris BA, et al. Acute kidney injury increases risk of ESRD among elderly. *J Am Soc Nephrol.* 2009;20(1):223-8. doi: 10.1681/ASN.2007080837. Epub 2008 Nov 19.

5. Molitoris BA. Therapeutic translation in acute kidney injury: the epithelial/endothelial axis. *J Clin Invest.* 2014;124(6):2355-63. doi: 10.1172/JCI72269. Epub 2014 Jun 2.

6. Cavaille-Coll M, Bala S, Velidedeoglu E, Hernandez A, Archdeacon P, Gonzalez G, et al. Summary of FDA workshop on ischemia reperfusion injury in kidney transplantation. *Am J Transplant.* 2013;13(5):1134-48.

7. Lechevallier E, Dussol B, Luccioni A, Thirion X, Vacher-Copomat H, Jaber K, et al. Posttransplantation acute tubular necrosis: risk factors and implications for graft survival. *Am J Kidney Dis.* 1998;32(6):984-91.

8. Irish WD, McCollum DA, Tesi RJ, Owen AB, Brennan DC, Bailly JE, et al. Nomogram for predicting the likelihood of delayed graft function in adult cadaveric renal transplant recipients. *J Am Soc Nephrol.* 2003;14(11):2967-74.

9. Amdur RL, Chawla LS, Amodeo S, Kimmel PL, and Palant CE. Outcomes following diagnosis of acute renal failure in U.S. veterans: focus on acute tubular necrosis. *Kidney Int.* 2009;76(10):1089-97. doi: 10.38/ki.2009.332. Epub Sep 9.

10. Lo LJ, Go AS, Chertow GM, McCulloch CE, Fan D, Ordonez JD, et al. Dialysis-requiring acute renal failure increases the risk of progressive chronic kidney disease. *Kidney Int.* 2009;76(8):893-9. doi: 10.1038/ki.2009.289. Epub Jul 29.

11. Yarlagadda SG, Coca SG, Formica RN, Poggio ED, and Parikh CR. Association between delayed graft function and allograft and patient survival: a systematic review and meta-analysis. *Nephrol Dial Transpl.* 2009;24(3):1039-47.

12. Legendre C, Canaud G, and Martinez F. Factors influencing long-term outcome after kidney transplantation. *Transpl Int.* 2014;27(1):19-27.

13. Linkermann A, Chen G, Dong G, Kunzendorf U, Krautwald S, and Dong Z. Regulated cell death in AKI. *J Am Soc Nephrol.* 2014;25(12):2689-701.

14. Sharfuddin AA, and Molitoris BA. Pathophysiology of ischemic acute kidney injury. *Nat Rev Nephrol.* 2011;7(4):189-200. doi: 10.1038/nrneph.2011.16. Epub Mar 1.

15. Basile DP. The endothelial cell in ischemic acute kidney injury: implications for acute and chronic function. *Kidney Int.* 2007;72(2):151-6. Epub 2007 May 2.

16. Basile DP, Friedrich JL, Spahic J, Knipe N, Mang H, Leonard EC, et al. Impaired endothelial proliferation and mesenchymal transition contribute to vascular rarefaction following acute kidney injury. *Am J Physiol Renal Physiol.* 2011;300(3):F721-33. doi: 10.1152/ajprenal.00546.2010. Epub 2010 Dec 1.

17. Horbelt M, Lee SY, Mang HE, Knipe NL, Sado Y, Kribben A, et al. Acute and chronic microvascular alterations in a mouse model of ischemic acute kidney injury. *Am J Physiol Renal Physiol.* 2007;293(3):F688-95. Epub 2007 Jul 11.

18. Basile DP, Donohoe DL, Roethe K, and Mattson DL. Chronic renal hypoxia after acute ischemic injury: effects of L-arginine on hypoxia and secondary damage. *Am J Physiol Renal Physiol.* 2003;284(2):F338-48. Epub 2002 Oct 1.

19. Basile DP, Donohoe D, Roethe K, and Osborn JL. Renal ischemic injury results in permanent damage to peritubular capillaries and influences long-term function. *Am J Physiol Renal Physiol.* 2001;281(5):F887-99.

20. Basile DP, and Yoder MC. Renal endothelial dysfunction in acute kidney ischemia reperfusion injury. *Cardiovasc Hematol Disord Drug Targets.* 2014;14(1):3-14.

21. Steegh FM, Gelens MA, Nieman FH, van Hooff JP, Cleutjens JP, van Suylen RJ, et al. Early loss of peritubular capillaries after kidney transplantation. *J Am Soc Nephrol.* 2011;22(6):1024-9. doi: 10.681/ASN.2010050531. Epub 2011 May 12.

22. Ehling J, Babickova J, Gremse F, Klinkhammer BM, Baetke S, Knuechel R, et al. Quantitative Micro-Computed Tomography Imaging of Vascular Dysfunction in Progressive

Kidney Diseases. *J Am Soc Nephrol.* 2016;27(2):520-32. doi: 10.1681/ASN.2015020204. Epub 2015 Jul 20.

23. Babickova J, Klinkhammer BM, Buhl EM, Djudjaj S, Hoss M, Heymann F, et al. Regardless of etiology, progressive renal disease causes ultrastructural and functional alterations of peritubular capillaries. *Kidney Int.* 2017;91(1):70-85. doi: 10.1016/j.kint.2016.07.038. Epub Sep 24.

24. Menshikh A, Scarfe L, Delgado R, Finney C, Zhu Y, Yang H, et al. Capillary rarefaction is more closely associated with CKD progression after cisplatin, rhabdomyolysis, and ischemia-reperfusion-induced AKI than renal fibrosis. *Am J Physiol Renal Physiol.* 2019;317(5):F1383-F97.

25. Zhang X, Zheng X, Sun H, Feng B, Chen G, Vladau C, et al. Prevention of renal ischemic injury by silencing the expression of renal caspase 3 and caspase 8. *Transplantation.* 2006;82(12):1728-32.

26. Yang B, Lan S, Dieude M, Sabo-Vatasescu JP, Karakeussian-Rimbaud A, Turgeon J, et al. Caspase-3 Is a Pivotal Regulator of Microvascular Rarefaction and Renal Fibrosis after Ischemia-Reperfusion Injury. *J Am Soc Nephrol.* 2018;29(7):1900-16.

27. Yang B, Dieude M, Hamelin K, Henault-Rondeau M, Patey N, Turgeon J, et al. Anti-LG3 Antibodies Aggravate Renal Ischemia-Reperfusion Injury and Long-Term Renal Allograft Dysfunction. *American journal of transplantation : official journal of the American Society of Transplantation and the American Society of Transplant Surgeons.* 2016;16(12):3416-29.

28. Langenberg C, Gobe G, Hood S, May CN, and Bellomo R. Renal histopathology during experimental septic acute kidney injury and recovery. *Crit Care Med.* 2014;42(1):e58-67.

29. Chow BSM, and Allen TJ. Mouse Models for Studying Diabetic Nephropathy. *Curr Protoc Mouse Biol.* 2015;5(2):85-94.

30. Racusen LC, Solez K, Colvin RB, Bonsib SM, Castro MC, Cavallo T, et al. The Banff 97 working classification of renal allograft pathology. *Kidney Int.* 1999;55(2):713-23.

31. Sirois I, Groleau J, Pallet N, Brassard N, Hamelin K, Londono I, et al. Caspase activation regulates the extracellular export of autophagic vacuoles. *Autophagy.* 2012;8(6):927-37.

32. Ehling J, Babickova J, Gremse F, Klinkhammer BM, Baetke S, Knuechel R, et al. Quantitative Micro-Computed Tomography Imaging of Vascular Dysfunction in Progressive Kidney Diseases. *J Am Soc Nephrol.* 2016;27(2):520-32.

33. Ghanavati S, Yu LX, Lerch JP, and Sled JG. A perfusion procedure for imaging of the mouse cerebral vasculature by X-ray micro-CT. *J Neurosci Methods.* 2014;221:70-7.

34. Babickova J, Klinkhammer BM, Buhl EM, Djudjaj S, Hoss M, Heymann F, et al. Regardless of etiology, progressive renal disease causes ultrastructural and functional alterations of peritubular capillaries. *Kidney Int.* 2017;91(1):70-85.

35. Ferrero ME. In vivo vascular leakage assay. *Methods Mol Med.* 2004;98:191-8.

36. Westhorpe CL, Bayard JE, O'Sullivan KM, Hall P, Cheng Q, Kitching AR, et al. In Vivo Imaging of Inflamed Glomeruli Reveals Dynamics of Neutrophil Extracellular Trap Formation in Glomerular Capillaries. *Am J Pathol.* 2017;187(2):318-31.

37. Molitoris BA. Therapeutic translation in acute kidney injury: the epithelial/endothelial axis. *J Clin Invest.* 2014;124(6):2355-63.

38. Basile DP. The case for capillary rarefaction in the AKI to CKD progression: insights from multiple injury models. *Am J Physiol Renal Physiol.* 2019;317(5):F1253-F4.

39. Zager RA, Johnson ACM, Andress D, and Becker K. Progressive endothelin-1 gene activation initiates chronic/end-stage renal disease following experimental ischemic/reperfusion injury. *Kidney International.* 2013;84(4):703-12.

40. Basile DP, Donohoe D, Roethe K, and Osborn JL. Renal ischemic injury results in permanent damage to peritubular capillaries and influences long-term function. *Am J Physiol Renal Physiol.* 2001;281(5):F887-99.

41. Yang L, Besschetnova TY, Brooks CR, Shah JV, and Bonventre JV. Epithelial cell cycle arrest in G2/M mediates kidney fibrosis after injury. *Nat Med.* 2010;16(5):535-43, 1p following 143.

42. Grgic I, Campanholle G, Bijol V, Wang C, Sabbisetti VS, Ichimura T, et al. Targeted proximal tubule injury triggers interstitial fibrosis and glomerulosclerosis. *Kidney Int.* 2012;82(2):172-83.

43. Fu Y, Tang C, Cai J, Chen G, Zhang D, and Dong Z. Rodent models of AKI-CKD transition. *Am J Physiol Renal Physiol.* 2018;315(4):F1098-F106.

44. Skrypnyk NI, Harris RC, and de Caestecker MP. Ischemia-reperfusion Model of Acute Kidney Injury and Post Injury Fibrosis in Mice. *Jove-J Vis Exp.* 2013(78).

45. Forni LG, Darmon M, Ostermann M, Oudemans-van Straaten HM, Pettila V, Prowle JR, et al. Renal recovery after acute kidney injury. *Intensive Care Med.* 2017;43(6):855-66.

46. Rippe C, Rippe A, Larsson A, Asgeirsson D, and Rippe B. Nature of glomerular capillary permeability changes following acute renal ischemia-reperfusion injury in rats. *Am J Physiol Renal Physiol.* 2006;291(6):F1362-8.

47. Picken M, Long J, Williamson GA, and Polichnowski AJ. Progression of Chronic Kidney Disease After Acute Kidney Injury: Role of Self-Perpetuating Versus Hemodynamic-Induced Fibrosis. *Hypertension.* 2016;68(4):921-8.

48. Sutton TA, Mang HE, Campos SB, Sandoval RM, Yoder MC, and Molitoris BA. Injury of the renal microvascular endothelium alters barrier function after ischemia. *Am J Physiol Renal Physiol.* 2003;285(2):F191-8.

49. Olof P, Hellberg A, Kallskog O, and Wolgast M. Red cell trapping and postischemic renal blood flow. Differences between the cortex, outer and inner medulla. *Kidney Int.* 1991;40(4):625-31.

50. Sutton TA. Alteration of microvascular permeability in acute kidney injury. *Microvasc Res.* 2009;77(1):4-7.

51. Ko GJ, Grigoryev DN, Linfert D, Jang HR, Watkins T, Cheadle C, et al. Transcriptional analysis of kidneys during repair from AKI reveals possible roles for NGAL and KIM-1 as biomarkers of AKI-to-CKD transition. *Am J Physiol Renal Physiol.* 2010;298(6):F1472-83.

52. Schaub JA, and Parikh CR. Biomarkers of acute kidney injury and associations with short- and long-term outcomes. *F1000Res.* 2016;5.

53. Chou YH, Huang TM, and Chu TS. Novel insights into acute kidney injury-chronic kidney disease continuum and the role of renin-angiotensin system. *Journal of the Formosan Medical Association.* 2017;116(9):652-9.

54. Devarajan P. The Use of Targeted Biomarkers for Chronic Kidney Disease. *Adv Chronic Kidney D.* 2010;17(6):469-79.

55. Sirois I, Raymond MA, Brassard N, Cailhier JF, Fedjaev M, Hamelin K, et al. Caspase-3-dependent export of TCTP: a novel pathway for antiapoptotic intercellular communication. *Cell death and differentiation.* 2011;18(3):549-62.

56. Futrakul N, and Futrakul P. Biomarker for early renal microvascular and diabetic kidney diseases. *Ren Fail.* 2017;39(1):505-11.

57. Cardinal H, Dieude M, and Hebert MJ. Endothelial Dysfunction in Kidney Transplantation. *Front Immunol.* 2018;9:1130.

58. Dieude M, Bell C, Turgeon J, Beillevaire D, Pomerleau L, Yang B, et al. The 20S proteasome core, active within apoptotic exosome-like vesicles, induces autoantibody production and accelerates rejection. *Sci Transl Med.* 2015;7(318):318ra200.

59. Chade AR. Small Vessels, Big Role: Renal Microcirculation and Progression of Renal Injury. *Hypertension.* 2017;69(4):551-63.

60. Ohnishi Y, Yasudo H, Suzuki Y, Furuta T, Matsuguma C, Azuma Y, et al. Circulating endothelial glycocalyx components as a predictive marker of coronary artery lesions in Kawasaki disease. *Int J Cardiol.* 2019;292:236-40.

61. Powell TC, Powell SL, Allen BK, Griffin RL, Warnock DG, and Wang HE. Association of inflammatory and endothelial cell activation biomarkers with acute kidney injury after sepsis. *Springerplus.* 2014;3:207.

62. Chironi GN, Boulanger CM, Simon A, Dignat-George F, Freyssinet JM, and Tedgui A. Endothelial microparticles in diseases. *Cell Tissue Res.* 2009;335(1):143-51.

63. Xu J, Buchwald JE, and Martins PN. Review of Current Machine Perfusion Therapeutics for Organ Preservation. *Transplantation.* 2020;104(9):1792-803.

64. Ferrari RS, and Andrade CF. Oxidative Stress and Lung Ischemia-Reperfusion Injury. *Oxidative Medicine and Cellular Longevity.* 2015;2015:1-14.

65. Feltes CM, Hassoun HT, Lie ML, Cheadle C, and Rabb H. Pulmonary endothelial cell activation during experimental acute kidney injury. *Shock.* 2011;36(2):170-6.

66. Gonzalez LM, Moeser AJ, and Blikslager AT. Animal models of ischemia-reperfusion-induced intestinal injury: progress and promise for translational research. *Am J Physiol Gastrointest Liver Physiol.* 2015;308(2):G63-75.

67. Homsi E, Janino P, and de Faria JB. Role of caspases on cell death, inflammation, and cell cycle in glycerol-induced acute renal failure. *Kidney Int.* 2006;69(8):1385-92.

68. Nydam TL, Plenter R, Jain S, Lucia S, and Jani A. Caspase Inhibition During Cold Storage Improves Graft Function and Histology in a Murine Kidney Transplant Model. *Transplantation.* 2018;102(9):1487-95.

69. Zhang X, Zheng X, Sun H, Feng B, Chen G, Vladau C, et al. Prevention of renal ischemic injury by silencing the expression of renal caspase 3 and caspase 8. *Transplantation.* 2006;82(12):1728-32.

70. Yang C, Zhao T, Zhao Z, Jia Y, Li L, Zhang Y, et al. Serum-stabilized naked caspase-3 siRNA protects autotransplant kidneys in a porcine model. *Mol Ther.* 2014;22(10):1817-28.
71. Baskin-Bey ES, Washburn K, Feng S, Oltersdorf T, Shapiro D, Huyghe M, et al. Clinical Trial of the Pan-Caspase Inhibitor, IDN-6556, in Human Liver Preservation Injury. *American journal of transplantation : official journal of the American Society of Transplantation and the American Society of Transplant Surgeons.* 2007;7(1):218-25.

Figure legends

Figure 1: Caspase-3 deficient mice show reduced long-term tubular and microvascular injury after renal IRI and better-preserved renal function after severe IRI. (A) Serum creatinine levels in wild-type and caspase-$3^{-/-}$ (KO) mice at baseline (pre-operation), and 1, 2, 7 and 21 days post 30 min and 60 min IRI. (B) Left panel: Representative haematoxylin and eosin (H&E) stained renal sections showing tubular injury from wild-type and caspase-$3^{-/-}$ mice at 21 days post 60 min IRI. Black arrow: polynuclear neutrophil; green arrow: cast formation; blue arrow: tubular dilation (magnification 200X and 400X). Right panel: Mean tubular injury scores of ten randomly chosen high-power fields in mice renal cortical sections at pre-operation and post-IRI at 1, 2, 7 and 21 days from wild-type and caspase-$3^{-/-}$ mice that underwent 30 min and 60 min IRI. (C) Left panel: Representative H&E-stained murine renal sections showing rouleaux formation at 21 days post 60 min IRI (magnification 200X and 400 X). Red arrow: rouleaux formation (vascular congestion). Right panel: Quantification of rouleaux formation in H&E-stained renal cortical sections at pre-operation and post-IRI at 1, 2, 7 and 21 days from wild-type and caspase-$3^{-/-}$ mice that underwent 30 min and 60 min IRI. Scale bar = 50 μm (magnification 200X), scale bar = 100 μm (magnification 400X). Values are mean ± SEM. * $P < 0.05$ between group.

Figure 2: Caspase-3 deficiency preserves the integrity of peritubular capillaries post-IRI. (A) Upper panel: Representative images of MECA-32 immunohistochemistry in the whole kidney and renal cortical-medullary junction from wild-type and caspase-$3^{-/-}$ mice that underwent 60 min IRI and were sacrificed 21 days post-IRI or sham-operation (magnification 200X). Lower panel: Quantification of MECA-32 positive peritubular capillary (PTC) in murine renal cortical-medullary junction sections at 21 days post 30 min and 60 min IRI or sham group. (B) Left panel: Representative images of MECA-32 immunohistochemistry staining within glomeruli from wild-type and caspase-$3^{-/-}$ mice that underwent 60 min IRI and were sacrificed 21 days post-IRI or sham-operation (magnification 200X). Right panel: Quantification of MECA-32 positive glomeruli in murine renal sections at 21 days post 30 min and 60 min IRI or sham group. Scale bar = 50 μm. Values are mean ± SEM.* $P < 0.05$ between group. # $P < 0.05$ compared to WT or KO SHAM.

Figure 3: Caspase-3 deficiency prevents endothelial apoptosis after severe IRI. (A-C): Representative electron micrographs of PTC from wild-type mice that underwent 60 min IRI and sacrificed 21 days post-IRI. (D-F): Representative EM images of PTC from caspase-$3^{-/-}$ mice that underwent 60 min IRI and sacrificed 21 days post-IRI. Blue arrow: apoptotic bodies; red arrow: apoptotic exosome-like vesicles; yellow arrow: nuclear condensation; black arrow: capillary endothelium fenestration; scale bar = 2 μm.

Figure 4: Caspase-3 deficiency prevents microvascular rarefaction of peritubular capillaries in mild and severe forms of IRI. (A) Representative microCT 3D reconstruction images of whole renal microvasculature from wild-type and caspase-$3^{-/-}$ mice that underwent 30 min and 60 min IRI and were sacrificed at 21 days post-IRI or pre-operation. Terminal capillaries in the kidney are labeled as green dots, scale bar = 1000 μm. (B) Quantification of total renal blood vessel volume from wild-type and caspase-$3^{-/-}$ mice at 21 days post 30 min and 60 min IRI or sham-operation. (C) Quantification of renal terminal capillary number from wild-type and caspase-$3^{-/-}$ mice at 21 days post 30 min and 60 min IRI or sham-operation. Values are mean ± SEM. * $P < 0.05$ between group. # $P < 0.05$ compared to WT or KO SHAM.

Figure 5: Caspase-3 deficient mice show reduced long-term endothelial permeability disturbances after mild and severe IRI. (A) Representative intra-vital live images showing renal microvascular endothelial permeability and perfusion from wild-type and caspase-$3^{-/-}$ mice that underwent 30 min and 60 min IRI and were sacrificed 21 days post-IRI. Green channel: fluorescein isothiocyanate-labeled dextran (2000 kDa); red channel: Evans Blue dye; white arrow: peritubular capillary (PTC) permeability depicted by Evans Blue leaking, scale bar = 50 μm. (B) Quantification of the length of non-perfused renal PTC from wild-type and caspase-$3^{-/-}$ mice at 21 days post 30 min and 60 min IRI. (C) Quantification of renal PTC perfusion ratio from wild-type and caspase-$3^{-/-}$ mice at 21 days post 30 min and 60 min IRI. (D) Left panel: Representative images of a retrieved ischemic kidney after Evans Blue perfusion from wild-type and caspase-$3^{-/-}$ mice that underwent 60 min IRI and were sacrificed 21 days post-IRI. Right panel: Quantification of renal *ex vivo* Evans Blue extravasation volume from wild-type and caspase-$3^{-/-}$ mice at 21 days post 30 min and 60 min IRI or sham-operation. Values are mean ± SEM. * $P < 0.05$ between group. # $P < 0.05$ compared to WT or KO SHAM.

Figure 6: Caspase-3 deficiency attenuates long-term collagen deposition in peritubular capillary after mild and severe IRI. (A) Left panel: Representative images of Sirius Red staining within peritubular capillary (PTC) in renal cortical-medullary junction sections from wild-type and caspase-$3^{-/-}$ mice that underwent 60 min IRI and were sacrificed 21 days post-IRI, or sham-operation. Arrowheads show collagen deposition in PTC (magnification 200X), scale bar = 50 μm. Right panel: Quantification of Sirius Red positive area within PTC in murine renal cortical-medullary junction sections at pre-operation, sham-operation, and 21 days post 30 min and 60 min IRI. (B) Left panel: Representative Sirius Red positive glomeruli in renal cortical section from wild-type and caspase-$3^{-/-}$ mice that underwent 60 min IRI and were sacrificed 21 days post-IRI, or sham-operation (magnification 200X), scale bar = 50 μm. Right panel: Quantification of Sirius Red positive glomeruli in renal cortical section from wild-type and caspase-$3^{-/-}$ mice at pre-operation, sham-operation and 21 days post 30 min and 60 min IRI. (C) Representative electron micrographs of collagen deposition in PTC from wild-type and caspase-$3^{-/-}$ mice that underwent 60 min IRI and were sacrificed 21 days post-IRI (magnification 3200X), arrowhead: collagen deposition in PTC, scale bar = 2 μm. Values are mean ± SEM.* $P < 0.05$ between group. # $P < 0.05$ compared to WT or KO SHAM.

Figure 7: Caspase-3 deficient mice show reduced long-term renal fibrosis after mild and severe IRI. (A) Upper panel: Representative α-SMA immunohistochemistry staining in whole murine kidney section 21 days after 60 min IRI. Middle panel: Representative α-SMA immunohistochemistry staining within peritubular capillary (PTC) in renal cortical section at day 21 after 60 min IRI (magnification 200X), scale bar = 50 μm. Lower panel: Representative α-SMA immunohistochemistry staining within glomeruli in renal cortical section at day 21 after 60 min IRI (magnification 200X), scale bar = 50 μm. (B) Quantification of α-SMA positive PTC in renal cortical sections from wild-type and caspase-$3^{-/-}$ mice at 21 days post 30 min and 60 min IRI. (C) Quantification of α-SMA positive glomeruli in renal cortical sections from wild-type and caspase-$3^{-/-}$ mice at 21 days post 30 min and 60 min IRI. (D) Quantification of α-SMA positive cells in macrovessels in renal sections from wild-type and caspase-$3^{-/-}$ mice at 21 days post 30 min and 60 min IRI. Values are mean ± SEM. * $P < 0.05$ between group. # $P < 0.05$ compared to WT or KO SHAM.

Figure 8： Impact of caspase-3 on microvascular endothelial injury and renal fibrosis and dysfunction post-IRI. Microvascular injury induced by renal IRI increases distrubances in microvascular permeability and microvascular rarefaction. It promotes secondary tubular injury, collagen deposition and myofibroblast differentiation, which result in long-term renal dysfunction and renal interstitial fibrosis. Caspase-3 is a pivotal regulator of renal dysfunction as its deficiency largely prevents the above pathophysiological changes.

Supplementary Figure legends

Supplementary Figure 1: Caspase-3 deficiency ameliorates long-term renal tubular injury and microvascular injury after mild IRI. (A) Tubular injury in representative renal sections from wild-type and caspase-$3^{-/-}$ mice at day 21 post 30 min of IRI and stained with haematoxylin and eosin (H&E). (magnifications 200X and 400X). (B) Representative H&E-stained renal sections showing rouleaux formation at day 21 post 30 min of IRI (magnifications 200X and 400X). Scale bar = 50 μm (magnification 200X), scale bar = 100 μm (magnification 400X).

Supplementary Figure 2: Description of multiple morphologies in MECA-32 immunohistochemistry staining in peritubular capillaries (PTCs). Upper panel: Representative images of MECA-32 immunohistochemistry (magnification 200X), scale bar = 50 μm. Lower panel: a: Capillary lumen is clearly stained; b: Capillary lumen is weakly stained; c: Capillary lumen is weakly stained, but the structural outline is visible; d: Smaller positive capillary; e: Capillary lumen is invisible, but the longitudinal axis is visible; f: Capillary lumen is visible, with cellular circulation inside.

Supplementary Figure 3: Caspase-3 deficiency prevents endothelial apoptosis post severe IRI. (A) Representative images of caspase-3 immunohistochemistry from wild-type and caspase-$3^{-/-}$ mice that underwent 60 min IRI (magnification 200X). Arrow: caspase-3 positive endothelial-like cells. (B) Quantification of caspase-3 positive endothelial-like cells in PTC from wild-type mice and caspase-$3^{-/-}$ mice at 21 days post 60 min IRI. Scale bar = 50 μm. Values are mean ± SEM.* $P < 0.05$.

Supplementary Figure 4: Caspase-3 deficiency does not modulate long term renal glomerulosclerosis post severe IRI. (A) Representative photos of silver-stained renal sections showing glomerulosclerosis at day 21 post 60 min of IRI (magnification 200X). (B) Quantification of glomerulosclerosis in murine renal glomeruli at day 21 post 60 min of IRI, scale bar = 50 μm. Values are mean ± SEM.* $P < 0.05$.

Supplementary Figure 5: Intra-vital images of renal capillary perfusion in sham-operated mice. (A) Upper panel: intra-vital images of peritubular capillaries prior to Evans Blue injection and 30 seconds, 5 minutes, and 15 minutes post-injection in sham-operated WT mice. (B) Lower panel: intra-vital images of peritubular capillaries prior to Evans Blue injection and 30 seconds, 5 minutes, and 15 minutes post-injection in sham-operated caspase-$3^{-/-}$ mice. Scale bar = 50 μm.

Supplementary Figure 6: Definitions of different types of renal capillaries in intra-vital live confocal imaging. (A) Definition and example of capillary segments quantification. (B) Definitions and examples of multiple types of renal peritubular capillaries (PTCs) post-IRI.

Supplementary Figure 7: Caspase-3 deficiency ameliorates tubular hypoxia after AKI. (A) Quantification of HIF-1α in murine renal cortical section at day 21 post 30 min and 60 min of IRI. (B) Quantification of HIF-1α at the cortical-medullary junction at day 21 post 30 min and 60 min of IRI. Values are mean ± SEM.* $P < 0.05$.

Video 1: Z stack image showing PTC leaking in WT mice at day 21 post IR for 60 min (zoom 3). Red area: Evans Blue leakage. Yellow/Green: Capillary. Blue: Tubules.

Video 2: Z stack image showing PTC leaking in caspase-$3^{-/-}$ mice at day 21 post IR for 60 min (zoom 3). Red area: Evans Blue leakage. Yellow/Green: Capillary. Blue: Tubules.

Video 3: Live imaging showing PTC perfusion in WT mice at day 21 post IR for 60 min (zoom1-zoom3). Red area: Evans Blue leakage. Yellow/Green: Capillary. Blue: Tubules.

Video 4: Live imaging showing PTC perfusion in caspase-$3^{-/-}$ mice at day 21 post IR for 60 min (zoom1-zoom3). Red area: Evans Blue leakage. Yellow/Green: Capillary. Blue: Tubules.

Video 5: Live imaging showing glomerular leakage in WT mice at day 21 post IR for 30 min (zoom 1). Red area: Evans Blue leakage. Yellow/Green: Capillary. Blue: Tubules. Star: Glomerular leakage of Evans Blue in tubular lumen.

Video 6: Live imaging showing PTC leakage and glomerular leakage in caspase-3$^{-/-}$ mice at day 21 post IR for 30 min (zoom 1). Red area: Evans Blue leakage. Yellow/Green: Capillary. Blue: Tubules. Arrow: PTC leakage of Evans Blue. Star: Glomerular leakage of Evans Blue in tubular lumen.

Video 7: Live imaging showing PTC leaking process (zoom 1). Red area: Evans Blue leakage. Yellow/Green: Capillary. Blue: Tubules. Arrow: PTC leakage of Evans Blue.

Video 8: Live imaging showing glomerular leaking process (zoom 3). Red area: Evans Blue leakage. Yellow/Green: Capillary. Blue: Tubules. Star: Glomerular leakage of Evans Blue in tubular lumen.

Video 9: Live imaging showing different renal PTCs definitions post-IRI (zoom 3). Arrowhead: non-perfused PTC; Arrow: perfused PTC without circulation; Star: PTC with normal circulation.

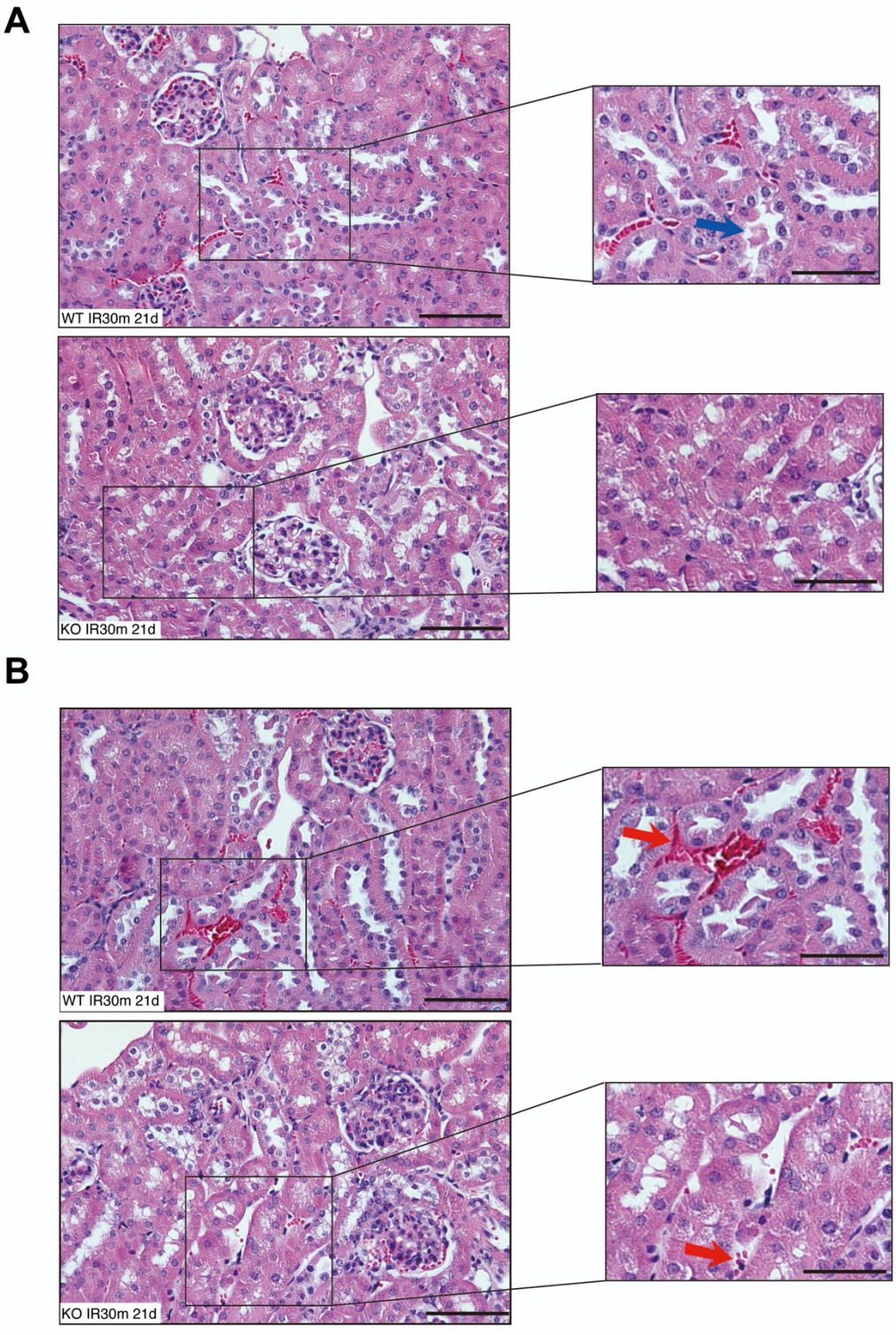

Supplementary Figure 1: Caspase-3 deficiency ameliorates long-term renal tubular injury and microvascular injury after mild IRI.

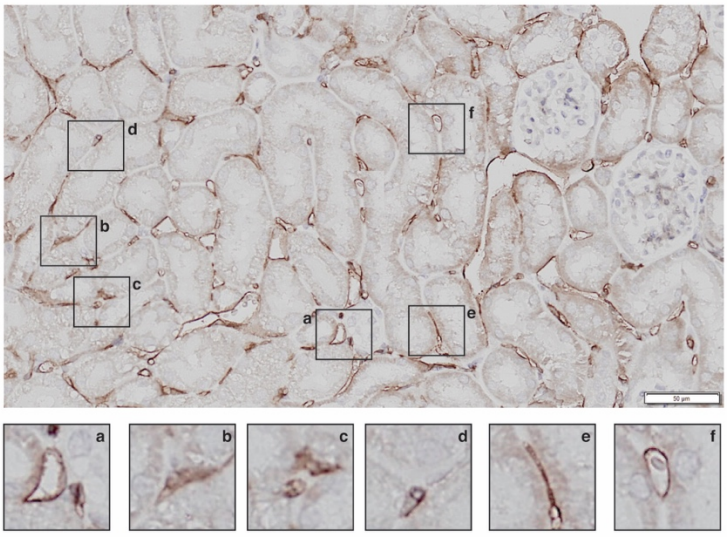

Supplementary Figure 2: Description of multiple morphology in peritubular capillries (PTCs).

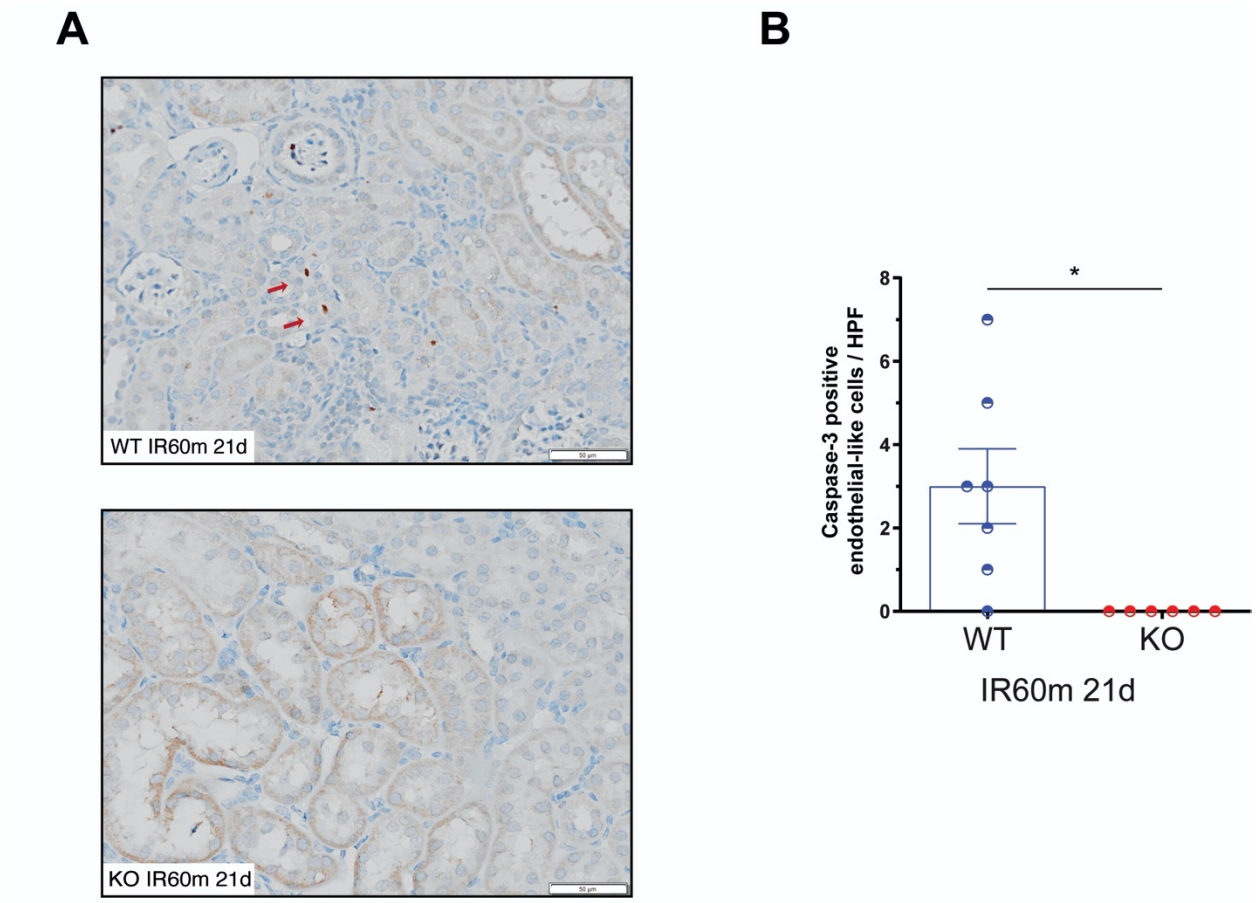

Supplementary Figure 3: Caspase-3 deficiency inhibits endothelial apoptosis post severe IRI.

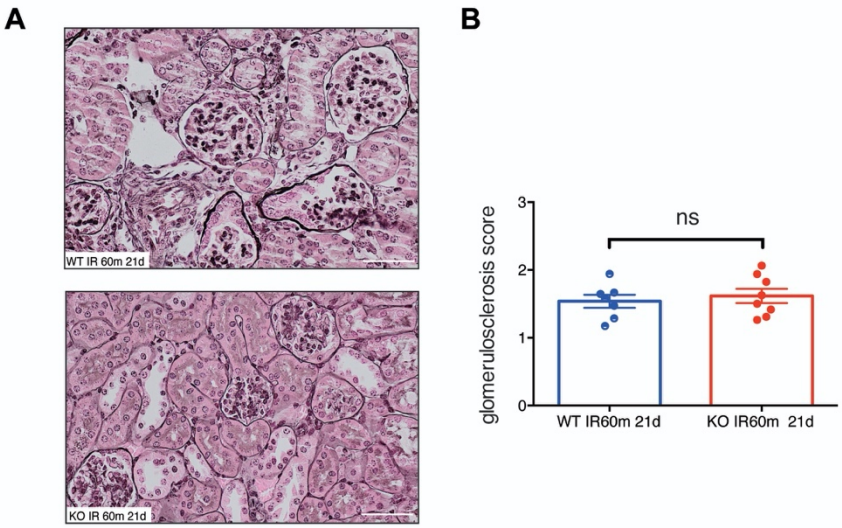

Supplementary Figure 4: Caspase-3 deficiency does not modulate long term renal glomerulosclerosis post severe IRI.

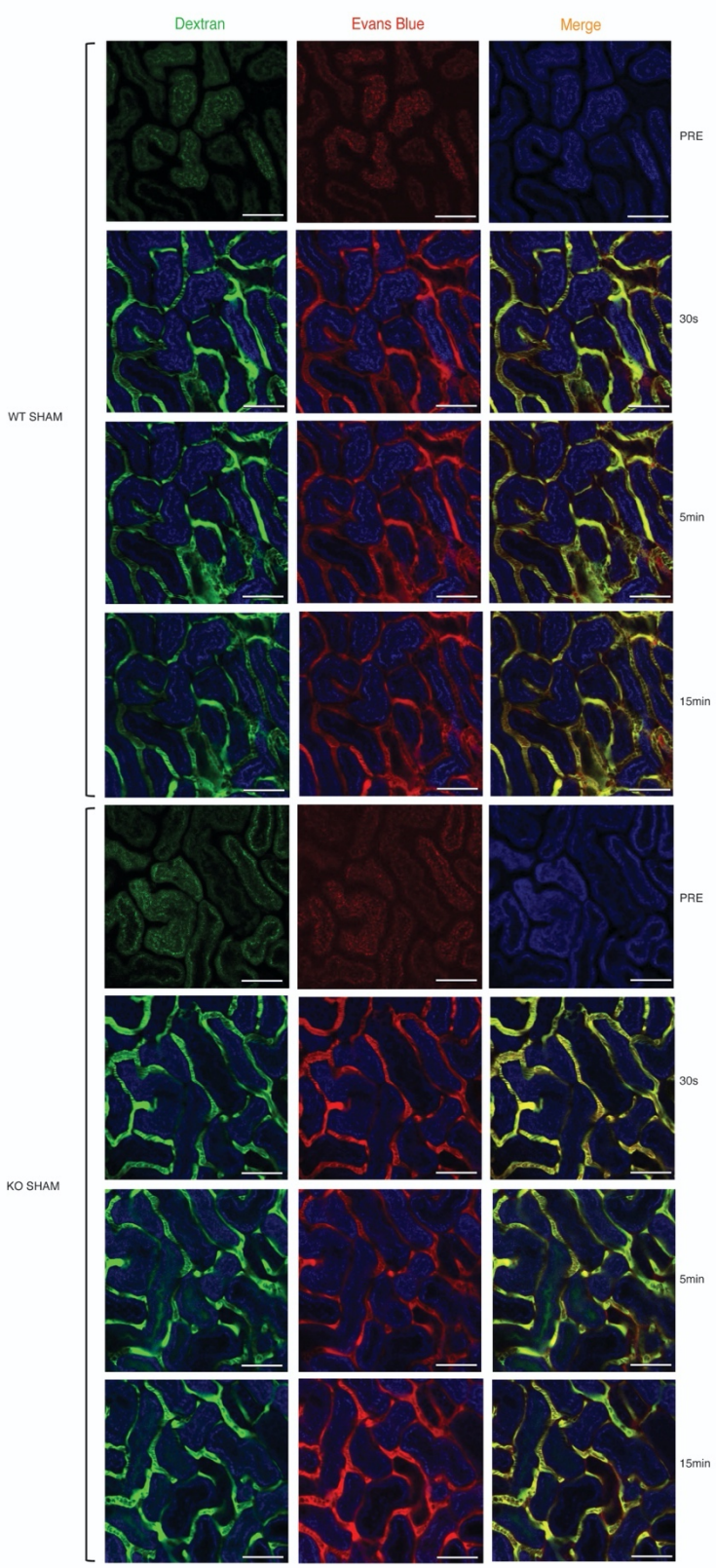

Supplementary Figure 5: Intra-vital images of renal capillary perfusion in sham-operated mice.

A

Definition: capillary=one segment between two nearby visible endpoints

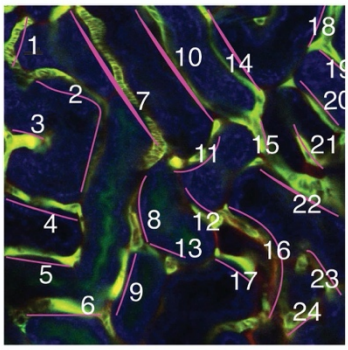

B

Definition: perfused capillary with circulation
= yellow/green fluorescence in capillary lumen (star)

perfused capillary without circulation
=yellow/green fluorescence in capillary lumen (arrow)

non-perfused capillary
= red fluorescence in capillary lumen (arrowhead)

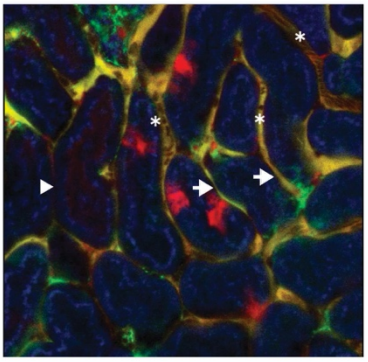

Supplementary Figure 6: Definitions of different types of renal capillaries in intra-vital live confocal imaging.

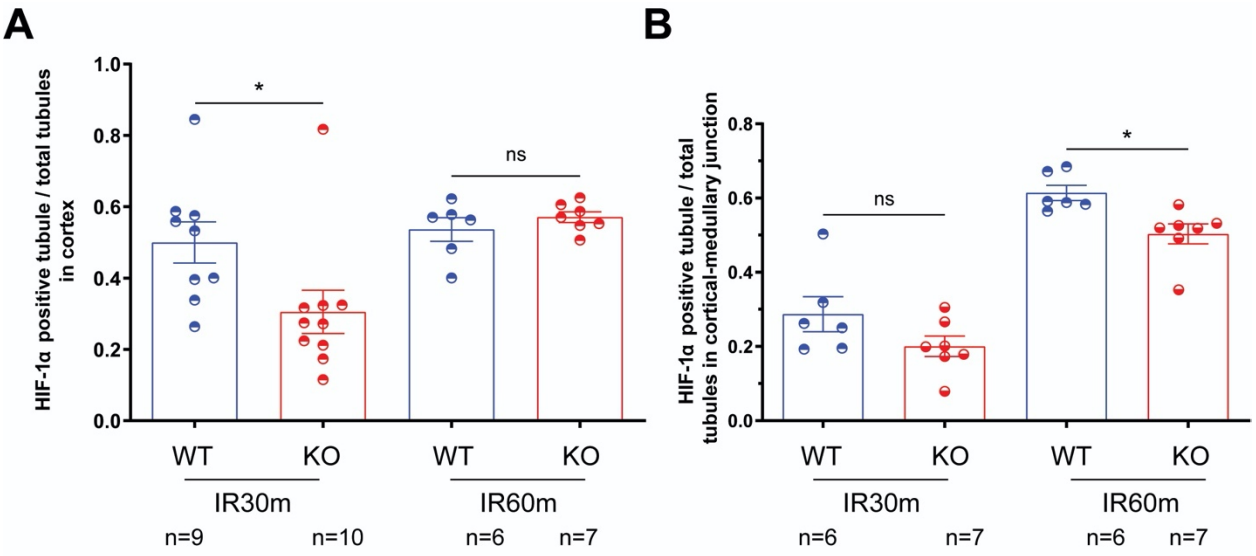

Supplementary Figure 7: Caspase-3 deficiency ameliorates tubular hypoxia after AKI.

Discussion

In summary, my work demonstrates the different impacts of the tubular epithelial compartment and the microvascular endothelial compartment on renal fibrosis and progressive renal dysfunction in the context of IRI-induced renal damage. IR and hypoxia-reoxygenation, experimental stresses that we chose to mimic IRI's effect *in vivo* and *in vitro*, activate cell death crosstalk and renal parenchymal dysfunction.

Compared with early tubular epithelial injury, my work has demonstrated that microvascular injury functions as a predominant driver of progressive renal dysfunction, especially peritubular capillary (PTC) injury and the subsequent microvascular rarefaction, displaying a solid correlation with secondary tubular atrophy, long-term interstitial fibrosis progression, and renal function decline.

To clarify the cellular stress and death responses in different renal compartments post-IRI, we performed in vitro and in vivo experiments with renal epithelial and endothelial cells and murine renal tissue in both the short term and long term. As opposed to our initial hypothesis, we found a different impact of caspase-3 invalidation on tubular and microvascular injury at the early AKI stage. However, in the long term, caspase-3 deficient animals showed better preservation of both compartments and reduced long-term renal fibrogenesis. In the early stage post-IRI, renal microvascular endothelial cells chose caspase-3 dependent apoptosis as the primary cell death pathway, while tubular epithelial cells headed to necroptosis as a predominant cell fate.

Also, we studied the impact of caspase-3 deficiency on long-term renal function in both mild and severe IRI. We found that caspase-3 deficiency attenuates microvascular rarefaction, better maintains endothelial permeability, attenuates tubular hypoxia, and reduces collagen deposition and myofibroblast differentiation, regardless of the severity of IRI. The endothelium is a semi-permeable barrier located at the interface of the blood flow and the vessel wall. Endothelial permeability is enhanced following endothelial cell injury, cytoskeleton alteration, and leukocyte-endothelial interactions. In an ischemic microvascular environment, damaged ECs fail to maintain vascular tone and normal vascular permeability because of a loss in endothelial junctions. As a result, endothelial permeability enhancement induces plasma concentration through water outflow. The alteration of permeability also promotes immune cell recruitment

and adhesion and activation of the inflammatory cascade. While PTC rarefaction leads to a drop-out of the microvasculature, it also implies detachment of pericytes from the vascular wall and secondary tubular atrophy. Pericytes are necessary for stabilizing the microvasculature in physiological conditions (Humphreys, Lin et al. 2010, Schrimpf, Xin et al. 2012). In pathological conditions, the detachment of pericytes from the microvasculature and their differentiation towards myofibroblasts further perturbs local homeostasis.

1. Impact of renal IRI on delayed graft function (DGF) and graft survival

Renal IRI-induced AKI in the context of transplantation is defined as DGF, which is a frequent outcome especially after deceased organ donation with a 20%-40% incidence (Muth, Astor et al. 2016). DGF occurrence is dependent on multiple factors, such as donor age, ischemia time, sex, existing disease, etc. The development of DGF is positively associated with oliguria, dialysis requirement after transplantation, and occurrence of rejection. Donation type is also associated with the risk and severity of DGF. The reported incidence of DGF for standard-criteria and extended-criteria donors is around 22% and 30% respectively in the USA respectively (Selby and Taal 2019). In the field of deceased organ donation, Brain Dead Donor (BDD) and Donation after Cardiac-Circulatory Death (DCD) are associated with a higher risk of DGF. Transplanted kidneys from DCD donors display an increased incidence of DGF compared with BDD due to a more prolonged exposure to warm ischemia. However, BDD is more prone to trigger progressive renal dysfunction, possibly because of a dysfunctional inflammatory environment, unstable hemodynamic features, and immune hyperreactivity in BDD donors (Saat, Susa et al. 2014).

Our work demonstrated the implication of renal microvascular endothelial cell death in AKI-CKD transition triggered by IRI, renal fibrosis, and long-term renal dysfunction. Meanwhile, inflammation and endothelial permeability alteration were also found in our IRI model with different degrees of severity, combined with previous data from our lab where administration of anti-LG3 autoantibody demonstrated an aggravated impact of renal IRI on peritubular capillary rarefaction with deteriorated renal function and interstitial fibrosis. Collectively, my results and previous work from the laboratory concur in establishing the importance of microvascular injury

as a significant determinant of AKI-CKD transition. These results could be further investigated to determine whether endothelial damage leads to the release of immunogenic extracellular vesicles and whether autoantibodies participate in enhanced immune reactivity and reduced long-term outcomes in organs from BDD donors.

2. Characteristics of the IRI model and relevance to the clinical context

There are several animal models of AKI-CKD transition, such as IRI, nephrotic AKI, sepsis, rhabdomyolysis, etc. However, one of our team's primary research objectives was to clarify the mechanisms of AKI-induced renal allograft dysfunction and the links with long-term renal transplant outcomes. Undoubtedly, an allogeneic renal transplant model is the ideal model to mimic human transplantation. However, it would be challenging to differentiate mechanisms of IRI-induced cell death from those induced by allogeneic immune activation in a transplantation model. Therefore, the IRI model is the optimal option to characterize the cell death pathways that are inevitably activated following ischemia-reperfusion during organ transplantation (Basile 2019).

As the most used experimental model of AKI and AKI-CKD transition, different severities of ischemic insults could induce mild and moderate AKI, or severe AKI with progression to CKD transition. Among multiple IRI models, uIRIx was performed in our study due to its similarity to renal transplantation in humans.

uIRIx has the advantages of allowing investigators to evaluate renal function at various time points, which provides an optimal setting for assessing dynamic curves of renal dysfunction and tissue damage. Compared with uIRI, uIRIx prevents contralateral kidney functional compensation, which would preclude the assessment of systemic renal function parameters. However, this model is associated with some technical challenges, especially when inducing severe renal injury, due to high mortality occurrence. In a study generating severe IRI in mice, up to 30% of the animals died in the first two weeks post-op (Fu, Tang et al. 2018). Moreover, significant variations were observed in this model compared with the uIRI model. One option of reducing mortality post-injury is to perform delayed uIRIx, which involves removing the

intact kidney several days post injury. Nonetheless, with delayed nephrectomy, monitoring renal dysfunction at multiple time points is difficult because of the contralateral kidney's compensation before nephrectomy.

In our study, we performed mild and severe IRI using the uIRIx murine model. In the severe IRI model, we did have the problem of the poor survival rate. However, we systematically standardized a detailed surgical protocol, specifying animal body temperature, rectal probing temperature, ischemic time, mice species, and sex features. We found that body temperature was positively associated with animal survival post-ischemic injury, especially in the severe IRI murine model. Cellular damage is highly dependent on temperature, a crucial factor for IRI severity. As a result, a duration of cold ischemia much longer than warm ischemia is necessary for inducing a similar severity, as higher temperatures under the same duration greatly exacerbated injury (Wei, Wang et al. 2019).

It is not common to perform multiple IRI severity levels in the same project due to the poor survival rate of animals in association with severe IRI. After a series of surgical technical troubleshooting in our severe IRI model, we systemically standardized murine IRI surgical protocol by modifying multiple parameters, including ischemic temperature setting, rectal probing temperature monitoring, ischemic time, operating time, mice species, and sex features, etc., ensuring project feasibility. After troubleshooting on the severe IRI model, we found that variations in heating carpet temperatures at the time of ischemia significantly impact the animal survival rate. A much lower survival rate was found in the IR60-minute group by increasing the carpet temperature, decreasing the survival rate from 92% to 62% by increasing the temperature from 37°C to 40°C in the IR60-minute group (not yet published). Our finding of a relationship between the survival rate and the elevated ischemic temperature is in line with the consensus in the literature (Skrypnyk, Harris et al. 2013, Ramesh and Ranganathan 2014, Fu, Tang et al. 2018).

In our preliminary work, different severities of IR were induced in female mice by performing warm ischemic time for 30 minutes, 45 minutes, and 60 minutes. The systems of 30 minutes and 60 minutes were analyzed and compared in the WT group and caspase-3 KO group. The injury induced in these two models is similar to mild and severe AKI in the clinic according to the serum creatinine elevation. However, the ischemia 45-minute group presented a

considerable variation within the group; some of the animals presented short-term alteration, but some have entered the chronic phase of AKI. Our team has recently been planning a new project to observe renal dysfunction post IRI both in male and female mice, trying to determine the influence of sex on renal dysfunction discrepancy in our models.

3. Predominant role of apoptosis in microvascular endothelial injury induced by IRI

In the context of AKI caused by IRI, we initially hypothesized that apoptosis is the predominant mode of cell death, and that caspase-3 deficiency would have global protective effects. Using a mouse model of AKI, we have shown that during the acute phase of IRI, the absence of caspase-3 worsens acute renal dysfunction. In terms of tissue damage, we have observed a decrease in microvascular damage but an increase in tubular damage linked to an aggravation of necroptosis in the tubular cells. These results indicate that ECs and tubular epithelial cells have different cell death programs, and that caspase-3-dependent apoptosis plays a predominant role in microvascular insults induced by IRI during the acute phase of AKI.

One of the most common causes of AKI is IRI. Tubular necrosis is classically considered a key feature of AKI. There is growing evidence to suggest that microvascular damage is also an essential contributor to renal dysfunction (Bonventre 2007, Chatauret, Badet et al. 2014, Verma and Molitoris 2015). Our results suggest that tubular damage has a predominant effect on renal dysfunction in the acute phase. Numerous studies have shown that programmed cell death plays a crucial role in tubular and microvascular damage induced by IRI. The different cell deaths implicated in microvascular damage, however, have not been identified. Our work is in line with studies by other research groups which identify necroptosis as the predominant type of cell death in tubular damage during the acute phase of IRI-induced AKI (Linkermann, De Zen et al. 2012, Linkermann, Hackl et al. 2013, Linkermann, Chen et al. 2014). However, investigations on necroptosis were more concentrated in the acute phase of IRI. Several studies, although not many, describe the impact of necroptosis in AKI-CKD transition and the chronic stage of CKD progression (Chen, Fang et al. 2018, Imamura, Moon et al. 2018). These results suggest that in the murine UUO model, RIPK3, a necroptosis mediator, promotes renal fibrosis via the AKT-dependent ATP citrate lyase pathway.

Further investigation on this topic is still needed. Our results provide novel insights into the importance of apoptosis in controlling microvascular damage during both the acute phase and the transition of AKI to CKD. Unlike epithelial cells, ECs in PTCs do not choose necroptosis as an alternative pathway in the condition of caspase-3 deficiency. Our preliminary work has proven that the absence of caspase-3 preserved renal microvascular density and ameliorated interstitial fibrosis. Based on these findings, we now hypothesize that another cell survival pathway, autophagy, is also involved in the endothelial stress response. Autophagy is a stress response that can exert a protective effect on the microvascular endothelial structure. In our preliminary observation of Electron Microscopy (EM) images from renal PTCs after IRI, an autophagolysosome-like structure was found in the cytoplasm of ECs within PTCs of caspase-3 KO mice, but not in the WT group. However, further investigations are underway to assess the impact of endothelial autophagy in the prevention of renal fibrosis post-IRI. Therefore, a follow-up project should aim at studying endothelial autophagy in the environment of renal IRI. Furthermore, besides findings in the mild IRI model, we also found similar results in the severe IRI model, with a protective role of a caspase-3 deficiency on microvascular preservation and renal fibrogenesis. However, no significant difference in the degree of tubular injury degree was found between the control group and the caspase-3 KO group in the early stage in the severe IRI model, including the histopathological parameters of tubular necrosis, tubular dilation, cast formation, and neutrophil infiltration both in the renal cortex and cortical-medullary junction sections. A possible explanation for this finding is that the severe IRI promoted necroptosis maximally in tubular epithelial cells, in control mice and caspase-3 KO mice, therefore preventing further activation of necroptosis in caspase-3 deficient mice.

Short-term renal endothelial dysfunction post-IRI was found to be ameliorated by caspase-3 deficiency, but the epithelial injury was found to be aggravated. One possible explanation is that TECs and ECs choose different regulated death pathways in the absence of caspase-3. Our results proved that TECs progress to necroptosis while ECs still develop apoptosis as a predominant cell death pathway. The mechanism regulating activation of different modes of cell death in tubular epithelial cells and microvascular endothelial cells perhaps correlates with varying sources of embryology. The tubular system develops from the intermediate mesoderm while peritubular and glomerular endothelial cells originate from the lateral mesoderm (Dekel,

Hochman et al. 2004). Therefore, our results imply that renal microvascular endothelial function was preserved by blocking the caspase-dependent apoptotic pathway both in mild and severe IRI forms. At the same time, tubular epithelial injury was aggravated by caspase-3 inhibition in the mild form, but there was no further deterioration in the severe form, possibly due to maximal activation in epithelial cells.

It would be interesting to confirm the effect of apoptosis on microvascular damage using mice with EC-specific caspase-3 deletion (Conditional Knockout, CKO) (Rongvaux, Jackson et al. 2014). We extrapolate that CKO mice would have reduced long-term renal dysfunction, microvascular and tubular damage, as well as decreased interstitial fibrosis, compared to WT mice. Caspase-3 deficiency in cell types other than the endothelium (especially fibroblasts) can affect the pro-fibrotic process. It would also be exciting to compare the CKO and general caspase3-/- mice at 21 days, which would allow us to distinguish how these cells contribute to post-IRI fibrosis.

Compared with microvascular ECs, TECs death pathways post-IRI have been studied for decades, and multiple cell death pathways have been reported in models of IRI (Linkermann, Chen et al. 2014, Sancho-Martinez, Lopez-Novoa et al. 2015, Wang, Zhang et al. 2016, Muller, Dewitz et al. 2017). Our study agrees with the literature that necroptosis is the predominant form of cell death in TECs in early AKI induced by IRI (Lau, Wang et al. 2013). Based on the literature, one study revealed that RIPK3-mediated necroptosis contributes to endothelial cell damage in a murine cardiac transplant model (Pavlosky, Lau et al. 2014). However, there are no investigations observing the impact of RIPK3 on microvascular rarefaction post renal IRI. It was expected that RIPK3 deficiency would protect against microvascular damage induced by IRI. However, another investigation using RIPK3/caspase-8 double knockout mice post-IRI suggested that necroptosis inhibition cannot rescue cell injury in TECs due to the compensatory upregulation of intrinsic apoptosis (Liu, Liu et al. 2019, Sung, Su et al. 2019), which supports the presence of multiple levels of cross-talk between cell death pathways. In addition, RIPK3 was proven to contribute to renal fibrosis by activating AKT-dependent ATP citrate lyase in UUO murine model (Imamura, Moon et al. 2018). These findings show the complexity of cell death crosstalk in the IRI context and the link between cell death and long-term fibrogenesis.

These results suggest that the RIPK1/RIPK3/MLKL signal pathway is positively associated with primary tubulointerstitial injury and long-term fibrosis post-IRI.

4. Contribution risk factors in AKI-CKD transition

4.1. Contribution of microvascular rarefaction in AKI-CKD transition

The renal microvasculature can be classified according to its volume and location, including the segmental artery, interlobar artery, arcuate artery, interlobular artery, and peritubular capillary (figure 10). Microvascular rarefaction can possibly occur in any segment of the renal vascular branches; however, it usually attacks PTCs and arterioles. In our study, our results were consistent with the literature. By visualizing total renal microvasculature using a micro-Computed Tomography (microCT) scan and 3D reconstruction, we found that loss of micro-blood vessels is principally focused on the terminal capillary level, not the segmental or the interlobar vessels.

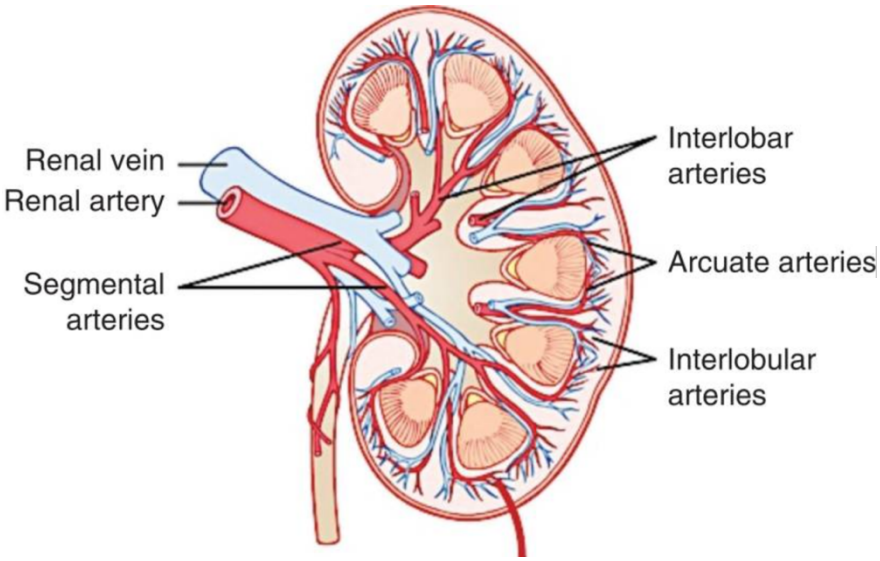

Figure 10. Distribution of renal microvasculature (Chade 2013).

Mounting evidence suggests that microvascular rarefaction is positively associated with renal interstitial fibrosis in patients with CKD, including ischemic nephropathy, IgA nephropathy, focal segmental glomerulosclerosis, kidney transplant, etc. Both microvascular rarefaction and renal fibrosis are considered highly related to CKD transition in multiple clinical settings

(Eardley, Kubal et al. 2008, Fliser 2010, Eirin, Zhu et al. 2011, Fiorentino, Grandaliano et al. 2018).

Although microvascular rarefaction is classically thought to result from insults that act on the vasculature, activation of endothelial injury sometimes starts from internal stimuli to the microvasculature, such as changes in circulation dynamics, endothelial phenotype transition, and cell death accompanied by insufficient regeneration (Chade 2013). The cascade of endothelial alterations contributes to secondary renal interstitial hypoxia and profibrotic pathway activation and microvascular drop-out. Some possible mechanisms include profibrotic gene upregulation and epigenetic alternation regulated by hypoxic insult, endothelial permeability disturbances, and myofibroblast transition. IRI and antibody-mediated rejection are two significant causes of microvascular injury in the context of renal transplantation (Doreille, Dieude et al. 2019).

However, clinical studies in patients can rarely reveal the mechanisms of AKI-CKD transition; animal models are therefore used to explore the detailed molecular and cellular mechanisms in CKD progression. In our murine model, microvascular rarefaction is in line with renal interstitial fibrotic alterations, as well as renal dysfunction, suggesting a strong link between endothelial dysfunction, renal fibrosis, and CKD transition. In the acute phase, we observed different impacts of caspase-3 deficiency in tubular and microvascular systems, namely reduced microvascular injury but aggravated tubular epithelial injury. Our results demonstrate that in the chronic phase, casp3$^{-/-}$ mice are both protected from microvascular depletion and severe tubular damage. Fibrosis, a key feature of CKD, was also reduced in the casp3$^{-/-}$ group demonstrating that microvascular damage is a driving force for CKD development.

Microvascular rarefaction and fibrosis have been considered closely related in a number of animal models, including IRI. However, as opposed to the current consensus, recent studies suggest that microvascular rarefaction and fibrosis are not always linked in the same pathway in some other animal renal disease models. According to recent reports with multiple AKI animal models, PTC rarefaction has a predominant impact on CKD progression over renal fibrosis (Menshikh, Scarfe et al. 2019). They reported capillary rarefaction and renal dysfunction without interstitial fibrosis in mice with cisplatin-induced AKI. In rhabdomyolysis-induced AKI, renal fibrosis developed but without severe capillary rarefaction or progressive

renal dysfunction. In the IRI model, PTCs were restored in the long-term, which is in line with renal function restoration, but renal interstitial fibrosis was found ongoing. Of note, the delayed contralateral nephrectomy IRI murine model was used, which potentially helped restore capillary number. However, renal interstitial fibrogenesis progression was not modulated (Menshikh, Scarfe et al. 2019). Collectively, these findings suggest that capillary rarefaction is more important than renal fibrosis for predicting progressive renal function decline. This is a reminder that different etiology could trigger different pathophysiological changes and that mechanisms that pertain to IRI may differ from those of other AKI models. The finding in the IRI model of this report where microvascular rarefaction displays a weak link with renal interstitial fibrosis (Menshikh, Scarfe et al. 2019) is somehow contradictory with ours. The possible explanation of this discrepancy is the animal model applied. Delayed nephrectomy performed with compensation from the contralateral kidney prevents the development of uremia, potentially preventing uremia-induced microvascular rarefaction and further CKD progression.

4.2. Contribution of other risk factors in AKI-CKD transition

Besides known classical risk factors of CKD progression, uremic toxins (UTs) are another risk factor that could further deteriorate renal function. There are different types of UTs, among which asymmetric dimethylarginine (ADMA), indoxyl sulfate (IS), p-cresyl sulfate (pCS) have been associated with CKD progression and renal dysfunction (Fujii, Goto et al. 2018). For example, ADMA is an endogenous inhibitor of nitric oxide (NO) synthase, and it works as an anti-atherosclerotic factor by reducing NO production. Therefore, serum ADMA concentration is considered a predictive marker of endothelial dysfunction (Cooke 2004). In kidneys with renal failure and interstitial hypoxia, ADMA contributes to PTCs loss and interstitial fibrogenesis, accentuating CKD progression. Plasma ADMA concentration increase upregulates apoptosis and prevents endothelial cell proliferation by decreasing NO level. In addition, ADMA inhibits NO synthase and bioavailability by increasing oxidative stress (Antoniades, Shirodaria et al. 2009). Different from ADMA, IS is a tryptophan derivative and binds to albumin in circulation. It participates in AKI progression by affecting the NO pathway and reducing the number of EPCs, which postpones recovery of renal function and favors CKD development. Furthermore, IS was shown to promote epithelial-mesenchymal transition and renal tubular epithelial

apoptosis, by activating ERK1/2 pathway and p38 MAP kinase (MAPK) (Kim, Yu et al. 2012). Also, IS displayed a pro-inflammatory function, which is similar to the effect of pCS, inducing inflammatory associated gene upregulation in cultured mice proximal tubular cells. (Sun, Hsu et al. 2013).

In addition, Renin-Angiotensin System (RAS) has been proven to significantly promote CKD development in patients. RAS is known to play a significant impact on renal physiology, therefore, RAS participates in both physiological and pathophysiological environments. RAS inhibitors have been found to effectively block CKD progression in clinical trials, and therefore represent potential therapeutic targets for CKD prevention (Laffer, Elijovich et al. 2020, Singhania, Bansal et al. 2020, Garcia-Prieto, Verdalles et al. 2021, Loutradis, Price et al. 2021, Sanidas, Papadopoulos et al. 2021).

4.3. Link between microvascular dysfunction and AKI-CKD transition in our study

In our study, severe AKI showed, as expected, a higher number of injured tubules than mild AKI (Yang, Lan et al. 2018, Dong, Zhang et al. 2019). Intriguingly, microvascular congestion was significantly less critical in severe AKI than mild AKI due to poorly preserved microvasculature (Basile, Donohoe et al. 2001). In severe AKI, renal peritubular capillaries collapse which dramatically narrows the vascular lumen, inducing a limitation for circulatory blood flow in renal capillaries. As a result, much less microvascular congestion was found in severe AKI compared to mild AKI. Furthermore, ex-vivo Evans Blue extravasation test displayed less endothelial leaking in the caspase-3 KO group than the control group post mild AKI. There was no significant difference between these two groups in the severe form of AKI. One possible explanation is that severe IRI led to greatly reduced PTC perfusion therefore preventing leakage. This suggests that the Evans Blue assay is not appropriate for assessing microvascular permeability in the severe AKI model. Consequently, we should keep in mind that the severity of the renal insult can influence some parameters aimed at evaluating microvascular function.

Our findings also confirmed the lack of Scr sensitivity as a biomarker of renal fibrosis in mild AKI. No difference was observed between casp3$^{-/-}$ and WT mice despite higher tubular injury

in the WT group. Scr and BUN are widely used clinically as biomarkers for evaluating renal function. However, they are far from ideal for detecting mild and moderate changes in GFR. Scr and BUN blood levels do not rise rapidly enough if the non-attacked renal nephrons maintain a near-normal function (Bonventre, Vaidya et al. 2010). A requirement for validating more sensitive biomarkers of subclinical renal dysfunction is needed to detect early renal dysfunction and predict progressive dysfunction. Figure 11 below shows various biomarker candidates for detecting early renal injury, such as KIM-1, NGAL, Cystatin C, IL-18, TIMP2, and IGFBP7. Urinary KIM-1 was detected in a renal tubular injury model and in patients with acute tubular necrosis (Han, Bailly et al. 2002). IL-18 levels in urinary samples of AKI patients were shown to increase before serum creatinine elevation, demonstrating its advantage as an early-stage injury marker (Awad and El-Sharif 2011). In addition, the urinary level of Cystatin C was also found to be more sensitive than serum creatinine in adult and pediatric patients with AKI (Pirgakis, Makris et al. 2014, Lagos-Arevalo, Palijan et al. 2015, Benoit, Ciccia et al. 2020). Current investigations reveal various potential biomarkers for detecting renal tubular damage early, but biomarkers focusing on renal microvascular injury are still lacking. However, a large number of studies, including our work, have illustrated the crucial association between microvascular dysfunction/rarefaction and long-term renal function, in both transplanted kidney and naïve kidneys (Afsar, Afsar et al. 2018, Polichnowski 2018, Yang, Lan et al. 2018, Basile 2019, Menshikh, Scarfe et al. 2019). Therefore, the validation of microvascular injury biomarkers should be considered an essential topic for renal disease research.

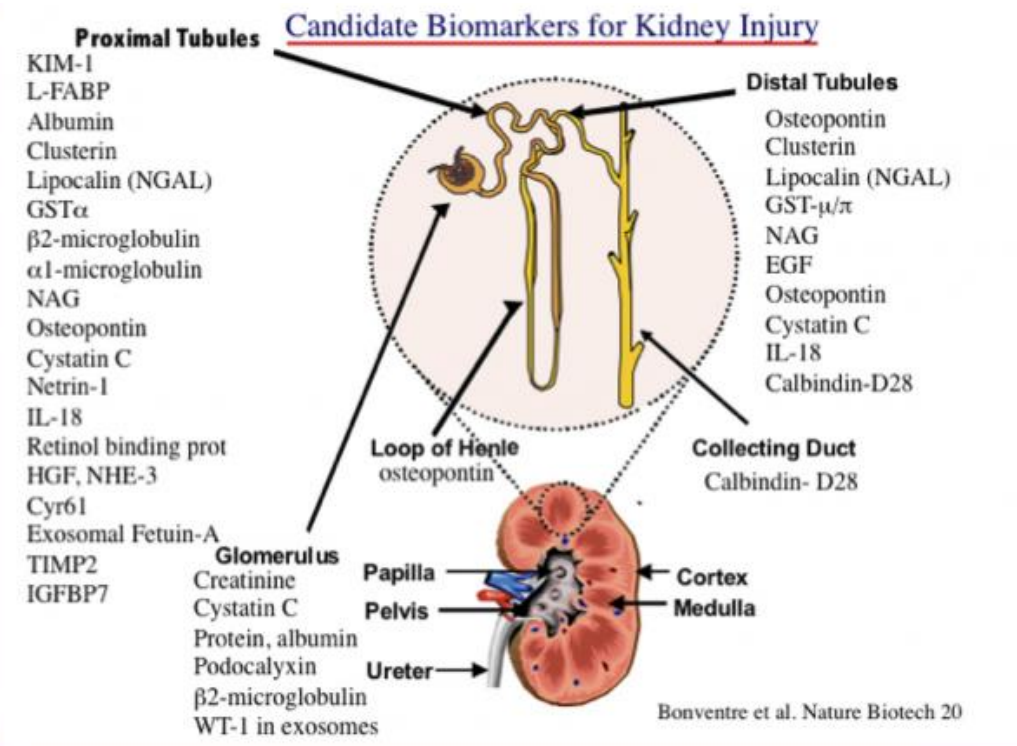

Figure 11. Potential candidate biomarkers of kidney injury (Bonventre, Vaidya et al. 2010).

Better preservation of microvascular function protected tubular function and reduced secondary tubular hypoxia as illustrated by decreased expression levels of HIF-1α in the cortex and cortical-medullary junction in mild and severe AKI. These results further support the pivotal role of PTC damage in secondary tubular hypoxia (Tanaka, Tanaka et al. 2014), where long-term secondary tubular hypoxic status results in the development of CKD, as demonstrated by tubular atrophy and interstitial fibrosis (Grgic, Campanholle et al. 2012, Humphreys 2018).

The mechanisms involved in the transition from AKI to CKD are complex and still need to be characterized. The distribution of blood supply and oxygen in the renal cortex and medulla differs greatly, with 90% in the cortex and around 10% in the medulla (Dimke, Sparks et al. 2015). In some pathophysiological conditions, the hypoxic status may extend to the cortex, contributing to peritubular capillary ischemic injury, which could be regarded as a CKD and AKI-CKD transition (de Braganca, Volpini et al. 2016). Several studies have described a feedback loop between microvascular rarefaction and impaired tubular regeneration. They have

identified this loop as the key pathophysiological process in the transition from AKI to CKD (Hsu 2012, Tanaka, Tanaka et al. 2014, Venkatachalam, Weinberg et al. 2015). Figure 12 displays multiple mechanisms and crosstalk between capillary rarefaction and renal dysfunction. In our work, with decreased microvascular damage and increased tubular damage during the acute phase of AKI, casp3$^{-/-}$ mice allowed us to create a unique model to distinguish the relative contribution of these two compartments to AKI to CKD transition. The results of our project demonstrated that early microvascular insults, but not epithelial injury play a key role in the transition from AKI to CKD. These results add a new experimental argument for the need to assess microvascular rarefaction in CKD patients.

Besides microvascular rarefaction, microvascular dysfunction induced by injury also contributes to CKD progression. With the progression of CKD, the latest phase could be uremic. However, uremia can also happen following AKI when it develops quickly. Additionally, uremia is a consequence of CKD and may function as a contributor to CKD progression. For example, uremic toxins such as IS could accentuate microvascular dysfunction by upregulating platelet hyperactivity and favoring thrombus formation (Allison 2017).

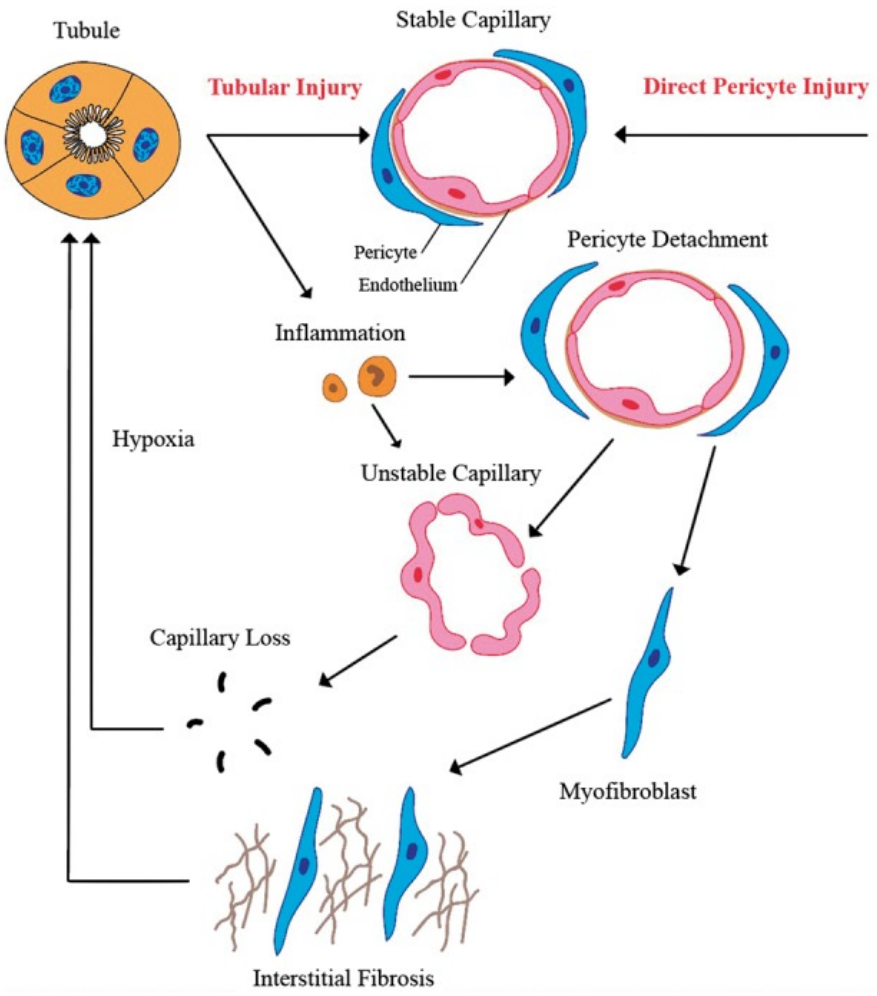

Figure 12. Crosstalk between capillary rarefaction and progressive renal damage (Afsar, Afsar et al. 2018).

5. Mechanisms of renal fibrosis in AKI-CKD transition

5.1 Myofibroblast differentiation

Regardless of etiology, interstitial fibrosis is a common histopathological finding of CKD. The differentiation of fibroblasts into myofibroblasts (myofibroblast differentiation) is crucial in developing fibrosis (Grgic, Duffield et al. 2012, Humphreys 2018). Many studies have identified an essential role for ROS in myofibroblast differentiation and in organ fibrosis (Siani and Tirelli

2014, Zhang, He et al. 2014, Andersson-Sjoland, Karlsson et al. 2016, He, Xiong et al. 2016, Bernard, Yang et al. 2020).

During progressive renal damage, connective tissue accumulation induces a series of actions triggering interstitial fibrosis and matrix deposition in the space between PTCs and tubules. Diverse links between renal fibrosis and CKD progression are shown in Figure 13. The deposited matrix contains collagen I, III, V, VI, VII, XV, and fibronectin. In the normal kidney, the primary collagen is collagen IV; in a pathological environment, the synthesis of collagen I is upregulated while the collagen IV level can remain unchanged, increased, or reduced (Sanna-Cherchi 2008, Genovese, Manresa et al. 2014). The myofibroblast is considered a matrix secreting cell (Kramann, Dirocco et al. 2013), although other cell types can also contribute to matrix deposition. The most common myofibroblast marker is α-smooth muscle actin (α-SMA), which illustrates the capacity of myofibroblasts to form stress fibers and acquire enhanced contractile capabilities. Other myofibroblast markers include vimentin, collagen-1alpha, fibronectin, and PDGFR- β (Lin, Kisseleva et al. 2008). In our research work, both the control and casp3$^{-/-}$ group display increased collagen deposition and enhanced levels of α-SMA in PTCs at 21 days post-IRI. Moreover, electron microscopy images also show an enlarged sub-endothelial space with deposition of extracellular matrix and collagen fibers. Compared with the control group, the casp3$^{-/-}$ group demonstrates reduced myofibroblast and collagen deposition, suggesting a protective effect of caspase-3 on renal interstitial fibrosis.

The collagen matrix produced by myofibroblasts reduces the blood flow to the PTCs by narrowing the capillary lumen, further inducing secondary tubular hypoxia and PTCs dropout. This secondary tubular hypoxia plays an important role in development and progression of CKD (Evans, Ow et al. 2015). In this cascade of chronic tubular hypoxia, HIF-1α is a vital regulator of the tubular hypoxic epithelial cells (Tanaka and Nangaku 2010). PTC rarefaction and secondary tubular hypoxia further impact the surrounding tubules, triggering pro-fibrotic pathways. We detected tubular hypoxia using HIF-1α immunohistochemistry staining of murine kidneys. Caspase-3 KO mice displayed a lower level of HIF-1α expression within the renal cortex after mild IRI. In the severe IRI model, caspase-3 deficiency was associated with reduced long-term secondary tubular hypoxia post-IRI, alleviated interstitial fibrosis and reduced CKD progression compared to controls.

5.2 Pericytes and myofibroblast differentiation

Pericytes surrounding endothelial cells in capillary blood vessels have a function in vessel maturation, angiogenesis, and endothelial response to injury. They also work as mesenchymal cells participating in injury repair and renal fibrogenesis. It is commonly accepted that myofibroblasts drive renal fibrosis by producing extracellular matrix and forming interstitial scar in the long term. A recent investigation using an IRI model in mice found that pericytes are also sources of myofibroblasts by converting from an inactive quiescent subtype to an active mode through a hypermethylation process (Chou, Pan et al. 2020). Another investigation also reported that myofibroblasts proliferate from a perivascular location in a murine kidney fibrosis model (Mack and Yanagita 2015). Collagen 1α GFP positive pericytes converted to α-SMA+ myofibroblast post insult in a murine model UUO (Lin, Kisseleva et al. 2008). We observed reduced α-SMA positive PTCs in caspase-3 KO mice. Follow-up studies should take advantage of cell tracing strategies to address the role of renal pericytes in interstitial fibrosis progression in our model.

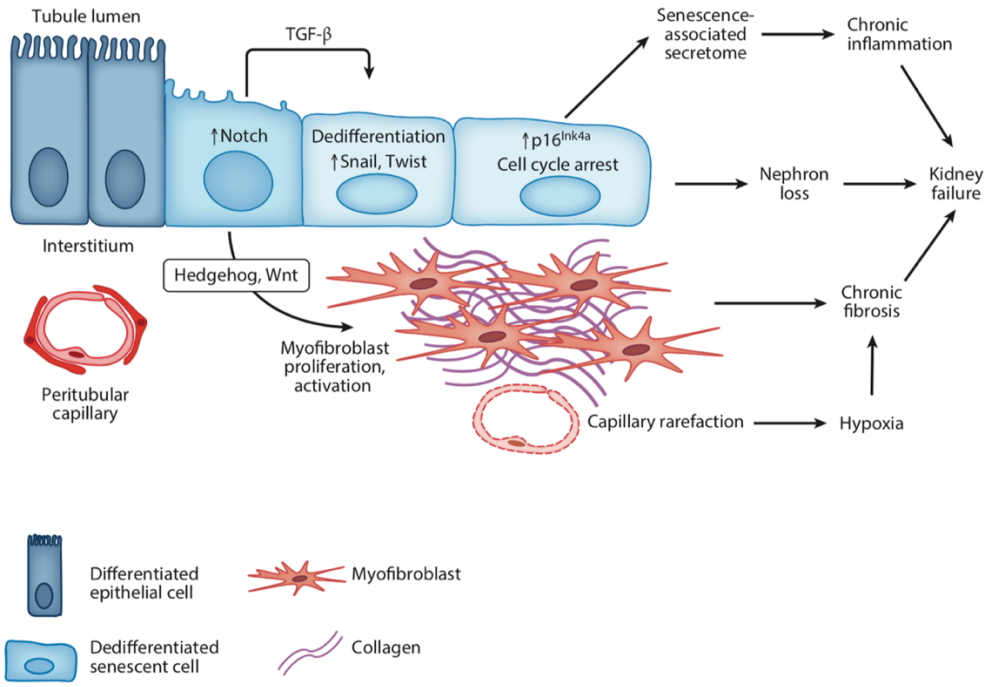

Figure 13. Signaling pathways involved in renal fibrosis and CKD progression (Humphreys 2018).

6. Identification of markers of microvascular injury post-IRI

Unlike the above-mentioned well-characterized tubular damage biomarkers, there are currently no reliable biomarkers of microvascular damage for IRI-induced AKI (Krawczeski, Vandevoorde et al. 2010, Ma, Li et al. 2010, Genovese, Manresa et al. 2014, Srisawat, Murugan et al. 2014, Alge and Arthur 2015, Tan, Yap et al. 2016, Carmona, Aguera et al. 2017, Gunay and Mertoglu 2019, Zhang, Li et al. 2019, Quaglia, Dellepiane et al. 2020). Since microvascular damage plays a crucial role in the pathophysiology of AKI and the progression to CKD, which tubular epithelial injury markers usually fail to predict, it would be essential to identify specific biomarkers for renal microvascular damage (Ince 2014). Several endothelial damage-related proteins or molecules represent potential endothelial injury biomarkers, e.g., soluble thrombomodulin, VCAM-1, ICAM-1, E-selectin, PAI-1, Angiopoietin-2, extracellular vesicles, etc.

Characterizing circulating markers present in WT mice after IRI and the absence of reduced casp3$^{-/-}$ mice represent a unique opportunity to characterize microvascular injury biomarkers. Casp3$^{-/-}$ mice present enhanced early tubular epithelial damage and reduced microvascular injury.

A number of molecules are currently being assessed as potential markers of vascular injury in various clinical disease states, including renal transplant. We should also envision whether circulating levels of the following candidate biomarkers correlate with microvascular depletion at six months post-transplantation. Multiple types of biomarkers could be validated for detecting early-stage renal injury and predicting prognosis in the transplant context, such as proteins, EVs, RNA, microRNA, etc. Among these candidate biomarkers, EVs are attracting a lot of attention due to their stability in biological fluids (discussed further in section 6.7).

6.1 Soluble Thrombomodulin (sTB)

Thrombomodulin (Malek and Nematbakhsh) is an endothelial cell surface transmembrane glycoprotein composed of 5 domains. It has a role in anticoagulant and anti-inflammatory activities by binding thrombin and activating protein C under normal conditions. Protein C

functions as an anti-apoptotic and anti-fibrotic mediator. When ECs are damaged, TB is released from the endothelial membrane in a soluble form and exerts a protective role on the endothelium (Martin, Murphy et al. 2013). In a hypoxic environment, anticoagulant and anti-inflammatory functions of TB are decreased due to separation from the endothelial membrane, contributing to a hypercoagulable and pro-inflammatory state within the microvasculature (Verma and Molitoris 2015). A correlation between soluble thrombomodulin (sTB) and the severity of chronic renal failure has been described (Sharain, Hoppensteadt et al. 2013). Also, in pediatric CKD cases, sTB was correlated with CKD, renal dysfunction, and oxidative stress (Drozdz, Latka et al. 2018). It could be interesting to explore the correlation between sTB and renal microvascular rarefaction in renal transplant patient biopsies.

6.2 Cellular adhesion molecules (VCAM-1, ICAM-1, E-selectin)

The selectin family includes three transmembrane types of glycoprotein receptors, named according to their main expression sites: E-selectin, expressed by activated ECs; P-selectin, produced by platelets; and L-selectin, expressed by lymphocytes. They are essential initiators of leukocyte adhesion to the endothelium (Telen 2014, McEver 2015). The soluble form of E-selectin is mainly generated by enzymatic cleavage in damaged ECs. One of the most promising biomarkers is soluble E-selectin. Its serum level increases significantly in several diseases where endothelial damage is an important manifestation, including stroke and diabetes (Prugger, Luc et al. 2013).

In addition to selectins, the inflammatory environment also triggers increased endothelial cell synthesis of some other cell adhesion molecules, including vascular cell adhesion protein 1 (VCAM-1) and ICAM-1, but reduced synthesis of anticoagulatory molecules, such as TB (Jourde-Chiche, Fakhouri et al. 2019).

However, in our preliminary work, we performed VCAM-1 immunohistochemistry staining in the renal tissue of our mice post-IRI. Intriguingly, we did not find a difference between the control group and the caspase-3 KO group in the mild AKI model, although more preserved endothelial cells and ameliorated microvascular permeability were observed in the caspase-3 KO group. However, the most common tested form of VCAM-1 in animal models and cohorts of patients is soluble VCAM-1. One clinical study reported a moderate relationship between

urinary soluble VCAM-1 and CKD stages in Systemic Lupus Erythematosus (SLE) patients. They also reported an even closer association between VCAM-1 and CKD stages in SLE patients with a history of Lupus Nephritis (LN). High levels of urinary soluble VCAM-1 were found in patients with severe renal dysfunction for more than 10 years (Parodis, Gokaraju et al. 2020). Another clinical cohort study showed an inverse correlation between circulatory VCAM-1 and residual renal function in peritoneal dialysis patients (Wang, Lam et al. 2005).

One possible interpretation of our data is that renal tissue VCAM-1 immunohistochemistry staining may not correlate with soluble VCAM-1 levels. Another possibility is that endothelial injury induced by mild IRI is insufficient to up-regulate cellular adhesion molecules and recruit immune cells on ECs. In support of the latter hypothesis, we found few CD45 positive leukocytes in the renal microvasculature in our model. However, we did not test serum levels of soluble VCAM-1 and ICAM-1 neither in the mild nor severe AKI model. It would be interesting to investigate these potential endothelial biomarkers in AKI-CKD transition.

6.3 PAI-1 and uPA

The urokinase-type plasminogen activator (uPA) is a serine protease involved in the breakdown of ECM. uPA is believed to play an essential role in increasing VEGF-induced vascular permeability. It has been reported that the increase in uPA correlates with the sepsis severity (Yang, Liu et al. 2011). Urokinase receptor (uPAR), a glycosylated protein binding and activating uPA, is expressed by endothelial cells, neutrophils, monocytes, and epithelial cells. Plasminogen activator inhibitor (PAI-1), the most potent inhibitor of uPA, is regarded as a biomarker of chronic inflammation, such as CKD progression and metabolic syndrome (Eddy and Fogo 2006, Ahirwar, Jain et al. 2015). Once PAI-1 binds to the uPA-uPAR complex, both uPA and PAI-1 are degraded. In the uPAR KO murine model, severe renal fibrogenesis post-UUO was observed, possibly attributed to increased interstitial PAI-1 (Zhang, Kim et al. 2003). uPAR was recently reported as a sensitive biomarker of CKD progression. However, the mechanisms that underpin this association include increased inflammation or podocyte activation (Saleem 2018).

6.4 Angiopoietin-2 and other mediators of angiogenesis

Angiopoietin-2 (Ang-2) is a Tie2 receptor antagonist ligand expressed by ECs. In a physiological context where ECs are quiescent, it is stored in the Weibel-Palade bodies (WPB). When ECs are damaged/activated, Ang-2 is quickly released as a pro-inflammatory factor. Increased circulating Ang-2 has been documented in various diseases that display microvascular damage, including diabetes, allograft arteriosclerosis, and acute coronary syndrome (Lee, Lip et al. 2004, Lim, Lip et al. 2005). It has also been shown to act as an independent predictor of microvascular dysfunction in kidney transplant recipients (Molnar, Kumpers et al. 2014). Ang-1 is another endothelial stabilizing factor and it inhibits EC apoptosis. The ratio of Ang-2 and Ang-1 might be a potential candidate for predicting the endothelial response post-injury. A clinical study testing Ang2/Ang1 ratio in stage 5 CKD patients found higher ratios in diabetes mellitus (DM) patients, which suggested that it behaves as an early endothelial injury marker but does not show predicting power for mortality (Carmona, Aguera et al. 2017). The urinary level of Ang 2 and Tie2 in patients was positively correlated with the severity of AKI development after a cardiac bypass operation (Jongman, van Klarenbosch et al. 2015). Since the Ang/Tie system has been proven to be associated with AKI and CKD, it would be interesting to test, in our IRI model, whether Ang2/Ang1 serum levels predict microvascular rarefaction and AKI-CKD development.

VEGF is a central mediator of angiogenesis. Some VEGF-associated mediators are also considered endothelial injury biomarkers. Endocan is a soluble proteoglycan that ECs can secrete. Soluble fms-type tyrosine kinase-1 (sFlt-1 or VEGFR-1) is a splicing variant of the VEGF receptor-1. Both of these proteins play an essential role in VEGF signaling pathways. Their expression levels have been shown to increase in various diseases that cause microvascular damage (Kose, Emet et al. 2015, Hammadah, Georgiopoulou et al. 2016, Bicer, Guler et al. 2017).

6.5 Glycocalyx marker (Syndecan-1)

Endothelial cells are located on the inner side of the microvasculature. Between the ECs and the blood flow, there is a layer called the glycocalyx, consisting of proteoglycans as well as

glycoproteins (Alphonsus and Rodseth 2014). This glycocalyx layer is involved in vascular permeability mediation and ECs-basement membrane attachment.

In some contexts, damage to the glycocalyx is synchronous with endothelial injury. Some plasma biomarkers of glycocalyx were found elevated in association with AKI and reflecting mortality. One multi-centric clinical study investigated the Syndecan-1 (SDC-1) level in AKI patients admitted to ICU. Nighty-day survivors displayed lower levels of SDC-1 compared to non-survivors, suggesting a predictive role for better survival. Lower levels of sTB were also found in patients with better clinical outcomes. These results indicate that higher SDC-1 and sTB are in line with poor survival in severe AKI patients (Inkinen, Pettilä et al. 2019). SDC-1 RNA, and protein expression level were also proven to be predictive for both moderate and severe AKI superimposed on CKD in murine IRI and/or aristolochic acid administration models (Jiang, Wang et al. 2020). In addition, plasma SDC-1 has been shown to be elevated in stage 3-5 CKD patients, suggesting an association between the loss of glycocalyx integrity and renal insufficiency (Padberg, Wiesinger et al. 2014). These findings suggest that the level of glycocalyx markers, such as SDC-1, is highly associated with long-term renal function in CKD cases and correlated with the survival of AKI patients admitted in ICU.

6.6 CD146

CD146 is one of the transmembrane glycoproteins expressed in the human endothelium, which was found to participate in EC adhesion, migration, angiogenesis, and differentiation (Fan, Fei et al. 2018). A recent study reported elevated circulating levels of soluble CD146 in patients with CKD and DM, suggesting that CD146 could reflect endothelial injury (Bardin, Moal et al. 2003, Saito, Saito et al. 2007).

6.7 Extracellular vesicles

Extracellular vesicles (EVs) have been recognized as a way of intercellular communication and material transfer in the past two decades. EVs can be produced by healthy cells, as well as apoptotic cells. EVs include microvesicles, exosomes, microparticles, etc. (Gyorgy, Szabo et al. 2011). The terminology “exosome” is usually used to refer to EVs between 40-100nm in diameter, released by fusing multivesicular endosomes (MVE) with the cellular plasma

membrane. The carriers within EVs are likely composed of endosome-related protein, fatty acid, mRNA, and miRNA. Exosomes are uptaken by recipient cells and transfer intracellular information through paracrine signalling (Montecalvo, Larregina et al. 2012).

In the context of ischemia, the hypoxic environment induces HIF formation, activating hypoxia response gene expression. This cascade of alterations allows for plasma membrane structural change, which is beneficial for EVs release. In the context of renal IRI, multiple cells, including macrophages, DC, and neutrophils, can release EVs, triggering complex proinflammatory cellular and tissue responses. As well as immune cells, renal TECs and ECs also release EVs. The EVs shed by tubular and endothelial cells display an essential effect on inflammatory and pro-fibrotic progression and favor the development of rejection by activating autoimmune and alloimmune immune responses (Quaglia, Dellepiane et al. 2020). Moreover, because of several advantages of EVs—the stability in multiple body fluids, unique biogenic process, production by numerous cells, transfer of protein and miRNA (LeBleu and Kalluri 2020), and the small measuring volume required—they are being considered as a potential early-stage biomarker for predicting endothelial injury post-IRI. In renal disease, urinary EV levels are widely investigated as a non-invasive marker of renal dysfunction. Some studies assessing EV serum levels are also ongoing. However, the main source of urinary detected EVs comes from shedding by different renal tubular segments. They are therefore less likely to predict primary microvascular damage. Moreover, urinary samples are not always easy to acquire in AKI patients, especially during the oliguric stage. Therefore, circulatory EVs derived from injured endothelial cells could be a potential biomarker of renal endothelial injury due to their endothelial source and availability.

However, the use of EVs as biomarkers have some limitations. EVs can be produced by multiple cells, both in physiological and pathophysiological conditions, which makes the circulatory vesicles a mixture of different EVs. EVs secreted by various cells are considered as carrying specific markers sourced from original cells, but no unique specific marker is widely accepted for identifying EVs. Therefore, identifying EVs by multiple markers is currently the most commonly used approach, with source cell markers and vesicle carrying materiel markers. The equipment and technique for identifying EV markers are not yet popularized due to the high cost.

Endothelial EVs are protective for parenchymal tissue cells by clearing caspase-3 in the biological environment (Cocucci, Racchetti et al. 2009). In the context of ischemia, overexpressed caspase-3 could withstand the EVs removing effect, triggering programmed cell death. Our team has shown that apoptotic endothelial cells released exosome-like vesicles containing 20S proteasome which contribute to recruiting adaptive immune cells and auto-antibody generation, such as an anti-perlecan, anti-angiotensin-1 receptor, and anti-dsDNA (Dieude, Bell et al. 2015, Cardinal, Dieude et al. 2018, Gunaratnam 2018). Therefore, EVs released by renal endothelial cells after IRI appear associated with endothelial injury and immune response.

Our team has already begun a preliminary work of injecting apoptotic exosome-like vesicles into the circulation of renal IR mice, to investigate the effect of these vesicles on renal dysfunction post-IRI. Preliminary data showed a strong tendency of inflammation up-regulation with exosome-like vesicles injection.

Endothelial Biomarker	**Advantages**	**Limitation**
sTB	Easy to test in serum	Correlation with CKD was proved, further observations are needed to determine the correlation with renal microvascular injury
VCAM-1	Soluble form is easy to test in serum and urine, correlated with CKD development	Immunohistochemistry in tissue is challenging to reflect endothelial injury
ICAM-1	Soluble form is promising	Immunohistochemistry in tissue is difficult to reflect endothelial injury
E-selectin	Produced by ECs, serum level increased in multiple diseases, stroke, diabetes	
PAI-1	Biomarker of chronic inflammation	
uPA	Predicting endothelial permeability change, sepsis	

Angiopoietin-2	Circulating level increased in microvascular damage, including diabetes, arteriosclerosis, acute coronary syndrome, a predictor for renal microvascular function post-transplant	
Syndecan-1	Involved in endothelial permeability, predicting endothelial injury and long-term function	
CD146	Reflecting endothelial injury in diabetes, CKD	
Extracellular vesicles (EVs)	1. Stable in the fluid sample, 2. Produced by multiple cells, 3. Carry protein. miRNA, etc., 4. Predict endothelial injury and inflammation	1. No specific marker, difficult to identify, 2. Urinary secreted EVs can't be used for evaluating endothelial injury

Tableau IV. Potential endothelial biomarkers.

7. Potential therapeutic strategies for preventing microvascular dysfunction

Due to the limited repair capacity of the endothelium and the association with long-term renal dysfunction, prevention of microvascular injury is crucial for renal function maintenance post-IRI. Based on mechanisms contributing to revascularization, some potential therapeutic strategies are regarded as promising in the field of endothelial function preservation.

7.1 Angiogenesis

Angiogenesis is the formation of new blood vessels by the germination and lengthening of existing vessels. Targeted therapies for inhibiting angiogenesis were developed for several disease contexts, notably cancers (El-Kenawi and El-Remessy 2013, Vasudev and Reynolds 2014, Neuzillet, Tijeras-Raballand et al. 2015). In the context of IR-induced AKI, pro-angiogenic therapies could be potentially useful, angiogenesis is regulated by numerous cytokines that could potentially serve as therapeutic targets (Ribatti and Crivellato 2012).

7.1.1 Hypoxia inducible factors (HIFs)

In the kidneys, different molecular response pathways are activated by hypoxia. The central mediators of these pathways are HIFs (Molnar, Kumpers et al.). HIFs belong to a group of transcription factors that are characterized by a helix-loop-helix-PAS structure. The activity of HIF is mainly regulated by the oxygen-dependent degradation of the HIF-α subunit by proteasomes. Under hypoxic conditions, the HIF heterodimer can migrate to the nucleus. The binding of HIF to hypoxia response elements leads to the transcriptional activation of genes inducible by hypoxia, including a series of pro-angiogenic factors (Rhim, Lee et al. 2013, Tanaka, Tanaka et al. 2014).

Activation of HIFs has been demonstrated in several kidney diseases, including diabetic nephropathy, IgA glomerulonephritis, and chronic allograft nephropathy (Fine and Norman 2008). The effect of HIF activation on the progression of kidney disease is still debated. It has been reported in a transgenic mouse model of IRI that HIF1$\alpha^{+/-}$ mice displayed severe renal injury compared with the littermate group, suggesting a protective role against ischemic damage of HIF (Hill, Shukla et al. 2008). In another study using a rat hind-limb ischemia model, stabilization of HIF by carbon monoxide and an inhibitor of prolyl hydroxylation 2 (PHD2) improved limb angiogenesis post-ischemia (Schellinger, Cordasic et al. 2017). However, in our study, attenuated up-regulation of tubular HIF-1α was found in the renal tissue within the caspase-3 KO group at 21 days post-IRI, suggesting ameliorated secondary tubular hypoxia in the condition of caspase-3 invalidation (Yang, Lan et al. 2018).

7.1.2 Vascular endothelial growth factor (VEGF)

The VEGF family includes several angiogenic factors, including the most potent factor VEGF-A, whose expression is mainly regulated by HIFs at the transcriptional level (Nakagawa, Sato et al. 2013, Tanaka and Nangaku 2013).

Two tyrosine kinase receptors (Pons, Reichardt et al.) have been identified for VEGF binding, VEGFR1 (Flt-1) and VEGFR2 (KDR/Flk-1). VEGF-A regulates angiogenesis by binding to the VEGFR2. The role of VEGFR-1 in angiogenesis is not yet fully understood, with weak tyrosine kinase activity. VEGFR-1 is considered an anti-angiogenic receptor because it acts as a decoy receptor for VEGF-A. However, intracellular VEGFR-1 signaling has been shown to stimulate

angiogenesis in specific cell types, including ECs and stromal cells (Schwartz, Rowinsky et al. 2010).

It is generally accepted that VEGFR-2 plays a predominant role in the transduction of pro-angiogenic signals induced by VEGF-A. Once VEGFR-2 is stimulated, tip cells increase the expression of Delta-like protein 4 (DLL4) and activate the Notch signaling pathway in stalk cells. Activation of the Notch pathway results in a decrease in VEGFR-1 in stem cells, allowing advanced cells to direct the vessel's germination and lengthening (Phng, Potente et al. 2009).

In an animal model of IRI-induced AKI, it was been shown that VEGF-A was decreased post-IRI (Basile, Fredrich et al. 2008), and VEGF-A administration was preserved post-IRI microvascularization (Leonard, Friedrich et al. 2008). In addition to VEGF-A, VEGF-C is also reported to protect myocardial cells after IRI in a rat model by inhibiting cardiomyocyte apoptosis. While VEGF antagonism administration displayed reduced tissue damage in mice brain IRI (Chen, Lv et al. 2016, Ueno, Samura et al. 2016). In a rat retinal IRI model, endothelial permeability augmentation happened dependent on VEGFR-2 activation (Muthusamy, Lin et al. 2013). Based on recent investigations, VEGF is considered as an endothelial injury marker and is investigated as a therapeutic strategy for preventing microvascular endothelial injury post-IRI in multiple organs.

Translational therapeutic investigations using VEGF were also performed. VEGF has been proven to be closely correlated with renal capillary loss post-AKI, and administration of VEGF-121 better preserved renal microvascular density and prevented renal fibrosis progression (Leonard, Friedrich et al. 2008, Tanaka, Tanaka et al. 2014). The VEGF family members display a potential of predicting endothelial injury and AKI-CKD transition, by indicating endothelial dysfunction and renal capillary loss.

7.1.3 The Angiopoietin-1 (Ang-1) Tie-2 pathway

Angiopoietins (Ang) belong to a family of secretory glycoproteins, of which four forms have been identified: Ang-1, Ang-2, Ang-3, and Ang-4 (Kumar, Velayutham et al. 2017, Akwii, Sajib et al. 2019, Bilimoria and Singh 2019, He, Zhang et al. 2019), the best investigated Ang are Ang-1 and Ang-2. Tie-2 (Tyrosine kinase with immunoglobulin and EGF domains) is an angiopoietin receptor expressed exclusively in ECs. It is generally accepted that Ang-1 is an

agonist for Tie-2, and Ang-2 is an antagonist interfering in the phosphorylation of Tie-2 (Scholz, Plate et al. 2015). In physiological contexts, Ang-1 stabilizes the capillaries by promoting the survival of ECs and reducing vascular permeability, through stimulating Tie-2. In the context of microvascular injury, damaged ECs secrete more Ang-2, which competitively inhibits the Ang-1/Tie-2 signaling pathway, thereby destabilizing the vessels. The fate of these ECs depends on the presence of VEGF. In the presence of VEGF, ECs begin to migrate and proliferate to form new vessels. They stop migrating in the absence of VEGF (Lobov, Brooks et al. 2002).

There is no study on the prediction of AKI-CKD transition by Ang-1/Tie-2 axis but serum Ang-1 levels have been shown to decrease in patients with CKD (Futrakul, Butthep et al. 2008). An increased circulatory level of Ang-2 was shown to be associated with arterial collagen deposition and inflammation in CKD patients (Chang, Chiang et al. 2014). In an animal model of IRI-induced AKI, Ang-1 administration provided protective effects against AKI (Jung, Kim et al. 2009), suggesting a close link between the Ang-1/Tie-2 signal and renal endothelial dysfunction. Moreover, a pharmacological activator of Tie-2 reduced adhesion molecules within PTCs and glomeruli, decreased inflammatory cell infiltration, and ameliorated renal fibrosis in murine kidney transplantation (Thamm, Njau et al. 2016). This evidence brings us a potential perspective of Ang-1/Tie-2 pathway as a therapeutic strategy for AKI-CKD management.

Therefore, it would be interesting to assess these signaling pathways in the cohort of transplant patients mentioned above. It is expected that DGF patients with severe microvascular rarefaction will show a lower level of VEGF-1 and Ang-1 in post-transplant serum. We are expecting a close association between these biomarkers and microvascular dropout at six months post-transplant.

It would also be interesting to verify whether the level of VEGF-A and Ang-1 in the perfusate of renal grafts predicts DGF progression. If true, the application of certain treatments increasing VEGF-A and Ang-1 could benefit patient outcomes post-transplant.

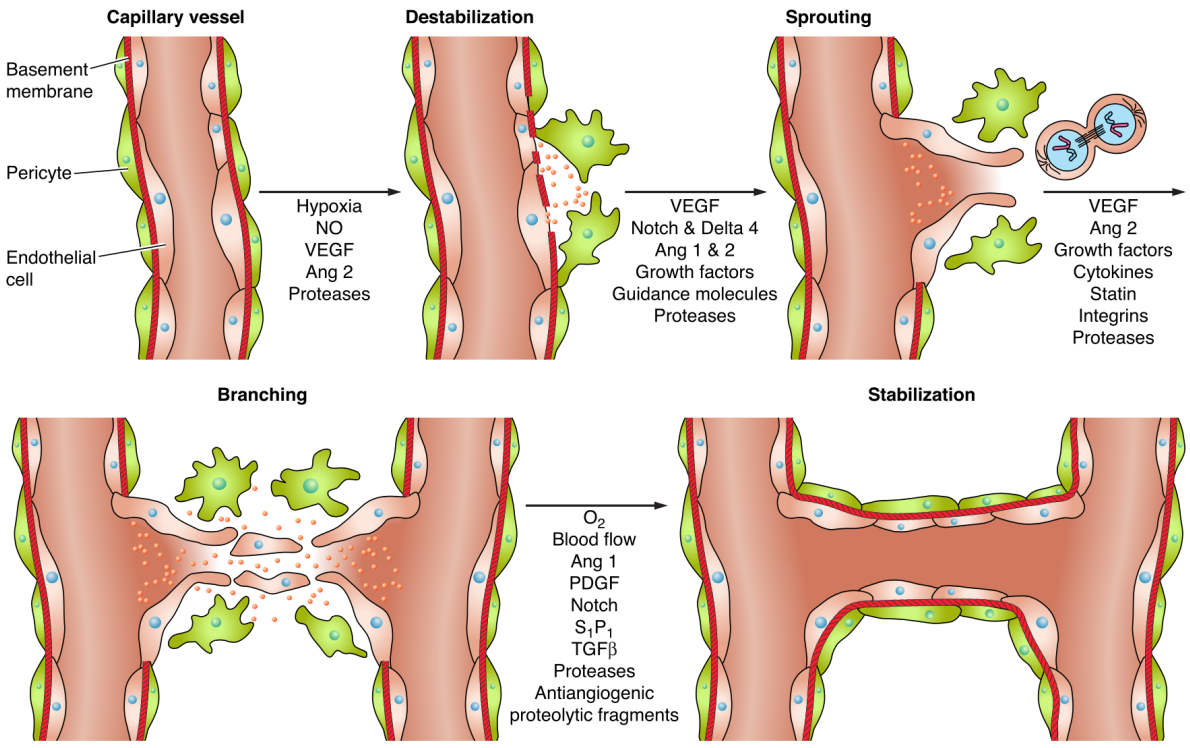

Figure 14. Cells and pathways involved in angiogenesis (Clapp, Thebault et al. 2009).

7.2 Progenitor endothelial cells and microvascular repair

Another potential therapeutic strategy for preventing microvascular rarefaction is the use of progenitor cells. Peripheral blood stem cells (PBSCs) and in situ progenitor cells are part of endothelial repair and regeneration mechanisms. After endothelial damage, the microvasculature begins to initiate repair mechanisms. Damaged ECs have been shown to be replaced by cells originating from two sources: (1) Activation and proliferation of neighboring ECs; (2) Circulating endothelial progenitor cells (EPCs).

The source and characteristics of EPCs are still in debate. The bone marrow is considered the predominant source of EPCs, but perhaps not the only source because progenitor cells with the endothelial-like makers were also found in peripheral blood, myocardial tissue, and adipose fat tissue. Therefore, ECPs are regarded as a group of heterogeneous progenitor cells, with markers

including CD34+, VEGF-R2+, and early progenitor cell marker CD133+ (Goligorsky, Kuo et al. 2009). ECPs are probably positive in the circulation with c-kit, Sca-1, and HSCs (hematopoietic stem cells) markers. After further differentiation with endothelial linage, the ECPs loses these markers and acquires endothelial markers, such as VE-cadherin (Hristov, Erl et al. 2003).

It is widely accepted that EPCs are involved in initiating microvascular repair (Reinders, Rabelink et al. 2006, Goligorsky, Yasuda et al. 2010).

Following signals released by microvascular damage, EPCs migrate from the bone marrow into the circulation to damaged sites to promote microvascular repair and tissue reperfusion (Schatteman, Dunnwald et al. 2007). The protective effect of EPCs on AKI has been demonstrated by several studies (Reinders, Rabelink et al. 2006, Schatteman, Dunnwald et al. 2007, Jung, Kim et al. 2009). However, EPCs from CKD patients with endothelial injury displayed decreased adhesion, reduced endothelial growth potential, and reduced anti-thrombotic function. This work suggests that the protective effect of EPCs requires not only a significant number of circulating EPCs but also a permissive microenvironment (Krenning, Dankers et al. 2009).

One investigation of the administration of progenitor cells in the kidney suggested an endothelial protective effect with rescued microvascular rarefaction, ameliorated renal function, reduced fibrosis in a stenotic kidney model (Chade, Zhu et al. 2009). The positive effects of progenitor cell administration are not entirely attributed to the presence of these cells in the damaged area. Administration of progenitor cells stimulates microvascular cell proliferation and protects the resident microvasculature through autocrine and paracrine activation. Additionally, activating pro-angiogenic mediators is another function of progenitor cells, which mobilizes resident and bone marrow progenitor cells. Nano-vesicles smaller than 100nm released by EPCs work on neighboring tubular epithelial cells by paracrine mode (Ozkok and Yildiz 2018), enhancing epithelial cell proliferation and preventing leukocyte infiltration. For evaluating the preservation of endothelial cells, immunohistochemistry staining of CD34 was performed in murine renal tissue post-IRI in our preliminary work. However, CD34 labels both ECs and EPCs, therefore we applied MECA-32 to label murine renal ECs in the published figures. For the CD34 immunohistochemistry evaluation, we did find increased CD34 positive cells in the casp3$^{-/-}$

group, but only in the short term. One possibility is that CD34 positive endothelial progenitor cells recruited from bone marrow or in situ favour the preservation or repair of PTCs. It may also be that tubular epithelial injury, in the initiation phase, favors the recruitment of EPCs as a helper for tubular epithelial regeneration and recovery.

In summary, the rescue of microvascular rarefaction and induction of new vessel production in the kidney appears a potential therapeutic strategy for alleviating microvascular endothelial injury. However, the therapeutic time window is narrow due to the early initiation time and limited repair capacity.

7.3 Caspase-3 inhibitor for prevention of endothelial injury

Our results suggest that caspase-3 inhibition should be considered a potential therapeutic strategy for preventing CKD transition post-acute kidney injury. Caspase-3 siRNA and inhibitors have been investigated in multiple IRI models, displaying controversial findings. siRNA has been tested on early renal outcomes in a number of IRI animal models with somewhat conflicting results (Zhang, Zheng et al. 2006, Yang, Zhao et al. 2014, Nydam, Plenter et al. 2018). siRNA caspase-3 treatment showed a protective impact on renal function in a porcine kidney autotransplant study (Yang, Zhao et al. 2014). Although caspase inhibition has yet to be tested in human renal IRI, a pan-caspase inhibitor has been evaluated in clinical trials in the context of liver transplantation (NCT00080236) but, to our knowledge, only early time points were assessed. Further clinical studies to address the use of caspase inhibition in preventing progressive renal dysfunction after IRI are still lacking. Our current results point to the need to address this question in future clinical studies that will investigate acute and long-term renal IRI consequences in patients.

However, the expected negative impact of caspase-3 inhibition in renal transplantation should also be considered and discussed. One of the possible outcomes of caspase-3 inhibition is to accentuate early-stage renal epithelial injury due to shifting to inflammatory necroptosis in tubular epithelial cells. Several potential strategies for avoiding the above-mentioned negative impacts on renal function could be effective, such as the combined administration of caspase-3 inhibitor and RIPK3 inhibitor, blocking both apoptosis and necroptosis in tubular epithelial compartment. Another option is to administer caspase-3 inhibitor and autophagy inducer

concomitantly, aiming to simultaneously activate the autophagic survival pathway of caspase-dependent apoptosis inhibition. Further research is necessary to better understand the complex crosstalk among different cell stress and death responses after IRI, which could be influenced by severity, ischemic temperature, age, pre-existing disease, etc.

One of our following projects investigates the effect of autophagy in our IRI model, especially in renal microvascular injury, by using GFP-LC3 transgenic mice that label LC3 puncta once autophagy is activated. This project has already started; the preliminary data present a higher elevation of Scr post-IRI in the condition of autophagy inhibition by pharmacological agents. Also, fluorescence LC3 puncta were visualized in the short-term post-IRI in intra-vital imaging.

In summary, our study identified caspase-3 as an essential regulator of renal microvascular dysfunction and rarefaction, and renal fibrogenesis post-IRI. Since the degree of caspase-3 dependent PTC rarefaction is considered a predictor associated with AKI-CKD transition, these findings bring a new direction for identifying predictors of AKI-CKD transition post-IRI, as caspase-3 could be regulated as a novel target for preserving long-term renal graft function.

Conclusion

It has been shown by various studies that both renal tubular and microvascular compartments play essential roles in the context of IRI-induced AKI, but the contributions of each of these two compartments were not yet clear. We have created a unique murine model, which allows us to distinguish the roles of microvascular damage and tubular damage on AKI to CKD transition.

In this study, we have demonstrated that the cell death pathway plays a crucial role in the pathophysiology of IRI-induced AKI, especially as the development of ECs apoptosis contributes to microvascular dysfunction, microvascular rarefaction, and long-term renal fibrogenesis. In the mild AKI model, we showed that caspase-3 deficiency worsened renal dysfunction in the early-stage. Interestingly, we observed an amelioration in microvascular damage but an increase in tubular damage. This discrepancy between these two renal compartments indicates that TECs choose necroptosis while ECs develop apoptosis as predominant cell death. In the long-term, both microvascular injury and tubular epithelial injury were rescued by the absence of caspase-3. Our findings reveal the dominant role of caspase-3 in IRI-induced microvascular insults during all phases of mild AKI.

In the following project, we performed a severe AKI model and further evaluated microvascular dysfunction post-IRI in both AKI forms. Our results demonstrated that caspase-3 deficiency is also protective for renal microvascular endothelial permeability, microvascular rarefaction, and renal fibrogenesis in the severe AKI model. The severity of PTCs disturbances post-IRI is an important predictor of AKI-CKD transition.

Taken together, our results suggest important roles of programmed cell deaths in the pathophysiology of IRI-induced AKI, as well as in the crucial link between microvascular dysfunction and long-term renal dysfunction. There is currently no treatment targeting microvascular injury or microvascular rarefaction in the setting of IRI-induced AKI or other kidney diseases. It would be interesting to study alterations in the angiogenesis pathway during IRI-induced AKI for therapeutic purposes. Our findings open a new direction for defining predictors of AKI-CKD transition and identify caspase-3 as a novel target for preventing long-term renal dysfunction.

Bibliographie

Aachoui, Y., V. Sagulenko, E. A. Miao and K. J. Stacey (2013). "Inflammasome-mediated pyroptotic and apoptotic cell death, and defense against infection." Curr Opin Microbiol **16**(3): 319-326.

Acosta-Ochoa, I., J. Bustamante-Munguira, A. Mendiluce-Herrero, J. Bustamante-Bustamante and A. Coca-Rojo (2019). "Impact on Outcomes across KDIGO-2012 AKI Criteria According to Baseline Renal Function." J Clin Med **8**(9).

Afsar, B., R. E. Afsar, T. Dagel, E. Kaya, S. Erus, A. Ortiz, et al. (2018). "Capillary rarefaction from the kidney point of view." Clin Kidney J **11**(3): 295-301.

Ahirwar, A. K., A. Jain, A. Singh, B. Goswami, M. K. Bhatnagar and J. Bhatacharjee (2015). "The study of markers of endothelial dysfunction in metabolic syndrome." Horm Mol Biol Clin Investig **24**(3): 131-136.

Akwii, R. G., M. S. Sajib, F. T. Zahra and C. M. Mikelis (2019). "Role of Angiopoietin-2 in Vascular Physiology and Pathophysiology." Cells **8**(5).

Alge, J. L. and J. M. Arthur (2015). "Biomarkers of AKI: a review of mechanistic relevance and potential therapeutic implications." Clin J Am Soc Nephrol **10**(1): 147-155.

Allison, S. J. (2017). "Chronic kidney disease: Uraemic toxin-induced platelet hyperactivity." Nat Rev Nephrol **13**(5): 261.

Alphonsus, C. S. and R. N. Rodseth (2014). "The endothelial glycocalyx: a review of the vascular barrier." Anaesthesia **69**(7): 777-784.

Andersson-Sjoland, A., J. C. Karlsson and K. Rydell-Tormanen (2016). "ROS-induced endothelial stress contributes to pulmonary fibrosis through pericytes and Wnt signaling." Laboratory Investigation **96**(2): 206-217.

Annaldas, S., M. A. Saifi, A. Khurana and C. Godugu (2019). "Nimbolide ameliorates unilateral ureteral obstruction-induced renal fibrosis by inhibition of TGF-beta and EMT/Slug signalling." Mol Immunol **112**: 247-255.

Antoniades, C., C. Shirodaria, P. Leeson, A. Antonopoulos, N. Warrick, T. Van-Assche, et al. (2009). "Association of plasma asymmetrical dimethylarginine (ADMA) with elevated vascular superoxide production and endothelial nitric oxide synthase uncoupling: implications for endothelial function in human atherosclerosis." Eur Heart J **30**(9): 1142-1150.

Asahara, T. and A. Kawamoto (2004). "Endothelial progenitor cells for postnatal vasculogenesis." Am J Physiol Cell Physiol **287**(3): C572-579.

Atala, A. (2012). "Re: VHL-Regulated miR-204 Suppresses Tumor Growth Through Inhibition of LC3B-Mediated Autophagy in Renal Clear Cell Carcinoma Editorial Comment." Journal of Urology **188**(6): 2434-2434.

Awad, A. S. and A. A. El-Sharif (2011). "Curcumin immune-mediated and anti-apoptotic mechanisms protect against renal ischemia/reperfusion and distant organ induced injuries." International Immunopharmacology **11**(8): 992-996.

Babickova, J., B. M. Klinkhammer, E. M. Buhl, S. Djudjaj, M. Hoss, F. Heymann, et al. (2017). "Regardless of etiology, progressive renal disease causes ultrastructural and functional alterations of peritubular capillaries." Kidney Int **91**(1): 70-85.

Bakogiannis, C., D. Tousoulis, E. Androulakis, A. Briasoulis, N. Papageorgiou, G. Vogiatzi, et al. (2012). "Circulating endothelial progenitor cells as biomarkers for prediction of cardiovascular outcomes." Curr Med Chem **19**(16): 2597-2604.

Barber, B. E., M. J. Grigg, K. A. Piera, T. William, D. J. Cooper, K. Plewes, et al. (2018). "Intravascular haemolysis in severe Plasmodium knowlesi malaria: association with endothelial activation, microvascular dysfunction, and acute kidney injury." Emerg Microbes Infect **7**(1): 106.

Bardin, N., V. Moal, F. Anfosso, L. Daniel, P. Brunet, J. Sampol, et al. (2003). "Soluble CD146, a novel endothelial marker, is increased in physiopathological settings linked to endothelial junctional alteration." Thrombosis and Haemostasis **90**(5): 915-920.

Barnes, J. L. and Y. Gorin (2011). "Myofibroblast differentiation during fibrosis: role of NAD(P)H oxidases." Kidney Int **79**(9): 944-956.

Basile, D. P. (2004). "Rarefaction of peritubular capillaries following ischemic acute renal failure: a potential factor predisposing to progressive nephropathy." Curr Opin Nephrol Hypertens **13**(1): 1-7.

Basile, D. P. (2007). "The endothelial cell in ischemic acute kidney injury: implications for acute and chronic function." Kidney Int **72**(2): 151-156.

Basile, D. P. (2019). "The case for capillary rarefaction in the AKI to CKD progression: insights from multiple injury models." Am J Physiol Renal Physiol **317**(5): F1253-F1254.

Basile, D. P., M. D. Anderson and T. A. Sutton (2012). "Pathophysiology of acute kidney injury." Compr Physiol **2**(2): 1303-1353.

Basile, D. P., D. Donohoe, K. Roethe and J. L. Osborn (2001). "Renal ischemic injury results in permanent damage to peritubular capillaries and influences long-term function." Am J Physiol Renal Physiol **281**(5): F887-899.

Basile, D. P., K. Fredrich, B. Chelladurai, E. C. Leonard and A. R. Parrish (2008). "Renal ischemia reperfusion inhibits VEGF expression and induces ADAMTS-1, a novel VEGF inhibitor." Am J Physiol Renal Physiol **294**(4): F928-936.

Basile, D. P., K. Fredrich, D. Weihrauch, N. Hattan and W. M. Chilian (2004). "Angiostatin and matrix metalloprotease expression following ischemic acute renal failure." Am J Physiol Renal Physiol **286**(5): F893-902.

Basile, D. P., J. L. Friedrich, J. Spahic, N. Knipe, H. Mang, E. C. Leonard, et al. (2011). "Impaired endothelial proliferation and mesenchymal transition contribute to vascular rarefaction following acute kidney injury." Am J Physiol Renal Physiol **300**(3): F721-733.

Basile, D. P. and M. C. Yoder (2014). "Renal endothelial dysfunction in acute kidney ischemia reperfusion injury." Cardiovasc Hematol Disord Drug Targets **14**(1): 3-14.

Becherucci, F., B. Mazzinghi, E. Ronconi, A. Peired, E. Lazzeri, C. Sagrinati, et al. (2009). "The role of endothelial progenitor cells in acute kidney injury." Blood Purif **27**(3): 261-270.

Benoit, S. W., E. A. Ciccia and P. Devarajan (2020). "Cystatin C as a biomarker of chronic kidney disease: latest developments." Expert Rev Mol Diagn: 1-8.

Bernard, M., M. Dieude, B. Yang, K. Hamelin, K. Underwood and M. J. Hebert (2014). "Autophagy fosters myofibroblast differentiation through MTORC2 activation and downstream upregulation of CTGF." Autophagy **10**(12): 2193-2207.

Bernard, M., M. Dieude, B. Yang, K. Hamelin, K. Underwood and M. J. Hebert (2014). "Autophagy fosters myofibroblast differentiation through MTORC2 activation and downstream upregulation of CTGF." Autophagy **10**(12): 2193-2207.

Bernard, M., B. Yang, F. Migneault, J. Turgeon, M. Dieude, M. A. Olivier, et al. (2020). "Autophagy drives fibroblast senescence through MTORC2 regulation." Autophagy.

Bertram, J. F., R. N. Douglas-Denton, B. Diouf, M. D. Hughson and W. E. Hoy (2011). "Human nephron number: implications for health and disease." Pediatr Nephrol **26**(9): 1529-1533.

Bhandari, S., P. Johnston, R. C. Fowler, A. Joyce and J. H. Turney (1995). "Non-dilated bilateral ureteric obstruction." Nephrol Dial Transplant **10**(12): 2337-2339.

Bicer, M., A. Guler, G. U. Kocabas, C. Imamoglu, A. Baloglu, O. Bilgir, et al. (2017). "Endocan is a predictor of increased cardiovascular risk in women with polycystic ovary syndrome." Endocrine Research **42**(2): 145-153.

Bilimoria, J. and H. Singh (2019). "The Angiopoietin ligands and Tie receptors: potential diagnostic biomarkers of vascular disease." J Recept Signal Transduct Res **39**(3): 187-193.

Black, L. M., J. M. Lever, A. M. Traylor, B. Chen, Z. Yang, S. K. Esman, et al. (2018). "Divergent effects of AKI to CKD models on inflammation and fibrosis." Am J Physiol Renal Physiol **315**(4): F1107-F1118.

Bohle, A., K. E. Grund, S. Mackensen and M. Tolon (1977). "Correlations between Renal Interstitium and Level of Serum Creatinine - Morphometric Investigations of Biopsies in Peri-Membranous Glomerulonephritis." Virchows Archiv a-Pathological Anatomy and Histopathology **373**(1): 15-22.

Bonegio, R. and W. Lieberthal (2002). "Role of apoptosis in the pathogenesis of acute renal failure." Curr Opin Nephrol Hypertens **11**(3): 301-308.

Bonora, M., M. R. Wieckowski, C. Chinopoulos, O. Kepp, G. Kroemer, L. Galluzzi, et al. (2015). "Molecular mechanisms of cell death: central implication of ATP synthase in mitochondrial permeability transition." Oncogene **34**(12): 1475-1486.

Bonventre, J. V. (2007). "Pathophysiology of acute kidney injury: roles of potential inhibitors of inflammation." Contrib Nephrol **156**: 39-46.

Bonventre, J. V., V. S. Vaidya, R. Schmouder, P. Feig and F. Dieterle (2010). "Next-generation biomarkers for detecting kidney toxicity." Nat Biotechnol **28**(5): 436-440.

Bonventre, J. V. and L. Yang (2011). "Cellular pathophysiology of ischemic acute kidney injury." J Clin Invest **121**(11): 4210-4221.

Brodsky, S. V., T. Yamamoto, T. Tada, B. Kim, J. Chen, F. Kajiya, et al. (2002). "Endothelial dysfunction in ischemic acute renal failure: rescue by transplanted endothelial cells." Am J Physiol Renal Physiol **282**(6): F1140-1149.

Broekema, M., M. C. Harmsen, M. J. van Luyn, J. A. Koerts, A. H. Petersen, T. G. van Kooten, et al. (2007). "Bone marrow-derived myofibroblasts contribute to the renal interstitial

myofibroblast population and produce procollagen I after ischemia/reperfusion in rats." J Am Soc Nephrol **18**(1): 165-175.

Bullok, K. E., D. Maxwell, A. H. Kesarwala, S. Gammon, J. L. Prior, M. Snow, et al. (2007). "Biochemical and in vivo characterization of a small, membrane-permeant, caspase-activatable far-red fluorescent peptide for imaging apoptosis." Biochemistry **46**(13): 4055-4065.

Burt, L. E., M. S. Forbes, B. A. Thornhill, S. C. Kiley, J. J. Minor and R. L. Chevalier (2007). "Renal vascular endothelial growth factor in neonatal obstructive nephropathy. II. Exogenous VEGF." American Journal of Physiology-Renal Physiology **292**(1): F168-F174.

Cailhier, J. F., P. Laplante and M. J. Hebert (2006). "Endothelial apoptosis and chronic transplant vasculopathy: recent results, novel mechanisms." Am J Transplant **6**(2): 247-253.

Cakiroglu, F., S. M. Enders-Comberg, H. Pagel, J. Rohwedel, H. Lehnert and J. Kramer (2016). "Erythropoietin-enhanced endothelial progenitor cell recruitment in peripheral blood and renal vessels during experimental acute kidney injury in rats." Cell Biol Int **40**(3): 298-307.

Cambar, J., C. Dorian and J. C. Cal (1987). "[Chronobiology and renal physiopathology]." Pathol Biol (Paris) **35**(6): 977-984.

Cao, Y. and D. J. Klionsky (2007). "Physiological functions of Atg6/Beclin 1: a unique autophagy-related protein." Cell Res **17**(10): 839-849.

Cao, Y., Z. W. Yi, H. Zhang, X. Q. Dang, X. C. Wu and A. W. Huang (2013). "Etiology and outcomes of acute kidney injury in Chinese children: a prospective multicentre investigation." BMC Urol **13**: 41.

Cardinal, H., M. Dieude and M. J. Hebert (2018). "Endothelial Dysfunction in Kidney Transplantation." Front Immunol **9**: 1130.

Carmona, A., M. L. Aguera, C. Luna-Ruiz, P. Buendia, L. Calleros, A. Garcia-Jerez, et al. (2017). "Markers of endothelial damage in patients with chronic kidney disease on hemodialysis." Am J Physiol Renal Physiol **312**(4): F673-F681.

Cavaille-Coll, M., S. Bala, E. Velidedeoglu, A. Hernandez, P. Archdeacon, G. Gonzalez, et al. (2013). "Summary of FDA Workshop on Ischemia Reperfusion Injury in Kidney Transplantation." American Journal of Transplantation **13**(5): 1134-1148.

Chade, A. R. (2013). "Renal vascular structure and rarefaction." Compr Physiol **3**(2): 817-831.

Chade, A. R., X. Zhu, R. Lavi, J. D. Krier, S. Pislaru, R. D. Simari, et al. (2009). "Endothelial progenitor cells restore renal function in chronic experimental renovascular disease." Circulation **119**(4): 547-557.

Chang, F. C., W. C. Chiang, M. H. Tsai, Y. H. Chou, S. Y. Pan, Y. T. Chang, et al. (2014). "Angiopoietin-2-induced arterial stiffness in CKD." J Am Soc Nephrol **25**(6): 1198-1209.

Chang, F. C., Y. H. Chou, Y. T. Chen and S. L. Lin (2012). "Novel insights into pericyte-myofibroblast transition and therapeutic targets in renal fibrosis." J Formos Med Assoc **111**(11): 589-598.

Chatauret, N., L. Badet, B. Barrou and T. Hauet (2014). "Ischemia-reperfusion: From cell biology to acute kidney injury." Prog Urol **24 Suppl 1**: S4-12.

Chen, D. L., J. T. Engle, E. A. Griffin, J. P. Miller, W. Chu, D. Zhou, et al. (2015). "Imaging caspase-3 activation as a marker of apoptosis-targeted treatment response in cancer." Mol Imaging Biol **17**(3): 384-393.

Chen, H., Y. Fang, J. Wu, H. Chen, Z. Zou, X. Zhang, et al. (2018). "RIPK3-MLKL-mediated necroinflammation contributes to AKI progression to CKD." Cell Death Dis **9**(9): 878.

Chen, X. G., Y. X. Lv, D. Zhao, L. Zhang, F. Zheng, J. Y. Yang, et al. (2016). "Vascular endothelial growth factor-C protects heart from ischemia/reperfusion injury by inhibiting cardiomyocyte apoptosis." Mol Cell Biochem **413**(1-2): 9-23.

Cheng, O., R. Thuillier, E. Sampson, G. Schultz, P. Ruiz, X. Zhang, et al. (2006). "Connective tissue growth factor is a biomarker and mediator of kidney allograft fibrosis." Am J Transplant **6**(10): 2292-2306.

Chien, C. T., S. K. Shyue and M. K. Lai (2007). "Bcl-xL augmentation potentially reduces ischemia/reperfusion induced proximal and distal tubular apoptosis and autophagy." Transplantation **84**(9): 1183-1190.

Choi, Y. J., S. Chakraborty, V. Nguyen, C. Nguyen, B. K. Kim, S. I. Shim, et al. (2000). "Peritubular capillary loss is associated with chronic tubulointerstitial injury in human kidney: altered expression of vascular endothelial growth factor." Hum Pathol **31**(12): 1491-1497.

Chou, Y. H., S. Y. Pan, Y. H. Shao, H. M. Shih, S. Y. Wei, C. F. Lai, et al. (2020). "Methylation in pericytes after acute injury promotes chronic kidney disease." J Clin Invest.

Clapp, C., S. Thebault, M. C. Jeziorski and G. Martinez De La Escalera (2009). "Peptide hormone regulation of angiogenesis." Physiol Rev **89**(4): 1177-1215.

Cocucci, E., G. Racchetti and J. Meldolesi (2009). "Shedding microvesicles: artefacts no more." Trends in Cell Biology **19**(2): 43-51.

Conrad, M., J. P. Angeli, P. Vandenabeele and B. R. Stockwell (2016). "Regulated necrosis: disease relevance and therapeutic opportunities." Nat Rev Drug Discov **15**(5): 348-366.

Cooke, J. P. (2004). "Asymmetrical dimethylarginine: the Uber marker?" Circulation **109**(15): 1813-1818.

Cotran, R. S. and T. Mayadas-Norton (1998). "Endothelial adhesion molecules in health and disease." Pathol Biol (Paris) **46**(3): 164-170.

Daniels, R. C. and T. E. Bunchman (2013). "Renal complications and therapy in the PICU: hypertension, CKD, AKI, and RRT." Crit Care Clin **29**(2): 279-299.

de Braganca, A. C., R. A. Volpini, P. Mehrotra, L. Andrade and D. P. Basile (2016). "Vitamin D deficiency contributes to vascular damage in sustained ischemic acute kidney injury." Physiol Rep **4**(13).

de Duve, C. (1983). "Lysosomes revisited." Eur J Biochem **137**(3): 391-397.

Dejana, E., K. K. Hirschi and M. Simons (2017). "The molecular basis of endothelial cell plasticity." Nat Commun **8**: 14361.

Dekel, B., E. Hochman, M. J. Sanchez, N. Maharshak, N. Amariglio, A. R. Green, et al. (2004). "Kidney, blood, and endothelium: developmental expression of stem cell leukemia during nephrogenesis." Kidney Int **65**(4): 1162-1169.

Demaria, M., N. Ohtani, S. A. Youssef, F. Rodier, W. Toussaint, J. R. Mitchell, et al. (2014). "An Essential Role for Senescent Cells in Optimal Wound Healing through Secretion of PDGF-AA." Developmental Cell **31**(6): 722-733.

Dieude, M., C. Bell, J. Turgeon, D. Beillevaire, L. Pomerleau, B. Yang, et al. (2015). "The 20S proteasome core, active within apoptotic exosome-like vesicles, induces autoantibody production and accelerates rejection." Sci Transl Med **7**(318): 318ra200.

Dimke, H., M. A. Sparks, B. R. Thomson, S. Frische, T. M. Coffman and S. E. Quaggin (2015). "Tubulovascular cross-talk by vascular endothelial growth factor a maintains peritubular microvasculature in kidney." J Am Soc Nephrol **26**(5): 1027-1038.

Dinarello, C. A. (1999). "IL-18: A TH1-inducing, proinflammatory cytokine and new member of the IL-1 family." J Allergy Clin Immunol **103**(1 Pt 1): 11-24.

Dirkes, S. M. (2016). "Acute Kidney Injury vs Acute Renal Failure." Crit Care Nurse **36**(6): 75-76.

Dobaczewski, M., M. Bujak, N. Li, C. Gonzalez-Quesada, L. H. Mendoza, X. F. Wang, et al. (2010). "Smad3 signaling critically regulates fibroblast phenotype and function in healing myocardial infarction." Circ Res **107**(3): 418-428.

Dong, Y., Q. Zhang, J. Wen, T. Chen, L. He, Y. Wang, et al. (2019). "Ischemic Duration and Frequency Determines AKI-to-CKD Progression Monitored by Dynamic Changes of Tubular Biomarkers in IRI Mice." Front Physiol **10**: 153.

Donnahoo, K. K., X. Meng, A. Ayala, M. P. Cain, A. H. Harken and D. R. Meldrum (1999). "Early kidney TNF-alpha expression mediates neutrophil infiltration and injury after renal ischemia-reperfusion." Am J Physiol **277**(3): R922-929.

Doreille, A., M. Dieude and H. Cardinal (2019). "The determinants, biomarkers, and consequences of microvascular injury in kidney transplant recipients." Am J Physiol Renal Physiol **316**(1): F9-F19.

Drozdz, D., M. Latka, T. Drozdz, K. Sztefko and P. Kwinta (2018). "Thrombomodulin as a New Marker of Endothelial Dysfunction in Chronic Kidney Disease in Children." Pediatric Nephrology **33**(10): 1875-1875.

Duann, P., E. A. Lianos, J. Ma and P. H. Lin (2016). "Autophagy, Innate Immunity and Tissue Repair in Acute Kidney Injury." Int J Mol Sci **17**(5).

Duffield, J. S., K. M. Park, L. L. Hsiao, V. R. Kelley, D. T. Scadden, T. Ichimura, et al. (2005). "Restoration of tubular epithelial cells during repair of the postischemic kidney occurs independently of bone marrow-derived stem cells." J Clin Invest **115**(7): 1743-1755.

Eardley, K. S., C. Kubal, D. Zehnder, M. Quinkler, J. Lepenies, C. O. Savage, et al. (2008). "The role of capillary density, macrophage infiltration and interstitial scarring in the pathogenesis of human chronic kidney disease." Kidney Int **74**(4): 495-504.

Eddy, A. A. and A. B. Fogo (2006). "Plasminogen activator inhibitor-1 in chronic kidney disease: evidence and mechanisms of action." J Am Soc Nephrol **17**(11): 2999-3012.

Ehling, J., J. Babickova, F. Gremse, B. M. Klinkhammer, S. Baetke, R. Knuechel, et al. (2016). "Quantitative Micro-Computed Tomography Imaging of Vascular Dysfunction in Progressive Kidney Diseases." J Am Soc Nephrol **27**(2): 520-532.

Eirin, A., X. Y. Zhu, V. H. Urbieta-Caceres, J. P. Grande, A. Lerman, S. C. Textor, et al. (2011). "Persistent kidney dysfunction in swine renal artery stenosis correlates with outer cortical microvascular remodeling." Am J Physiol Renal Physiol **300**(6): F1394-1401.

Eisenberg, T., M. Abdellatif, S. Schroeder, U. Primessnig, S. Stekovic, T. Pendl, et al. (2016). "Cardioprotection and lifespan extension by the natural polyamine spermidine." Nat Med **22**(12): 1428-1438.

El-Kenawi, A. E. and A. B. El-Remessy (2013). "Angiogenesis inhibitors in cancer therapy: mechanistic perspective on classification and treatment rationales." Br J Pharmacol **170**(4): 712-729.

Erslev, A. J. (1975). "Renal biogenesis of erythropoietin." Am J Med **58**(1): 25-30.

Evans, R. G., C. P. Ow and P. Bie (2015). "The chronic hypoxia hypothesis: the search for the smoking gun goes on." Am J Physiol Renal Physiol **308**(2): F101-102.

Fabian, S. L., R. R. Penchev, B. St-Jacques, A. N. Rao, P. Sipila, K. A. West, et al. (2012). "Hedgehog-Gli pathway activation during kidney fibrosis." Am J Pathol **180**(4): 1441-1453.

Fan, Y., Y. Fei, L. Zheng, J. Wang, W. Xiao, J. Wen, et al. (2018). "Expression of Endothelial Cell Injury Marker Cd146 Correlates with Disease Severity and Predicts the Renal Outcomes in Patients with Diabetic Nephropathy." Cell Physiol Biochem **48**(1): 63-74.

Ferenbach, D. A. and J. V. Bonventre (2015). "Mechanisms of maladaptive repair after AKI leading to accelerated kidney ageing and CKD." Nat Rev Nephrol **11**(5): 264-276.

Ferrannini, M., G. Vischini and N. Di Daniele (2008). "Cystatin C: a promising misunderstood biomarker for the diagnosis of acute kidney injury." Kidney Int **74**(12): 1623; author reply 1623-1624.

Ferreyra, C., F. Vargas, I. Rodriguez-Gomez, R. Perez-Abud, F. O'Valle and A. Osuna (2013). "Preconditioning with triiodothyronine improves the clinical signs and acute tubular necrosis induced by ischemia/reperfusion in rats." PLoS One **8**(9): e74960.

Fine, L. G. and J. T. Norman (2008). "Chronic hypoxia as a mechanism of progression of chronic kidney diseases: from hypothesis to novel therapeutics." Kidney International **74**(7): 867-872.

Finn, W. F. (1980). "Enhanced recovery from postischemic acute renal failure. Micropuncture studies in the rat." Circ Res **46**(3): 440-448.

Finn, W. F., E. Fernandezrepollet, D. Goldfarb, A. Iaina and H. E. Eliahou (1984). "Attenuation of Injury Due to Unilateral Renal Ischemia - Delayed-Effects of Contralateral Nephrectomy." Journal of Laboratory and Clinical Medicine **103**(2): 193-203.

Fiorentino, M., G. Grandaliano, L. Gesualdo and G. Castellano (2018). "Acute Kidney Injury to Chronic Kidney Disease Transition." Contrib Nephrol **193**: 45-54.

Fliser, D. (2010). "Perspectives in renal disease progression: the endothelium as a treatment target in chronic kidney disease." Journal of Nephrology **23**(4): 369-376.

Fu, Y., C. Tang, J. Cai, G. Chen, D. Zhang and Z. Dong (2018). "Rodent models of AKI-CKD transition." Am J Physiol Renal Physiol **315**(4): F1098-F1106.

Fujii, H., S. Goto and M. Fukagawa (2018). "Role of Uremic Toxins for Kidney, Cardiovascular, and Bone Dysfunction." Toxins (Basel) **10**(5).

Fujita, Y., J. Araya, S. Ito, K. Kobayashi, N. Kosaka, Y. Yoshioka, et al. (2015). "Suppression of autophagy by extracellular vesicles promotes myofibroblast differentiation in COPD pathogenesis." J Extracell Vesicles **4**: 28388.

Futrakul, N., P. Butthep and P. Futrakul (2008). "Altered vascular homeostasis in chronic kidney disease." Clin Hemorheol Microcirc **38**(3): 201-207.

Galluzzi, L., J. M. Bravo-San Pedro, I. Vitale, S. A. Aaronson, J. M. Abrams, D. Adam, et al. (2015). "Essential versus accessory aspects of cell death: recommendations of the NCCD 2015." Cell Death Differ **22**(1): 58-73.

Galluzzi, L., O. Kepp and G. Kroemer (2014). "MLKL regulates necrotic plasma membrane permeabilization." Cell Res **24**(2): 139-140.

Galluzzi, L., F. Pietrocola, B. Levine and G. Kroemer (2014). "Metabolic control of autophagy." Cell **159**(6): 1263-1276.

Galluzzi, L., I. Vitale, J. M. Abrams, E. S. Alnemri, E. H. Baehrecke, M. V. Blagosklonny, et al. (2012). "Molecular definitions of cell death subroutines: recommendations of the Nomenclature Committee on Cell Death 2012." Cell Death Differ **19**(1): 107-120.

Garcia-Prieto, A. M., U. Verdalles and M. Goicoechea (2021). "Use of renin-angiotensin-aldosterone system blockade in controversial chronic kidney disease populations." Med Clin (Barc).

Gastman, B. R. (2001). "Apoptosis and its clinical impact." Head Neck **23**(5): 409-425.

Genovese, F., A. A. Manresa, D. J. Leeming, M. A. Karsdal and P. Boor (2014). "The extracellular matrix in the kidney: a source of novel non-invasive biomarkers of kidney fibrosis?" Fibrogenesis Tissue Repair **7**(1): 4.

Goligorsky, M. S., M. C. Kuo, D. Patschan and M. C. Verhaar (2009). "Review article: endothelial progenitor cells in renal disease." Nephrology (Carlton) **14**(3): 291-297.

Goligorsky, M. S., K. Yasuda and B. Ratliff (2010). "Dysfunctional endothelial progenitor cells in chronic kidney disease." J Am Soc Nephrol **21**(6): 911-919.

Grgic, I., G. Campanholle, V. Bijol, C. Wang, V. S. Sabbisetti, T. Ichimura, et al. (2012). "Targeted proximal tubule injury triggers interstitial fibrosis and glomerulosclerosis." Kidney Int **82**(2): 172-183.

Grgic, I., J. S. Duffield and B. D. Humphreys (2012). "The origin of interstitial myofibroblasts in chronic kidney disease." Pediatric Nephrology **27**(2): 183-193.

Guan, X. F., Q. J. Chen, X. C. Zuo, R. Guo, X. D. Peng, J. L. Wang, et al. (2017). "Contrast Media-Induced Renal Inflammation Is Mediated Through HMGB1 and Its Receptors in Human Tubular Cells." DNA Cell Biol **36**(1): 67-76.

Gunaratnam, L. (2018). "New Answers to Old Conundrums: What Antibodies, Exosomes and Inflammasomes Bring to the Conversation. Canadian National Transplant Research Program International Summit Report (vol 102, pg 209, 2018)." Transplantation **102**(7): E360-E360.

Gunay, M. and C. Mertoglu (2019). "Increase of endocan, a new marker for inflammation and endothelial dysfunction, in acute kidney injury." North Clin Istanb **6**(2): 124-128.

Gurney, M. A., C. Huang, J. M. Ramil, N. Ravindran, A. M. Andres, J. Sin, et al. (2015). "Measuring cardiac autophagic flux in vitro and in vivo." Methods Mol Biol **1219**: 187-197.

Guzzi, F., L. Cirillo, R. M. Roperto, P. Romagnani and E. Lazzeri (2019). "Molecular Mechanisms of the Acute Kidney Injury to Chronic Kidney Disease Transition: An Updated View." Int J Mol Sci **20**(19).

Gyorgy, B., T. G. Szabo, M. Pasztoi, Z. Pal, P. Misjak, B. Aradi, et al. (2011). "Membrane vesicles, current state-of-the-art: emerging role of extracellular vesicles." Cell Mol Life Sci **68**(16): 2667-2688.

Hakroush, S., M. J. Moeller, F. Theilig, B. Kaissling, T. P. Sijmonsma, M. Jugold, et al. (2009). "Effects of increased renal tubular vascular endothelial growth factor (VEGF) on fibrosis, cyst formation, and glomerular disease." Am J Pathol **175**(5): 1883-1895.

Hamed, H. M., S. A. El-Sherbini, N. A. Barakat, T. M. Farid and E. A. Rasheed (2013). "Serum cystatin C is a poor biomarker for diagnosing acute kidney injury in critically-ill children." Indian J Crit Care Med **17**(2): 92-98.

Hammadah, M., V. V. Georgiopoulou, A. P. Kalogeropoulos, M. Weber, X. Wang, M. A. Samara, et al. (2016). "Elevated Soluble Fms-Like Tyrosine Kinase-1 and Placental-Like Growth Factor Levels Are Associated With Development and Mortality Risk in Heart Failure." Circulation-Heart Failure **9**(1).

Han, W. K., V. Bailly, R. Abichandani, R. Thadhani and J. V. Bonventre (2002). "Kidney Injury Molecule-1 (KIM-1): a novel biomarker for human renal proximal tubule injury." Kidney Int **62**(1): 237-244.

Harris, M. B., H. Ju, V. J. Venema, H. Liang, R. Zou, B. J. Michell, et al. (2001). "Reciprocal phosphorylation and regulation of endothelial nitric-oxide synthase in response to bradykinin stimulation." J Biol Chem **276**(19): 16587-16591.

Hassan, M., H. Watari, A. AbuAlmaaty, Y. Ohba and N. Sakuragi (2014). "Apoptosis and molecular targeting therapy in cancer." Biomed Res Int **2014**: 150845.

Havasi, A. and S. C. Borkan (2011). "Apoptosis and acute kidney injury." Kidney Int **80**(1): 29-40.

He, F. F., D. Zhang, Q. Chen, Y. Zhao, L. Wu, Z. Q. Li, et al. (2019). "Angiopoietin-Tie signaling in kidney diseases: an updated review." FEBS Lett **593**(19): 2706-2715.

He, T., J. Xiong, L. Nie, Y. Yu, X. Guan, X. Xu, et al. (2016). "Resveratrol inhibits renal interstitial fibrosis in diabetic nephropathy by regulating AMPK/NOX4/ROS pathway." J Mol Med (Berl) **94**(12): 1359-1371.

Hernandez-Gea, V., Z. Ghiassi-Nejad, R. Rozenfeld, R. Gordon, M. I. Fiel, Z. Y. Yue, et al. (2012). "Autophagy Releases Lipid That Promotes Fibrogenesis by Activated Hepatic Stellate Cells in Mice and in Human Tissues." Gastroenterology **142**(4): 938-946.

Hill, P., D. Shukla, M. G. Tran, J. Aragones, H. T. Cook, P. Carmeliet, et al. (2008). "Inhibition of hypoxia inducible factor hydroxylases protects against renal ischemia-reperfusion injury." J Am Soc Nephrol **19**(1): 39-46.

Homsi, E., P. Janino and J. B. de Faria (2006). "Role of caspases on cell death, inflammation, and cell cycle in glycerol-induced acute renal failure." Kidney Int **69**(8): 1385-1392.

Horbelt, M., S. Y. Lee, H. E. Mang, N. L. Knipe, Y. Sado, A. Kribben, et al. (2007). "Acute and chronic microvascular alterations in a mouse model of ischemic acute kidney injury." Am J Physiol Renal Physiol **293**(3): F688-695.

Hoste, E. A. and J. A. Kellum (2006). "Acute kidney injury: epidemiology and diagnostic criteria." Curr Opin Crit Care **12**(6): 531-537.

Hristov, M., W. Erl and P. C. Weber (2003). "Endothelial progenitor cells: mobilization, differentiation, and homing." Arterioscler Thromb Vasc Biol **23**(7): 1185-1189.

Hsu, C. Y. (2012). "Yes, AKI truly leads to CKD." J Am Soc Nephrol **23**(6): 967-969.

Hsu, R. K., C. E. McCulloch, R. A. Dudley, L. J. Lo and C. Y. Hsu (2013). "Temporal changes in incidence of dialysis-requiring AKI." J Am Soc Nephrol **24**(1): 37-42.

Hu, D., D. Zhang, B. Liu, Y. Liu, Y. Zhou, Y. Yu, et al. (2020). "Human ucMSCs seeded in a decellularized kidney scaffold attenuate renal fibrosis by reducing epithelial-mesenchymal transition via the TGF-beta/Smad signaling pathway." Pediatr Res.

Hu, J. B., D. Liu, J. Qi, K. J. Lu, F. Y. Jin, X. Y. Ying, et al. (2018). "An E-selectin targeting and MMP-2-responsive dextran-curcumin polymeric prodrug for targeted therapy of acute kidney injury." Biomater Sci **6**(12): 3397-3409.

Huang, K. and D. C. Fingar (2014). "Growing knowledge of the mTOR signaling network." Semin Cell Dev Biol **36**: 79-90.

Huen, S. C., L. Huynh, A. Marlier, Y. Lee, G. W. Moeckel and L. G. Cantley (2015). "GM-CSF Promotes Macrophage Alternative Activation after Renal Ischemia/Reperfusion Injury." J Am Soc Nephrol **26**(6): 1334-1345.

Humphreys, B. D. (2018). "Mechanisms of Renal Fibrosis." Annu Rev Physiol **80**: 309-326.

Humphreys, B. D., S. L. Lin, A. Kobayashi, T. E. Hudson, B. T. Nowlin, J. V. Bonventre, et al. (2010). "Fate tracing reveals the pericyte and not epithelial origin of myofibroblasts in kidney fibrosis." Am J Pathol **176**(1): 85-97.

Humphreys, B. D., M. T. Valerius, A. Kobayashi, J. W. Mugford, S. Soeung, J. S. Duffield, et al. (2008). "Intrinsic epithelial cells repair the kidney after injury." Cell Stem Cell **2**(3): 284-291.

Imamura, M., J. S. Moon, K. P. Chung, K. Nakahira, T. Muthukumar, R. Shingarev, et al. (2018). "RIPK3 promotes kidney fibrosis via AKT-dependent ATP citrate lyase." JCI Insight **3**(3).

Ince, C. (2014). "The central role of renal microcirculatory dysfunction in the pathogenesis of acute kidney injury." Nephron Clin Pract **127**(1-4): 124-128.

Inkinen, N., V. Pettilä, P. Lakkisto, A. Kuitunen, S. Jukarainen, S. Bendel, et al. (2019). "Association of endothelial and glycocalyx injury biomarkers with fluid administration, development of acute kidney injury, and 90-day mortality: data from the FINNAKI observational study." Ann Intensive Care **9**(1): 103.

Inkinen, N., V. Pettila, P. Lakkisto, A. Kuitunen, S. Jukarainen, S. Bendel, et al. (2019). "Association of endothelial and glycocalyx injury biomarkers with fluid administration, development of acute kidney injury, and 90-day mortality: data from the FINNAKI observational study." Ann Intensive Care **9**(1): 103.

Ionescu-Tirgoviste, C. and D. Bodoia (1969). "[The endocrine function of the kidney. 3. Renal medullin]." Med Interna (Bucur) **21**(10): 1163-1166.

Ishani, A., J. L. Xue, J. Himmelfarb, P. W. Eggers, P. L. Kimmel, B. A. Molitoris, et al. (2009). "Acute Kidney Injury Increases Risk of ESRD among Elderly." Journal of the American Society of Nephrology **20**(1): 223-228.

Iwai-Kanai, E., H. Yuan, C. Huang, M. R. Sayen, C. N. Perry-Garza, L. Kim, et al. (2008). "A method to measure cardiac autophagic flux in vivo." Autophagy **4**(3): 322-329.

Iwano, M., D. Plieth, T. M. Danoff, C. Xue, H. Okada and E. G. Neilson (2002). "Evidence that fibroblasts derive from epithelium during tissue fibrosis." Journal of Clinical Investigation **110**(3): 341-350.

Jamison, R. J. (1987). "The renal concentrating mechanism." Kidney Int Suppl **21**: S43-50.

Jang, H. R. and H. Rabb (2015). "Immune cells in experimental acute kidney injury." Nat Rev Nephrol **11**(2): 88-101.

Jezek, J., K. T. Chang, A. M. Joshi and R. Strich (2019). "Mitochondrial translocation of cyclin C stimulates intrinsic apoptosis through Bax recruitment." EMBO Rep **20**(9): e47425.

Jiang, M., K. Liu, J. Luo and Z. Dong (2010). "Autophagy is a renoprotective mechanism during in vitro hypoxia and in vivo ischemia-reperfusion injury." Am J Pathol **176**(3): 1181-1192.

Jiang, W., X. Wang, X. Geng, Y. Gu, M. Guo, X. Ding, et al. (2020). "Novel predictive biomarkers for acute injury superimposed on chronic kidney disease." Nefrologia.

Jiang, Y. H., B. N. Jahagirdar, R. L. Reinhardt, R. E. Schwartz, C. D. Keene, X. R. Ortiz-Gonzalez, et al. (2002). "Pluripotency of mesenchymal stem cells derived from adult marrow." Nature **418**(6893): 41-49.

Joannidis, M., W. Druml, L. G. Forni, A. B. J. Groeneveld, P. M. Honore, E. Hoste, et al. (2017). "Prevention of acute kidney injury and protection of renal function in the intensive care unit: update 2017 : Expert opinion of the Working Group on Prevention, AKI section, European Society of Intensive Care Medicine." Intensive Care Med **43**(6): 730-749.

Jongman, R. M., J. van Klarenbosch, G. Molema, J. G. Zijlstra, A. J. de Vries and M. van Meurs (2015). "Angiopoietin/Tie2 Dysbalance Is Associated with Acute Kidney Injury after Cardiac Surgery Assisted by Cardiopulmonary Bypass." PLoS One **10**(8): e0136205.

Jourde-Chiche, N., F. Fakhouri, L. Dou, J. Bellien, S. Burtey, M. Frimat, et al. (2019). "Endothelium structure and function in kidney health and disease." Nat Rev Nephrol **15**(2): 87-108.

Jung, Y. J., D. H. Kim, A. S. Lee, S. Lee, K. P. Kang, S. Y. Lee, et al. (2009). "Peritubular capillary preservation with COMP-angiopoietin-1 decreases ischemia-reperfusion-induced acute kidney injury." Am J Physiol Renal Physiol **297**(4): F952-960.

Kalamas, A. G. and C. U. Niemann (2013). "Patients with chronic kidney disease." Med Clin North Am **97**(6): 1109-1122.

Kanagasundaram, N. S. (2015). "Pathophysiology of ischaemic acute kidney injury." Ann Clin Biochem **52**(Pt 2): 193-205.

Kang, R., H. J. Zeh, M. T. Lotze and D. Tang (2011). "The Beclin 1 network regulates autophagy and apoptosis." Cell Death Differ **18**(4): 571-580.

Karch, J. and J. D. Molkentin (2012). "Is p53 the Long-Sought Molecular Trigger for Cyclophilin D-Regulated Mitochondrial Permeability Transition Pore Formation and Necrosis?" Circulation Research **111**(10): 1258-1260.

Kardideh, B., Z. Samimi, F. Norooznezhad, S. Kiani and K. Mansouri (2019). "Autophagy, cancer and angiogenesis: where is the link?" Cell Biosci **9**: 65.

Karlberg, L., B. J. Norlen, G. Ojteg and M. Wolgast (1983). "Impaired medullary circulation in postischemic acute renal failure." Acta Physiol Scand **118**(1): 11-17.

Katayama, S., S. Nunomiya, K. Koyama, M. Wada, T. Koinuma, Y. Goto, et al. (2017). "Markers of acute kidney injury in patients with sepsis: the role of soluble thrombomodulin." Crit Care **21**(1): 229.

Kaushal, G. P. and S. V. Shah (2016). "Autophagy in acute kidney injury." Kidney Int **89**(4): 779-791.

Kaye, K. W. and M. E. Goldberg (1982). "Applied anatomy of the kidney and ureter." Urol Clin North Am **9**(1): 3-13.

Kelly, K. J., N. R. Baird and A. L. Greene (2001). "Induction of stress response proteins and experimental renal ischemia/reperfusion." Kidney Int **59**(5): 1798-1802.

Kerr, J. F., A. H. Wyllie and A. R. Currie (1972). "Apoptosis: a basic biological phenomenon with wide-ranging implications in tissue kinetics." Br J Cancer **26**(4): 239-257.

Kida, Y. and J. S. Duffield (2011). "Pivotal role of pericytes in kidney fibrosis." Clin Exp Pharmacol Physiol **38**(7): 467-473.

Kim, J. S., L. He and J. J. Lemasters (2003). "Mitochondrial permeability transition: a common pathway to necrosis and apoptosis." Biochem Biophys Res Commun **304**(3): 463-470.

Kim, S. H., M. A. Yu, E. S. Ryu, Y. H. Jang and D. H. Kang (2012). "Indoxyl sulfate-induced epithelial-to-mesenchymal transition and apoptosis of renal tubular cells as novel mechanisms of progression of renal disease." Laboratory Investigation **92**(4): 488-498.

Kimura, T., Y. Takabatake, A. Takahashi, J. Y. Kaimori, I. Matsui, T. Namba, et al. (2011). "Autophagy protects the proximal tubule from degeneration and acute ischemic injury." J Am Soc Nephrol **22**(5): 902-913.

Kinsey, G. R., L. Li and M. D. Okusa (2008). "Inflammation in acute kidney injury." Nephron Experimental Nephrology **109**(4): E102-E107.

Kitamura, H., D. Nakano, Y. Sawanobori, T. Asaga, H. Yokoi, M. Yanagita, et al. (2018). "Guanylyl Cyclase A in Both Renal Proximal Tubular and Vascular Endothelial Cells Protects the Kidney against Acute Injury in Rodent Experimental Endotoxemia Models." Anesthesiology **129**(2): 296-310.

Klionsky, D. J., K. Abdelmohsen, A. Abe, M. J. Abedin, H. Abeliovich, A. Acevedo Arozena, et al. (2016). "Guidelines for the use and interpretation of assays for monitoring autophagy (3rd edition)." Autophagy **12**(1): 1-222.

Klionsky, D. J., Z. Elazar, P. O. Seglen and D. C. Rubinsztein (2008). "Does bafilomycin A(1) block the fusion of autophagosomes with lysosomes?" Autophagy **4**(7): 849-850.

Kose, M., S. Emet, T. S. Akpinar, M. Kocaaga, R. Cakmak, M. Akarsu, et al. (2015). "Serum Endocan Level and the Severity of Coronary Artery Disease: A Pilot Study." Angiology **66**(8): 727-731.

Koyner, J. L., M. R. Bennett, E. M. Worcester, Q. Ma, J. Raman, V. Jeevanandam, et al. (2008). "Urinary cystatin C as an early biomarker of acute kidney injury following adult cardiothoracic surgery." Kidney Int **74**(8): 1059-1069.

Kramann, R., D. P. Dirocco, O. H. Maarouf and B. D. Humphreys (2013). "Matrix Producing Cells in Chronic Kidney Disease: Origin, Regulation, and Activation." Curr Pathobiol Rep **1**(4).

Kramann, R., R. K. Schneider, D. P. DiRocco, F. Machado, S. Fleig, P. A. Bondzie, et al. (2015). "Perivascular Gli1+ progenitors are key contributors to injury-induced organ fibrosis." Cell Stem Cell **16**(1): 51-66.

Krawczeski, C. D., R. G. Vandevoorde, T. Kathman, M. R. Bennett, J. G. Woo, Y. Wang, et al. (2010). "Serum cystatin C is an early predictive biomarker of acute kidney injury after pediatric cardiopulmonary bypass." Clin J Am Soc Nephrol **5**(9): 1552-1557.

Krenning, G., P. Y. Dankers, J. W. Drouven, F. Waanders, C. F. Franssen, M. J. van Luyn, et al. (2009). "Endothelial progenitor cell dysfunction in patients with progressive chronic kidney disease." Am J Physiol Renal Physiol **296**(6): F1314-1322.

Kroemer, G. (2015). "Autophagy: a druggable process that is deregulated in aging and human disease." Journal of Clinical Investigation **125**(1): 1-4.

Kroemer, G. and B. Levine (2008). "Autophagic cell death: the story of a misnomer." Nat Rev Mol Cell Biol **9**(12): 1004-1010.

Kulkarni, O. P., I. Hartter, S. R. Mulay, J. Hagemann, M. N. Darisipudi, S. Kumar Vr, et al. (2014). "Toll-like receptor 4-induced IL-22 accelerates kidney regeneration." J Am Soc Nephrol **25**(5): 978-989.

Kumar, N. P., B. Velayutham, D. Nair and S. Babu (2017). "Angiopoietins as biomarkers of disease severity and bacterial burden in pulmonary tuberculosis." Int J Tuberc Lung Dis **21**(1): 93-99.

Kumar, S. (2018). "Cellular and molecular pathways of renal repair after acute kidney injury." Kidney Int **93**(1): 27-40.

Kurts, C., U. Panzer, H. J. Anders and A. J. Rees (2013). "The immune system and kidney disease: basic concepts and clinical implications." Nat Rev Immunol **13**(10): 738-753.

Kuypers, D. R., C. Metalidis, E. Lerut, S. H. van Vuuren, R. Broekhuizen, Y. Vanrenterghem, et al. (2012). "Urinary Connective Tissue Growth Factor (CTGFu) as a Marker and Early Predictor of Chronic Renal Allograft Injury." Transplantation **94**(10): 82-82.

Kwon, O., C. L. Phillips and B. A. Molitoris (2002). "Ischemia induces alterations in actin filaments in renal vascular smooth muscle cells." Am J Physiol Renal Physiol **282**(6): F1012-1019.

Kwong, J. M., C. Hoang, R. T. Dukes, R. W. Yee, B. D. Gray, K. Y. Pak, et al. (2014). "Bis(zinc-dipicolylamine), Zn-DPA, a new marker for apoptosis." Invest Ophthalmol Vis Sci **55**(8): 4913-4921.

Laffer, C. L., F. Elijovich, M. Sahinoz, A. Pitzer and A. Kirabo (2020). "New Insights Into the Renin-Angiotensin System in Chronic Kidney Disease." Circ Res **127**(5): 607-609.

Lagos-Arevalo, P., A. Palijan, L. Vertullo, P. Devarajan, M. R. Bennett, V. Sabbisetti, et al. (2015). "Cystatin C in acute kidney injury diagnosis: early biomarker or alternative to serum creatinine?" Pediatr Nephrol **30**(4): 665-676.

Lameire, N., W. Van Biesen and R. Vanholder (2005). "Acute renal failure." The Lancet **365**(9457): 417-430.

Laplante, P., I. Sirois, M. A. Raymond, V. Kokta, A. Beliveau, A. Prat, et al. (2010). "Caspase-3-mediated secretion of connective tissue growth factor by apoptotic endothelial cells promotes fibrosis." Cell Death Differ **17**(2): 291-303.

Lau, A., S. Wang, J. Jiang, A. Haig, A. Pavlosky, A. Linkermann, et al. (2013). "RIPK3-mediated necroptosis promotes donor kidney inflammatory injury and reduces allograft survival." Am J Transplant **13**(11): 2805-2818.

LeBleu, V. S. and R. Kalluri (2020). "Exosomes as a Multicomponent Biomarker Platform in Cancer." Trends in Cancer **6**(9): 767-774.

LeBleu, V. S., G. Taduri, J. O'Connell, Y. Teng, V. G. Cooke, C. Woda, et al. (2013). "Origin and function of myofibroblasts in kidney fibrosis." Nat Med **19**(8): 1047-1053.

Lech, M., R. Grobmayr, M. Ryu, G. Lorenz, I. Hartter, S. R. Mulay, et al. (2014). "Macrophage Phenotype Controls Long-Term AKI Outcomes-Kidney Regeneration versus Atrophy." Journal of the American Society of Nephrology **25**(2): 292-304.

Lee, K. W., G. Y. Lip and A. D. Blann (2004). "Plasma angiopoietin-1, angiopoietin-2, angiopoietin receptor tie-2, and vascular endothelial growth factor levels in acute coronary syndromes." Circulation **110**(16): 2355-2360.

Leite de Oliveira, R., S. Deschoemaeker, A. T. Henze, K. Debackere, V. Finisguerra, Y. Takeda, et al. (2012). "Gene-targeting of Phd2 improves tumor response to chemotherapy and prevents side-toxicity." Cancer Cell **22**(2): 263-277.

Leonard, E. C., J. L. Friedrich and D. P. Basile (2008). "VEGF-121 preserves renal microvessel structure and ameliorates secondary renal disease following acute kidney injury." Am J Physiol Renal Physiol **295**(6): F1648-1657.

Leung, K. C., M. Tonelli and M. T. James (2013). "Chronic kidney disease following acute kidney injury-risk and outcomes." Nat Rev Nephrol **9**(2): 77-85.

Levine, B. and G. Kroemer (2008). "Autophagy in the pathogenesis of disease." Cell **132**(1): 27-42.

Levine, B., M. Packer and P. Codogno (2015). "Development of autophagy inducers in clinical medicine." The Journal of clinical investigation **125**(1): 14-24.

Li, J., S. G. Kim and J. Blenis (2014). "Rapamycin: one drug, many effects." Cell Metab **19**(3): 373-379.

Li, J., X. Qu and J. F. Bertram (2009). "Endothelial-myofibroblast transition contributes to the early development of diabetic renal interstitial fibrosis in streptozotocin-induced diabetic mice." Am J Pathol **175**(4): 1380-1388.

Li, L., R. Black, Z. Ma, Q. Yang, A. Wang and F. Lin (2012). "Use of mouse hematopoietic stem and progenitor cells to treat acute kidney injury." Am J Physiol Renal Physiol **302**(1): F9-F19.

Li, L., J. Tan, Y. Miao, P. Lei and Q. Zhang (2015). "ROS and Autophagy: Interactions and Molecular Regulatory Mechanisms." Cell Mol Neurobiol **35**(5): 615-621.

Li, S., L. Yu, A. He and Q. Liu (2019). "Klotho Inhibits Unilateral Ureteral Obstruction-Induced Endothelial-to-Mesenchymal Transition via TGF-beta1/Smad2/Snail1 Signaling in Mice." Front Pharmacol **10**: 348.

Lim, H. S., G. Y. Lip and A. D. Blann (2005). "Angiopoietin-1 and angiopoietin-2 in diabetes mellitus: relationship to VEGF, glycaemic control, endothelial damage/dysfunction and atherosclerosis." Atherosclerosis **180**(1): 113-118.

Lin, F. M., K. Cordes, L. H. Li, L. Hood, W. G. Couser, S. J. Shankland, et al. (2003). "Hematopoietic stem cells contribute to the regeneration of renal tubules after renal ischemia-reperfusion injury in mice." Journal of the American Society of Nephrology **14**(5): 1188-1199.

Lin, F. M., A. Moran and P. Igarashi (2005). "Intrarenal cells, not bone marrow-derived cells, are the major source for regeneration in postischemic kidney." Journal of Clinical Investigation **115**(7): 1756-1764.

Lin, S. L., F. C. Chang, C. Schrimpf, Y. T. Chen, C. F. Wu, V. C. Wu, et al. (2011). "Targeting endothelium-pericyte cross talk by inhibiting VEGF receptor signaling attenuates kidney microvascular rarefaction and fibrosis." Am J Pathol **178**(2): 911-923.

Lin, S. L., T. Kisseleva, D. A. Brenner and J. S. Duffield (2008). "Pericytes and perivascular fibroblasts are the primary source of collagen-producing cells in obstructive fibrosis of the kidney." Am J Pathol **173**(6): 1617-1627.

Linkermann, A., G. Chen, G. Dong, U. Kunzendorf, S. Krautwald and Z. Dong (2014). "Regulated cell death in AKI." J Am Soc Nephrol **25**(12): 2689-2701.

Linkermann, A., F. De Zen, J. Weinberg, U. Kunzendorf and S. Krautwald (2012). "Programmed necrosis in acute kidney injury." Nephrol Dial Transplant **27**(9): 3412-3419.

Linkermann, A., M. J. Hackl, U. Kunzendorf, H. Walczak, S. Krautwald and A. M. Jevnikar (2013). "Necroptosis in immunity and ischemia-reperfusion injury." Am J Transplant **13**(11): 2797-2804.

Liu, L., D. Feng, G. Chen, M. Chen, Q. Zheng, P. Song, et al. (2012). "Mitochondrial outer-membrane protein FUNDC1 mediates hypoxia-induced mitophagy in mammalian cells." Nat Cell Biol **14**(2): 177-185.

Liu, Y. P., T. Liu, T. T. Lei, D. D. Zhang, S. Y. Du, L. Girani, et al. (2019). "RIP1/RIP3-regulated necroptosis as a target for multifaceted disease therapy (Review)." International Journal of Molecular Medicine **44**(3): 771-786.

Lo, L. J., A. S. Go, G. M. Chertow, C. E. McCulloch, D. Fan, J. D. Ordonez, et al. (2009). "Dialysis-requiring acute renal failure increases the risk of progressive chronic kidney disease." Kidney Int **76**(8): 893-899.

Lobov, I. B., P. C. Brooks and R. A. Lang (2002). "Angiopoietin-2 displays VEGF-dependent modulation of capillary structure and endothelial cell survival in vivo." Proc Natl Acad Sci U S A **99**(17): 11205-11210.

Lonskaya, I., M. L. Hebron, N. M. Desforges, J. B. Schachter and C. E. Moussa (2014). "Nilotinib-induced autophagic changes increase endogenous parkin level and ubiquitination, leading to amyloid clearance." J Mol Med (Berl) **92**(4): 373-386.

Loutradis, C., A. Price, C. J. Ferro and P. Sarafidis (2021). "Renin-angiotensin system blockade in patients with chronic kidney disease: benefits, problems in everyday clinical use, and open questions for advanced renal dysfunction." J Hum Hypertens.

Luo, Q., Z. Cai, J. Tu, Y. Ling, D. Wang and Y. Cai (2019). "Total flavonoids from Smilax glabra Roxb blocks epithelial-mesenchymal transition and inhibits renal interstitial fibrosis by targeting miR-21/PTEN signaling." J Cell Biochem **120**(3): 3861-3873.

Luthra, A. and A. Tyagi (2019). "[TIMP-2]*[IGFBP7] for Predicting Early AKI." Anaesth Crit Care Pain Med **38**(6): 677.

Ma, Y., Q. Li, J. Wang, Z. Xu, C. Song, R. Zhuang, et al. (2010). "Cystatin C, a novel urinary biomarker for sensitive detection of acute kidney injury during haemorrhagic fever with renal syndrome." Biomarkers **15**(5): 410-417.

Mack, M. and M. Yanagita (2015). "Origin of myofibroblasts and cellular events triggering fibrosis." Kidney Int **87**(2): 297-307.

MacPherson, D. J., C. L. Mills, M. J. Ondrechen and J. A. Hardy (2019). "Tri-arginine exosite patch of caspase-6 recruits substrates for hydrolysis." J Biol Chem **294**(1): 71-88.

Madar, I., H. Ravert, B. Nelkin, M. Abro, M. Pomper, R. Dannals, et al. (2007). "Characterization of membrane potential-dependent uptake of the novel PET tracer 18F-fluorobenzyl triphenylphosphonium cation." Eur J Nucl Med Mol Imaging **34**(12): 2057-2065.

Maekawa, H. and R. Inagi (2019). "Pathophysiological Role of Organelle Stress/Crosstalk in AKI-to-CKD Transition." Semin Nephrol **39**(6): 581-588.

Malek, M. and M. Nematbakhsh (2015). "Renal ischemia/reperfusion injury; from pathophysiology to treatment." J Renal Inj Prev **4**(2): 20-27.

Mari, M., J. Griffith, E. Rieter, L. Krishnappa, D. J. Klionsky and F. Reggiori (2010). "An Atg9-containing compartment that functions in the early steps of autophagosome biogenesis." Journal of Cell Biology **190**(6): 1005-1022.

Marschner, J. A., H. Schafer, A. Holderied and H. J. Anders (2016). "Optimizing Mouse Surgery with Online Rectal Temperature Monitoring and Preoperative Heat Supply. Effects on Post-Ischemic Acute Kidney Injury." PLoS One **11**(2): e0149489.

Martin, F. A., R. P. Murphy and P. M. Cummins (2013). "Thrombomodulin and the vascular endothelium: insights into functional, regulatory, and therapeutic aspects." American Journal of Physiology-Heart and Circulatory Physiology **304**(12): H1585-H1597.

Matthys, E., M. K. Patton, R. W. Osgood, M. A. Venkatachalam and J. H. Stein (1983). "Alterations in vascular function and morphology in acute ischemic renal failure." Kidney Int **23**(5): 717-724.

Mayer, G. (2011). "Capillary rarefaction, hypoxia, VEGF and angiogenesis in chronic renal disease." Nephrology Dialysis Transplantation **26**(4): 1132-1137.

McEver, R. P. (2015). "Selectins: initiators of leucocyte adhesion and signalling at the vascular wall." Cardiovascular Research **107**(3): 331-339.

Meersch, M., C. Schmidt, H. Van Aken, S. Martens, J. Rossaint, K. Singbartl, et al. (2014). "Urinary TIMP-2 and IGFBP7 as early biomarkers of acute kidney injury and renal recovery following cardiac surgery." PLoS One **9**(3): e93460.

Meng, X. M. (2019). "Inflammatory Mediators and Renal Fibrosis." Adv Exp Med Biol **1165**: 381-406.

Menshikh, A., L. Scarfe, R. Delgado, C. Finney, Y. Zhu, H. Yang, et al. (2019). "Capillary rarefaction is more closely associated with CKD progression after cisplatin, rhabdomyolysis, and ischemia-reperfusion-induced AKI than renal fibrosis." Am J Physiol Renal Physiol **317**(5): F1383-F1397.

Mizushima, N. and M. Komatsu (2011). "Autophagy: renovation of cells and tissues." Cell **147**(4): 728-741.

Mizushima, N., A. Kuma, Y. Kobayashi, A. Yamamoto, M. Matsubae, T. Takao, et al. (2003). "Mouse Apg16L, a novel WD-repeat protein, targets to the autophagic isolation membrane with the Apg12-Apg5 conjugate." J Cell Sci **116**(Pt 9): 1679-1688.

Mizushima, N., T. Yoshimori and B. Levine (2010). "Methods in mammalian autophagy research." Cell **140**(3): 313-326.

Mohsenin, V. (2017). "Practical approach to detection and management of acute kidney injury in critically ill patient." J Intensive Care **5**: 57.

Molnar, M. Z., P. Kumpers, J. T. Kielstein, M. Schiffer, M. E. Czira, A. Ujszaszi, et al. (2014). "Circulating Angiopoietin-2 levels predict mortality in kidney transplant recipients: a 4-year prospective case-cohort study." Transpl Int **27**(6): 541-552.

Montecalvo, A., A. T. Larregina, W. J. Shufesky, D. B. Stolz, M. L. G. Sullivan, J. M. Karlsson, et al. (2012). "Mechanism of transfer of functional microRNAs between mouse dendritic cells via exosomes." Blood **119**(3): 756-766.

Moore-Morris, T., N. Guimaraes-Camboa, I. Banerjee, A. C. Zambon, T. Kisseleva, A. Velayoudon, et al. (2014). "Resident fibroblast lineages mediate pressure overload-induced cardiac fibrosis." J Clin Invest **124**(7): 2921-2934.

Morselli, E., M. C. Maiuri, M. Markaki, E. Megalou, A. Pasparaki, K. Palikaras, et al. (2010). "Caloric restriction and resveratrol promote longevity through the Sirtuin-1-dependent induction of autophagy." Cell Death Dis **1**: e10.

Moulis, M. and C. Vindis (2017). "Methods for Measuring Autophagy in Mice." Cells **6**(2).

Muller, T., C. Dewitz, J. Schmitz, A. S. Schroder, J. H. Brasen, B. R. Stockwell, et al. (2017). "Necroptosis and ferroptosis are alternative cell death pathways that operate in acute kidney failure." Cell Mol Life Sci **74**(19): 3631-3645.

Muth, B. L., B. C. Astor, J. Turk, M. Mohamed, S. Parajuli, D. B. Kaufman, et al. (2016). "Outpatient Management of Delayed Graft Function Is Associated With Reduced Length of Stay Without an Increase in Adverse Events." American Journal of Transplantation **16**(5): 1604-1611.

Muthusamy, A., C. M. Lin, H. Lindner, S. Shanmugam, S. Abcouwer, D. Antonetti, et al. (2013). "Early Ischemia-reperfusion Injury Induces Retinal Vascular Permeability in a VEGF Receptor 2 Dependent Manner Followed by Occludin Phosphorylation and Ubiquitination." Investigative Ophthalmology & Visual Science **54**(15).

Nakagawa, T., W. Sato, T. Kosugi and R. J. Johnson (2013). "Uncoupling of VEGF with Endothelial NO as a Potential Mechanism for Abnormal Angiogenesis in the Diabetic Nephropathy." Journal of Diabetes Research **2013**.

Nash, K., A. Hafeez and S. Hou (2002). "Hospital-acquired renal insufficiency." Am J Kidney Dis **39**(5): 930-936.

Neuzillet, C., A. Tijeras-Raballand, R. Cohen, J. Cros, S. Faivre, E. Raymond, et al. (2015). "Targeting the TGFbeta pathway for cancer therapy." Pharmacol Ther **147**: 22-31.

Niu, G. and X. Chen (2010). "Apoptosis imaging: beyond annexin V." J Nucl Med **51**(11): 1659-1662.

Nony, P. A. and R. G. Schnellmann (2003). "Mechanisms of renal cell repair and regeneration after acute renal failure." J Pharmacol Exp Ther **304**(3): 905-912.

Nydam, T. L., R. Plenter, S. Jain, S. Lucia and A. Jani (2018). "Caspase Inhibition During Cold Storage Improves Graft Function and Histology in a Murine Kidney Transplant Model." Transplantation **102**(9): 1487-1495.

Obermuller, N., H. Geiger, C. Weipert and A. Urbschat (2014). "Current developments in early diagnosis of acute kidney injury." Int Urol Nephrol **46**(1): 1-7.

Ohashi, R., H. Kitamura and N. Yamanaka (2000). "Peritubular capillary injury during the progression of experimental glomerulonephritis in rats." J Am Soc Nephrol **11**(1): 47-56.

Ohashi, R., A. Shimizu, Y. Masuda, H. Kitamura, M. Ishizaki, Y. Sugisaki, et al. (2002). "Peritubular capillary regression during the progression of experimental obstructive nephropathy." J Am Soc Nephrol **13**(7): 1795-1805.

Ohnishi, Y., H. Yasudo, Y. Suzuki, T. Furuta, C. Matsuguma, Y. Azuma, et al. (2019). "Circulating endothelial glycocalyx components as a predictive marker of coronary artery lesions in Kawasaki disease." Int J Cardiol **292**: 236-240.

Okugawa, Y., C. Miki, Y. Toiyama, Y. Koike, T. Yokoe, S. Saigusa, et al. (2010). "Soluble VCAM-1 and its relation to disease progression in colorectal carcinoma." Experimental and Therapeutic Medicine **1**(3): 463-469.

Ozkok, A. and A. Yildiz (2018). "Endothelial Progenitor Cells and Kidney Diseases." Kidney Blood Press Res **43**(3): 701-718.

Ozretic, P., I. Alvir, B. Sarcevic, Z. Vujaskovic, Z. Rendic-Miocevic, A. Roguljic, et al. (2018). "Apoptosis regulator Bcl-2 is an independent prognostic marker for worse overall survival in triple-negative breast cancer patients." Int J Biol Markers **33**(1): 109-115.

Padberg, J. S., A. Wiesinger, G. S. di Marco, S. Reuter, A. Grabner, D. Kentrup, et al. (2014). "Damage of the endothelial glycocalyx in chronic kidney disease." Atherosclerosis **234**(2): 335-343.

Park, M. Y., S. J. Choi, J. K. Kim, S. D. Hwang and Y. W. Lee (2013). "Urinary cystatin C levels as a diagnostic and prognostic biomarker in patients with acute kidney injury." Nephrology (Carlton) **18**(4): 256-262.

Parodis, I., S. Gokaraju, A. Zickert, K. Vanarsa, T. Zhang, D. Habazi, et al. (2020). "ALCAM and VCAM-1 as urine biomarkers of activity and long-term renal outcome in systemic lupus erythematosus." Rheumatology **59**(9): 2237-2249.

Patschan, D., K. Schwarze, E. Henze, S. Patschan and G. A. Muller (2016). "Endothelial autophagy and Endothelial-to-Mesenchymal Transition (EndoMT) in eEPC treatment of ischemic AKI." J Nephrol **29**(5): 637-644.

Pavlosky, A., A. Lau, Y. Su, D. Lian, X. Huang, Z. Yin, et al. (2014). "RIPK3-mediated necroptosis regulates cardiac allograft rejection." Am J Transplant **14**(8): 1778-1790.

Pedersen, J. I., J. G. Ghazarian, N. R. Orme-Johnson and H. F. DeLuca (1976). "Isolation of chick renal mitochondrial ferredoxin active in the 25-hydroxyvitamin D3-1alpha-hydroxylase system." J Biol Chem **251**(13): 3933-3941.

Perry, H. M., L. Huang, H. Ye, C. Liu, S. J. Sung, K. R. Lynch, et al. (2016). "Endothelial Sphingosine 1Phosphate Receptor1 Mediates Protection and Recovery from Acute Kidney Injury." J Am Soc Nephrol **27**(11): 3383-3393.

Phng, L. K., M. Potente, J. D. Leslie, J. Babbage, D. Nyqvist, I. Lobov, et al. (2009). "Nrarp coordinates endothelial Notch and Wnt signaling to control vessel density in angiogenesis." Dev Cell **16**(1): 70-82.

Piera-Velazquez, S., Z. Li and S. A. Jimenez (2011). "Role of endothelial-mesenchymal transition (EndoMT) in the pathogenesis of fibrotic disorders." Am J Pathol **179**(3): 1074-1080.

Pirgakis, K. M., K. Makris, I. Dalainas, A. M. Lazaris, C. K. Maltezos and C. D. Liapis (2014). "Urinary cystatin C as an early biomarker of acute kidney injury after open and endovascular abdominal aortic aneurysm repair." Ann Vasc Surg **28**(7): 1649-1658.

Polichnowski, A. J. (2018). "Microvascular rarefaction and hypertension in the impaired recovery and progression of kidney disease following AKI in preexisting CKD states." Am J Physiol Renal Physiol **315**(6): F1513-F1518.

Polichnowski, A. J., K. A. Griffin, H. Licea-Vargas, R. Lan, M. M. Picken, J. Long, et al. (2020). "Pathophysiology of unilateral ischemia-reperfusion injury: importance of renal counterbalance and implications for the AKI-CKD transition." Am J Physiol Renal Physiol **318**(5): F1086-F1099.

Pons, M., C. M. Reichardt, D. Hennig, A. Nathan, N. Kiweler, C. Stocking, et al. (2018). "Loss of Wilms tumor 1 protein is a marker for apoptosis in response to replicative stress in leukemic cells." Arch Toxicol **92**(6): 2119-2135.

Popolo, A., S. Adesso, A. Pinto, G. Autore and S. Marzocco (2014). "L-Arginine and its metabolites in kidney and cardiovascular disease." Amino Acids **46**(10): 2271-2286.

Powell, J. T., D. S. Tsapepas, S. T. Martin, M. A. Hardy and L. E. Ratner (2013). "Managing renal transplant ischemia reperfusion injury: novel therapies in the pipeline." Clin Transplant **27**(4): 484-491.

Prakoura, N., J. Hadchouel and C. Chatziantoniou (2019). "Novel Targets for Therapy of Renal Fibrosis." J Histochem Cytochem **67**(9): 701-715.

Preuss, H. G. (1993). "Basics of renal anatomy and physiology." Clin Lab Med **13**(1): 1-11.

Prugger, C., G. Luc, B. Haas, P. E. Morange, J. Ferrieres, P. Amouyel, et al. (2013). "Multiple biomarkers for the prediction of ischemic stroke: the PRIME study." Arterioscler Thromb Vasc Biol **33**(3): 659-666.

Quaglia, M., S. Dellepiane, G. Guglielmetti, G. Merlotti, G. Castellano and V. Cantaluppi (2020). "Extracellular Vesicles as Mediators of Cellular Crosstalk Between Immune System and Kidney Graft." Frontiers in Immunology **11**.

Rabadi, M. M., T. Ghaly, M. S. Goligorksy and B. B. Ratliff (2012). "HMGB1 in renal ischemic injury." Am J Physiol Renal Physiol **303**(6): F873-885.

Rabb, H., M. D. Griffin, D. B. McKay, S. Swaminathan, P. Pickkers, M. H. Rosner, et al. (2016). "Inflammation in AKI: Current Understanding, Key Questions, and Knowledge Gaps." J Am Soc Nephrol **27**(2): 371-379.

Rahal, A., A. Kumar, V. Singh, B. Yadav, R. Tiwari, S. Chakraborty, et al. (2014). "Oxidative stress, prooxidants, and antioxidants: the interplay." Biomed Res Int **2014**: 761264.

Ramesh, G. and P. Ranganathan (2014). "Mouse models and methods for studying human disease, acute kidney injury (AKI)." Methods Mol Biol **1194**: 421-436.

Ramesh, G. and W. B. Reeves (2004). "Salicylate reduces cisplatin nephrotoxicity by inhibition of tumor necrosis factor-alpha." Kidney Int **65**(2): 490-499.

Randow, F. and R. J. Youle (2014). "Self and nonself: how autophagy targets mitochondria and bacteria." Cell Host Microbe **15**(4): 403-411.

Reilly, M., R. M. Miller, M. H. Thomson, V. Patris, P. Ryle, L. McLoughlin, et al. (2013). "Randomized, double-blind, placebo-controlled, dose-escalating phase I, healthy subjects study of intravenous OPN-305, a humanized anti-TLR2 antibody." Clin Pharmacol Ther **94**(5): 593-600.

Reinders, M. E., T. J. Rabelink and D. M. Briscoe (2006). "Angiogenesis and endothelial cell repair in renal disease and allograft rejection." J Am Soc Nephrol **17**(4): 932-942.

Rewa, O. and S. M. Bagshaw (2014). "Acute kidney injury-epidemiology, outcomes and economics." Nat Rev Nephrol **10**(4): 193-207.

Rhim, T., D. Y. Lee and M. Lee (2013). "Hypoxia as a target for tissue specific gene therapy." Journal of Controlled Release **172**(2): 484-494.

Ribatti, D. and E. Crivellato (2012). ""Sprouting angiogenesis", a reappraisal." Dev Biol **372**(2): 157-165.

Rieckmann, P., J. M. Tuscano and J. H. Kehrl (1997). "Tumor necrosis factor-alpha (TNF-alpha) and interleukin-6 (IL-6) in B-lymphocyte function." Methods **11**(1): 128-132.

Rongvaux, A., R. Jackson, C. C. Harman, T. Li, A. P. West, M. R. de Zoete, et al. (2014). "Apoptotic caspases prevent the induction of type I interferons by mitochondrial DNA." Cell **159**(7): 1563-1577.

Roy, J. P. and P. Devarajan (2019). "Acute Kidney Injury: Diagnosis and Management." Indian J Pediatr.

Saat, T. C., D. Susa, H. P. Roest, N. F. Kok, S. van den Engel, J. N. Ijzermans, et al. (2014). "A comparison of inflammatory, cytoprotective and injury gene expression profiles in kidneys from brain death and cardiac death donors." Transplantation **98**(1): 15-21.

Sadler, J. E. (1997). "Thrombomodulin structure and function." Thromb Haemost **78**(1): 392-395.

Saikumar, P. and M. A. Venkatachalam (2003). "Role of apoptosis in hypoxic/ischemic damage in the kidney." Semin Nephrol **23**(6): 511-521.

Saito, T., O. Saito, T. Kawano, H. Tamemoto, E. Kusano, M. Kawakami, et al. (2007). "Elevation of serum adiponectin and CD146 levels in diabetic nephropathy." Diabetes Res Clin Pract **78**(1): 85-92.

Saleem, M. A. (2018). "What is the Role of Soluble Urokinase-Type Plasminogen Activator in Renal Disease?" Nephron **139**(4): 334-341.

Sampaio, F. J. B. and A. H. M. Aragao (1990). "Anatomical Relationship between the Intrarenal Arteries and the Kidney Collecting System." Journal of Urology **143**(4): 679-681.

Sancho-Martinez, S. M., J. M. Lopez-Novoa and F. J. Lopez-Hernandez (2015). "Pathophysiological role of different tubular epithelial cell death modes in acute kidney injury." Clin Kidney J **8**(5): 548-559.

Sanidas, E., D. Papadopoulos, M. Chatzis, M. Velliou and J. Barbetseas (2021). "Renin Angiotensin Aldosterone System Inhibitors in Chronic Kidney Disease: A Difficult Equation." Am J Cardiovasc Drugs.

Sanna-Cherchi, S. (2008). "Quantifying collagen in mouse kidneys." Kidney Int **73**(9): 987-989.

Sarkar, S. (2013). "Chemical screening platforms for autophagy drug discovery to identify therapeutic candidates for Huntington's disease and other neurodegenerative disorders." Drug Discov Today Technol **10**(1): e137-144.

Saydam, O., E. Turkmen, O. Portakal, M. Arici, R. Dogan, M. Demircin, et al. (2018). "Emerging biomarker for predicting acute kidney injury after cardiac surgery: cystatin C." Turk J Med Sci **48**(6): 1096-1103.

Schatteman, G. C., M. Dunnwald and C. Jiao (2007). "Biology of bone marrow-derived endothelial cell precursors." Am J Physiol Heart Circ Physiol **292**(1): H1-18.

Schaub, J. A. and C. R. Parikh (2016). "Biomarkers of acute kidney injury and associations with short- and long-term outcomes." F1000Res **5**.

Schellinger, I. N., N. Cordasic, J. Panesar, B. Buchholz, J. Jacobi, A. Hartner, et al. (2017). "Hypoxia inducible factor stabilization improves defective ischemia-induced angiogenesis in a rodent model of chronic kidney disease." Kidney Int **91**(3): 616-627.

Scherz-Shouval, R. and Z. Elazar (2011). "Regulation of autophagy by ROS: physiology and pathology." Trends Biochem Sci **36**(1): 30-38.

Scholz, A., K. H. Plate and Y. Reiss (2015). "Angiopoietin-2: a multifaceted cytokine that functions in both angiogenesis and inflammation." Annals Reports, Vol 1347 **1347**: 45-51.

Schrimpf, C., O. E. Teebken, M. Wilhelmi and J. S. Duffield (2014). "The role of pericyte detachment in vascular rarefaction." J Vasc Res **51**(4): 247-258.

Schrimpf, C., C. Xin, G. Campanholle, S. E. Gill, W. Stallcup, S. L. Lin, et al. (2012). "Pericyte TIMP3 and ADAMTS1 modulate vascular stability after kidney injury." J Am Soc Nephrol **23**(5): 868-883.

Schwartz, J. D., E. K. Rowinsky, H. Youssoufian, B. Pytowski and Y. Wu (2010). "Vascular endothelial growth factor receptor-1 in human cancer: concise review and rationale for development of IMC-18F1 (Human antibody targeting vascular endothelial growth factor receptor-1)." Cancer **116**(4 Suppl): 1027-1032.

Selby, N. M. and M. W. Taal (2019). "Long-term outcomes after AKI-a major unmet clinical need." Kidney Int **95**(1): 21-23.

Seo, J. B., Y. K. Choi, H. I. Woo, Y. A. Jung, S. Lee, S. Lee, et al. (2019). "Gemigliptin Attenuates Renal Fibrosis Through Down-Regulation of the NLRP3 Inflammasome." Diabetes Metab J **43**(6): 830-839.

Sharain, K., D. Hoppensteadt, V. Bansal, A. Singh and J. Fareed (2013). "Progressive increase of inflammatory biomarkers in chronic kidney disease and end-stage renal disease." Clin Appl Thromb Hemost **19**(3): 303-308.

Sharfuddin, A. A. and B. A. Molitoris (2011). "Pathophysiology of ischemic acute kidney injury." Nat Rev Nephrol **7**(4): 189-200.

Shigeoka, A. A., T. D. Holscher, A. J. King, F. W. Hallt, W. B. Kiosses, P. S. Tobias, et al. (2007). "TLR2 is constitutively expressed within the kidney and participates in ischemic renal injury through both MyD88-dependent and -independent pathways." Journal of Immunology **178**(10): 6252-6258.

Shin, Y. J., S. H. Han, D. S. Kim, G. H. Lee, W. H. Yoo, Y. M. Kang, et al. (2010). "Autophagy induction and CHOP under-expression promotes survival of fibroblasts from rheumatoid arthritis patients under endoplasmic reticulum stress." Arthritis Research & Therapy **12**(1).

Siani, A. and N. Tirelli (2014). "Myofibroblast differentiation: main features, biomedical relevance, and the role of reactive oxygen species." Antioxid Redox Signal **21**(5): 768-785.

Singbartl, K. and J. A. Kellum (2012). "AKI in the ICU: definition, epidemiology, risk stratification, and outcomes." Kidney Int **81**(9): 819-825.

Singhania, N., S. Bansal, S. Mohandas, D. P. Nimmatoori, A. A. Ejaz and G. Singhania (2020). "Role of renin-angiotensin-aldosterone system inhibitors in heart failure and chronic kidney disease." Drugs Context **9**.

Sirois, I., M. A. Raymond, N. Brassard, J. F. Cailhier, M. Fedjaev, K. Hamelin, et al. (2011). "Caspase-3-dependent export of TCTP: a novel pathway for antiapoptotic intercellular communication." Cell Death Differ **18**(3): 549-562.

Skouta, R., S. J. Dixon, J. Wang, D. E. Dunn, M. Orman, K. Shimada, et al. (2014). "Ferrostatins inhibit oxidative lipid damage and cell death in diverse disease models." J Am Chem Soc **136**(12): 4551-4556.

Skrypnyk, N. I., R. C. Harris and M. P. de Caestecker (2013). "Ischemia-reperfusion model of acute kidney injury and post injury fibrosis in mice." J Vis Exp(78).

Skrypnyk, N. I., R. C. Harris and M. P. de Caestecker (2013). "Ischemia-reperfusion Model of Acute Kidney Injury and Post Injury Fibrosis in Mice." Jove-Journal of Visualized Experiments(78).

Slee, E. A., C. Adrain and S. J. Martin (2001). "Executioner caspase-3, -6, and -7 perform distinct, non-redundant roles during the demolition phase of apoptosis." J Biol Chem **276**(10): 7320-7326.

Srisawat, N., R. Murugan and J. A. Kellum (2014). "Repair or progression after AKI: a role for biomarkers?" Nephron Clin Pract **127**(1-4): 185-189.

Stasi, A., A. Intini, C. Divella, R. Franzin, E. Montemurno, G. Grandaliano, et al. (2017). "Emerging role of Lipopolysaccharide binding protein in sepsis-induced acute kidney injury." Nephrol Dial Transplant **32**(1): 24-31.

Strutz, F. and G. A. Muller (2006). "Renal fibrosis and the origin of the renal fibroblast." Nephrology Dialysis Transplantation **21**(12): 3368-3370.

Strutz, F. and M. Zeisberg (2006). "Renal fibroblasts and myofibroblasts in chronic kidney disease." Journal of the American Society of Nephrology **17**(11): 2992-2998.

Sturmlechner, I., M. Durik, C. J. Sieben, D. J. Baker and J. M. van Deursen (2017). "Cellular senescence in renal ageing and disease." Nat Rev Nephrol **13**(2): 77-89.

Sun, C. Y., H. H. Hsu and M. S. Wu (2013). "p-Cresol sulfate and indoxyl sulfate induce similar cellular inflammatory gene expressions in cultured proximal renal tubular cells." Nephrol Dial Transplant **28**(1): 70-78.

Sung, B., Y. Su, J. Jiang, P. McLeod, W. Liu, A. Haig, et al. (2019). "Loss of receptor interacting protein kinases 3 and caspase-8 augments intrinsic apoptosis in tubular epithelial cell and promote kidney ischaemia-reperfusion injury." Nephrology (Carlton) **24**(6): 661-669.

Sutton, T. A., H. E. Mang, S. B. Campos, R. M. Sandoval, M. C. Yoder and B. A. Molitoris (2003). "Injury of the renal microvascular endothelium alters barrier function after ischemia." Am J Physiol Renal Physiol **285**(2): F191-198.

Tait, S. W. and D. R. Green (2010). "Mitochondria and cell death: outer membrane permeabilization and beyond." Nat Rev Mol Cell Biol **11**(9): 621-632.

Tan, H. L., J. Q. Yap and Q. Qian (2016). "Acute Kidney Injury: Tubular Markers and Risk for Chronic Kidney Disease and End-Stage Kidney Failure." Blood Purif **41**(1-3): 144-150.

Tanaka, S., T. Tanaka and M. Nangaku (2014). "Hypoxia as a key player in the AKI-to-CKD transition." Am J Physiol Renal Physiol **307**(11): F1187-1195.

Tanaka, S., T. Tanaka and M. Nangaku (2015). "Hypoxia and Dysregulated Angiogenesis in Kidney Disease." Kidney Dis (Basel) **1**(1): 80-89.

Tanaka, T. and M. Nangaku (2010). "The role of hypoxia, increased oxygen consumption, and hypoxia-inducible factor-1 alpha in progression of chronic kidney disease." Current Opinion in Nephrology and Hypertension **19**(1): 43-50.

Tanaka, T. and M. Nangaku (2013). "Angiogenesis and hypoxia in the kidney." Nat Rev Nephrol **9**(4): 211-222.

Tannous, P., H. X. Zhu, A. Nemchenko, J. M. Berry, J. L. Johnstone, J. M. Shelton, et al. (2008). "Intracellular Protein Aggregation Is a Proximal Trigger of Cardiomyocyte Autophagy." Circulation Research **103**(5): E53-E53.

Telen, M. J. (2014). "Cellular adhesion and the endothelium: E-selectin, L-selectin, and pan-selectin inhibitors." Hematol Oncol Clin North Am **28**(2): 341-354.

Teng, X., A. Degterev, P. Jagtap, X. Xing, S. Choi, R. Denu, et al. (2005). "Structure-activity relationship study of novel necroptosis inhibitors." Bioorg Med Chem Lett **15**(22): 5039-5044.

Thamm, K., F. Njau, P. Van Slyke, D. J. Dumont, J.-K. Park, H. Haller, et al. (2016). "Pharmacological Tie2 activation in kidney transplantation." World journal of transplantation **6**(3): 573-582.

Tian, F., Z. Wang, J. He, Z. Zhang and N. Tan (2020). "4-Octyl itaconate protects against renal fibrosis via inhibiting TGF-beta/Smad pathway, autophagy and reducing generation of reactive oxygen species." Eur J Pharmacol **873**: 172989.

Tian, S., L. Zhang, J. Tang, X. Guo, K. Dong and S. Y. Chen (2015). "HMGB1 exacerbates renal tubulointerstitial fibrosis through facilitating M1 macrophage phenotype at the early stage of obstructive injury." Am J Physiol Renal Physiol **308**(1): F69-75.

Tian, Y., W. Song, D. Li, L. Cai and Y. Zhao (2019). "Resveratrol As A Natural Regulator Of Autophagy For Prevention And Treatment Of Cancer." OncoTargets and therapy **12**: 8601-8609.

Togashi, Y., Y. Sakaguchi, M. Miyamoto and Y. Miyamoto (2012). "Urinary cystatin C as a biomarker for acute kidney injury and its immunohistochemical localization in kidney in the CDDP-treated rats." Exp Toxicol Pathol **64**(7-8): 797-805.

Togel, F., Z. M. Hu, K. Weiss, J. Isaac, C. Lange and C. Westenfelder (2005). "Administered mesenchymal stem cells protect against ischemic acute renal failure through differentiation-independent mechanisms." American Journal of Physiology-Renal Physiology **289**(1): F31-F42.

Tonnus, W. and A. Linkermann (2019). "Gasdermin D and pyroptosis in acute kidney injury." Kidney Int **96**(5): 1061-1063.

Uchino, S., R. Bellomo, D. Goldsmith, S. Bates and C. Ronco (2006). "An assessment of the RIFLE criteria for acute renal failure in hospitalized patients." Crit Care Med **34**(7): 1913-1917.

Uchino, S., J. A. Kellum, R. Bellomo, G. S. Doig, H. Morimatsu, S. Morgera, et al. (2005). "Acute renal failure in critically ill patients: a multinational, multicenter study." JAMA **294**(7): 813-818.

Ueno, K., M. Samura, T. Nakamura, Y. Tanaka, Y. Takeuchi, D. Kawamura, et al. (2016). "Increased plasma VEGF levels following ischemic preconditioning are associated with downregulation of miRNA-762 and miR-3072-5p." Sci Rep **6**: 36758.

van der Vaart, A., M. Mari and F. Reggiori (2008). "A picky eater: exploring the mechanisms of selective autophagy in human pathologies." Traffic **9**(3): 281-289.

Vanden Berghe, T., A. Linkermann, S. Jouan-Lanhouet, H. Walczak and P. Vandenabeele (2014). "Regulated necrosis: the expanding network of non-apoptotic cell death pathways." Nat Rev Mol Cell Biol **15**(2): 135-147.

Vasudev, N. S. and A. R. Reynolds (2014). "Anti-angiogenic therapy for cancer: current progress, unresolved questions and future directions." Angiogenesis **17**(3): 471-494.

Venkatachalam, M. A., J. M. Weinberg, W. Kriz and A. K. Bidani (2015). "Failed Tubule Recovery, AKI-CKD Transition, and Kidney Disease Progression." J Am Soc Nephrol **26**(8): 1765-1776.

Verma, S. K. and B. A. Molitoris (2015). "Renal endothelial injury and microvascular dysfunction in acute kidney injury." Semin Nephrol **35**(1): 96-107.

Vescarelli, E., A. Pilloni, F. Dominici, P. Pontecorvi, A. Angeloni, A. Polimeni, et al. (2017). "Autophagy activation is required for myofibroblast differentiation during healing of oral mucosa." Journal of Clinical Periodontology **44**(10): 1039-1050.

Waikar, S. S., K. D. Liu and G. M. Chertow (2008). "Diagnosis, epidemiology and outcomes of acute kidney injury." Clin J Am Soc Nephrol **3**(3): 844-861.

Waikar, S. S. and G. M. McMahon (2018). "Expanding the Role for Kidney Biopsies in Acute Kidney Injury." Semin Nephrol **38**(1): 12-20.

Wan, Z. H., J. J. Wang, S. L. You, H. L. Liu, B. Zhu, H. Zang, et al. (2013). "Cystatin C is a biomarker for predicting acute kidney injury in patients with acute-on-chronic liver failure." World J Gastroenterol **19**(48): 9432-9438.

Wang, A. Y., C. W. Lam, M. Wang, J. Woo, I. H. Chan, S. F. Lui, et al. (2005). "Circulating soluble vascular cell adhesion molecule 1: relationships with residual renal function, cardiac hypertrophy, and outcome of peritoneal dialysis patients." Am J Kidney Dis **45**(4): 715-729.

Wang, F., W. Fang, M. Zhao, Z. Wang, S. Ji, Y. Li, et al. (2008). "Imaging paclitaxel (chemotherapy)-induced tumor apoptosis with 99mTc C2A, a domain of synaptotagmin I: a preliminary study." Nucl Med Biol **35**(3): 359-364.

Wang, S., C. Zhang, L. Hu and C. Yang (2016). "Necroptosis in acute kidney injury: a shedding light." Cell Death Dis **7**: e2125.

Wang, W., A. Mitra, B. Poole, S. Falk, M. S. Lucia, S. Tayal, et al. (2004). "Endothelial nitric oxide synthase-deficient mice exhibit increased susceptibility to endotoxin-induced acute renal failure." American Journal of Physiology-Renal Physiology **287**(5): F1044-F1048.

Wang, Y., L. Chen, K. Wang, Y. Da, M. Zhou, H. Yan, et al. (2019). "Suppression of TRPM2 reduces renal fibrosis and inflammation through blocking TGF-beta1-regulated JNK activation." Biomed Pharmacother **120**: 109556.

Wang, Y. and N. Tjandra (2013). "Structural insights of tBid, the caspase-8-activated Bid, and its BH3 domain." J Biol Chem **288**(50): 35840-35851.

Wang, Z., S. Li, Y. Wang, X. Zhang, L. Chen and D. Sun (2019). "GDNF enhances the anti-inflammatory effect of human adipose-derived mesenchymal stem cell-based therapy in renal interstitial fibrosis." Stem Cell Res **41**: 101605.

Waters, D. W., K. E. C. Blokland, P. S. Pathinayake, J. K. Burgess, S. E. Mutsaers, C. M. Prele, et al. (2018). "Fibroblast senescence in the pathology of idiopathic pulmonary fibrosis." Am J Physiol Lung Cell Mol Physiol **315**(2): L162-L172.

Wei, J., Y. Wang, J. Zhang, L. Wang, L. Fu, B. J. Cha, et al. (2019). "A mouse model of renal ischemia-reperfusion injury solely induced by cold ischemia." Am J Physiol Renal Physiol **317**(3): F616-F622.

Wei, Q., G. Dong, J. K. Chen, G. Ramesh and Z. Dong (2013). "Bax and Bak have critical roles in ischemic acute kidney injury in global and proximal tubule-specific knockout mouse models." Kidney International **84**(1): 138-148.

Wei, Q. Q. and Z. Dong (2012). "Mouse model of ischemic acute kidney injury: technical notes and tricks." American Journal of Physiology-Renal Physiology **303**(11): F1487-F1494.

Weiner, C. P., R. G. Knowles, S. E. Nelson and L. D. Stegink (1994). "Pregnancy increases guanosine 3',5'-monophosphate in the myometrium independent of nitric oxide synthesis." Endocrinology **135**(6): 2473-2478.

Weiss, R., M. Meersch, H. J. Pavenstadt and A. Zarbock (2019). "Acute Kidney Injury." Dtsch Arztebl Int **116**(49): 833-842.

Willinger, C. C., H. Schramek, K. Pfaller and W. Pfaller (1992). "Tissue distribution of neutrophils in postischemic acute renal failure." Virchows Arch B Cell Pathol Incl Mol Pathol **62**(4): 237-243.

Xavier, S., R. Vasko, K. Matsumoto, J. A. Zullo, R. Chen, J. Maizel, et al. (2015). "Curtailing endothelial TGF-beta signaling is sufficient to reduce endothelial-mesenchymal transition and fibrosis in CKD." J Am Soc Nephrol **26**(4): 817-829.

Xiao, L., D. Zhou, R. J. Tan, H. Fu, L. Zhou, F. F. Hou, et al. (2016). "Sustained Activation of Wnt/beta-Catenin Signaling Drives AKI to CKD Progression." J Am Soc Nephrol **27**(6): 1727-1740.

Xu, J., S. Lamouille and R. Derynck (2009). "TGF-beta-induced epithelial to mesenchymal transition." Cell Res **19**(2): 156-172.

Xu-Dubois, Y. C., J. Peltier, I. Brocheriou, C. Suberbielle-Boissel, A. Djamali, S. Reese, et al. (2016). "Markers of Endothelial-to-Mesenchymal Transition: Evidence for Antibody-Endothelium Interaction during Antibody-Mediated Rejection in Kidney Recipients." J Am Soc Nephrol **27**(1): 324-332.

Yagoda, N., M. von Rechenberg, E. Zaganjor, A. J. Bauer, W. S. Yang, D. J. Fridman, et al. (2007). "RAS-RAF-MEK-dependent oxidative cell death involving voltage-dependent anion channels." Nature **447**(7146): 864-868.

Yamamoto, T., T. Tada, S. V. Brodsky, H. Tanaka, E. Noiri, F. Kajiya, et al. (2002). "Intravital videomicroscopy of peritubular capillaries in renal ischemia." Am J Physiol Renal Physiol **282**(6): F1150-1155.

Yang, B., S. A. Hosgood and M. L. Nicholson (2011). "Naked small interfering RNA of caspase-3 in preservation solution and autologous blood perfusate protects isolated ischemic porcine kidneys." Transplantation **91**(5): 501-507.

Yang, B., S. Lan, M. Dieude, J. P. Sabo-Vatasescu, A. Karakeussian-Rimbaud, J. Turgeon, et al. (2018). "Caspase-3 Is a Pivotal Regulator of Microvascular Rarefaction and Renal Fibrosis after Ischemia-Reperfusion Injury." J Am Soc Nephrol **29**(7): 1900-1916.

Yang, C., T. Zhao, Z. Zhao, Y. Jia, L. Li, Y. Zhang, et al. (2014). "Serum-stabilized naked caspase-3 siRNA protects autotransplant kidneys in a porcine model." Mol Ther **22**(10): 1817-1828.

Yang, K. Y., K. T. Liu, Y. C. Chen, C. S. Chen, Y. C. Lee, R. P. Perng, et al. (2011). "Plasma soluble vascular endothelial growth factor receptor-1 levels predict outcomes of pneumonia-related septic shock patients: a prospective observational study." Crit Care **15**(1): R11.

Yang, L., T. Y. Besschetnova, C. R. Brooks, J. V. Shah and J. V. Bonventre (2010). "Epithelial cell cycle arrest in G2/M mediates kidney fibrosis after injury." Nat Med **16**(5): 535-543, 531p following 143.

Yang, W. S., R. SriRamaratnam, M. E. Welsch, K. Shimada, R. Skouta, V. S. Viswanathan, et al. (2014). "Regulation of ferroptotic cancer cell death by GPX4." Cell **156**(1-2): 317-331.

Yang, Z. and D. J. Klionsky (2010). "Mammalian autophagy: core molecular machinery and signaling regulation." Curr Opin Cell Biol **22**(2): 124-131.

Yarlagadda, S. G., S. G. Coca, R. N. Formica, E. D. Poggio and C. R. Parikh (2009). "Association between delayed graft function and allograft and patient survival: a systematic review and meta-analysis." Nephrology Dialysis Transplantation **24**(3): 1039-1047.

Yeh, C. H., S. P. Hsu, C. C. Yang, C. T. Chien and N. P. Wang (2010). "Hypoxic preconditioning reinforces HIF-alpha-dependent HSP70 signaling to reduce ischemic renal failure-induced renal tubular apoptosis and autophagy." Life Sci **86**(3-4): 115-123.

Yin, Q. and H. Liu (2019). "Connective Tissue Growth Factor and Renal Fibrosis." Adv Exp Med Biol **1165**: 365-380.

Yoshii, S. R., A. Kuma and N. Mizushima (2017). "Transgenic rescue of Atg5-null mice from neonatal lethality with neuron-specific expression of ATG5: Systemic analysis of adult Atg5-deficient mice." Autophagy **13**(4): 763-764.

Yoshimori, T., A. Yamamoto, Y. Moriyama, M. Futai and Y. Tashiro (1991). "Bafilomycin-A1, a Specific Inhibitor of Vacuolar-Type H+-Atpase, Inhibits Acidification and Protein-Degradation in Lysosomes of Cultured-Cells." Journal of Biological Chemistry **266**(26): 17707-17712.

Young, A. R. J., E. Y. W. Chan, X. W. Hu, R. Koch, S. G. Crawshaw, S. High, et al. (2006). "Starvation and ULK1-dependent cycling of mammalian Atg9 between the TGN and endosomes." Journal of Cell Science **119**(18): 3888-3900.

Yu, W. K., J. B. McNeil, N. E. Wickersham, C. M. Shaver, J. A. Bastarache and L. B. Ware (2019). "Vascular endothelial cadherin shedding is more severe in sepsis patients with severe acute kidney injury." Crit Care **23**(1): 18.

Yuan, Q., R. J. Tan and Y. Liu (2019). "Myofibroblast in Kidney Fibrosis: Origin, Activation, and Regulation." Adv Exp Med Biol **1165**: 253-283.

Yue, L., Q. Xia, G. H. Luo and Y. P. Lu (2010). "Urinary Connective Tissue Growth Factor Is a Biomarker in a Rat Model of Chronic Nephropathy." Transplantation Proceedings **42**(5): 1875-1880.

Yunos, N. M., I. B. Kim, R. Bellomo, M. Bailey, L. Ho, D. Story, et al. (2011). "The biochemical effects of restricting chloride-rich fluids in intensive care." Crit Care Med **39**(11): 2419-2424.

Zager, R. A., L. A. Baltes, H. M. Sharma and M. S. Jurkowitz (1984). "Responses of the ischemic acute renal failure kidney to additional ischemic events." Kidney Int **26**(5): 689-700.

Zager, R. A., A. C. Johnson and K. Becker (2011). "Acute unilateral ischemic renal injury induces progressive renal inflammation, lipid accumulation, histone modification, and "end-stage" kidney disease." Am J Physiol Renal Physiol **301**(6): F1334-1345.

Zeisberg, E. M., S. E. Potenta, H. Sugimoto, M. Zeisberg and R. Kalluri (2008). "Fibroblasts in kidney fibrosis emerge via endothelial-to-mesenchymal transition." J Am Soc Nephrol **19**(12): 2282-2287.

Zhang, C., H. Dong, F. Chen, Y. Wang, J. Ma and G. Wang (2019). "The HMGB1-RAGE/TLR-TNF-alpha signaling pathway may contribute to kidney injury induced by hypoxia." Exp Ther Med **17**(1): 17-26.

Zhang, G., H. Kim, X. Cai, J. M. Lopez-Guisa, P. Carmeliet and A. A. Eddy (2003). "Urokinase receptor modulates cellular and angiogenic responses in obstructive nephropathy." J Am Soc Nephrol **14**(5): 1234-1253.

Zhang, L., Y. L. He, Q. Z. Li, X. H. Hao, Z. F. Zhang, J. X. Yuan, et al. (2014). "N-acetylcysteine alleviated silica-induced lung fibrosis in rats by down-regulation of ROS and mitochondrial apoptosis signaling." Toxicol Mech Methods **24**(3): 212-219.

Zhang, N., H. Hartig, I. Dzhagalov, D. Draper and Y. W. He (2005). "The role of apoptosis in the development and function of T lymphocytes." Cell Research **15**(10): 749-769.

Zhang, R., R. Li and Y. Tang (2019). "Soluble vascular endothelial cadherin: a promising marker of critical illness?" Crit Care **23**(1): 57.

Zhang, W., Y. Sha, K. Wei, C. Wu, D. Ding, Y. Yang, et al. (2018). "Rotenone ameliorates chronic renal injury caused by acute ischemia/reperfusion." Oncotarget **9**(36): 24199-24208.

Zhang, X., X. Zheng, H. Sun, B. Feng, G. Chen, C. Vladau, et al. (2006). "Prevention of renal ischemic injury by silencing the expression of renal caspase 3 and caspase 8." Transplantation **82**(12): 1728-1732.

Zhao, J., S. Jitkaew, Z. Y. Cai, S. Choksi, Q. N. Li, J. Luo, et al. (2012). "Mixed lineage kinase domain-like is a key receptor interacting protein 3 downstream component of TNF-induced necrosis." Proceedings of the National Academy of Sciences of the United States of America **109**(14): 5322-5327.

Zhou, C., J. Liu, Y. Ge, Y. Zhu, L. Zhou, L. Xu, et al. (2020). "Remote Ischemic Preconditioning Ameliorates Renal Fibrosis After Ischemia-Reperfusion Injury via Transforming Growth Factor beta1 (TGF-beta1) Signalling Pathway in Rats." Med Sci Monit **26**: e919185.

Zimmerhackl, B., C. R. Robertson and R. L. Jamison (1985). "The microcirculation of the renal medulla." Circ Res **57**(5): 657-667.

Zuk, A. and J. V. Bonventre (2016). "Acute Kidney Injury." Annu Rev Med **67**: 293-307.

Appendices

Middle author publication and detailed contribution

1. Yang, B., M. Dieude, K. Hamelin, M. Henault-Rondeau, N. Patey, J. Turgeon, et al. (2016). "Anti-LG3 Antibodies Aggravate Renal Ischemia-Reperfusion Injury and Long-Term Renal Allograft Dysfunction." Am J Transplant **16**(12): 3416-3429.

Contribution: Shanshan Lan performed part of murine renal IRI models independently and assisted in the other animal models. Besides, Shanshan participated in animal sacrifice, necropsy, sample collection, and preservation.

2. Cardinal, H., M. Dieude and M. J. Hebert (2018). "Endothelial Dysfunction in Kidney Transplantation." Front Immunol **9**: 1130.

Contribution: Shanshan Lan provided renal microvascular microCT images.

8th Annual ASTS
Leadership Development Program
September 23–26, 2018

The Premier Executive Management Course Designed Exclusively for the Field of Transplantation

In a field of increasing regulation and complexity, you need an edge to succeed.

The ASTS Leadership Development Program will introduce you to expert coaches to improve your transplant center's performance and accelerate your career success.

Learn. Lead. Succeed.

Register today at ASTS.org/LDP.

ASTS
American Society of Transplant Surgeons®

Kellogg School of Management
Northwestern

Northwestern University Kellogg School of Management James L. Allen Center, Evanston, IL

American Journal of Transplantation 2016; 16: 3416–3429
Wiley Periodicals Inc.

doi: 10.1111/ajt.13866

Anti-LG3 Antibodies Aggravate Renal Ischemia–Reperfusion Injury and Long-Term Renal Allograft Dysfunction

B. Yang[1,2,3], M. Dieudé[1,2,3], K. Hamelin[1,2,3], M. Hénault-Rondeau[1,2,3], N. Patey[1,2,3,4], J. Turgeon[1,2,3], S. Lan[1,2,3], L. Pomerleau[1], M. Quesnel[1], J. Peng[1], J. Tremblay[1], Y. Shi[1,3], J. S. Chan[1,3], M. J. Hébert[1,2,3,*,†] and H. Cardinal[1,2,3,*,†]

[1]*Research Centre, Centre Hospitalier de l'Université de Montréal (CRCHUM), Montreal, QC, Canada*
[2]*Canadian National Transplant Research Program, Edmonton, Alberta, T6G 2E1, Canada*
[3]*Université de Montréal, Montreal, QC, Canada*
[4]*Department of Pathology, CHU Ste-Justine, Université de Montréal, Montreal, QC, Canada*
*Corresponding authors: Marie-Josée Hébert and Héloïse Cardinal, marie-josee.hebert.chum@ssss.gouv.qc.ca and heloise.cardinal.chum@ssss.gouv.qc.ca
[†]*Both authors contributed equally.*

Pretransplant autoantibodies to LG3 and angiotensin II type 1 receptors (AT1R) are associated with acute rejection in kidney transplant recipients, whereas antivimentin autoantibodies participate in heart transplant rejection. Ischemia–reperfusion injury (IRI) can modify self-antigenic targets. We hypothesized that ischemia–reperfusion creates permissive conditions for autoantibodies to interact with their antigenic targets and leads to enhanced renal damage and dysfunction. In 172 kidney transplant recipients, we found that pretransplant anti-LG3 antibodies were associated with an increased risk of delayed graft function (DGF). Pretransplant anti-LG3 antibodies are inversely associated with graft function at 1 year after transplantation in patients who experienced DGF, independent of rejection. Pretransplant anti-AT1R and antivimentin were not associated with DGF or its functional outcome. In a model of renal IRI in mice, passive transfer of anti-LG3 IgG led to enhanced dysfunction and microvascular injury compared with passive transfer with control IgG. Passive transfer of anti-LG3 antibodies also favored intrarenal microvascular complement activation, microvascular rarefaction and fibrosis after IRI. Our results suggest that anti-LG3 antibodies are novel aggravating factors for renal IRI. These results provide novel insights into the pathways that modulate the severity of renal injury at the time of transplantation and their impact on long-term outcomes.

Abbreviations: α-SMA, α-smooth muscle actin; AKI, acute kidney injury; AT1R, angiotensin II type 1 receptor; BUN, blood urea nitrogen; CDC, complement-dependent cytotoxicity; CHUM, Centre Hospitalier de l'Université de Montréal; CI, confidence interval; COL, IVcollagen IV; cPRA, calculated panel reactive antibody; Ctrl, control; DGF, delayed graft function; eGFR, estimated GFR; ELISA, enzyme-linked immunosorbent assay; H&E, hematoxylin and eosin; HPF, high power field; I/R, ischemia–reperfusion; IRI, ischemia–reperfusion injury; MAC, membrane attack complex; NS, not significant; OR, odds ratio; PBS, phosphate-buffered saline; PTC, peritubular capillaries; SD, standard deviation.

Received 30 September 2015, revised 04 May 2016 and accepted for publication 07 May 2016

Introduction

In the immediate posttransplant period, ischemia–reperfusion injury (IRI) to kidney allografts leads to acute kidney injury (AKI) in 20–50% of transplantations from deceased donors (1–3). Posttransplant AKI manifests as delayed graft function (DGF), a condition that refers to the need for dialysis, or the failure of serum creatinine to decrease adequately in the first week after transplantation (4). DGF is associated with an increased risk of acute rejection (5) and reduced long-term graft survival in some (6,7) but not all studies (8,9). This suggests that undefined factors may synergize with DGF in some patients but not in others to durably alter renal function.

Renal epithelial cell injury and death are major hallmarks of AKI. In recent years, however, microvascular damage has emerged as a major contributor to acute and long-term renal dysfunction secondary to AKI (10). In the acute phases of AKI, injury to the peritubular capillaries (PTC) enhances renal hypoperfusion and tubular cell damage. In the long term, microvascular injury leads to microcapillary rarefaction, promoting interstitial fibrosis and contributing to progression of chronic kidney disease (11). Whether factors implicated in shaping the severity of microvascular damage during AKI could contribute to

the long-term impact of AKI on renal function remains to be evaluated.

An association between autoantibodies and acute or chronic vascular rejection in kidney, heart and lung transplant patients has been shown in recent years (12–16). Autoantibodies against angiotensin II type 1 receptors (AT1R), vimentin and perlecan LG3 fragment behave as accelerators of rejection in animal models of kidney, heart and/or aortic transplantation (13,16,17). In addition to their role in acceleration of rejection, mounting evidence suggests that some types of autoantibodies can also mediate tissue damage associated with IRI (18,19). In animal models of intestinal IRI, the binding of natural autoantibodies to self-antigenic targets leads to enhanced tissue damage through complement activation (20). Ischemia has been shown to enhance the vasoconstrictive effect of anti-AT1R autoantibodies (17,21). We showed previously that vascular ischemia greatly enhances the capacity of anti-LG3 antibodies to enhance vascular inflammation (17).

We hypothesized that IRI can create permissive conditions for autoantibodies such as anti-LG3, anti-AT1R and antivimentin to interact with their antigenic targets and potentially enhance renal damage and renal dysfunction, even in the absence of rejection. To test this hypothesis, we assessed whether these autoantibodies, measured immediately prior to transplantation, were associated with an increased risk of DGF and with lower long-term graft function in kidney transplant recipients. We then turned to an animal model of renal IRI to better understand the mechanisms by which autoantibodies modulate renal injury.

Methods

Human study

Study design and patients: We performed a retrospective cohort study of consecutive patients who received kidney transplantation at our center between June 1, 2008, and June 1, 2013. All patients participated in the Centre Hospitalier de l'Université de Montréal (CHUM) clinical and biological database, and sera were banked immediately prior to transplantation. Clinical information was retrieved from the electronic database and complemented by chart review by trained research nurses as needed. Patients entered the cohort on the date of transplantation and were followed until February 1, 2015. The study was approved by our local ethics review board.

Outcomes: The primary outcome was the occurrence of DGF. DGF was defined as the need for dialysis in the first posttransplant week, as the failure of serum creatinine to decrease by >10% on the first three postoperative days or as serum creatinine levels >250 μmol/L on postoperative day 5 in the presence of scintigraphic evidence of acute tubular necrosis (4). The secondary outcome was graft function at 1 year after transplantation, estimated with the MDRD four-variable equation (22).

Measurements: Anti-AT1R, antivimentin and anti-LG3 antibodies were measured on pretransplant sera. We used a locally developed enzyme-linked immunosorbent assay (ELISA) to measure anti-LG3 IgG antibodies, as described previously (17). We used a commercially available ELISA to measure anti-AT1R (One Lambda; Thermo Fisher Scientific, Waltham, MA) and antivimentin antibodies (Antibodies-online.com, Atlanta, GA). For anti-AT1R, the threshold for positivity was >17 U/mL; results between 10 and 17 U/mL were considered intermediate, and results <10 U/mL were considered negative. For antivimentin, values >1.31 (sample positivity index, semiquantitative measurement) were positive; values between 1 and 1.3 were considered intermediate, and values <1 were negative, according to the manufacturer's protocol. We collected data on recipient medical history and demographic characteristics (age, sex, renal disease, number of previous transplantations and pretransplant panel reactive antibodies), donor characteristics (donor type, age, height, weight, hypertension and diabetes), procedural and management characteristics (cold ischemic time, induction type and maintenance immunosuppressive protocol), and posttransplant outcomes (rejection according to the Banff 2013 classification (23), graft function, and patient and graft survival).

Statistical analyses: Continuous variables are reported as means and standard deviations, and categorical variables are summarized as proportions. Student t-tests were used to compare between-group differences for continuous variables according to their distribution. Chi-square or Fisher exact tests were used to determine differences between categorical variables. Logistic regression was used to assess whether pretransplant anti-LG3, anti-AT1R and antivimentin antibodies were associated with DGF. The pretransplant autoantibodies were analyzed as categorical variables. After plotting the median of each quartile of the distribution for each antibody against the log odds of cases to controls, we chose a cutoff of 225 (corresponding to the median of the last quartile) for anti-LG3 positivity. Because there was no visual signal for a potential cutoff between anti-AT1R or antivimentin and the outcome, we used the manufacturer's recommended cutoff for positivity. Variables with a p-value <0.05 on univariate analysis were included in the final multivariate model. No other variables were forced into the model to avoid overfitting. Linear regression was used to study the association between graft function at 1 year after transplant and pretransplant anti-LG3 titers. Analyses were performed using SAS version 9.3 (SAS Institute, Cary, NC).

Animal study

Animals and surgical procedures: Adult C57Bl/6 mice (20–25 g) were purchased from Charles River Laboratories (Wilmington, MA), maintained on a 12-h light/dark cycle and fed a normal diet *ad libitum*. All experiments on mice were approved by the institutional animal care and use committee of the CHUM research center. AKI in mice was carried out, as described previously (24). Briefly, mice were anaesthetized using isoflurane (2%) by inhalation and were placed on a heated surgical pad. A midline incision was made; microvascular clamps were placed on the left renal pedicle for 30 min and then released. The right kidney was removed after the release of microvascular clamps.

Production and passive transfer of murine anti-LG3 IgG: Naïve C57Bl/6 mice were injected subcutaneously with either recombinant LG3 (50 μg) or phosphate-buffered saline (PBS) and emulsified in incomplete Freund's adjuvant every 2 weeks for a total of four immunizations. Blood was recovered with cardiac puncture at sacrifice 12–14 days after the last immunization. Sera (diluted 1/100) were tested for the presence of anti-LG3 IgG, as described. IgG was isolated from pooled sera of either LG3-immunized mice (anti-LG3 IgG) or PBS-immunized mice (control IgG) using protein A Sepharose CL-4B (Sigma-Aldrich, St. Louis, MO) and

quantitated by the Micro BCA assay (Pierce; Thermo Fisher Scientific). For passive transfer of anti-LG3 IgGs, mice received tail-vein intravenous injections of 50 μg anti-LG3 IgG or control IgG. Each group received injections 2 days before surgery, the day of surgery and every other day until sacrifice. Three doses were given to mice that were sacrificed at day 2 after surgery, or four doses was given to those sacrificed at day 7 after surgery.

Immunohistochemistry: Clamped kidneys were recovered at day 2 or 7 after surgery; tissues were fixed with 10% neutral buffered formalin and were paraffin embedded, according to usual methods. Samples were cut into 4-μm slices. Immunohistochemistry was performed on paraffin-embedded sections using an automated immunostainer (ArtisanLink; Dako, Glostrup, Denmark), according to the manufacturer's protocols. The antibodies used in our study were C4d (1/1600, BI-RC4D; Alpco, Salem, NH), C5b-9 or membrane attack complex (MAC; 1/200, SC5b-9; Quidel, San Diego, CA), CD31 (1/20, CM303A; Biocare Medical, Concord, CA), α-smooth muscle actin (α-SMA; 1/500, clone 1A4; Dako), collagen IV (1/100, AB769; Millipore, Billerica, MA) and caspase 3 (1/50, CP229B; Biocare Medical). Digital images of stained tissues were captured by a Leica DMLS microscope and a Leica DFC420C camera (Leica Microsystems, Wetzlar, Germany). CD31-positive staining was quantified using Visiomorph (Visiopharm, Hoersholm, Denmark).

Histopathological scoring: Histopathological scoring was done in renal sections stained with hematoxylin and eosin, as described previously (25). Briefly, the percentage of damaged tubules in the renal cortex was estimated using a five-point scale based on the following criteria: brush border loss, tubular dilatation, cast deposition and cellular necrosis in 10 randomly selected, nonoverlapping fields (×200 magnification). Lesions were graded on a scale from 0 to 5: 0 indicated normal; 1 indicated mild, involvement of <10% of the cortex; 2 indicated moderate, involvement of 10–25% of the cortex; 3 indicated severe, involvement of 25–50% of the cortex; 4 indicated very severe, involvement of 50–75% of cortex; and 5 indicated extensive damage, involvement of >75% of the cortex (25).

Biochemical analysis: The Vitros CREA method was performed for measurement of serum creatinine using the Vitros CREA Slides and the Vitros Chemistry Products (Vitros 250/350 Chemistry Systems; Ortho Clinical Diagnostics, Raritan, NJ). Levels of blood urea nitrogen (BUN) were measured using the Quantichrom urea assay kit (BioAssay Systems, Hayward, CA).

Results

Among the 173 patients included in this study, one died from myocardial infarction immediately after transplantation and another died within 1 year after transplant (Figure 1). Recipient, donor and periprocedural

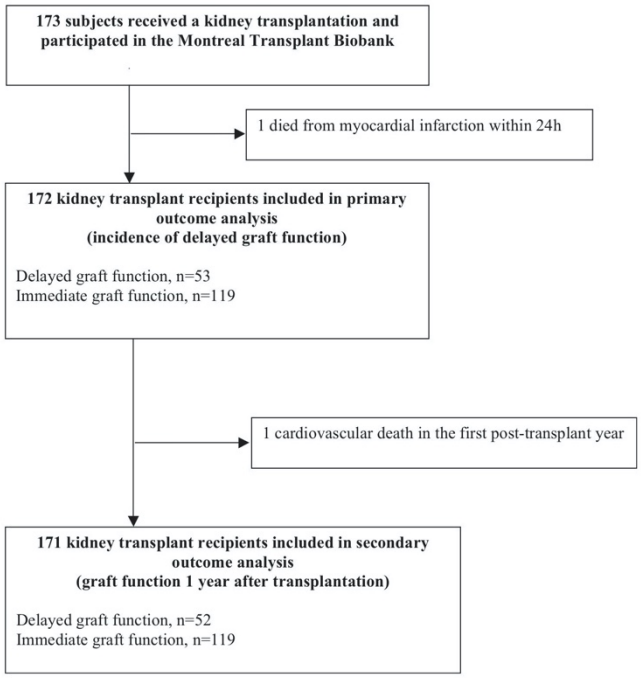

Figure 1: Patient flow chart.

Table 1: Recipient and donor characteristics (n = 172)

Characteristics	Results
Age in years, mean (SD)	50 (12)
Male sex, n (%)	107 (62)
Race, n (%)	
White	149 (86)
Black	13 (8)
Other	10 (6)
Cause of chronic kidney disease, n (%)[1]	
Glomerular diseases	51 (30)
Diabetes	25 (15)
Hypertension/vascular	9 (5)
Polycystic kidney diseases	39 (23)
Autoimmune diseases	8 (5)
Other	47 (27)
Pretransplant CDC panel reactive antibodies >20%, n (%)	6 (4)
First transplantation, n (%)	148 (86)
Living donor, n (%)	69 (40)
Deceased donor, n (%)	
Neurological determination of death	96 (56)
Donor after cardiocirculatory arrest	7 (4)
Cold ischemic time in hours, mean (SD)	8 (5)
Donor age in years, mean (SD)	47 (14)
Donor with hypertension or diabetes, n (%)	21 (12)
Donor height in meters, mean (SD)	1.67 (0.1)
Induction, n (%)[1]	
Thymoglobulin	52 (30)
Anti-CD25	131 (76)

CDC, complement-dependent cytotoxicity; SD, standard deviation.
[1]Number of patients exceeds 172 because some patients had two listed causes of chronic kidney disease or received more than one type of induction.

characteristics are shown in Table 1. All patients received tacrolimus, mycophenolate mofetil and prednisone, except for three patients who received cyclosporine in combination with mycophenolate mofetil and prednisone. Patient and graft survival over a median follow-up of 3.5 years were 95% and 89%, respectively. We observed no associations between pretransplant positivity for anti-LG3 and antivimentin antibodies and previous sensitizing events (transplantations, pregnancies or transfusions) or classical autoimmune diseases (lupus erythematosus, anti–neutrophil cytoplasmic antibodies or anti–glomerular basement membrane–associated vasculitis) (Figure S1). Positivity for anti-AT1R was more frequent in retransplant patients ($p < 0.01$) (Figure S1A). Pretransplant anti-LG3 titers were associated with antivimentin ($p = 0.23$, 95% confidence interval [CI] 0.08–0.37) but not with anti-AT1R titers ($p = 0.15$, 95% CI −0.01 to 0.29).

Pretransplant anti-LG3 titers are associated with an increased risk of DGF

Of the 172 study participants included in the primary outcome analysis, 53 (31%) experienced DGF, as defined above, of whom 12 needed hemodialysis in the first week after transplantation. Pretransplant anti-LG3 titers were higher in patients with DGF compared with those with immediate graft function, whereas pretransplant anti-AT1R and antivimentin antibody titers were similar in both groups (Figure 2). When antibodies were analyzed as dichotomous variables, we also observed a difference in pretransplant positivity status for anti-LG3 antibodies—but not in anti-AT1R or antivimentin—between patients who developed DGF and those who did not (Figure 3). This was also true when anti-AT1R and antivimentin

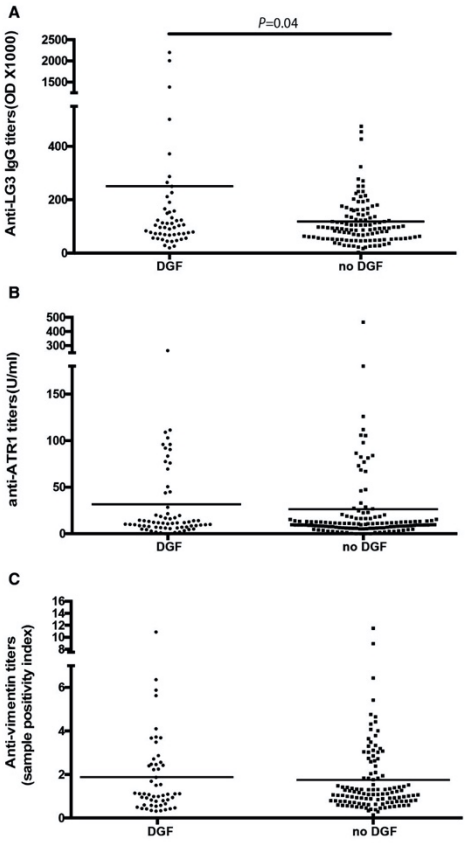

Figure 2: Pretransplant titers of anti-LG3, anti-AT1R, and antivimentin antibodies in patients with and without DGF. (A) Pretransplant anti-LG3 titers in patients who went on to develop DGF and those who did not. Mean titers were higher in patients who went on to develop DGF compared with those who did not (251 ± 449 vs. 118 ± 109 OD, $p = 0.04$). (B) Mean pretransplant anti-AT1R levels in patients with and without DGF (14 ± 20 vs. 13 ± 17 U/mL, $p = 0.75$). (C) Mean pretransplant antivimentin titers in patients with and without DGF (1.9 ± 1.9 vs. 1.7 ± 1.7 sample positivity index, $p = 0.66$). ATR1, angiotensin II type 1 receptor; DGF, delayed graft function; OD, optical density.

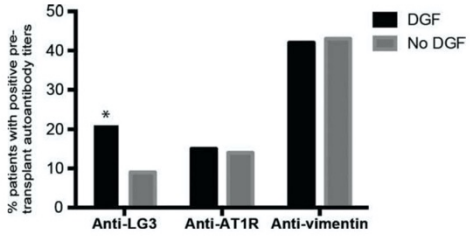

Figure 3: Pretransplant positivity status for anti-LG3, anti-AT1R, and antivimentin antibodies in patients with and without DGF. The proportion of patients who were positive for pretransplant anti-LG3 antibodies (titers >225 optical density) was greater in patients who went on to develop DGF than in those who did not (21% vs. 9%, *p = 0.03), whereas the proportions of patients with positive pretransplant antivimentin or anti-AT1R antibodies were similar in patients who went on to develop DGF and in those who did not (antivimentin: 42% vs. 43%, p = 0.87; anti-AT1R: 15% vs. 14%, p = 0.89). ATR1, angiotensin II type 1 receptor; DGF, delayed graft function.

antibodies were classified as positive, intermediate, and negative (data not shown). In univariate analyses, positive pretransplant anti-LG3 status was associated with DGF (odds ratio [OR] 2.57, 95% CI 1.03–6.38, p = 0.04), whereas positive pretransplant anti-AT1R status (OR 1.10, 95% CI 0.42–2.91, p = 0.84) and positive antivimentin status (OR 0.95, 95% CI 0.48–1.89, p = 0.88) were not (Table 2). Rejection was not associated with an increased risk of DGF (OR 1.61, 95% CI 0.50–5.51, p = 0.40). In multivariate analyses, positive pretransplant anti-LG3 status (OR 2.77, 95% CI 1.01–7.68), female sex (OR 0.35, 95% CI 0.16–0.79), donor type (deceased after neurological determination of death vs. living: OR 2.89, 95% CI 1.31–6.36; deceased after cardiocirculatory arrest vs. living: OR 16.00, 95% CI 2.32–110.75), and donor height (OR 0.64 per 10-cm increase, 95% CI 0.44–0.91) were independently associated with DGF.

Pretransplant anti-LG3 titers are associated with lower estimated GFR 1 year after transplantation in patients with DGF but not in those with immediate graft function

To evaluate whether autoantibodies can negatively affect renal function independent of their role in induction or acceleration of rejection, we evaluated the association between pretransplant autoantibody titers and renal function at 1 year. Among the 171 patients available for this analysis, estimated GFR (eGFR) at 1 year after transplantation was lower in patients with DGF compared with immediate graft function (44 ± 16 vs. 61 ± 22 mL/min per 1.73 m^2, p = 0.001). In patients with DGF, eGFR at 1 year after transplantation was significantly lower in patients who had positive pretransplant anti-LG3 antibodies (p = 0.003) (Figure 4).

Positive pretransplant anti-LG3 status, but not antivimentin or anti-AT1R status, was associated with reduced eGFR at 1 year after transplantation in patients with DGF (β = −15 mL/min per 1.73 m^2, 95% CI −24 to −5) (Table 3). Donor age (β = −3 mL/min per 1.73 m^2, 95% CI −19 to 0) and height (β = 4 mL/min per 1.73 m^2 per

Table 2: Factors associated with delayed graft function

Factor	Univariate OR (95% CI)	Multivariate OR (95% CI)
Positive pretransplant anti-LG3 titers[1]	2.57 (1.03–6.38)*	2.77 (1.01–7.68)*
Female sex (vs. male)	0.32 (0.15–0.67)*	0.35 (0.16–0.79)*
Donor type (vs. living donor)		
Donor after neurological determination of death	2.85 (1.35–6.02)*	2.89 (1.31–6.36)*
Donor after cardiocirculatory arrest	11.88 (2.05–68.61)*	16.00 (2.32–110.75)*
Donor height (per 10-cm increase)	0.67 (0.48–0.94)	0.64 (0.44–0.91)*
Acute rejection in the first 3 weeks after transplant	1.66 (0.50–5.51)	–
Donor age >60 years	1.82 (0.77–4.28)	–
Cold ischemic time (per 1-h increase)	1.06 (1.00–1.12)*	–
Recipient BMI (per 1-U increase)	1.07 (1.00–1.16)	–
Positive pretransplant antivimentin antibodies[1]	0.95 (0.48–1.89)	–
Positive pretransplant anti-AT1R antibodies[1]	1.10 (0.42–2.91)	

AT1R, angiotensin II type 1 receptor; CI, confidence interval; OR, odds ratio.
[1]Pretransplant anti-LG3 titers >225 optical density, pretransplant antivimentin titers ≥1.31 sample positivity index and pretransplant anti-AT1R antibodies >17 U/mL.
*p < 0.05.

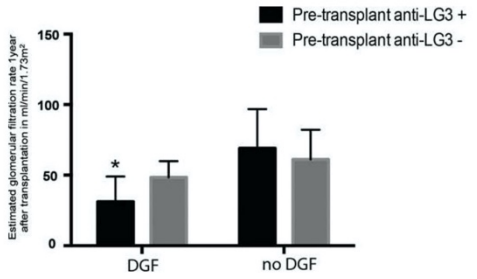

Figure 4: Estimated GFR (eGFR) 1 year after transplantation according to the presence of DGF and positive pretransplant anti-LG3 antibodies. In patients with DGF, eGFR at 1 year after transplantation was lower in patients with positive pretransplant anti-LG3 antibodies than in those who were negative (31 ± 18 vs. 47 ± 14 mL/min per 1.73 m^2, *p = 0.003). In contrast, in patients who did not experience DGF, eGFR at 1 year after transplant was not associated with pretransplant anti-LG3 status (69 ± 28 vs. 61 ± 22 mL/min per 1.73 m^2, p = 0.23). DGF, delayed graft function.

10-cm increase, 95% CI 1–8) were also associated with 1-year graft function in patients with DGF, whereas rejection and donor type were not (Table 3). We observed no relationship between any of the pretransplant autoantibodies and 1-year graft function in patients with immediate graft function. These results support the notion that in recipients of a renal allograft with DGF, elevated anti-LG3 titers at the time of transplantation durably and negatively affect renal function. This effect was specific to anti-LG3 antibodies; antivimentin and anti-AT1R antibodies were not associated with 1-year graft function.

Anti-LG3 antibodies enhance renal dysfunction following ischemia–reperfusion in mice

We turned to a murine model of renal IRI to characterize the mechanisms of aggravated renal dysfunction induced by anti-LG3 antibodies. Renal IRI in mice was induced by left renal artery clamping and contralateral nephrectomy. Mice were passively transferred with anti-LG3 IgG 2 days prior to renal artery clamping and every other day thereafter to reach and maintain anti-LG3 IgG titers within the range observed in renal transplant patients (Figure S2A) (17). Passive transfer of anti-LG3 antibodies is associated with injections of large amounts of fluid that protect against AKI (Figure S2B). Consequently, we used mice injected with equivalent amounts of mouse IgG and fluid as controls. After IRI, both control and anti-LG3 IgG–transferred mice showed deterioration in renal function and histological evidence of tubular and microvascular injury (Figures 5A–D). Compared with mice passively transferred with control IgG, BUN levels were significantly higher at day 2 after IRI in mice passively transferred with anti-LG3 antibodies (Figure 5A). There was a trend toward increased BUN levels at day 7 (Figure 5A). Serum creatinine levels were significantly higher in mice passively transferred with anti-LG3 antibodies at day 7 after IRI (Figure S2C). This was associated with increased tubular damage, as shown by an elevated tubular injury score at day 2 and further increase at day 7 (Figure 5C). Microvascular injury with microvascular congestion and rouleaux formation was also increased at day 2 and further enhanced at day 7 (Figures 5B and D). Activated caspase 3 staining was significantly increased in mice transferred with anti-LG3 antibodies compared with controls at days 2 and 7 (Figure 5E). We found a significant increase in caspase 3 staining between days 2 and 7 in anti-LG3–transferred mice, whereas caspase 3 staining in control mice remained relatively stable after IRI (Figure 5E), supporting the notion that anti-LG3 led to prolonged aggravation of renal injury after IRI. We also performed passive transfer of anti-LG3 IgG in the absence of renal IRI in another set of mice. This did not lead to alteration in renal function (Figure S2D) or histological evidence of renal injury (data not shown). Collectively, these results suggest that anti-LG3

Table 3: Factors associated with graft function 1 year after transplantation in patients with delayed graft function

Factor	Univariate β (95% CI)	Multivariate β (95% CI)
Positive pretransplant anti-LG3 titers[1]	−14 (−25 to −3)*	−15 (−24 to −5)*
Donor age (per 10-year increase)	−2 (−5 to 0)	−3 (−19 to 0)*
Donor type (reference living donor)		
Donor after neurological determination of death	2 (−8 to 13)	2 (−7 to 12)
Donor after cardiocirculatory arrest	7 (−10 to 24)	4 (−11 to 18)
Donor height (per 10-cm increase)	4 (0–8)*	4 (1–8)*
Rejection in the first posttransplant year	−1 (−11 to 8)	
Female sex	−3 (−13 to 8)	
Cold ischemic time (per 1-h increase)	0 (−1 to 0)	
Positive pretransplant antivimentin antibodies[1]	−6 (−15 to 2)	
Positive pretransplant anti-AT1R antibodies[1]	0 (−12 to 11)	

AT1R, angiotensin II type 1 receptor; CI, confidence interval.
[1]Pretransplant anti-LG3 titers >225 optical density, pretransplant antivimentin titers ≥1.31 sample positivity index and pretransplant anti-AT1R antibodies >17 U/mL.
*p < 0.05.

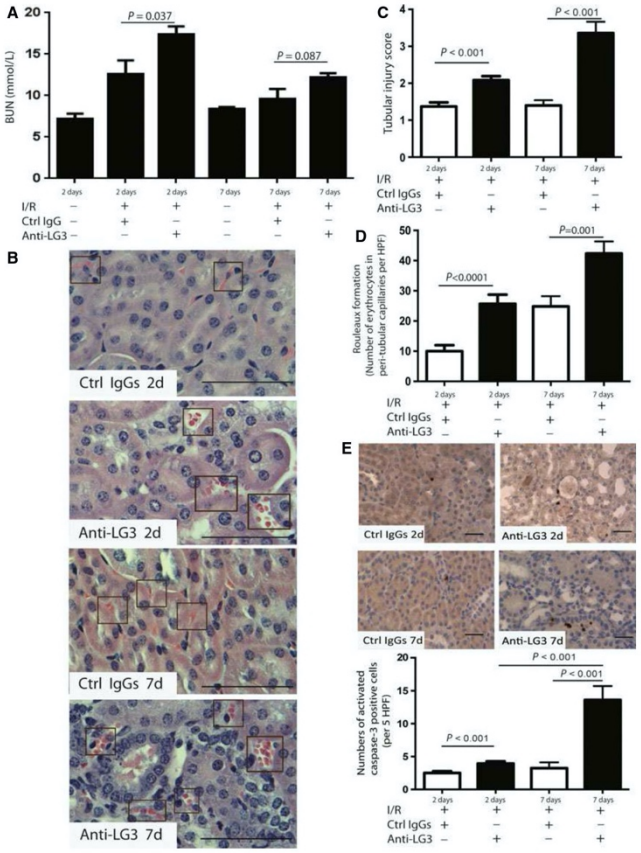

Figure 5: Anti-LG3 antibodies aggravate renal dysfunction after I/R. (A) BUN levels in mice after sham surgery or IRI and passively transferred with anti-LG3 IgG or control mouse IgG ($n \geq 4$ per group). (B) Representative H&E-stained kidney sections from mice submitted to IRI and passively transferred with anti-LG3 IgG or control mouse IgG and sacrificed 2 days (upper panels) and 7 days (lower panels) after surgery; black boxes show rouleaux formation. Scale bar = 50 μm. (C) Tubular injury score in H&E-stained kidney sections from mice submitted to IRI and passively transferred with anti-LG3 IgG or control mouse IgG and sacrificed 2 and 7 days after surgery ($n \geq 5$ per group). (D) Quantification of rouleaux formation in H&E-stained kidney sections from mice submitted to IRI and passively transferred with anti-LG3 IgG or control mouse IgG and sacrificed 2 and 7 days after surgery ($n \geq 5$ per group). (E) Immunohistochemistry and quantification for activated caspase 3 from mice submitted to IRI and passively transferred with anti-LG3 IgG or control mouse IgG and sacrificed 2 and 7 days after surgery ($n \geq 5$ per group). Scale bar = 50 μm. BUN, blood urea nitrogen; Ctrl, control; H&E, hematoxylin and eosin; HPF, high-power field; I/R, ischemia–reperfusion; IRI, ischemia–reperfusion injury.

antibodies lead to progressive and sustained aggravation of renal cell death after IRI.

Anti-LG3 antibodies trigger activation of the classical complement pathway and enhance renal microvascular injury after ischemia–reperfusion

Because LG3 is a cryptic fragment of perlecan—a constituent of vascular and, to a lesser extent, tubular basement membranes—we considered the possibility that, following IRI, anti-LG3 antibodies bind basement membranes and activate complement. In renal IRI, complement activation is classically associated with activation of the alternative pathway, with little contribution of the classical pathway (26). We quantified C4d and MAC staining at days 2 and 7 after IRI. There was a trend toward increased C4d staining in PTC at day 2 after IRI

in mice transferred with anti-LG3 IgG (see Figure 6 for the corticomedullary junction and Figure S3 for the superficial cortex), but this did not translate into increased MAC deposition (see Figure 7 for the corticomedullary junction and Figure S4 for the superficial cortex). C4d and MAC staining, however, were both significantly increased at day 7 after IRI within PTC sampled at the corticomedullary junction (Figures 6 and 7). C4d tubular staining was not enhanced in anti-LG3–transferred mice compared with IgG controls (see Figure 6C for the corticomedullary junction).

Taking into consideration the importance of complement activation in microvascular involution and fibrosis following IRI, we then evaluated whether CD31 α-SMA and collagen IV staining within PTC was modulated by anti-LG3 antibodies. Mice transferred with anti-LG3 IgG showed reduced peritubular CD31 staining (Figure 8A), increased collagen IV staining (Figure 8B) and increased α-SMA (Figure 8C) compared with controls, confirming enhanced microvascular rarefaction and fibrosis markers in mice transferred with anti-LG3 antibodies. Collectively, these results suggest that, when associated with IRI, anti-LG3 antibodies activate the classical complement pathway, further compromising microvascular integrity and enhancing renal injury and fibrosis.

Discussion

Ischemia–reperfusion is an integral component of renal transplantation. Whether IRI influences long-term outcomes in renal transplant patients is still debated (27). Although clinical factors such as donor age and type may influence the occurrence and functional impact of DGF (28), recent data show that autoantibodies can participate in IRI-mediated tissue damage (12,18). We identified

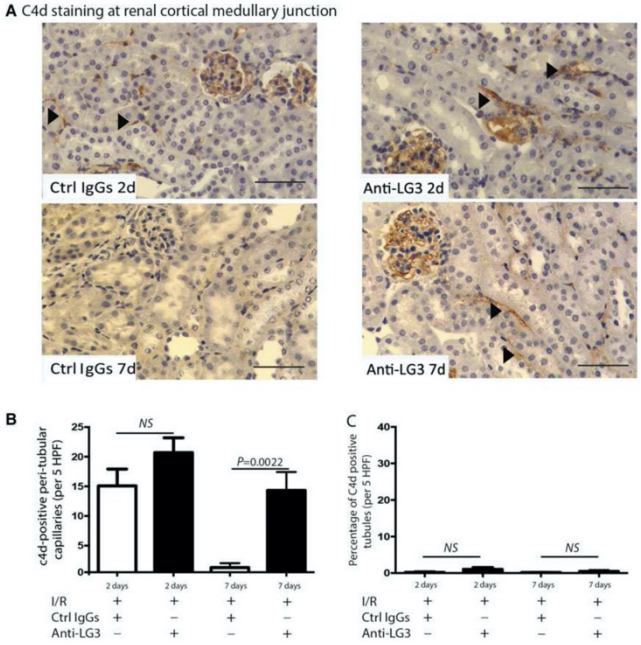

Figure 6: Anti-LG3 antibodies increase intrarenal C4d deposition after ischemia/reperfusion. (A) Immunohistochemistry for C4d deposition in corticomedullary kidney sections from mice submitted to ischemia–reperfusion injury (IRI) and passively transferred with anti-LG3 IgG or control mouse IgG and sacrificed 2 days (upper panels) and 7 days (lower panels) after surgery (magnification ×200); black arrowheads indicate positive peritubular capillary, scale bar = 50 μm (n ≥ 5 per group). (B) Number of C4d-positive peritubular capillaries, per 5 randomly chosen HPFs (×200) at the corticomedullary junction from mice submitted to IRI and passively transferred with anti-LG3 IgG or control mouse IgG and sacrificed 2 and 7 days after surgery (n ≥ 5 per group). (C) Percentage of C4d positive tubules per five randomly chosen HPFs (×200) at the corticomedullary junction from mice submitted to IRI and passively transferred with anti-LG3 IgG or control mouse IgG and sacrificed 2 and 7 days after surgery (n ≥ 5 per group). Ctrl, control; HPF, high-power field; I/R, ischemia–reperfusion; NS, not significant.

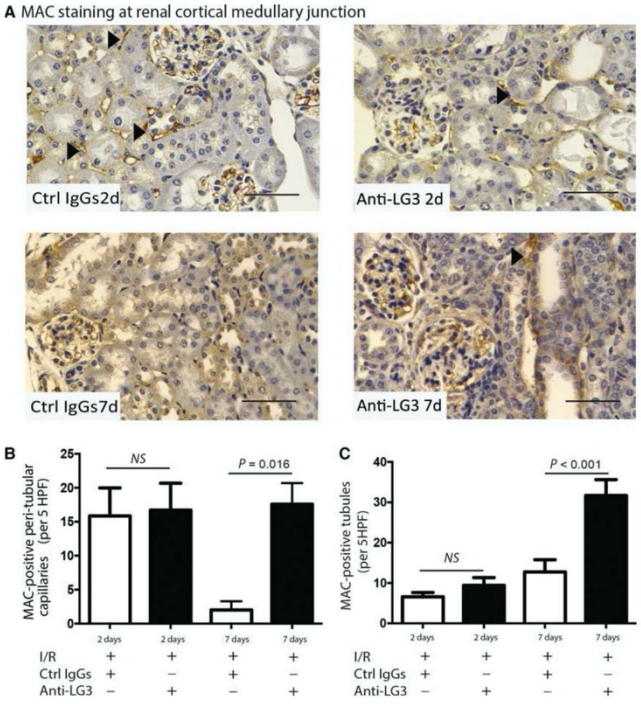

Figure 7: Anti-LG3 antibodies increase intrarenal deposition of MAC after I/R. (A) Representative MAC immunohistochemistry in corticomedullary kidney sections from mice submitted to I/R injury (IRI) and passively transferred with anti-LG3 IgG or control mouse IgG and sacrificed 2 days (upper panels) and 7 days (lower panels) after surgery (magnification ×200); black arrowheads indicate positive peritubular capillaries, scale bar = 50 μm. (B) Numbers of MAC-positive peritubular capillaries per five randomly chosen high power fields (×200) at the corticomedullary junction from mice submitted to IRI and passively transferred with anti-LG3 IgG or control mouse IgG and sacrificed 2 and 7 days after surgery ($n \geq 5$ per group). (C) Percentage of MAC-positive tubules per five randomly chosen high power fields (×200) at the corticomedullary junction from mice submitted to IRI and passively transferred with anti-LG3 IgG or control mouse IgG and sacrificed 2 and 7 days after surgery ($n \geq 5$ per group). Ctrl, control; HPF, high-power field; I/R, ischemia–reperfusion; MAC, membrane attack complex; NS, not significant.

antibodies against a C-terminal perlecan fragment (LG3) as novel modulators of AKI in response to IRI. In kidney transplant recipients, pretransplant anti-LG3 antibody titers are associated with an increased risk of DGF. Moreover, in patients with DGF but not in those with immediate graft function, anti-LG3 antibody titers assessed immediately before transplantation predicted lower graft function at 1 year after transplantation. The impact of anti-LG3 antibodies on the occurrence and functional impact of DGF cannot be attributed to a confounding effect of rejection because the latter was not associated with DGF or graft function at 1 year after transplantation in patients with DGF. Anti-AT1R and antivimentin were not associated with DGF or graft function at 1 year after transplant. These results suggest that, in addition to their function as accelerators of rejection, anti-LG3 antibodies can impair renal function through rejection-independent pathways, whereas anti-AT1R and antivimentin do not.

We turned to an animal model of IRI to investigate how anti-LG3 antibodies aggravate renal dysfunction. We chose a model of IRI and not renal transplantation because we wanted to evaluate whether anti-LG3 antibodies could accelerate renal dysfunction caused by IRI in the absence of any contributing mechanisms that stem from alloimmunity. We found that when present at high titers at the time of IRI, anti-LG3 antibodies enhance renal dysfunction in association with activation of the complement pathway within PTC. This was associated with enhanced microvascular rarefaction, demonstrated by reduced CD31 staining and increased levels of α-SMA

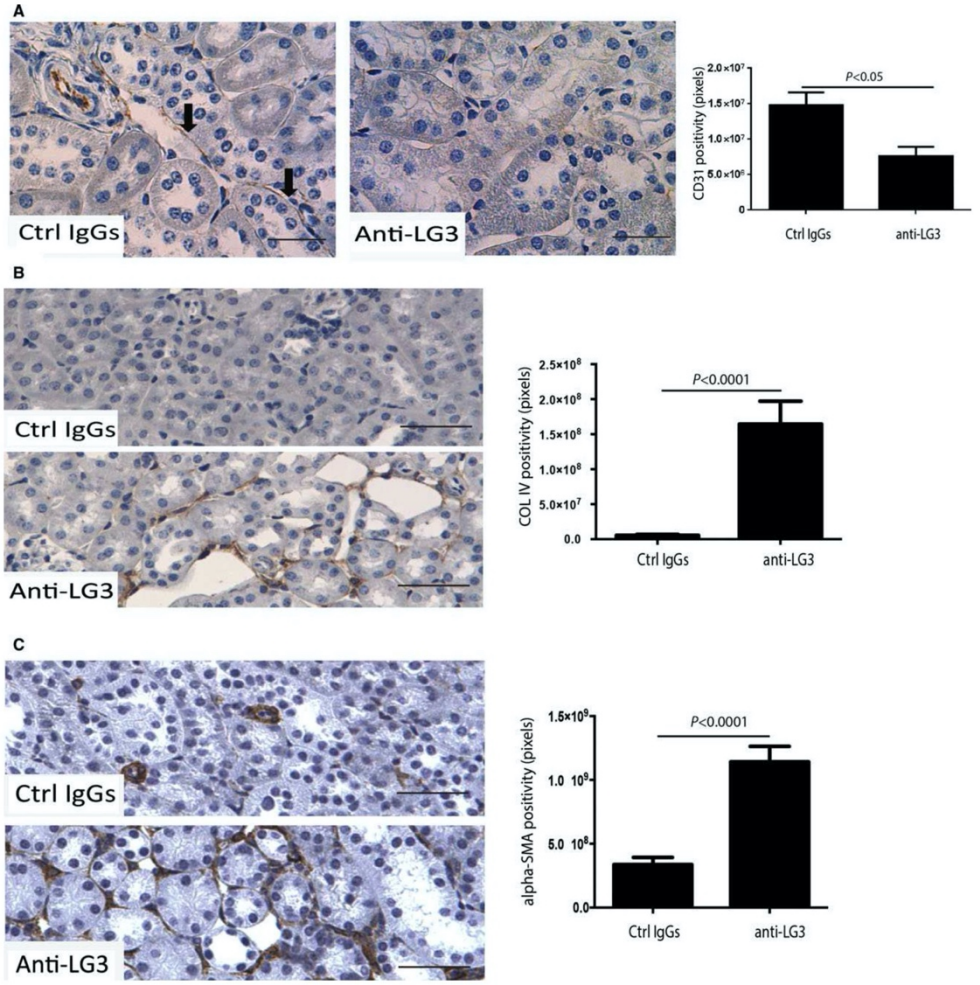

Figure 8: Anti-LG3 antibodies increase peritubular capillary loss and fibrotic markers after ischemia–reperfusion. (A) Immunohistochemistry and quantification of CD31 in kidney sections from mice submitted to ischemia–reperfusion injury (IRI) and passively transferred with anti-LG3 IgG or control mouse IgG and sacrificed 7 days after surgery (magnification ×630); arrows indicate CD31-positive peritubular capillaries, scale bar = 10 μm (n = 5 per group). (B) Immunohistochemistry and quantification of collagen IV in kidney sections from mice submitted to IRI and passively transferred with anti-LG3 IgG or control mouse IgG and sacrificed 7 days after surgery (×200), scale bar = 50 μm. (C) Immunohistochemistry and quantification of α-SMA in kidney sections from mice submitted to IRI and passively transferred with anti-LG3 IgG or control mouse IgG and sacrificed 7 days after surgery (×200), scale bar = 50 μm. α-SMA, α-smooth muscle actin; COL IV, collagen IV; Ctrl, control; MAC, membrane attack complex.

and collagen IV, two fibrotic markers. Nevertheless, in the absence of IRI, anti-LG3 antibodies did not induce renal dysfunction, confirming their role as aggravators but not inducers of renal dysfunction. Collectively, these results suggest that ischemia represents a permissive factor for intrarenal activation of complement by anti-LG3 antibodies, leading to enhanced microvascular injury, involution and fibrosis.

Tubular injury was also increased in mice transferred with anti-LG3 antibodies, but various elements argue for an indirect effect rather than direct epithelial toxicity. First, there was no evidence of C4d deposition within renal tubules at either day 2 or 7 after IRI, demonstrating the absence of classical complement activation within tubules; however, we found increased tubular MAC staining at day 7 after IRI in mice transferred with anti-LG3 antibodies, suggesting enhanced tubular activation of the alternative complement pathway. Future studies are needed to explain this finding. A potential explanation is that progressive microvascular involution (shown by reduced CD31 staining) caused by complement-induced microvascular injury associated with anti-LG3 leads to tubular ischemia, which in turn fuels tubular epithelial cell death leading to activation of the alternative complement pathway. This possibility would be consistent with our findings showing progressive increase in caspase 3 staining in mice transferred with anti-LG3 antibodies. This possibility is also consistent with previous publications demonstrating a role for tubular ischemia in activation of the alternative complement pathway in renal tubular cells (29). Delineating the contributions of the classical and alternative pathways in anti-LG3–dependent renal injury will be key to developing clinically relevant strategies of complement inhibition for prevention of progressive renal dysfunction.

Injury to the microvasculature is emerging as an important contributor to renal dysfunction after IRI (11,30,31). Endothelial injury and apoptosis contribute to renal dysfunction by durably limiting perfusion of tubules and perpetuating tubular damage (32,33). Microvascular dropout also favors tubulointerstitial fibrosis, myofibroblast differentiation and progressive loss of renal function (32,34). Endothelial injury and apoptosis also contribute to the processing of perlecan and production of LG3 (35,36), and circulating LG3 has been recently reported to be an early predictor of AKI in heart surgery patients with AKI (37). The mechanisms responsible for increased LG3 levels in association with AKI are still incompletely defined. Recent results from our group identified apoptotic exosomelike vesicles, a novel type of membrane vesicles released by dying vascular cells, as a central trigger for anti-LG3 production (36). The presence of LG3 and active 20S proteasome complex within these vesicles plays a major role in the immunogenic processing of perlecan required for anti-LG3 production. We also showed that acute vascular injury, whether renal or not, increases circulating levels of these vesicles *in vivo*. Other mechanisms of LG3 production associated with IRI include the possibility that proteolytic enzymes released by infiltrating leukocytes (38) contribute to the proteolysis of perlecan and to the production of LG3. Further studies are needed to characterize the full spectrum of mechanisms by which ischemia–reperfusion favors the production of LG3 and anti-LG3–dependent microvascular injury in transplantation and other clinical situations associated with IRI.

Interactions between auto- and alloimmune pathways after solid organ transplantation are increasingly recognized as a risk factor for rejection. In kidney transplant patients, pretransplant anti-LG3, anti-AT1R and autoreactive antibodies against apoptotic cells have been linked with severe acute rejection (13,14,17,39). Antiagrin, antifibronectin, anti–collagen IV and antivimentin autoantibodies have been linked to transplant glomerulopathy (40,41) and tubular atrophy/interstitial fibrosis (42). Our present work, however, is the first report of an interaction between a circulating autoantibody and the severity of AKI following renal ischemia–reperfusion in transplant patients.

We considered the possibility that autoantibodies could aggravate posttransplant AKI, leading to an increased risk of DGF, based on two observations. First, in murine models of intestinal IRI, binding of natural autoantibodies to self-antigenic targets were shown to increase tissue damage through complement activation following ischemia–reperfusion (18). Second, recent data in human lung transplant patients demonstrated an association between pretransplant levels of autoantibodies to K-α1 tubulin and collagen V and increased incidence of primary graft dysfunction (12). We observed that pretransplant anti-LG3 antibodies were associated with the occurrence and functional impact of DGF, whereas anti-AT1R and antivimentin were not. This result suggests that autoantibodies to cryptic antigens that may become exposed or mobilized by ischemia can behave as accelerators of injury at the time of transplantation. Although our data suggest that this is the case for LG3, AT1R and vimentin may not be as susceptible to ischemic modifications, explaining their lack of association with DGF.

The mechanisms that support the production of anti-LG3, anti-AT1R and antivimentin antibodies in patients awaiting a renal transplantation also remain ill characterized. Although other studies have reported an association between anti-AT1R, lupus erythematosus and systemic sclerosis (43–46), we did not find an association between the autoantibodies we studied and autoimmune diseases. This conclusion, however, is limited by the small number of patients with autoimmune diseases (n = 8) included in the present cohort. In previous work, we also showed in pregnant women that anti-LG3 antibodies do not correlate with anti-AT1R autoantibodies and that both antibodies do not increase in association with normal pregnancy (47). In the present study, however, we found an association between anti-AT1R and prior transplantation, whereas anti-LG3 and antivimentin were not associated with classical allosensitizing events. Collectively, these results suggest that the factors associated with the production of anti-LG3 and anti-AT1R antibodies are

likely different from classical autoimmune conditions and from one another.

In addition to anti-LG3, donor age and height were associated with graft function at 1 year after transplantation in patients with DGF, whereas donor type and cold ischemic time were not. Other studies have also shown that recipients of kidneys from donors after cardiocirculatory arrest experience more DGF but that this does not affect graft survival (48,49). Cold ischemic time was not associated with DGF or its functional impact in multivariate analyses, probably because of relatively homogeneous and short cold ischemic times at our center (Table 1).

In summary, we showed that high titers of anti-LG3 antibodies at the time of transplantation are associated with an increased risk of DGF and with lower long-term renal function after DGF. Anti-LG3 antibodies also aggravate AKI after IRI in mice, in association with activation of the classical complement pathway in PTC, increased tubular activation of the alternative complement pathway at a distance from IRI, and increased microvascular damage and involution. Our results identified anti-LG3 antibodies as novel regulators of IRI in renal transplant patients, providing new insights into the pathways that modulate the severity of renal injury at the time of transplantation and their impact on long-term outcomes.

Acknowledgments

This work was supported by a research grant from the Kidney Foundation of Canada (KFOC140012) to H.C. and a research grant from the Canadian Institutes of Health Research (CIHR) (MOP-15447) and Kidney Foundation of Canada to M.J.H. H.C. is a research scholar of the Fonds de recherche du Québec (FRQ) santé, and a KRESCENT new investigator. B.Y. is a recipient of a research fellowship from the University of Montreal Nephrology Research Consortium and a CNTRP student. M.J.H. is the holder of the Shire Chair in Nephrology, Transplantation and Renal Regeneration of l'Université de Montréal. We thank the J.-L. Levesque Foundation for renewed support.

Disclosure

The authors of this manuscript have no conflicts of interest to disclose as described by the *American Journal of Transplantation*.

References

1. Cavaille-Coll M, Bala S, Velidedeoglu E, et al. Summary of FDA workshop on ischemia reperfusion injury in kidney transplantation. Am J Transplant 2013; 13: 1134–1148.
2. Irish WD, McCollum DA, Tesi RJ, et al. Nomogram for predicting the likelihood of delayed graft function in adult cadaveric renal transplant recipients. J Am Soc Nephrol 2003; 14: 2967–2974.
3. Lechevallier E, Dussol B, Luccioni A, et al. Posttransplantation acute tubular necrosis: Risk factors and implications for graft survival. Am J Kidney Dis 1998; 32: 984–991.
4. Yarlagadda SG, Coca SG, Garg AX, et al. Marked variation in the definition and diagnosis of delayed graft function: A systematic review. Nephrol Dial Transplant 2008; 23: 2995–3003.
5. Wu WK, Famure O, Li Y, Kim SJ. Delayed graft function and the risk of acute rejection in the modern era of kidney transplantation. Kidney Int 2015; 88: 851–858.
6. Legendre C, Canaud G, Martinez F. Factors influencing long-term outcome after kidney transplantation. Transpl Int 2014; 27: 19–27.
7. Yarlagadda SG, Coca SG, Formica RN Jr, Poggio ED, Parikh CR. Association between delayed graft function and allograft and patient survival: A systematic review and meta-analysis. Nephrol Dial Transplant 2009; 24: 1039–1047.
8. Boom H, Mallat MJ, de Fijter JW, de Fijter J, Zwinderman AH, Paul LC. Delayed graft function influences renal function, but not survival. Kidney Int 2000; 58: 859–862.
9. Lapointe I, Lachance JG, Noel R, et al. Impact of donor age on long-term outcomes after delayed graft function: 10-year follow-up. Transpl Int 2013; 26: 162–169.
10. Verma SK, Molitoris BA. Renal endothelial injury and microvascular dysfunction in acute kidney injury. Semin Nephrol 2015; 35: 96–107.
11. Basile DP. The endothelial cell in ischemic acute kidney injury: Implications for acute and chronic function. Kidney Int 2007; 72: 151–156.
12. Bharat A, Saini D, Steward N, et al. Antibodies to self-antigens predispose to primary lung allograft dysfunction and chronic rejection. Ann Thorac Surg 2010; 90: 1094–1101.
13. Dragun D, Muller DN, Brasen JH, et al. Angiotensin II type 1-receptor activating antibodies in renal-allograft rejection. N Engl J Med 2005; 352: 558–569.
14. Gao B, Moore C, Porcheray F, et al. Pretransplant IgG reactivity to apoptotic cells correlates with late kidney allograft loss. Am J Transplant 2014; 14: 1581–1591.
15. Jurcevic S, Ainsworth ME, Pomerance A, et al. Antivimentin antibodies are an independent predictor of transplant-associated coronary artery disease after cardiac transplantation. Transplantation 2001; 71: 886–892.
16. Mahesh B, Leong HS, McCormack A, Sarathchandra P, Holder A, Rose ML. Autoantibodies to vimentin cause accelerated rejection of cardiac allografts. Am J Pathol 2007; 170: 1415–1427.
17. Cardinal H, Dieude M, Brassard N, et al. Antiperlecan antibodies are novel accelerators of immune-mediated vascular injury. Am J Transplant 2013; 13: 861–874.
18. Zhang M, Alicot EM, Carroll MC. Human natural IgM can induce ischemia/reperfusion injury in a murine intestinal model. Mol Immunol 2008; 45: 4036–4039.
19. Zhang M, Carroll MC. Natural IgM-mediated innate autoimmunity: A new target for early intervention of ischemia-reperfusion injury. Expert Opin Biol Ther 2007; 7: 1575–1582.
20. Zhang M, Austen WG Jr, Chiu I, et al. Identification of a specific self-reactive IgM antibody that initiates intestinal ischemia/reperfusion injury. Proc Natl Acad Sci USA 2004; 101: 3886–3891.
21. Lukitsch I, Kehr J, Chaykovska L, et al. Renal ischemia and transplantation predispose to vascular constriction mediated by angiotensin II type 1 receptor-activating antibodies. Transplantation 2012; 94: 8–13.

22. Shaffi K, Uhlig K, Perrone RD, et al. Performance of creatinine-based GFR estimating equations in solid-organ transplant recipients. Am J Kidney Dis 2014; 63: 1007–1018.
23. Haas M, Sis B, Racusen LC, et al. Banff 2013 meeting report: Inclusion of c4d-negative antibody-mediated rejection and antibody-associated arterial lesions. Am J Transplant 2014; 14: 272–283.
24. Wei Q, Dong Z. Mouse model of ischemic acute kidney injury: Technical notes and tricks. Am J Physiol Renal Physiol 2012; 303: F1487–F1494.
25. Leemans JC, Stokman G, Claessen N, et al. Renal-associated TLR2 mediates ischemia/reperfusion injury in the kidney. J Clin Invest 2005; 115: 2894–2903.
26. McCullough JW, Renner B, Thurman JM. The role of the complement system in acute kidney injury. Semin Nephrol 2013; 33: 543–556.
27. Ponticelli C. Ischaemia-reperfusion injury: A major protagonist in kidney transplantation. Nephrol Dial Transplant 2014; 29: 1134–1140.
28. Irish WD, Ilsley JN, Schnitzler MA, Feng S, Brennan DC. A risk prediction model for delayed graft function in the current era of deceased donor renal transplantation. Am J Transplant 2010; 10: 2279–2286.
29. Thurman JM. Altered renal tubular expression of the complement inhibitor Crry permits complement activation after ischemia/reperfusion. J Clin Invest 2006; 116: 357–368.
30. Sharfuddin AA, Molitoris BA. Pathophysiology of ischemic acute kidney injury. Nat Rev Nephrol 2011; 7: 189–200.
31. Molitoris BA. Therapeutic translation in acute kidney injury: The epithelial/endothelial axis. J Clin Investig 2014; 124: 2355–2363.
32. Basile DP, Friedrich JL, Spahic J, et al. Impaired endothelial proliferation and mesenchymal transition contribute to vascular rarefaction following acute kidney injury. Am J Physiol Renal Physiol 2011; 300: F721–F733.
33. Horbelt M, Lee SY, Mang HE, et al. Acute and chronic microvascular alterations in a mouse model of ischemic acute kidney injury. Am J Physiol Renal Physiol 2007; 293: F688–F695.
34. Basile DP, Yoder MC. Renal endothelial dysfunction in acute kidney ischemia reperfusion injury. Cardiovasc Hematol Disord Drug Targets 2014; 14: 3–14.
35. Soulez M, Pilon EA, Dieude M, et al. The perlecan fragment LG3 is a novel regulator of obliterative remodeling associated with allograft vascular rejection. Circ Res 2012; 110: 94–104.
36. Dieude M, Bell C, Turgeon J, et al. The 20S proteasome core, active within apoptotic exosome-like vesicles, induces autoantibody production and accelerates rejection. Sci Transl Med 2015; 7: 318ra200.
37. Haase M, Bellomo R, Albert C, et al. The identification of three novel biomarkers of major adverse kidney events. Biomark Med 2014; 8: 1207–1217.
38. Sutton TA, Mang HE, Campos SB, Sandoval RM, Yoder MC, Molitoris BA. Injury of the renal microvascular endothelium alters barrier function after ischemia. Am J Physiol Renal Physiol 2003; 285: F191–F198.
39. Giral M, Foucher Y, Dufay A, et al. Pretransplant sensitization against angiotensin II type 1 receptor is a risk factor for acute rejection and graft loss. Am J Transplant 2013; 13: 2567–2576.
40. Angaswamy N, Klein C, Tiriveedhi V, et al. Immune responses to collagen-IV and fibronectin in renal transplant recipients with transplant glomerulopathy. Am J Transplant 2014; 14: 685–693.
41. Joosten SA, Sijpkens YW, van Ham V, et al. Antibody response against the glomerular basement membrane protein agrin in patients with transplant glomerulopathy. Am J Transplant 2005; 5: 383–393.
42. Besarani D, Cerundolo L, Smith JD, et al. Role of anti-vimentin antibodies in renal transplantation. Transplantation 2014; 98: 72–78.
43. Riemekasten G, Philippe A, Nather M, et al. Involvement of functional autoantibodies against vascular receptors in systemic sclerosis. Ann Rheum Dis 2011; 70: 530–536.
44. Becker MO, Kill A, Kutsche M, et al. Vascular receptor autoantibodies in pulmonary arterial hypertension associated with systemic sclerosis. Am J Respir Crit Care Med 2014; 190: 808–817.
45. Kill A, Tabeling C, Undeutsch R, et al. Autoantibodies to angiotensin and endothelin receptors in systemic sclerosis induce cellular and systemic events associated with disease pathogenesis. Arthritis Res Ther 2014; 16: R29.
46. Xiong J, Liang Y, Yang H, Zhu F, Wang Y. The role of angiotensin II type 1 receptor-activating antibodies in patients with lupus nephritis. Int J Clin Pract 2013; 67: 1066–1067.
47. Hirt-Minkowski P, Roth M, Honger G, Amico P, Hopfer H, Schaub S. Soluble CD30 correlates with clinical but not subclinical renal allograft rejection. Transpl Int 2013; 26: 75–83.
48. Summers DM, Johnson RJ, Allen J, et al. Analysis of factors that affect outcome after transplantation of kidneys donated after cardiac death in the UK: A cohort study. Lancet 2010; 376: 1303–1311.
49. Singh RP, Farney AC, Rogers J, et al. Kidney transplantation from donation after cardiac death donors: Lack of impact of delayed graft function on post-transplant outcomes. Clin Transplant 2011; 25: 255–264.

Supporting Information

Additional Supporting Information may be found in the online version of this article.

Figure S1: Anti-LG3, anti-AT1R and antivimentin and allosensitizing events and classical autoimmune diseases. Positive pretransplant anti-AT1R antibody status was more frequent in recipients of retransplant than in patients with a first kidney transplant (42% vs. 10%, $p < 0.001$). Positive pretransplant status for anti-LG3 (13% in both groups, $p = 0.25$) and antivimentin (50% vs. 41%, $p = 0.42$) was similar in patients who had received a previous transplantation compared with those who had not. (B) Positive pretransplant status for anti-LG3 (8% vs. 14%, $p = 0.42$), anti-AT1R (18% vs. 14%, $p = 0.16$) and antivimentin (38% vs. 44%, $p = 0.47$) were similar in patients who had a history of pregnancy compared with those who did not. (C) Positive pretransplant status for anti-LG3 (14% vs. 12%, $p = 0.81$), anti-AT1R (19% vs. 12%, $p = 0.27$) and antivimentin (47% vs. 40%, $p = 0.41$) were similar in patients who had a history of transfusions compared with those who did not. (D) Positive pretransplant status for anti-LG3 (0% vs. 13%, $p = 0.32$), anti-AT1R (0% vs. 15%, $p = 0.60$) and antivimentin (50% vs. 42%, $p = 0.72$) were similar in patients who had a history of autoimmune disease compared with those who did not. (E) Positive pretransplant

status for anti-LG3 (0% vs. 13%, p = 0.43), anti-AT1R (33% vs. 14%, p = 0.17) and antivimentin (33% vs. 43%, p = 0.30) were similar in patients with pretransplant calculated panel reactive antibody >20% compared with <20%. AT1R, angiotensin II type 1 receptor.

Figure S2: (A) Enzyme-linked immunosorbent assay dosage of anti-LG3 IgG titers at 2 days after renal artery clamping in mice passively transferred with anti-LG3 antibodies or control mouse IgG (n ≥ 8 per group). (B) Blood urea nitrogen (BUN) levels in control, sham-operated or ischemia–reperfusion injury (IRI) mice with or without injection of phosphate-buffered saline (vehicle for IgG control and anti-LG3; n ≥ 4 per group) at 2 days after renal artery clamping. (C) Serum creatinine levels in mice passively transferred with anti-LG3 IgG or control mouse IgG and sacrificed 2 or 7 days after IRI. (D) BUN levels in nonoperated mice injected with IgG control or anti-LG3 IgG every 2 days and sacrificed 2 or 7 days after the second injection.

Figure S3: (A) Immunohistochemistry and quantification of C4d staining (superficial cortex) in kidney sections from mice submitted to ischemia–reperfusion injury (IRI) and passively transferred with anti-LG3 IgG or control mouse IgG and sacrificed 2 and 7 days after surgery (n ≥ 5 per group); black arrowheads indicate positive peritubular capillary, scale bars = 50 μm. (B) Numbers of C4d-positive peritubular capillaries per five randomly chosen high-power fields (×200) in superficial cortex of mice submitted to IRI and passively transferred with anti-LG3 IgG or control mouse IgG and sacrificed 2 and 7 days after surgery (n ≥ 5 per group).

Figure S4: (A) Immunohistochemistry of membrane attack complex (MAC) staining (superficial cortex) in kidney sections from mice submitted to ischemia–reperfusion injury (IRI) and passively transferred with anti-LG3 IgG or control mouse IgG and sacrificed 2 days (upper panels) and 7 days (lower panels) after surgery (n ≥ 5 per group); arrowheads indicate positive peritubular capillary, scale bars = 50 μm. (B) Numbers of MAC-positive peritubular capillaries per five randomly chosen high-power fields (×200) in superficial cortex of mice submitted to IRI and passively transferred with anti-LG3 IgG or control mouse IgG and sacrificed 2 and 7 days after surgery (n ≥ 5 per group).

frontiers in Immunology

MINI REVIEW
published: 23 May 2018
doi: 10.3389/fimmu.2018.01130

Endothelial Dysfunction in Kidney Transplantation

Héloïse Cardinal[1,2,3], *Mélanie Dieudé*[1,2] *and Marie-Josée Hébert*[1,2,3]*

[1] Research Centre, Centre hospitalier de l'Université de Montréal (CRCHUM), Montreal, QC, Canada, [2] Canadian National Transplant Research Program, Montreal, QC, Canada, [3] University of Montreal, Montreal, QC, Canada

Kidney transplantation entails a high likelihood of endothelial injury. The endothelium is a target of choice for injury by ischemia-reperfusion, alloantibodies, and autoantibodies. A certain degree of ischemia-reperfusion injury inevitably occurs in the immediate post-transplant setting and can manifest as delayed graft function. Acute rejection episodes, whether T-cell or antibody-mediated, can involve the graft micro- and macrovasculature, leading to endothelial injury and adverse long-term consequences on graft function and survival. In turn, caspase-3 activation in injured and dying endothelial cells favors the release of extracellular vesicles (apoptotic bodies and apoptotic exosome-like vesicles) that further enhance autoantibody production, complement deposition, and microvascular rarefaction. In this review, we present the evidence for endothelial injury, its causes and long-term consequences on graft outcomes in the field of kidney transplantation.

Keywords: kidney transplantation, endothelial injury, apoptosis, necroptosis, alloantibodies, autoantibodies

OPEN ACCESS

Edited by:
Thomas Luft, Universitätsklinikum Heidelberg, Germany

Reviewed by:
Philippe Saas, INSERM U1098 Interactions Hôte-Greffon-Tumeur & Ingénierie Cellulaire et Génique, France
Christophe Picard, Établissement Français du Sang, France

***Correspondence:**
Marie-Josée Hébert
marie-josee.hebert@umontreal.ca

Specialty section:
This article was submitted to Alloimmunity and Transplantation, a section of the journal Frontiers in Immunology

Received: *15 December 2017*
Accepted: *04 May 2018*
Published: *23 May 2018*

Citation:
Cardinal H, Dieudé M and Hébert M-J (2018) Endothelial Dysfunction in Kidney Transplantation. Front. Immunol. 9:1130. doi: 10.3389/fimmu.2018.01130

INTRODUCTION

The endothelium plays an important role in vascular biology and regulation of renal function. Healthy endothelial cells are involved in vasodilation through nitric oxide (NO) release, which also inhibits platelet adhesion and aggregation, as well as leukocyte adhesion. Conversely, injured endothelial cells can develop a vasoconstrictive, pro-inflammatory, and procoagulant phenotype. Endothelial dysfunction is associated with traditional cardiovascular risk factors such as hypertension and diabetes, and it predicts atherosclerosis progression and cardiovascular events in the general population (1, 2). A large body of data shows that chronic kidney disease (CKD) is associated with endothelial dysfunction and/or apoptosis (3–7). Increased levels of circulating microparticles from apoptotic endothelial cells have been observed in patients with CKD (5, 6). Uremic solutes foster the production of these microparticles by endothelial cells (6), which in turn decrease NO release and impair endothelium-mediated dilation (5).

Kidney transplantation is the best mode of renal replacement therapy, improving both quality of life and life expectancy compared to dialysis (8, 9). Kidney transplantation restores renal function and improves endothelial function compared to dialysis (10, 11). Nevertheless, kidney transplantation entails a high likelihood of endothelial injury in the allograft. Given its intimate contact with the blood, the allograft endothelium is a target of choice for interactions with circulating inflammatory cells, cytokines, antibodies, and circulating pharmacological agents. First, a certain degree of ischemia-reperfusion injury (IRI) inevitably occurs in the immediate posttransplant setting and manifests as delayed graft function (DGF). IRI is associated with both tubular and endothelial damage, especially in the peritubular capillary network. Second, acute rejection episodes, whether T-cell or antibody-mediated, occur in 15–20% of kidney transplant recipients (2) and can involve the graft micro- and macrovasculature, leading to endothelial injury. This can alter renal blood flow

and impair renal function, both acutely and on the long-term, favoring renal fibrosis and loss of renal function.

Last, the most commonly used immunosuppressive agents may have divergent impact on the graft endothelium after transplantation. Mycophenolic acid may protect the endothelium, but calcineurin inhibitors have an adverse impact on endothelial function and glucocorticoids can worsen endothelial function under physiological conditions and improve it in the presence of inflammation. While these topics are reviewed elsewhere (12–14), here we present the evidence for allograft endothelial injury that is associated with IRI, alloimmunity, and autoimmunity in kidney transplantation and describe its long-term consequences on graft outcomes.

IRI INDUCES ENDOTHELIAL DAMAGE, MICROVASCULAR RAREFACTION AND ADVERSE GRAFT OUTCOMES

The kidney transplant procedure is inevitably associated with a certain degree of IRI. Donor type (deceased after cardiocirculatory arrest and neurologically deceased versus living) and length of cold and warm ischemic times are important risk factors for IRI (15). Clinically significant IRI manifests as DGF, or acute kidney injury (AKI) in the immediate posttransplant period. DGF is defined as the need for hemodialysis in the first week posttransplantation or failure of serum creatinine to decrease by more than 10% on the first three postoperative days, although other definitions have been used (16). Episodes of AKI are strong predictors of CKD in the general population (17–20). Similarly, DGF is associated with decreased long-term kidney graft survival (15, 21).

In the past decade, microvascular injury and endothelial dysfunction have emerged as pivotal elements in the pathogenesis of AKI (22, 23). In experimental models of IRI, renal perfusion in peritubular capillaries is compromised within minutes of unclamping (24). Endothelial dysfunction/injury and apoptosis compromise microcirculatory renal blood flow through decreased vasodilatory capacity, coagulation activation and the formation of microvascular thrombi, and increased rolling/adhesion of inflammatory cells (23, 25).

Because the regenerative capacity of endothelial cells in peritubular capillaries appears limited (26–28), microvascular damage occurring during an episode of AKI can lead to permanent peritubular capillary rarefaction (26–28). Loss of peritubular capillaries favors chronic hypoxia, leading to overexpression of hypoxia inducible factor 1 α (HIF-1α), favoring transcription of fibrogenic genes such as transforming growth factor β (TGF-β) and connective tissue growth factor (CTGF). It also favors accumulation of α-smooth muscle actin (α-SMA) positive myofibroblasts and production of fibrogenic mediators (22, 23, 28–31).

These phenomena eventually lead to progressive interstitial fibrosis/tubular atrophy and renal dysfunction in animal models and in human AKI (31, 32). In kidney transplant patients, peritubular capillary loss, assessed by comparing capillary density on 3-month posttransplant biopsies with capillary density on preimplantation biopsies, is strongly associated with interstitial fibrosis/tubular atrophy and graft dysfunction 1 year posttransplant (33). Recent animal studies using *in vivo* imaging and electron microscopy in murine models of AKI demonstrated a tight correlation between peritubular capillary injury, rarefaction, and renal fibrosis (34, 35). Ultrastructural changes to peritubular capillaries include focal widening of the subendothelial space, higher numbers of endothelial vacuoles, reduced numbers of fenestrations, and increased thickness of the basement membrane (35). Human kidney biopsy samples with progressive renal fibrosis showed strikingly similar ultrastructural findings. Taken together, these studies support the concept that IRI-associated AKI can lead to microvascular rarefaction which in turn plays a pivotal role in favoring interstitial fibrosis and long-term renal dysfunction in patients with native kidney disease and in kidney transplant recipients.

Kidneys from older donors are more susceptible to IRI and more likely to develop DGF (36–39). Increasing age and the presence of age-associated disorders, such as hypertension and type 2 diabetes, favor the accumulation of senescent cells within the vasculature and the kidney. Senescence is characterized by proliferative arrest, cell flattening and enlargement, and the production of an array of pro-inflammatory cytokines (IL-1α, IL-1β, IL-6, IL-8, matrix metalloproteiases, CTGF) known as senescence associated secretory phenotype (40). Senescent cells lack replicative potential and hence tissues with higher levels of senescent cells display lower repair capacity in the face of injury. Increased microvascular rarefaction and enhanced fibrosis have been observed following IRI in rodent models and in transplant patients (41, 42).

IMMUNE-MEDIATED VASCULAR AND ENDOTHELIAL INJURY IS ASSOCIATED WITH ADVERSE KIDNEY GRAFT OUTCOMES

Acute rejection episodes occur in 15–20% of kidney transplant recipients (2). T-cell mediated rejections that involve the tubulointerstitial compartment are responsive to corticosteroid therapy and are reversible in a majority of cases. However, vascular involvement by the rejection process, also termed graft endarteritis, is an important risk factor for decreased long-term graft survival (43, 44). Endarteritis has classically been regarded as a T-cell-mediated phenomenon (45), with both alloreactive CD8+ and CD4+ T-cells infiltrating the allograft small-sized arteries (46). However, mounting evidence shows that endarteritis often clusters with microvascular inflammation (glomerulitis, peritubular capillaritis) and antibody-mediated damage (47). The deleterious impact of donor-specific alloantibodies (DSA) is illustrated by recent data showing that antibody-mediated rejection with endarteritis entails a worse prognosis than cell-mediated endarteritis alone (44). DSA can target class I human leukocyte antigen (HLA) molecules, which are constitutively expressed on all nucleated cells or class II HLA molecules, whose expression is restricted to B lymphocytes, antigen-presenting cells, and activated endothelial cells. Both class I and class II DSA can injure the endothelium though complement-dependent

mechanisms and antibody-dependent cell-mediated cytotoxicity. DSA class I binding also affects the graft endothelium by inducing intracellular signaling which results in migration, proliferation, and resistance to apoptosis and complement-induced death that can have an impact on vascular remodeling and chronic allograft rejection (48). The effect of HLA class II DSA on cell signaling remains to be fully defined given constraints in experimental systems due to the restricted expression of their antigenic target. Although DSA IgG have long been recognized as deleterious to the allograft, the clinical relevance of DSA IgM remains unclear. Some studies have reported associations between IgM DSA, rejection, and decreased graft survival (49, 50).

Even when the allograft arteries are not involved, DSA can affect the graft microcirculation, which is associated with adverse outcomes. A threefold increase in the risk of graft loss was reported in DSA-positive cases of rejection affecting only the microcirculation compared to pure cell-mediated tubulointerstitial rejection (44). In another study, diffuse C4d staining in peritubular capillaries, which marks antibody-mediated complement activation through the classical pathway, was an independent adverse prognostic factor in patients with concurrent cell-mediated rejection, whether or not the graft arteries were involved (51). Hence, the presence of antibody-mediated damage to the microcirculation has prognostic implications in cases of acute rejection, whether or not graft arterial involvement is also present.

Donor-specific antibodies lead to adverse outcomes by injuring the graft endothelium. In patients with antibody-mediated rejection, elevated levels of endothelial transcripts including von Willebrand's factor, caveolin 1, platelet/endothelial cell adhesion molecule, and E selectin have been found in the allograft tissue (52). The presence of circulating DSA and elevated endothelial transcripts in the allograft were associated with poorer long-term graft survival (52), even when evidence for complement activation was lacking (53). Taken together, these studies illustrate that endothelial injury in the allograft macro- or microvascular beds, especially when antibody-mediated, reduces graft survival. DSA-mediated endothelial damage can occur through both complement-dependent and independent pathways.

The persistence of cell- or antibody-mediated vascular and endothelial injury are closely linked with the development of allograft fibrosis and demise. In a swine kidney transplantation model, persistent inflammation in peritubular capillaries was strongly associated with the presence of proliferating α-actin positive myofibroblasts around peritubular capillaries and progression of interstitial fibrosis (54). Similar results were found in human kidney graft biopsies, where microvascular injury in peritubular capillaries (angioregression or capillary drop-out, apoptotic endothelial cells and lamination of the basement membrane) was strongly correlated with interstitial fibrosis, graft dysfunction, and proteinuria (55). Glomerular capillary loss was also associated with glomerular sclerosis and proteinuria.

Recent data suggest that, in addition to DSA, autoantibodies present at the time of transplantation or produced in the posttransplant period can accentuate and aggravate microvascular injury. This concept, coined "innate autoimmunity," was put forward by Carroll and co-workers, as they identified the aggravating role of naturally occurring polyspecific IgM autoantibodies targeting non muscle myosin heavy chain and glycogen phosphorylase in models of intestinal and skeletal muscle IRI (56–58). They also showed that blockade of this autoantibody attenuated tissue damage in a model of cardiac IRI (59). Our group identified anti-perlecan/LG3 IgG autoantibodies of the IgG1 and IgG3 sub-types that target a cryptic C-terminal fragment of perlecan (LG3), as predictors of renal dysfunction in a murine model of renal IRI and in renal transplant patients (60). Elevated levels of anti-perlecan/LG3 at the time of transplantation are associated with an increased risk of vascular rejection and DGF (60, 61). In patients with DGF, anti-perlecan/LG3 autoantibodies predict reduced long-term renal function (60). Anti-perlecan/LG3 autoantibodies exhibit a specific tropism for the ischemic vasculature. In experimental models of vascular rejection and renal IRI, deposition of anti-perlecan/LG3 autoantibodies was significantly increased by ischemia (60, 61). This led to enhanced activation of the classical complement pathway, C4d deposition, peritubular capillary rarefaction, and renal fibrosis. Other autoantibodies, such as anti-angiotensin II type 1 receptors (AT1R) and anti-fibronectin antibodies, have been implicated in accentuation of renal acute vascular rejection and transplant glomerulopathy (38, 39). Anti-AT1R IgG autoantibodies also increase the risk of acute rejection and graft loss in renal transplant patients (62, 63). Ischemia was shown to increase the contractile activity of AT1R autoantibodies in isolated renal artery rings (64), suggesting the possibility of enhanced renal vasoconstriction and ischemia. Collectively, these reports add further support to the notion that renal microvascular injury, either induced by IRI, allo- or autoantibodies or through synergistic interactions between these different factors, plays a major role in long-term renal allograft dysfunction.

ENDOTHELIAL CELL DEATH CONTRIBUTES TO VASCULAR REMODELING, AUTOIMMUNITY AND INFLAMMATION

The presence of dying renal cells in association with AKI or rejection episodes has been known for decades. However, the characterization of molecular pathways controlling regulated renal cell death responses is still an evolving field. Two major types of programmed cell death, apoptosis and necroptosis, have been characterized in association with AKI (23, 26, 65–73), although various death and inflammatory pathways such as ferroptosis and pyroptosis also likely contribute (74–76). Apoptosis can be initiated by two major initiating pathways: cell surface death receptors or mitochondrial outer membrane permeabilization. Both pathways converge on an effector phase triggered by caspases-3 activation and responsible for definitive degradation of key nuclear and cytoskeletal substrates leading to morphological changes such as membrane blebbing and nuclear condensation. However, ligation of death receptors, such as tumor necrosis factor or Fas, in conditions when caspases are inhibited can also activate a regulated form of necrosis referred to as "necroptosis" [reviewed in Ref. (77, 78)]. In this context, receptor-interacting protein 1 (RIPK1) phosphorylates RIPK3

and mixed lineage kinase domain-like protein (MLKL) leading to cell swelling and rupture (77, 78). Necroptosis is associated with an important inflammatory response secondary to the release of damage-associated molecular patterns and to the activation of the inflammasome leading to caspase-1 activation and release of IL-1β, IL-18, and IL-1α. Like necroptosis, pyroptosis is a type of regulated necrotic cell death. Pyroptosis is characterized by caspase-11/gasdermin D-dependent plasma membrane rupture, is highly pro-inflammatory, and has a unique feature: the caspase-1 dependent maturation of pro-inflammatory cytokines in a multiprotein complex called the inflammasome during the cell death process (71, 75).

Apoptosis has classically been considered as an inert or anti-inflammatory type of cell death, responsible for the physiological turnover of multiple cell types. During apoptosis, caspase activation inactivates mitochondrial DNA-induced type I interferon secretion and oxidizes danger signals. This inactivates danger associated molecular patterns (DAMP) molecules and prevents the development of an innate immune response to apoptotic cells (79). Effector caspase activation also leads to the release of chemotactic factors that recruit phagocytes and enhance the clearance of apoptotic cells, preventing secondary necrosis and the release of DAMP factors (79).

Nevertheless, the impact of apoptosis may vary according to cell type and in certain conditions also favor inflammatory responses. Apoptotic endothelial cells externalize phosphatidylserine (80), which binds Factor XII to promote coagulation (81). Apoptotic endothelial cells also interact with other cell types through the release of extracellular vesicles which can in turn promote inflammation. Extracellular vesicles include microvesicles, such as apoptotic bodies, that are produced by cytoplasmic membrane blebbing and shedding, and exosomes, that are smaller and stored in multivesicular bodies or alpha-granules (82). For example, endothelial apoptotic bodies that contain the full-length precursor and processed mature form of IL-1α have pro-inflammatory effects when injected in the peritoneal cavity of mice (83). Both types of vesicles are involved in cellular crosstalk, as will be discussed later.

The relative importance of regulated death pathways in AKI or rejection-induced microvascular injury is only beginning to be unraveled. It is generally accepted that broad caspase inhibition can prevent apoptosis at the expense of increased necroptosis

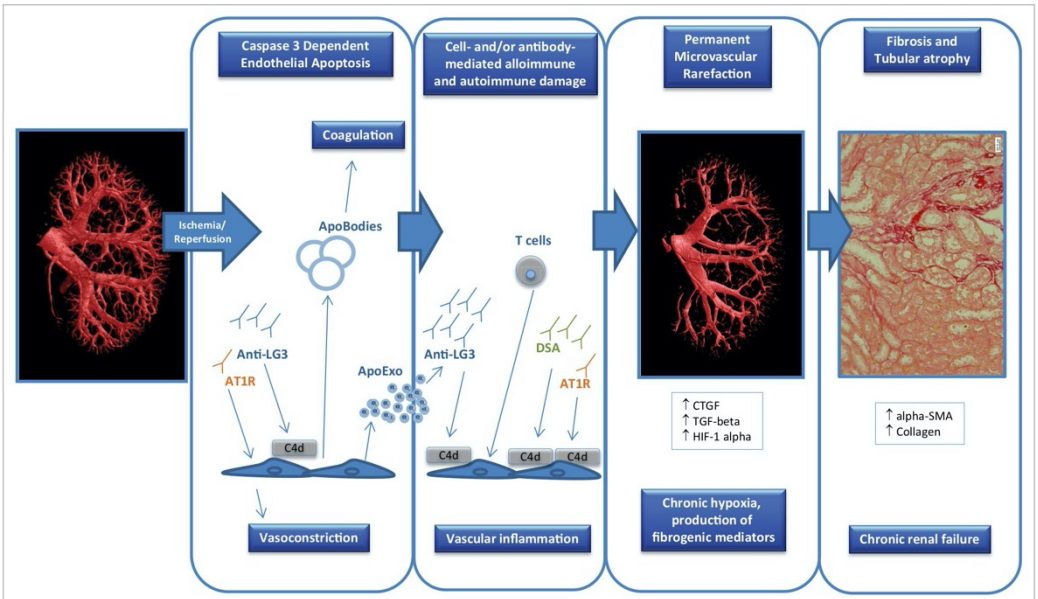

FIGURE 1 | Factors contributing to endothelial dysfunction in transplantation. Ischemia-reperfusion injury that occurs at the time of transplantation can trigger endothelial apoptosis through caspase-3 activation which can in turn release apoptotic bodies with procoagulant activity. In addition, apoptotic endothelial cells also release apoptotic exosome-like vesicles that favor the recruitment of inflammatory cells (e.g., T cells) and the production of autoantibodies such as anti-perlecan/LG3 antibodies (anti-LG3). The synergistic interactions between cellular alloimmunity and autoimmunity, donor-specific antibodies (DSA), and autoantibodies [anti-LG3, anti-angiotensin II type 1 receptors (AT1R)] amplify microvascular damage, through complement-dependent (C4d deposition) or -independent pathways, which leads to permanent peritubular capillary rarefaction. Loss of peritubular capillaries favors chronic hypoxia, leading to overexpression of hypoxia inducible factor 1 α (HIF-1α), favoring transcription of fibrogenic genes such as transforming growth factor β (TGF-β) and connective tissue growth factor (CTGF). It also favors accumulation of collagen, α-smooth muscle actin (α-SMA) positive myofibroblasts and of fibrogenic mediators. These phenomena eventually lead to progressive interstitial fibrosis/tubular atrophy and renal graft dysfunction.

and accentuated renal dysfunction (70, 78), a phenomenon well characterized in renal tubular epithelial cells (84, 85). Cardiac endothelial cells have also been shown to develop RIPK3-dependent cell death after TNF-alpha treatment *in vitro* and following transplantation *in vivo*. RIPK3−/− mice show better preservation of microvascular integrity in a model of cardiac rejection (86). Whether RIPK-dependent death also occurs in the renal microvasculature during AKI and/or rejection remains to be evaluated. However, microvascular apoptosis, evaluated by caspase-3 activation, has been documented in models of renal IRI and rejection (23, 87). Also, inhibition of caspase-3 at the time of renal IRI has generally been associated with improved long-term renal function and reduced extracellular matrix deposition (78, 88, 89). Collectively, these results suggest an important role for caspase-3 in regulating renal vascular cell death whereas the importance of RIPK-dependent death remains to be characterized. While pyroptosis has been observed in renal tubular epithelial cells in a rat model of renal IRI (90), this type of cell death has not been described in endothelial cells.

Endothelial caspase-3 activation can promote vascular dysfunction through various and non-mutually exclusive pathways (**Figure 1**). It favors the release of a number of fibroproliferative mediators, such as CTGF, LG3, and translationally controlled tumor protein, which can in turn favor neointima formation and myointimal thickening (91–94). Endothelial caspase-3 activation also leads to the release of apoptotic bodies or membrane blebs with procoagulant activity (95, 96). Recently, we showed that, in addition to apoptotic bodies, endothelial caspase-3 activation prompts the release of a novel type of extracellular vesicles whose protein content and function are dramatically different from classic apoptotic bodies (97). These apoptotic exosome-like vesicles (ApoExo) are smaller than apoptotic bodies, ranging from 30 to 100 nm and carry active 20S proteasome complexes with pro-inflammatory activity. ApoExo injection in mice favors the recruitment of T and B cells in a model of vascular allograft rejection (97). Endothelial ApoExos also favor the production of autoantibodies such as anti-perlecan/LG3 antibodies, anti-nuclear antibodies, and anti-double-stranded DNA antibodies (97), which in turn further aggravate vascular inflammation. In animal models, renal IRI favors the release of ApoExos within the bloodstream, followed by augmented levels of anti-perlecan/LG3 antibodies (97). Collectively, these results highlight an important role for vascular caspase-3 activation in triggering the release of a number of mediators and extracellular vesicles that will, both at the local and systemic levels, initiate multiple positive feedback mechanisms that favor vascular remodeling, inflammation, and autoimmunity.

CONCLUDING REMARKS

Kidney transplantation is associated with an elevated likelihood of damage to the graft macro- and microvasculature, given the IRI that occurs at the time of transplantation and the physical location of the graft endothelium that makes it a target of choice for cell- or antibody-mediated alloimmune injury. IRI, alloimmune damage, and autoantibodies can activate programmed cell death pathways in the graft endothelium, which can in turn trigger microvascular rarefaction, interstitial fibrosis, and graft dysfunction. These pathways represent potential targets for pharmacological intervention that could be delivered in preservation solutions during the period cold ischemia, with the aim of improving long-term graft outcomes.

AUTHOR CONTRIBUTIONS

HC, MD, and M-JH reviewed the literature and drafted the manuscript.

ACKNOWLEDGMENTS

HC is a research scholar of the Fonds de Recherche du Québec (FRQ) santé. M-JH holds the Shire Chair in Nephrology, Transplantation and Renal Regeneration of l'Université de Montréal. HC is an associate researcher on that chair. This work was supported by grants from the Canadian Institutes of Health Research (MOP 15447 and MOP 123436) and the Kidney Foundation of Canada to M-JH and HC. We thank Shanshan Lan and Bing Yang for their contribution to **Figure 1**. We thank the J.-L. Levesque Foundation for renewed support. MD is the scientific integration manager of the Canadian National Transplantation Research Program (CNTRP). HC, MD, and M-JH are CNTRP investigators.

REFERENCES

1. Heitzer T, Schlinzig T, Krohn K, Meinertz T, Munzel T. Endothelial dysfunction, oxidative stress, and risk of cardiovascular events in patients with coronary artery disease. *Circulation* (2001) 104:2673–8. doi:10.1161/hc4601.099485
2. Schachinger V, Britten MB, Zeiher AM. Prognostic impact of coronary vasodilator dysfunction on adverse long-term outcome of coronary heart disease. *Circulation* (2000) 101:1899–906. doi:10.1161/01.CIR.101.16.1899
3. Ghiadoni L, Cupisti A, Huang Y, Mattei P, Cardinal H, Favilla S, et al. Endothelial dysfunction and oxidative stress in chronic renal failure. *J Nephrol* (2004) 17:512–9.
4. Cardinal H, Raymond MA, Hebert MJ, Madore F. Uraemic plasma decreases the expression of ABCA1, ABCG1 and cell-cycle genes in human coronary arterial endothelial cells. *Nephrol Dial Transplant* (2007) 22:409–16. doi:10.1093/ndt/gfl619
5. Amabile N, Guerin AP, Leroyer A, Mallat Z, Nguyen C, Boddaert J, et al. Circulating endothelial microparticles are associated with vascular dysfunction in patients with end-stage renal failure. *J Am Soc Nephrol* (2005) 16:3381–8. doi:10.1681/ASN.2005050535
6. Faure V, Dou L, Sabatier F, Cerini C, Sampol J, Berland Y, et al. Elevation of circulating endothelial microparticles in patients with chronic renal failure. *J Thromb Haemost* (2006) 4:566–73. doi:10.1111/j.1538-7836.2005.01780.x
7. Goligorsky MS. Pathogenesis of endothelial cell dysfunction in chronic kidney disease: a retrospective and what the future may hold. *Kidney Res Clin Pract* (2015) 34:76–82. doi:10.1016/j.krcp.2015.05.003
8. Laupacis A, Keown P, Pus N, Krueger H, Ferguson B, Wong C, et al. A study of the quality of life and cost-utility of renal transplantation. *Kidney Int* (1996) 50:235–42. doi:10.1038/ki.1996.307
9. Wolfe RA, Ashby VB, Milford EL, Ojo AO, Ettenger RE, Agodoa LY, et al. Comparison of mortality in all patients on dialysis, patients on dialysis

awaiting transplantation, and recipients of a first cadaveric transplant. *N Engl J Med* (1999) 341:1725–30. doi:10.1056/NEJM199912023412303
10. Kocak H, Ceken K, Yavuz A, Yucel S, Gurkan A, Erdogan O, et al. Effect of renal transplantation on endothelial function in haemodialysis patients. *Nephrol Dial Transplant* (2006) 21:203–7. doi:10.1093/ndt/gfi119
11. Sharma J, Kapoor A, Muthu R, Prasad N, Sinha A, Khanna R, et al. Assessment of endothelial dysfunction in Asian Indian patients with chronic kidney disease and changes following renal transplantation. *Clin Transplant* (2014) 28:889–96. doi:10.1111/ctr.12398
12. Olejarz W, Bryk D, Zapolska-Downar D. Mycophenolate mofetil – a new atheropreventive drug? *Acta Pol Pharm* (2014) 71:353–61.
13. Verhoeven F, Prati C, Maguin-Gate K, Wendling D, Demougeot C. Glucocorticoids and endothelial function in inflammatory diseases: focus on rheumatoid arthritis. *Arthritis Res Ther* (2016) 18:258. doi:10.1186/s13075-016-1157-0
14. Lamas S. Cellular mechanisms of vascular injury mediated by calcineurin inhibitors. *Kidney Int* (2005) 68:898–907. doi:10.1111/j.1523-1755.2005.00472.x
15. Chapal M, Le Borgne F, Legendre C, Kreis H, Mourad G, Garrigue V, et al. A useful scoring system for the prediction and management of delayed graft function following kidney transplantation from cadaveric donors. *Kidney Int* (2014) 86:1130–9. doi:10.1038/ki.2014.188
16. Yarlagadda SG, Coca SG, Garg AX, Doshi M, Poggio E, Marcus RJ, et al. Marked variation in the definition and diagnosis of delayed graft function: a systematic review. *Nephrol Dial Transplant* (2008) 23:2995–3003. doi:10.1093/ndt/gfn158
17. Coca SG, Singanamala S, Parikh CR. Chronic kidney disease after acute kidney injury: a systematic review and meta-analysis. *Kidney Int* (2012) 81:442–8. doi:10.1038/ki.2011.379
18. Ishani A, Xue JL, Himmelfarb J, Eggers PW, Kimmel PL, Molitoris BA, et al. Acute kidney injury increases risk of ESRD among elderly. *J Am Soc Nephrol* (2009) 20:223–8. doi:10.1681/ASN.2007080837
19. Amdur RL, Chawla LS, Amodeo S, Kimmel PL, Palant CE. Outcomes following diagnosis of acute renal failure in U.S. veterans: focus on acute tubular necrosis. *Kidney Int* (2009) 76:1089–97. doi:10.1038/ki.2009.332
20. Lo LJ, Go AS, Chertow GM, McCulloch CE, Fan D, Ordonez JD, et al. Dialysis-requiring acute renal failure increases the risk of progressive chronic kidney disease. *Kidney Int* (2009) 76:893–9. doi:10.1038/ki.2009.289
21. Yarlagadda SG, Coca SG, Formica RN Jr, Poggio ED, Parikh CR. Association between delayed graft function and allograft and patient survival: a systematic review and meta-analysis. *Nephrol Dial Transplant* (2009) 24:1039–47. doi:10.1093/ndt/gfn667
22. Basile DP, Yoder MC. Renal endothelial dysfunction in acute kidney ischemia reperfusion injury. *Cardiovasc Hematol Disord Drug Targets* (2014) 14:3–14. doi:10.2174/1871529X1401140724093505
23. Molitoris BA. Therapeutic translation in acute kidney injury: the epithelial/endothelial axis. *J Clin Invest* (2014) 124:2355–63. doi:10.1172/JCI72269
24. Yamamoto T, Tada T, Brodsky SV, Tanaka H, Noiri E, Kajiya F, et al. Intravital videomicroscopy of peritubular capillaries in renal ischemia. *Am J Physiol Renal Physiol* (2002) 282:F1150–5. doi:10.1152/ajprenal.00310.2001
25. Goligorsky MS, Brodsky SV, Noiri E. NO bioavailability, endothelial dysfunction, and acute renal failure: new insights into pathophysiology. *Semin Nephrol* (2004) 24:316–23. doi:10.1016/j.semnephrol.2004.04.003
26. Basile DP, Friedrich JL, Spahic J, Knipe N, Mang H, Leonard EC, et al. Impaired endothelial proliferation and mesenchymal transition contribute to vascular rarefaction following acute kidney injury. *Am J Physiol Renal Physiol* (2011) 300:F721–33. doi:10.1152/ajprenal.00546.2010
27. Kwon O, Hong SM, Sutton TA, Temm CJ. Preservation of peritubular capillary endothelial integrity and increasing pericytes may be critical to recovery from postischemic acute kidney injury. *Am J Physiol Renal Physiol* (2008) 295:F351–9. doi:10.1152/ajprenal.90276.2008
28. Basile DP, Donohoe D, Roethe K, Osborn JL. Renal ischemic injury results in permanent damage to peritubular capillaries and influences long-term function. *Am J Physiol Renal Physiol* (2001) 281:F887–99. doi:10.1152/ajprenal.0050.2001
29. Horbelt M, Lee SY, Mang HE, Knipe NL, Sado Y, Kribben A, et al. Acute and chronic microvascular alterations in a mouse model of ischemic acute kidney injury. *Am J Physiol Renal Physiol* (2007) 293:F688–95. doi:10.1152/ajprenal.00452.2006
30. Basile DP, Donohoe DL, Roethe K, Mattson DL. Chronic renal hypoxia after acute ischemic injury: effects of L-arginine on hypoxia and secondary damage. *Am J Physiol Renal Physiol* (2003) 284:F338–48. doi:10.1152/ajprenal.00169.2002
31. Basile DP. The endothelial cell in ischemic acute kidney injury: implications for acute and chronic function. *Kidney Int* (2007) 72:151–6. doi:10.1038/sj.ki.5002312
32. Basile DP. Rarefaction of peritubular capillaries following ischemic acute renal failure: a potential factor predisposing to progressive nephropathy. *Curr Opin Nephrol Hypertens* (2004) 13:1–7. doi:10.1097/00041552-200401000-00001
33. Steegh FM, Gelens MA, Nieman FH, van Hooff JP, Cleutjens JP, van Suylen RJ, et al. Early loss of peritubular capillaries after kidney transplantation. *J Am Soc Nephrol* (2011) 22:1024–9. doi:10.1681/ASN.2010050531
34. Ehling J, Babickova J, Gremse F, Klinkhammer BM, Baetke S, Knuechel R, et al. Quantitative micro-computed tomography imaging of vascular dysfunction in progressive kidney diseases. *J Am Soc Nephrol* (2016) 27:520–32. doi:10.1681/ASN.2015020204
35. Babickova J, Klinkhammer BM, Buhl EM, Djudjaj S, Hoss M, Heymann F, et al. Regardless of etiology, progressive renal disease causes ultrastructural and functional alterations of peritubular capillaries. *Kidney Int* (2017) 91:70–85. doi:10.1016/j.kint.2016.07.038
36. Lim WH, Clayton P, Wong G, Campbell SB, Cohney S, Russ GR, et al. Outcomes of kidney transplantation from older living donors. *Transplantation* (2013) 95:106–13. doi:10.1097/TP.0b013e318277b2be
37. Slegtenhorst BR, Dor FJ, Elkhal A, Rodriguez H, Yang X, Edtinger K, et al. Mechanisms and consequences of injury and repair in older organ transplants. *Transplantation* (2014) 97:1091–9. doi:10.1097/TP.0000000000000072
38. Tasaki M, Saito K, Nakagawa Y, Ikeda M, Imai N, Narita I, et al. Effect of donor-recipient age difference on long-term graft survival in living kidney transplantation. *Int Urol Nephrol* (2014) 46:1441–6. doi:10.1007/s11255-014-0655-8
39. Oberhuber R, Ge X, Tullius SG. Donor age-specific injury and immune responses. *Am J Transplant* (2012) 12:38–42. doi:10.1111/j.1600-6143.2011.03798.x
40. van Willigenburg H, de Keizer PLJ, de Bruin RWF. Cellular senescence as a therapeutic target to improve renal transplantation outcome. *Pharmacol Res* (2018) 130:322–30. doi:10.1016/j.phrs.2018.02.015
41. Katsuumi G, Shimizu I, Yoshida Y, Minamino T. Vascular senescence in cardiovascular and metabolic diseases. *Front Cardiovasc Med* (2018) 5:18. doi:10.3389/fcvm.2018.00018
42. Clements ME, Chaber CJ, Ledbetter SR, Zuk A. Increased cellular senescence and vascular rarefaction exacerbate the progression of kidney fibrosis in aged mice following transient ischemic injury. *PLoS One* (2013) 8:e70464. doi:10.1371/journal.pone.0070464
43. Mueller A, Schnuelle P, Waldherr R, van der Woude FJ. Impact of the Banff '97 classification for histological diagnosis of rejection on clinical outcome and renal function parameters after kidney transplantation. *Transplantation* (2000) 69:1123–7. doi:10.1097/00007890-200003270-00017
44. Lefaucheur C, Loupy A, Vernerey D, Duong-Van-Huyen JP, Suberbielle C, Anglicheau D, et al. Antibody-mediated vascular rejection of kidney allografts: a population-based study. *Lancet* (2013) 381:313–9. doi:10.1016/S0140-6736(12)61265-3
45. Solez K, Colvin RB, Racusen LC, Haas M, Sis B, Mengel M, et al. Banff 07 classification of renal allograft pathology: updates and future directions. *Am J Transplant* (2008) 8:753–60. doi:10.1111/j.1600-6143.2008.02159.x
46. Nankivell BJ, Alexander SI. Rejection of the kidney allograft. *N Engl J Med* (2010) 363:1451–62. doi:10.1056/NEJMra0902927
47. Sis B, Einecke G, Chang J, Hidalgo LG, Mengel M, Kaplan B, et al. Cluster analysis of lesions in nonselected kidney transplant biopsies: microcirculation changes, tubulointerstitial inflammation and scarring. *Am J Transplant* (2010) 10:421–30. doi:10.1111/j.1600-6143.2009.02938.x
48. Valenzuela NM, Mulder A, Reed EF. HLA class I antibodies trigger increased adherence of monocytes to endothelial cells by eliciting an increase in endothelial P-selectin and, depending on subclass, by engaging FcgammaRs. *J Immunol* (2013) 190:6635–50. doi:10.4049/jimmunol.1201434
49. Babu A, Andreou A, Briggs D, Krishnan N, Higgins R, Mitchell D, et al. Clinical relevance of donor-specific IgM antibodies in HLA incompatible renal Transplantation: a retrospective single-center study. *Clin Transpl* (2016) 32:173–9.

50. Everly MJ, Rebellato LM, Haisch CE, Briley KP, Bolin P, Kendrick WT, et al. Impact of IgM and IgG3 anti-HLA alloantibodies in primary renal allograft recipients. *Transplantation* (2014) 97:494–501. doi:10.1097/01.TP.0000441362.11232.48
51. Herzenberg AM, Gill JS, Djurdjev O, Magil AB. C4d deposition in acute rejection: an independent long-term prognostic factor. *J Am Soc Nephrol* (2002) 13:234–41.
52. Sis B, Jhangri GS, Bunnag S, Allanach K, Kaplan B, Halloran PF. Endothelial gene expression in kidney transplants with alloantibody indicates antibody-mediated damage despite lack of C4d staining. *Am J Transplant* (2009) 9:2312–23. doi:10.1111/j.1600-6143.2009.02761.x
53. Sis B, Halloran PF. Endothelial transcripts uncover a previously unknown phenotype: C4d-negative antibody-mediated rejection. *Curr Opin Organ Transplant* (2010) 15:42–8. doi:10.1097/MOT.0b013e3283352a50
54. Shimizu A, Yamada K, Sachs DH, Colvin RB. Persistent rejection of peritubular capillaries and tubules is associated with progressive interstitial fibrosis. *Kidney Int* (2002) 61:1867–79. doi:10.1046/j.1523-1755.2002.00309.x
55. Ishii Y, Sawada T, Kubota K, Fuchinoue S, Teraoka S, Shimizu A. Injury and progressive loss of peritubular capillaries in the development of chronic allograft nephropathy. *Kidney Int* (2005) 67:321–32. doi:10.1111/j.1523-1755.2005.00085.x
56. Zhang M, Alicot EM, Carroll MC. Human natural IgM can induce ischemia/reperfusion injury in a murine intestinal model. *Mol Immunol* (2008) 45:4036–9. doi:10.1016/j.molimm.2008.06.013
57. Zhang M, Alicot EM, Chiu I, Li J, Verna N, Vorup-Jensen T, et al. Identification of the target self-antigens in reperfusion injury. *J Exp Med* (2006) 203:141–52. doi:10.1084/jem.20050390
58. Zhang M, Austen WG Jr, Chiu I, Alicot EM, Hung R, Ma M, et al. Identification of a specific self-reactive IgM antibody that initiates intestinal ischemia/reperfusion injury. *Proc Natl Acad Sci U S A* (2004) 101:3886–91. doi:10.1073/pnas.0400347101
59. Zhang M, Michael LH, Grosjean SA, Kelly RA, Carroll MC, Entman ML. The role of natural IgM in myocardial ischemia-reperfusion injury. *J Mol Cell Cardiol* (2006) 41:62–7. doi:10.1016/j.yjmcc.2006.02.006
60. Yang B, Dieude M, Hamelin K, Henault-Rondeau M, Patey N, Turgeon J, et al. Anti-LG3 antibodies aggravate renal ischemia-reperfusion injury and long-term renal allograft dysfunction. *Am J Transplant* (2016) 16:3416–29. doi:10.1111/ajt.13866
61. Cardinal H, Dieude M, Brassard N, Qi S, Patey N, Soulez M, et al. Antiperlecan antibodies are novel accelerators of immune-mediated vascular injury. *Am J Transplant* (2013) 13:861–74. doi:10.1111/ajt.12168
62. Giral M, Foucher Y, Dufay A, Van Huyen JP, Renaudin K, Moreau A, et al. Pretransplant sensitization against angiotensin II type 1 receptor is a risk factor for acute rejection and graft loss. *Am J Transplant* (2013) 13:2567–76. doi:10.1111/ajt.12397
63. Taniguchi M, Rebellato LM, Cai J, Hopfield J, Briley KP, Haisch CE, et al. Higher risk of kidney graft failure in the presence of anti-angiotensin II type-1 receptor antibodies. *Am J Transplant* (2013) 13:2577–89. doi:10.1111/ajt.12395
64. Lukitsch I, Kehr J, Chaykovska L, Wallukat G, Nieminen-Kelha M, Batuman V, et al. Renal ischemia and transplantation predispose to vascular constriction mediated by angiotensin II type 1 receptor-activating antibodies. *Transplantation* (2012) 94:8–13. doi:10.1097/TP.0b013e3182529bb7
65. Nogae S, Miyazaki M, Kobayashi N, Saito T, Abe K, Saito H, et al. Induction of apoptosis in ischemia-reperfusion model of mouse kidney: possible involvement of Fas. *J Am Soc Nephrol* (1998) 9:620–31.
66. Toronyi E, Lord R, Bowen ID, Perner F, Szende B. Renal tubular cell necrosis and apoptosis in transplanted kidneys. *Cell Biol Int* (2001) 25:267–70. doi:10.1006/cbir.2000.0620
67. Jaffe R, Ariel I, Beeri R, Paltiel O, Hiss Y, Rosen S, et al. Frequent apoptosis in human kidneys after acute renal hypoperfusion. *Exp Nephrol* (1997) 5:399–403.
68. Havasi A, Borkan SC. Apoptosis and acute kidney injury. *Kidney Int* (2011) 80:29–40. doi:10.1038/ki.2011.120
69. Kishino M, Yukawa K, Hoshino K, Kimura A, Shirasawa N, Otani H, et al. Deletion of the kinase domain in death-associated protein kinase attenuates tubular cell apoptosis in renal ischemia-reperfusion injury. *J Am Soc Nephrol* (2004) 15:1826–34. doi:10.1097/01.ASN.0000131527.59781.F2
70. Wang S, Zhang C, Hu L, Yang C. Necroptosis in acute kidney injury: a shedding light. *Cell Death Dis* (2016) 7:e2125. doi:10.1038/cddis.2016.37
71. Kers J, Leemans JC, Linkermann A. An overview of pathways of regulated necrosis in acute kidney injury. *Semin Nephrol* (2016) 36:139–52. doi:10.1016/j.semnephrol.2016.03.002
72. Linkermann A, Heller JO, Prokai A, Weinberg JM, De Zen F, Himmerkus N, et al. The RIP1-kinase inhibitor necrostatin-1 prevents osmotic nephrosis and contrast-induced AKI in mice. *J Am Soc Nephrol* (2013) 24:1545–57. doi:10.1681/ASN.2012121169
73. Linkermann A, Brasen JH, Darding M, Jin MK, Sanz AB, Heller JO, et al. Two independent pathways of regulated necrosis mediate ischemia-reperfusion injury. *Proc Natl Acad Sci U S A* (2013) 110:12024–9. doi:10.1073/pnas.1305538110
74. Linkermann A. Nonapoptotic cell death in acute kidney injury and transplantation. *Kidney Int* (2016) 89:46–57. doi:10.1016/j.kint.2015.10.008
75. Linkermann A, Chen G, Dong G, Kunzendorf U, Krautwald S, Dong Z. Regulated cell death in AKI. *J Am Soc Nephrol* (2014) 25:2689–701. doi:10.1681/ASN.2014030262
76. Linkermann A, Skouta R, Himmerkus N, Mulay SR, Dewitz C, De Zen F, et al. Synchronized renal tubular cell death involves ferroptosis. *Proc Natl Acad Sci U S A* (2014) 111:16836–41. doi:10.1073/pnas.1415518111
77. Weinlich R, Oberst A, Beere HM, Green DR. Necroptosis in development, inflammation and disease. *Nat Rev Mol Cell Biol* (2017) 18:127–36. doi:10.1038/nrm.2016.149
78. Hébert MJ, Jevnikar AM. The impact of regulated cell death pathways on alloimmune responses and graft injury. *Curr Transplant Rep* (2015) 2:242–58. doi:10.1007/s40472-015-0067-4
79. Saas P, Daguindau E, Perruche S. Concise review: apoptotic cell-based therapies-rationale, preclinical results and future clinical developments. *Stem Cells* (2016) 34:1464–73. doi:10.1002/stem.2361
80. Casciola-Rosen L, Rosen A, Petri M, Schlissel M. Surface blebs on apoptotic cells are sites of enhanced procoagulant activity: implications for coagulation events and antigenic spread in systemic lupus erythematosus. *Proc Natl Acad Sci U S A* (1996) 93:1624–9. doi:10.1073/pnas.93.4.1624
81. Yang A, Chen F, He C, Zhou J, Lu Y, Dai J, et al. The procoagulant activity of apoptotic cells is mediated by interaction with factor XII. *Front Immunol* (2017) 8:1188. doi:10.3389/fimmu.2017.01188
82. Ridger VC, Boulanger CM, Angelillo-Scherrer A, Badimon L, Blanc-Brude O, Bochaton-Piallat ML, et al. Microvesicles in vascular homeostasis and diseases. Position paper of the European Society of Cardiology (ESC) Working Group on atherosclerosis and vascular biology. *Thromb Haemost* (2017) 117:1296–316. doi:10.1160/TH16-12-0943
83. Berda-Haddad Y, Robert S, Salers P, Zekraoui L, Farnarier C, Dinarello CA, et al. Sterile inflammation of endothelial cell-derived apoptotic bodies is mediated by interleukin-1alpha. *Proc Natl Acad Sci U S A* (2011) 108:20684–9. doi:10.1073/pnas.1116848108
84. Lau A, Wang S, Jiang J, Haig A, Pavlosky A, Linkermann A, et al. RIPK3-mediated necroptosis promotes donor kidney inflammatory injury and reduces allograft survival. *Am J Transplant* (2013) 13:2805–18. doi:10.1111/ajt.12447
85. Linkermann A, Hackl MJ, Kunzendorf U, Walczak H, Krautwald S, Jevnikar AM. Necroptosis in immunity and ischemia-reperfusion injury. *Am J Transplant* (2013) 13:2797–804. doi:10.1111/ajt.12448
86. Pavlosky A, Lau A, Su Y, Lian D, Huang X, Yin Z, et al. RIPK3-mediated necroptosis regulates cardiac allograft rejection. *Am J Transplant* (2014) 14:1778–90. doi:10.1111/ajt.12779
87. Pallet N, Dieude M, Cailhier J, Hebert M. The molecular legacy of apoptosis in transplantation. *Am J Transplant* (2012) 12:1378–84. doi:10.1111/j.1600-6143.2012.04015.x
88. Zhang X, Zheng X, Sun H, Feng B, Chen G, Vladau C, et al. Prevention of renal ischemic injury by silencing the expression of renal caspase 3 and caspase 8. *Transplantation* (2006) 82:1728–32. doi:10.1097/01.tp.0000250764.17636.ba
89. Yang C, Zhao T, Zhao Z, Jia Y, Li L, Zhang Y, et al. Serum-stabilized naked caspase-3 siRNA protects autotransplant kidneys in a porcine model. *Mol Ther* (2014) 22:1817–28. doi:10.1038/mt.2014.111
90. Yang JR, Yao FH, Zhang JG, Ji ZY, Li KL, Zhan J, et al. Ischemia-reperfusion induces renal tubule pyroptosis via the CHOP-caspase-11 pathway. *Am J Physiol Renal Physiol* (2014) 306:F75–84. doi:10.1152/ajprenal.00117.2013

91. Sirois I, Raymond MA, Brassard N, Cailhier JF, Fedjaev M, Hamelin K, et al. Caspase-3-dependent export of TCTP: a novel pathway for antiapoptotic intercellular communication. *Cell Death Differ* (2011) 18:549–62. doi:10.1038/cdd.2010.126
92. Laplante P, Sirois I, Raymond MA, Kokta V, Beliveau A, Prat A, et al. Caspase-3-mediated secretion of connective tissue growth factor by apoptotic endothelial cells promotes fibrosis. *Cell Death Differ* (2010) 17:291–303. doi:10.1038/cdd.2009.124
93. Soulez M, Pilon EA, Dieude M, Cardinal H, Brassard N, Qi S, et al. The perlecan fragment LG3 is a novel regulator of obliterative remodeling associated with allograft vascular rejection. *Circ Res* (2012) 110:94–104. doi:10.1161/CIRCRESAHA.111.250431
94. Pilon EA, Dieude M, Qi S, Hamelin K, Pomerleau L, Beillevaire D, et al. The perlecan fragment LG3 regulates homing of mesenchymal stem cells and neointima formation during vascular rejection. *Am J Transplant* (2015) 15:1205–18. doi:10.1111/ajt.13119
95. Gao C, Xie R, Yu C, Ma R, Dong W, Meng H, et al. Thrombotic role of blood and endothelial cells in uremia through phosphatidylserine exposure and microparticle release. *PLoS One* (2015) 10:e0142835. doi:10.1371/journal.pone.0142835
96. Dignat-George F, Boulanger CM. The many faces of endothelial microparticles. *Arterioscler Thromb Vasc Biol* (2011) 31:27–33. doi:10.1161/ATVBAHA.110.218123
97. Dieude M, Bell C, Turgeon J, Beillevaire D, Pomerleau L, Yang B, et al. The 20S proteasome core, active within apoptotic exosome-like vesicles, induces autoantibody production and accelerates rejection. *Sci Transl Med* (2015) 7:318ra200. doi:10.1126/scitranslmed.aac9816

Conflict of Interest Statement: The authors declare that the research was conducted in the absence of any commercial or financial relationships that could be construed as a potential conflict of interest.